Fall 12-3-2018

Design and development of small molecule based biosensors for detection of pathogens

Amrita Das
Amrita Das

DESIGN AND DEVELOPMENT OF SMALL MOLECULE BASED BIOSENSORS FOR DETECTION OF PATHOGENS

by

AMRITA DAS

Under the Direction of Suri S Iyer. Ph.D.

ABSTRACT

Glycans are present on the cell surface of mammalian cells. In Dr. Iyer's laboratories, we aim to understand the interactions of cell surface glycans with toxins and pathogens at a molecular level and use that information to develop a point of care diagnostics. This thesis primarily focuses on the development of new technologies that could potentially be further developed towards the point of care diagnostics.

Chapter 1, the introduction chapter focuses on the biosensors, different recognition molecules, various reporters, techniques, testing parameters used in biosensors and point of care testing (POCT).

In chapter 2, the focus is on the development of a novel electrochemical assay that uses repurposed glucose meters for the detection of different analytes. Glucose meters have been used primarily for the detection of blood glucose. The Iyer group has been developing substrates for enzymes that release glucose when exposed to the enzyme. The released glucose can be detected using personal glucose meters. While previous research represents a significant advance, one major concern is that of background glucose present in blood and other matrices. To eliminate the effect of background glucose, we have developed an electrochemical assay to detect other molecules such as paracetamol or catechol in the presence of large amounts of glucose. The strips used for the assay were devoid of glucose oxidase or glucose dehydrogenase, and hence, glucose cannot get oxidized and will not pose a problem. The paracetamol/catechol gets oxidized directly on the surface of the strips and can be detected directly making the assay more robust. This assay was used to detect enzymes, influenza viruses, *S. pneumoniae,* and *E. coli.*

The novel assay uses non-glucose bearing sialic acid substrates. The non-glucose analyte is released when exposed to viral NA or intact viruses. The released non-glucose analyte can be

detected using repurposed glucose meters. Thus, personal glucose meters that were designed to assist diabetics and prediabetics monitor blood glucose can potentially be used to detect pathogens.

In chapter 3, the focus was on the detection of influenza virus using an immunoassay-based detection method. For the immunoassay-based approach biotinylated bivalent Zanamivir analogs as probes for influenza viruses were designed and synthesized. The compound was used in a "glycan" based sandwich assay; where glycans were immobilized on glass slides to capture strains of Influenza A H1N1, A/Brisbane/59/2007 virus and the biotinylated bivalent Zanamivir analog-labeled streptavidin complex was used as a reporter. This study indicated that glycans could be used for capturing and reporting influenza viruses and the biotinylated compounds could be used as probes for capturing and isolating influenza viruses from complex mixtures.

The work in chapter 4, we expanded the innovative concept described in chapter 2 to develop assays for blood disorders. As a first step towards this goal, synthesis of peptide substrates bearing electrochemically inactive molecules are required. In this chapter, the synthesis and characterization of novel catechol bearing substrate is described. We have designed a substrate that can directly measure the amount of thrombin in blood and the doctors can use this to adjust the dosage of anti-coagulants prescribed for high-risk patients. These compounds will be eventually used to develop assays that could potentially be used to monitor oral anticoagulant therapies and patients taking recombinant blood coagulation factors.

INDEX WORDS: electrochemical detection, glucose meter, paracetamol, glycosidase, influenza, *E. coli*, assured diagnostics, point of care detection.

DESIGN AND DEVELOPMENT OF SMALL MOLECULE BASED BIOSENSORS FOR DETECTION OF PATHOGENS

by

AMRITA DAS

A Thesis Submitted in Partial Fulfillment of the Requirements for the Degree of

Doctor of Philosophy

in the College of the Arts

Georgia State University

2018

DESIGN AND DEVELOPMENT OF SMALL MOLECULE BASED BIOSENSORS FOR DETECTION OF PATHOGENS

by

AMRITA DAS

Committee Chair: Dr. Suri. S. Iyer

Committee: Dr. George Wang

Dr. Gangli Wang

Dr. Kathryn Grant

Electronic Version Approved:

Office of Graduate Studies

College of the Arts

Georgia State University

December 2018

DEDICATION

I would like to dedicate this dissertation to my parents Dr. Sujit Das, Dr. Ila Das and my uncle, Dr. Tapas Saha. They have always supported and inspired me on this long journey. They have and will always stand by me through difficult times and have always inspired and encouraged me to overcome any difficulty that I have ever faced in my life. I would also like to thank my husband Susmit Majumder for his continued support and patience. I appreciate all my family and friends for all the good wishes and everything they have done for me and will be grateful forever.

ACKNOWLEDGEMENTS

I want to thank my committee members and my advisor Dr. Suri. S Iyer for his continued support at every point of my Ph.D. career. Dr. Iyer has provided me with an enormous amount of support, encouragement and learning opportunities during my Ph.D. Dr. Iyer is an excellent teacher who is kind, patient and was eager to help overcome any problems I faced during my journey. I will always be indebted to him for providing me with such an excellent education.

I want to thank my committee members Dr. George Wang and Dr. Kathryn Grant and Dr. Gangli Wang. Their advice and guidance were constructive.

I want to thank the Dr. Suri Iyer's Group, Dr. Dinh, Dr. Xiaohu Zhang, Dr. Abasaheb Dhawane, Dr. Bharat Gurale, Dr. Yang, Dr. Yun He, Dr. Xikai Cui, Joyce Sweeney, Dandan Liu, Jordyn Howard, Chadwick Dotson and Luong Pham for their help in research.

TABLE OF CONTENTS

LIST OF TABLES

LIST OF FIGURES

LIST OF ABBREVIATIONS

N, N Dimethyl formamide, DMF; Ethyl acetate, EA; Dichloromethane, DCM; Thin layer chromatography, TLC; Methanol, MeOH; Ethanol, EtOH; Triethylamine, NEt_3; Tetra butyl ammonium hydrogen sulfate, $TBHSO_4$; tert-Butyldimethylsilyl chloride, TBSCl; 4-Dimethylaminepyridine, DMAP; Sulphuric acid, H_2SO4,; Trifluoromethanesulfonic acid, TMSOTf; Sodium methoxide, NaOMe; Sodium hydroxide, NaOH; Sodium bicarbonate, Na_2CO_3; Hydrochloric acid, HCl; Glucose oxidase, GOD. Acetic acid AcOH; Acetyl chloride AcCl; Acetone CH_3COCH_3; Di-isopropyl ethylamine DIPEA; Ethyl acetate EtOAc; Dichloromethane DCM; Methanol MeOH; Triethylamine NEt_3; Sodium Methoxide NaOMe; Pyridine py; Palladium hydroxide $Pd(OH)_2$; Sodium hydroxide NaOH; Sodium thiosulphate $Na_2S_2O_3$; Hydrochloric acid HCl; Mercury(II) chloride $HgCl_2$ Dimethylamino pyridine, DMAP; Sodium bicarbonate, $NaHCO_3$; Trimethylsilylazide $TMSN_3$; Trimethylsilyltrifluoromethanesulfonate TMSOTf; Tri-Phenyl Phosphine PPh_3; Triflic Acid TFA; Di-tert-butyl dicarbonate $(Boc)_2O$; tert-Butyl alcohol t-BuOH; Cupric sulfate CuSO4; Thin layer chromatography TLC.

CHAPTER 1

1. INTRODUCTION

1.1 Biosensors

Biosensors can be thought of a sensing device that uses a biological agent. In the past, biosensors were considered to have only two components, first a biological agent capable of recognizing the analyte or changes in the analyte and second the transducer which converts the change into a measurable output. However, with advances in the biosensor field, sample preparation and output are also considered as unique parts of the biosensor. Some of the steps of the sample preparation involve filtration, centrifugation, selection using magnetic beads, etc. as shown in **Figure 1**. Biosensors can be designed to detect a plethora of biological parameters like enzymes, nucleic acids, antibodies, pathogens and changes in environmental conditions like changes in pH. A successful biosensor should be highly sensitive and selective towards the analyte to be detected, be independent of matrix effects and temperature and other environmental factors. The signal output should be accurate, reproducible and linear under a significant analytical range of the analyte. Potential applications of biosensors span from medical diagnostics, drug development, environmental sample monitoring, food industry, industrial waste control, defense, and security.

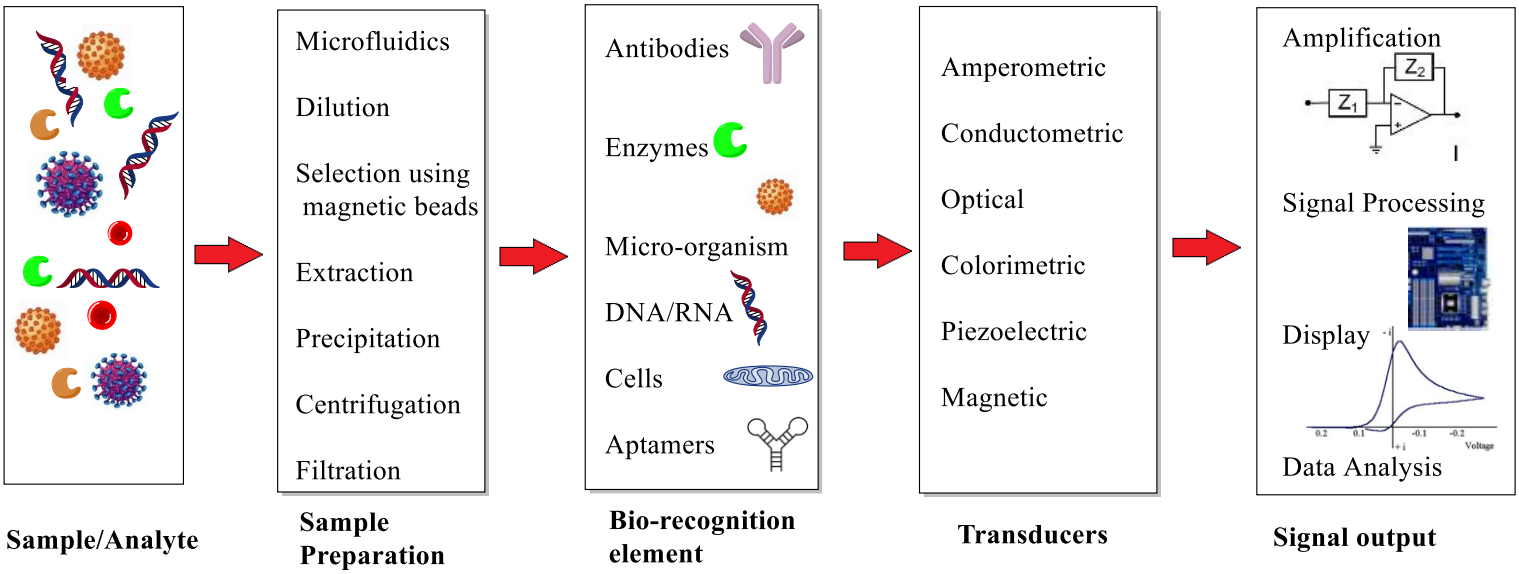

Figure 1. *Different components of a biosensor*

1.1.1 Economic impact

The field of biosensors is rapidly growing with new advances every year with an annual growth rate of ~ 9%. The estimated market for biosensors field is around 16.7 billion worldwide and is projected to double by 2022. Within the broad field of diagnostics, Point of Care (POC) testing occupies a niche subfield that has stringent requirements (discussed in detail later) and is expected to remain the largest application area for Biosensors reaching a projected US$11.5 billion by 2022 growing at a rate of 8.1% between 2017 (**Figure 2**) and 2022.[2]

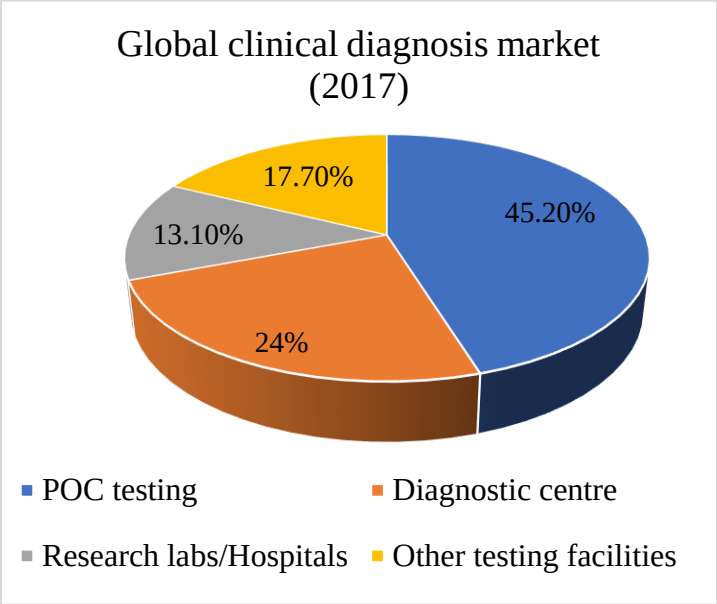

Figure 2. *Global clinical diagnosis market share 2017*
Adapted with permission[2]

1.1.2 History of biosensors

It has been well accepted that Professor Leyland Clark is widely regarded as the father of biosensors. In 1956, Professor Leyland Clark published a paper describing an oxygen electrode that measures oxygen concentration in blood. In 1962, at a New York Academy of Sciences symposium, he first elucidated the concept of biosensors where the first glucose sensor was described. He entrapped glucose oxidase enzyme on the Clark oxygen electrode using a dialysis membrane and then used this setup to measure glucose. This experiment led to increased research in this field where enzymes were immobilized onto electrodes, and the electrodes were transformed into powerful analytical tools which can be used to measure a variety of biological parameters. This laid the foundation for biosensor research.[3]

1916	First report on immobilization of proteins: adsorption of invertase on activated charcoal
1922	pH electrode was developed
1956	Invention of Glass electrode by Clark
1962	Amperometric biosensor for glucose developed by Clark; First description of biosensor
1969	Potentiometric biosensor: urease immobilized on ammonia electrode to detect urea
1970	Invention of Ion Selective Field-Effect Transistor (ISFET) (Bergveld)
1972	First commercial biosensor: Yellow spring instrument develops glucose sensor
1975	Divis first developed a microbial biosensor, detecting bacteria by measurement of alcohol. Invention of pO2/ pCO2 optode: a fiber-optic sensor by Lubbers and Optiz
1976	Glucose biosensor was integrated with artificial pancreas and marketed by Miles
1980	Fiber-optic pH sensor was developed for in vivo blood gases
1983	Surface Plasmon resonance (SPR) immunosensor was developed
1984	Use of electron mediators: Ferrocene was mediated with glucose oxidase for detection of glucose
1985	Roche (Switzerland) introduced the Lactate Analyzer LA 640 in which the soluble mediator, hexacyanoferrate, was used to shuttle electrons from lactate dehydrogenase to an electrode
1987	Launch of MediSense ExaTechTM blood glucose biosensor
1990	Launch of Pharmacia BIACore SPR based biosensor system
1992	i-STAT launches handheld blood analyzer
1996	Glucocard launched
1999	Use of quantum dots, nanoparticles nanowires, nanotubes, etc in biosensors
2018	Biosensor market globally accounts for $ 17 billion
2022	It is projected to grow to $25 billion with a robust growth rate of 9%

Table 1. *History of Biosensors*[3,5,7]

1.2 Classification

While a biosensor can be defined in several ways, a biosensor can be typically classified using 3 major parameters

i. *Based upon the bio-receptor interaction involving*: antibody/antigen, enzymes/ligands, nucleic acids/DNA, cellular structures/cells, or biomimetic material, etc.

ii. *Based upon the bio transducer*: electrochemical, optical, piezoelectric, thermometric, magnetic, micromechanical, etc.

iii. *Based upon the mode of use*: point of care, high throughput.

1.2.1 Bio-receptor interaction

Some of the significant biorecognition molecules are presented below.

1.2.1.1 Antibody/antigen interaction

There are several biosensors that use the antibody/antigen recognition element. The dissociation constants for antibodies are low around 10^{-9}M, which results in an irreversible complex formation. An example of a commercially available antigen/antibody-based device is the pregnancy kit. These types of ELISA based immunosensors are very robust and are used globally for the detection of a variety of diseases like Malaria, HIV, STDs.[5] However, despite their prevalence in biosensors, there are various drawbacks for using antibodies as biorecognition element in biosensors due to their high molecular weight, low stability and presence of disulfide bonds which makes it very difficult to handle. One way to overcome these include the use of engineered recombinant binding fragments like Fab, Fy scFv or VH or VHH domains. Another approach involves the engineering of small families of antigen binding proteins (AgBP), which

are approximately 100 amino-acid residues which are more stable, disulfide bonds and these bind specifically to a specific antigen. These molecules are selected using techniques such as phage display, ribosome display, yeast display or mRNA display.[6-10]

1.2.1.2 Enzymes/ligands

Enzymes are a very popular bio-recognition element for the development of biosensors owing to their specificity. The most successful biosensor is the glucose meter, which uses an immobilized enzyme and an electrochemical output. Almost 80% of the biosensors market is captured by glucose meters. Glucose meters use glucose oxidase or glucose dehydrogenase for the detection of glucose. The main reasons for the high use of enzymes are mainly the catalytic power of enzymes, it can catalyze many reactions, it can detect different types of analytes, can be used easily with various transducers and mainly since the enzymes are not consumed, it can be used continuously for a longer time. If enzymes are used as a bio-recognition element, lower limits of detection can be easily achieved. However, one of the drawbacks, however, is that the lifetime of the sensor is dependent on the stability of the enzyme.[10-15]

1.2.1.3 Nucleic acid interactions

Biosensors that employ nucleic acid interactions are referred to as genosensors. The recognition process is based on the principle of complementary base pairing property of adenine: thymine (A-T) and cytosine: guanine (G-C). Typically, a complementary sequence to the target sequence is synthesized and immobilized on the surface of the sensor. If the analyte contains the complementary target sequence, the binding event triggers a change which is detected by the transducers and converted into a readable output. The popular, readable outputs for nucleic acid-based sensors is either optical or electrochemical.[4, 7, 10]

1.2.2 Transducers

There is an alternate method of classifying biosensors i.e. by their transducers; the transducers are the detecting or the sensing element of the biosensors. The actual definition of a transducer is a device that converts one form of energy into another. Therefore, the transducer can detect a perturbation in the chemical, electrical or physical environment of the analyte and convert that change into a readable output. The biosensors can be divided into the following based on their transducers:

1.2.2.1 Electrochemical sensors

These types of sensors are based on redox chemical reactions. They use current flowing through the system (amperometric), the difference in electrical potential between the two electrodes (potentiometric) or change in the conductance (conductometric) of the system due to the presence of the analyte to quantify the amount of analyte. These are fast and highly sensitive can detect sub-nanomolar or lower concentrations of the analyte. Another significant advantage is that it can measure samples which are turbid/opaque and provide a quantified output. One of the most successful biosensors, i.e. the glucose meters fall in this category.[4-7]

1.2.2.2 Optical sensors

These biosensors employ parameters like light absorption, fluorescence, luminescence, reflectance, Raman scattering and refractive index to quantify analytes in a sample. Fluorescence is one of the most measured optical parameters. There are several advances in the detection of fluorescence and sensors that can detect intensity, decay time, quenching efficiency and luminescence energy transfer. These optical sensors have been automated and can detect thousands of samples in a day. Surface Plasmon Resonance (SPR) based sensors are also widely applicable.

This is a label-free flow-based technique exploiting electron charge density waves called plasmons. These plasmons are generated when light strikes an electrically conducting surface at the interface between two media. The resonant angle of these waves depends upon the refractive index of the medium, this, in turn, is dependent upon the local mass density of the surface. When the surface of the sensor is modified by the capture of the analyte by the antibodies on its surface, it changes the resonant angle. This change in the resonant angle can be quantified to the concentration of the analyte.[15-16]

1.2.2.3 Piezoelectric sensors

These are sensors that can measure small changes in the mass, the principle of these sensors relies on the use of piezoelectric materials that can be made to oscillate at a specific frequency by application of electric signals. The frequency of the oscillation is dependent upon the mass and the frequency of the electrical signal. When the mass of the crystals changes due to binding with the analytes that change in mass is directly related to the amount of analyte in the sample. The piezoelectric immunosensors have been very successful in the detection of HIV in samples.[14]

1.2.2.4 Thermometric/ calorimetric sensors

These sensors involve the measurement of heat that is generated in an enzymatic reaction. It utilizes thermistors that transform heat generated (or lost) during a reaction into an electrical signal. Examples of these types of sensors include enzyme thermistor, thermal enzyme-linked immunosorbent assay, Isothermal calorimetry-based assays, etc.

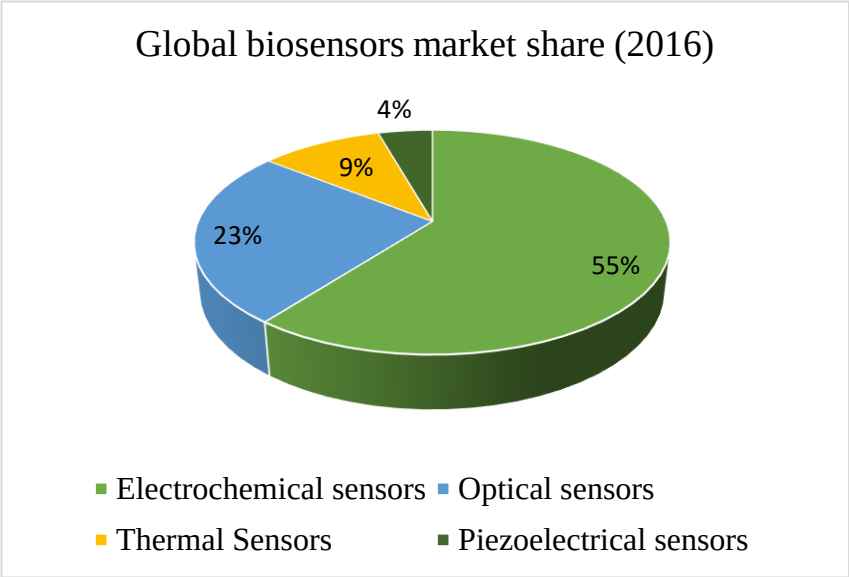

Figure 3. *Global biosensors market share 2016.*
Adapted with permission.[2]

The global market breakdown for these sensors is provided in **Figure 3**.

1.2.3 High throughput detection technology

Another way that biosensors can be classified is based upon their instrumentation. High throughput screening techniques for biosensing technology is equipped to screen a large number of analytes via the methods of automation, multiplexing and involves large-scale data analysis. These are highly sophisticated high-throughput machines capable of automation that is rapid, accurate and can measure a huge number of samples in a single day. These technologies are usually highly expensive and require highly skilled professionals to use. High throughput detection is mainly useful when the sample contains many non-target micro-organisms and other matrix effects, which imparts, low specificity and poor detection limit to a biosensor. [16]Thus, there is a need for integrated processes that is able to non-selectively concentrate the target analyte (amplification techniques like PCR, etc) or separate the target analyte from the non-specific sample matrix using filtration or employment of antibody-coated paramagnetic beads. These integrated

processes also possess the multiplexing capability. Multiplexing is an ability to detect huge number of analytes simultaneously using either a number of labels at the same time for detection while using a multichannel detector to detect the various analytes (Label multiplexing) or by the use of a large number of immobilized probes on separate sites detected using a single channel detector (Spatial multiplexing). Examples of this include the microarray technology.[17-20] The main success of the high-throughput technology is the ability to detect thousands of targets in a single assay and is being increasingly used by the pharmaceutical community to isolate potential drug targets. Some of the most successful HTS techniques are discussed below:

1.2.3.1 Microarray technology

Microarrays consist of a collection of analytes immobilized onto solid support so that each unique analyte forms a tiny feature, called a 'spot' or 'target.' These target analytes are then analyzed using a probe which after recognition gives out an output. Multiple microarray platforms exist, including printed glycan arrays, protein arrays, double-stranded DNA and oligonucleotide arrays, in situ-synthesized arrays, high-density bead arrays, electronic microarrays, and suspension bead arrays. Basic features of a microarray include an immobilized probe onto a solid support using mainly a chemical reaction in a distinctive pattern as spots. Thousands of probes can be immobilized on a single microarray plate. The unknown target is fluorescently labeled and then hybridized with the probes. The hybridization of the probe and labeled target leads to an increase of fluorescent intensity compared to background and then measured using a fluorescent reader. [21]

1.2.3.1.1 DNA microarrays

The principle for DNA microarray is a hybridization between the two strands of a DNA. A single strand of DNA (cDNA), oligonucleotides, etc are immobilized on the solid support, and fluorescently labeled targets are added. The hybridization of the complementary sequences results

in the increase of fluorescence intensity compared to the background. DNA microarrays are quantitative. The fluorescence intensity of the probes can quantitatively determine the amount of hybridization or the DNA. DNA microarray technology can be used for comparing genomic hybridization, i.e. for assessing genome content in closely related species, gene expression profiling, by measuring the expression level of thousands of genes in samples exposed to different pathogens or after undergoing several post-translational modifications or at different stages during disease prognosis.[17-18]

Affymetrix GeneChip is one of the successful DNA microarray platforms that are commercialized; these can be used for gene expression profiling, whole genome transcriptome mapping, etc.

Manufacture of GeneChip probe array

The GeneChip array is a 5 square inch wafer which is immobilized with DNA samples. At first, the wafer is modified covalently with a silane reagent, to get a surface layer of hydroxyalkyl groups. Next linker molecules with photo-labile protecting groups are then attached to these hydroxyalkyl groups. This layer now can be spatially activated by light. A photolithographic mask set is next designed which contains the array design and pattern to immobilize the probes at a specific position by either permitting or preventing the transmission of ultraviolet light. This ensures the oligonucleotide synthesis at precise locations of the quartz wafer thereby creating the microarray. Ultraviolet light removes the protecting groups at defined areas, and a single nucleotide is washed over the deprotected groups and undergoes coupling. This deprotection and coupling step is repeated until specific full-length probes (25-mers) are immobilized at specific regions of the quartz wafer. Using algorithms for designing the photolithographic mask ensures

that significantly less than 100 deprotection-coupling cycles are needed to synthesize the 25-mer sequences. [15]

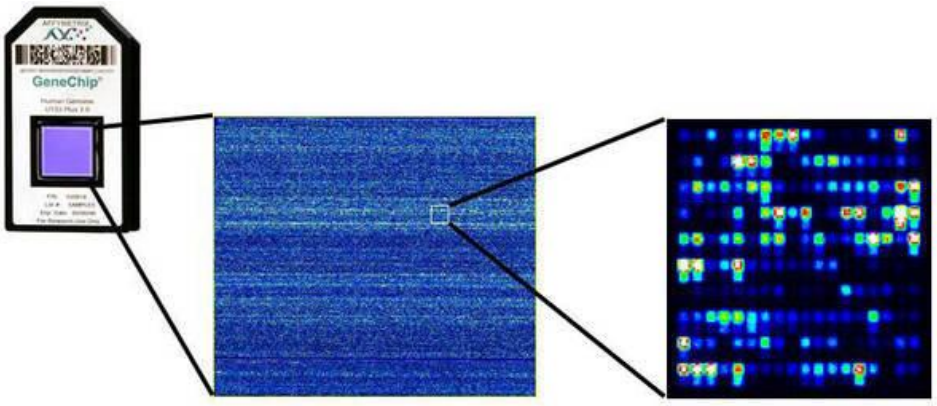

Figure 4. *GeneChip array probe with DNA microarray.*
Reprinted with permission[14]

GeneChip array analysis

The nucleic acid containing the target sample/analyte is selectively amplified and then undergoes reverse transcription and labeling of the sample. The labeled sample is injected into the GeneChip probe array and allowed to hybridize overnight. The stained array then is analyzed using Affymetrix GeneChip scanner, which reads the fluorescent intensity at each spot. To analyze the fluorescent readout two types of probes are used i) perfect match probe (PM), this probe has a complete complementary sequence to the target sequence ii) mismatch probe (MM) probes with a single mismatch to the target. Another set of probes are present which bind to the specific biotinylated oligonucleotide sequence added to the target labeled sample; these serve as controls. Based upon the fluorescent intensity pattern for each of the probes in the array the data is analyzed to give the gene expression studies, Single nucleotide polymorphism (SNP) profiling, gene mapping etc.[14-17]

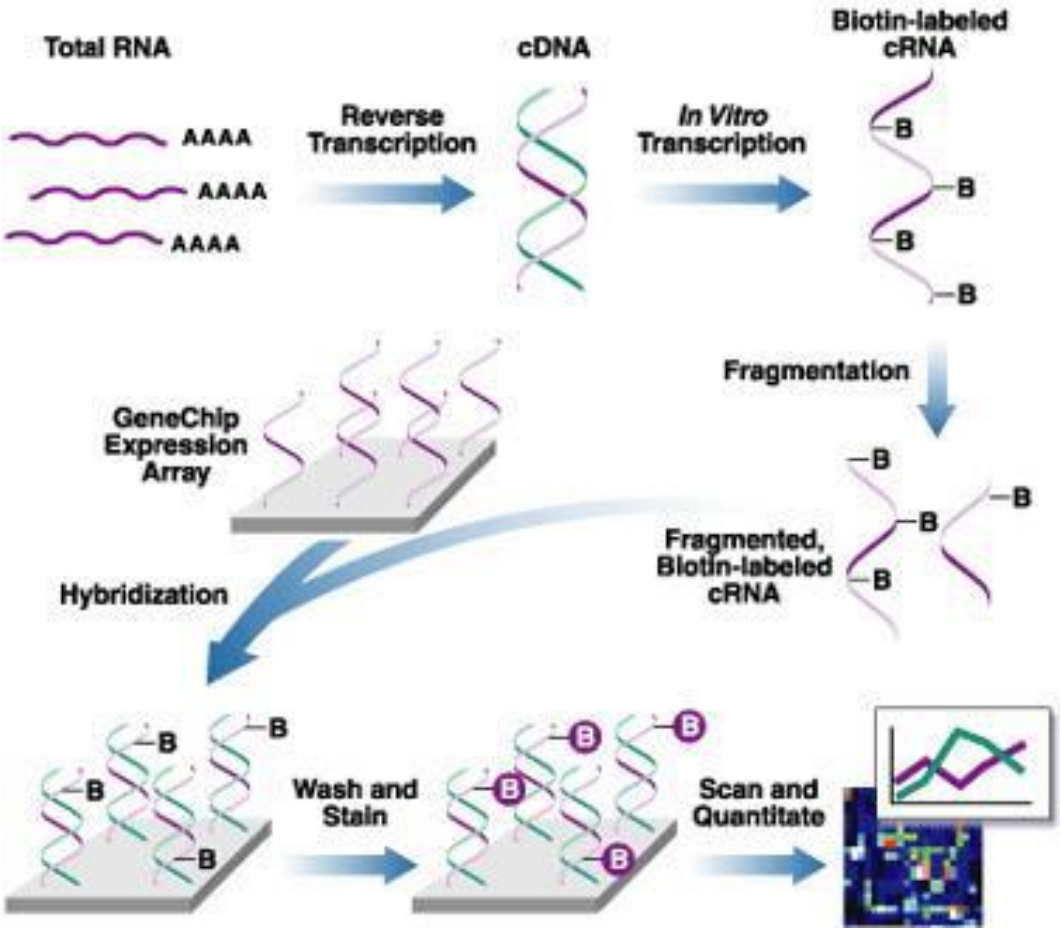

Figure 5. *DNA microarray analysis using Affymetrix GeneChip*
Reprinted with permission[15]

1.2.3.1.2 Protein/peptide microarrays

Protein microarrays were developed in early 1980 for profiling antibody-antigen interactions. They are now used for proteomic analysis. Protein microarrays have demonstrated numerous applications for studying biomarker discovery, protein-protein interaction, protein-ligand profiling, kinase activity and posttranslational modifications of proteins. Recently protein microarrays have been widely applied as a promising proteomic technology with great potential for protein expression profiling, biomarker screen, drug discovery, drug target identification and analysis of signaling pathways in health and disease. Based on the different detection techniques,

protein microarray detection techniques can be also classified as being label-based and label-free. The labeling strategies, such as fluorescent, chemiluminescent and radioactive labeling, have synthetic challenges, multiple label issues and may exhibit interference with the binding site and high background interference. Therefore, development of sensitive, reliable, high-throughput, label-free detection techniques is now attracting significant attention. Label-free detection techniques monitor biomolecular interactions and simplify the bioassays by eliminating the need for secondary reactants. These techniques include surface plasmon resonance mass spectrometry (SPR–MS), backscattering interferometry, UV fluorometry, surface enhanced laser desorption ionization time of- flight mass spectrometry (SELDI-TOF-MS), etc.[14, 20-25]

1.2.3.1.3 Glycan microarrays

The glycan microarray was first developed in the early twenty-first century for high throughput detection of glycan-binding proteins (GPB) and investigation of the biological role of glycans. The glycan microarray analysis has become one of the most sought-after detection strategies for host-pathogen interactions. Infectious diseases mainly use a cell surface glycan to gain entry inside the cell and subsequent invasion and immune response. The use of glycan libraries to detect and characterize pathogenic GBP is highly predominant. The arrays are created by immobilizing carbohydrates that are either derived from natural sources or obtained by chemical synthesis. The immobilization methods include non-covalent methods involving nitrocellulose and oxidized polystyrene using hydrophobic adsorption methods or by using covalent ligation methods like thiol coupling, cycloaddition, amine-functionalization, maleimide functionalization, etc. The detection of the target can be done using labeled or label-free ligands.[24-25] The labeled ligands include fluorescently labeled lectins and antibodies. Labeled streptavidin–avidin interactions are also used for binding and further structure elucidation of the glycan. The

label-free methods for glycan microarray include Surface Plasmon Resonance and Mass Spectroscopy. The glycan microarray technology has been used to detect infectious pathogens such as influenza using Hemagglutinin (HA) which bind to glycans containing sialic acid. The different serotypes of HA bind to the sialic acid-containing glycans differently enabling the profiling of influenza HA based upon the binding patterns.[27] This binding information has led to the development of several vaccines and other novel methods of therapy and detection. This method has also been applied to other pathogens where HIV-antibody 2G12, GPI from Plasmodium falciparum, isolated glycans from *Schistosoma mansoni, Closteridum diffile* has been investigated to determine promising glycan based epitopes.[28]

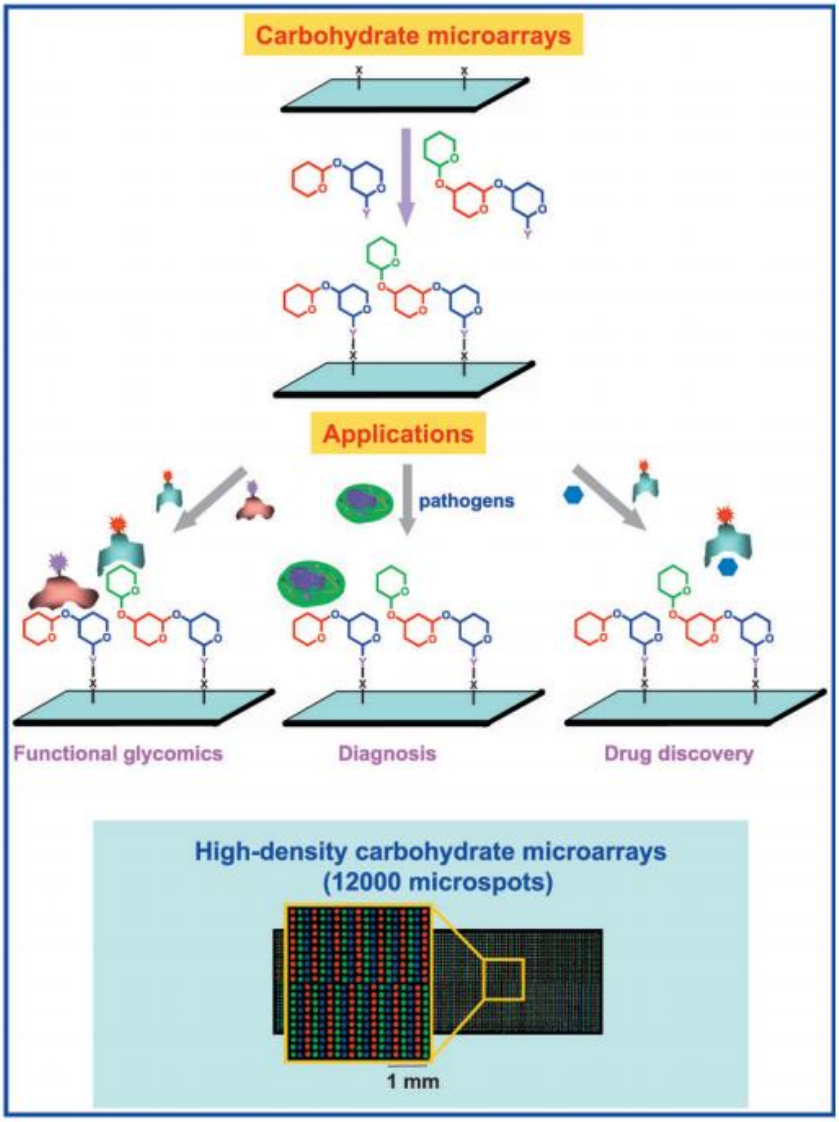

Figure 6. *Glycan microarrays, generated by different strategies, used for detection of a binding pattern of pathogens or antibody using fluorescent intensity*
The figure is taken from the publisher with permission.[23]

1.2.3.1.4 ***Polymerase chain reaction***

Polymerase chain reaction (PCR) is a highly sensitive and specific technique that can amplify and produce millions to billions of copies of a gene of interest in a very short amount of time. These gene copies can then be further analyzed for sequencing, cloning, and further analysis. An added advantage of qRT-PCR over PCR is that qRT-PCR can quantitatively measure the

amount of gene sequence and can be used to measure the gene expression levels in tumors or amount of gene present in a certain analyte containing a microbe, bacteria or viruses.

The advent of new strains of an infectious virus or detection of uncultivated pathogens or specific diagnosis of a certain pathogenic strain can be easily done using PCR methods. Owing to the high level of sensitivity of PCR, detection of the viruses can be done at very early stages of infection thereby giving physicians enough time to mitigate the disease. Using qRT-PCR, it is also possible to measure viral load and monitor and adjust the dosage of treatment. This is a very important part of the HIV treatment regime where the dose of the anti-retroviral drugs are adjusted according to the levels of viral load in blood.[29-30]

The essential components of a PCR include

i) *Template DNA*: Template DNA containing genomic DNA sample from a patient can be used in the single or double-stranded form. Closed circular DNA templates are amplified slightly less efficiently than linear DNAs. Ideally, PCR requires only a single copy of the target sequence as a template for the amplification.[34]

ii) *Oligonucleotide Primers:* A pair of synthetic oligonucleotides should be short, single-stranded, and complementary to the target. Standard reactions contain 0.1 - 0.5μM of each primer, which is sufficient for 30 cycles of amplification. Higher concentrations of primer increase the chances of mis-priming and may lead to non-specific amplification.[35]

iii) *Thermostable DNA polymerase:* A thermostable DNA polymerase, which can withstand the denaturation temperatures (94-95 ºC), is essential to catalyze the template-dependent synthesis of DNA. Earlier, Klenow fragment of

Escherichia coli pol I was used17. However, this enzyme being unstable at high temperature, had to be added after every denaturation step. Now DNA polymerase, Taq DNA polymerase isolated from thermophilic bacterium Thermus aquatics which is stable even at higher temperatures are used.

iv) *Deoxynucleoside triphoshates (dNTPs):*

- dCTP, Deoxycytidine triphosphate
- dTTP, Deoxythymidine triphosphate
- dATP, Deoxyadenosine triphosphate

dGTP, Deoxyguanosine triphosphate.

These dNTPs are available commercially and supplied as pyrophosphate free mixtures. These dNTPs are utilized during the amplification steps of PCR to form the target DNA sequences.

Amplification of the target sequence involves the following three steps:

1. Denaturation of the template at 95^0C heat.
2. Annealing of the oligonucleotide primers to single-stranded target sequences.
3 Extension of the annealed primers using thermostable DNA polymerase.

Denaturation

The first stage of PCR involves denaturation to convert the double-stranded DNA sequence to a single strand. For this process, higher temperatures are required the DNA sequences from their complementary sequences. PCRs catalyzed by Taq polymerase, the process of denaturation is carried out at 94-95 ºC, which is the highest temperature the enzyme can withstand for 30 or more cycles without being damaged. During the first cycle, denaturation is carried out for 5 minutes to ensure complete denaturation of the long molecules of template DNA. Higher temperatures may

be required to denature templates containing higher amounts of G+C. In addition, longer the DNA templates, greater is the denaturation time required.

Annealing

As the temperature is reduced, the single-stranded oligonucleotide sequences then combine to the available complementary probes (primers) and become double-stranded sequences which can undergo extension. The design of the primers is essential for successful PCR. Poor primer design leads to high non-specific amplification of unwanted DNA segments. Annealing temperatures range from 55-65 ºC depending on the primer sequence and length. The annealing temperature is also critical. When a high annealing temperature is used the primers will not anneal properly and the amount of DNA thus amplified will be too low for detection. At low annealing temperatures, there is a high amount of nonspecific annealing. This results in amplification of unwanted segments of DNA compared to the target sequence.[35]

Extension

DNA polymerase catalyzes the extension of oligonucleotide primers and thereby a new strand, having sequences complementary to template strand is synthesized. The optimal temperature for DNA synthesis may vary slightly depending on the DNA polymerase used. When Taq polymerase is used, the ideal temperature for DNA synthesis is about 72-78 ºC. Taq polymerase can insert about 2000 nucleotides every minute at this temperature. Leading to the formation of a very high amount of amplified target DNA sequence.[34,35]

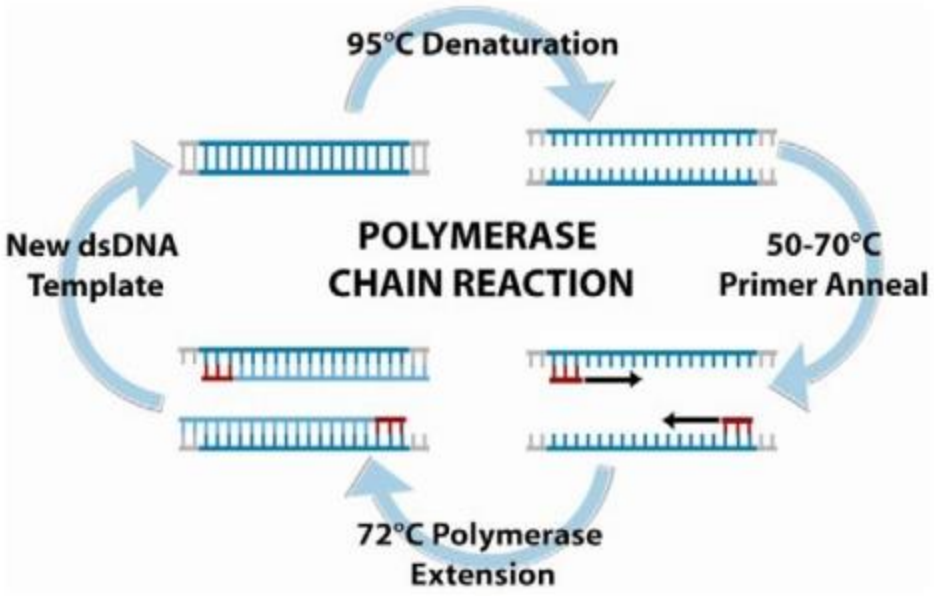

Figure 7. *Basic steps of Polymerase Chain reaction*
Reprinted with permission [29]

1.2.3.2 Surface Plasmon Resonance Spectroscopy

Surface plasmon resonance (SPR) was first demonstrated by Otto in 1968.[19] Biacore® (GE Healthcare) first commercialized the technology in 1990[19]. Since then SPR has been widely used for bimolecular interaction applications like binding studies, kinetic analysis of biomolecular interaction, antigen-antibody interaction, etc.

When a plane polarized monochromatic light strikes the interface of two media one with a lesser refractive index, then a part of the light is refracted and partly reflected in the same media. But when the angle of incidence becomes greater than the critical angle, then all of the light is reflected in the media, and no refraction occurs that is called total internal Reflection (TIR).[19,20]

SPR consists of a glass prism coated with Au film. This Au film contains free conducting electrons which oscillate at certain frequency and are called plasmons. The plasmons confined to the surface is called surface plasmons. These plasmons extend 500nm from the surface and are referred to as the detection zone. When the incident angle of the light beam is larger than the

critical angle, and it matches the resonant angle, surface plasmon resonance occurs. So when this happens, the light is absorbed by the detector at a certain incident angle.[21]

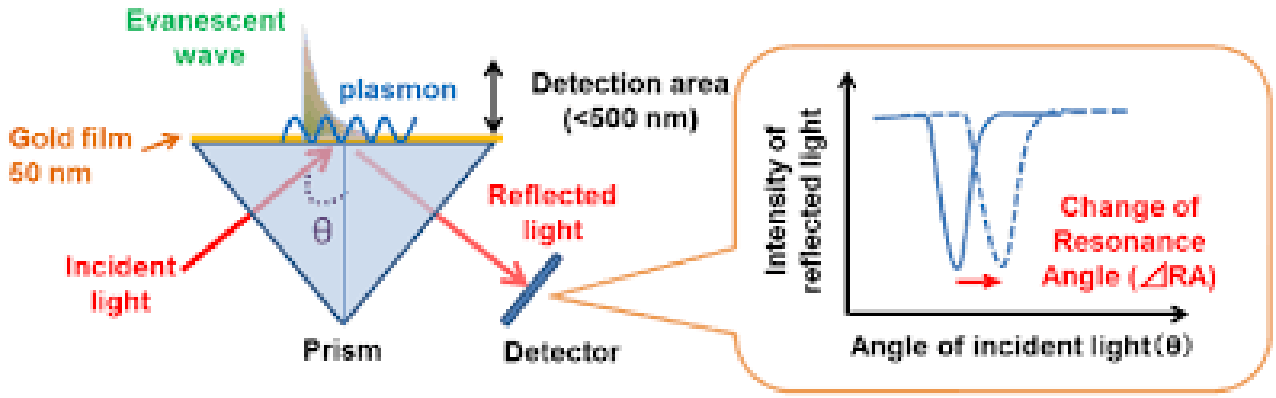

Figure 8. *Working principle of Surface Plasmon resonance*
Reprinted with permission[21]

When there is a change in the composition of the surface Au layer due to any binding by any target analyte then the resonance does not occur at the same angle of incidence, so there is a shift in the resonance angle, and this is known as SPR shift. This shift in the resonance is directly proportional to the binding incident with the analyte or the change in mass at the Au surface due to binding.

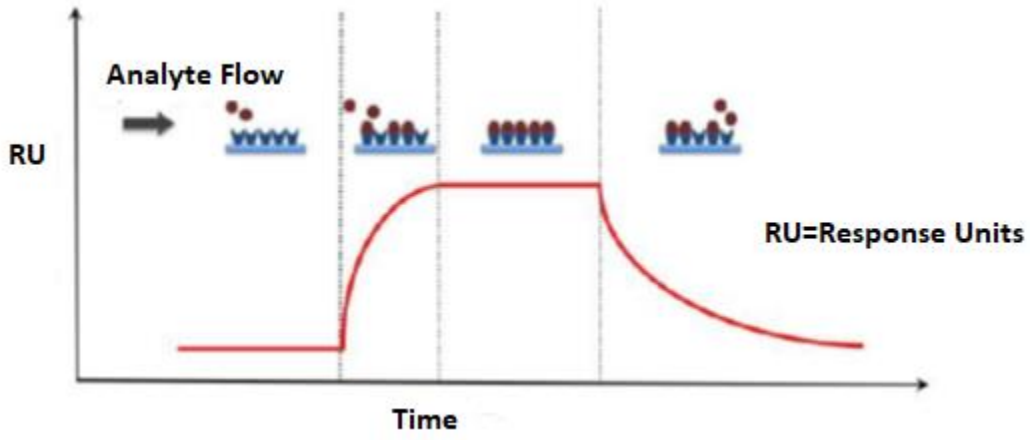

Figure 9. *Detection of binding events for Surface Plasmon Resonance.*
Reprinted with permission[21]

1.2.4 Point of Care (POC) technology

The growth of the population and as the burden of people at the hospitals and clinics increasing day by day, there has been an urgent need for the development of rapid accurate robust and easy to use devices at home. These are highly sought after in the health care industry as it allows the de-centralization of medical treatment from hospitals to the patients, which is ushering in a new change in the economic landscape of the diagnostic market. Point of care (POC) devices provide real-time results which are fast, accurate, sensitive at the convenience of home. Conventional analyses performed in a hospital or clinic are generally expensive, time-consuming and require skilled professionals to perform them.

In contrast, POC systems are simple easy to use, affordable and can be used in a poor resource setting, reducing the cost of analysis, and providing privacy of home. This type of devices are also highly significant for developing countries where though the burden of the disease is high, but they severely lack modern laboratory or fully automated and sophisticated medical testing facilities and trained personnel. POC devices require little or no resources and can provide fast and accurate results which helps a doctor diagnose and save thousands of lives every day in those poor resource areas.

An immense effort is being made to design and develop POC devices for the diseases that are of global health importance. The global market for point-of-care diagnostics is expected to reach $27.5 billion by the end of 2018 at an estimated compound annual growth rate (CAGR) of 9.3% from 2013–2018.[3] It is one of the most rapidly growing areas of research and development and in the past 10 years several new POC devices have been introduced in the market. The design of each POC is dependent upon the need of the user and the clinical setting, but some of the salient features include portable, affordable and easy to use. More recently WHO has laid out specific

design criteria and guidelines for the developers of POC devices and these are called as **ASSURED** criteria. For a POC biosensor to meet all the **ASSURED** criteria it must be **Affordable** by the people who are affected by the disease or the consumers who will buy the device or the sensor. **Sensitive**, meaning false negatives should be minimal. **Specific**, the device should only test positive for the desired pathogen or micro-organism hence low false positives. **User-friendly**, the tests must be simple enough that it can be done in a low resource setting, out of a hospital or clinic. **Rapid and Robust**, the test should ideally give a result within 15 minutes or less and should be stable under different environmental conditions. **Equipment free** such that it does not require any expensive machine for the output and can be stored in a very low resource setting. **Deliverable** to the end consumers in a hassle-free manner. Meeting all these criteria is a tall order, and most often there are trade-offs, but upon careful design consideration and proper optimization, these criteria can be achieved.[28] A comparison of the different tests available for Influenza virus is done based on the ASSURED criteria by WHO in the following table (Table 2)

Several prospective label-free biosensors, such as electrochemical, surface plasmon resonance (SPR), white light reflectance spectroscopy (WLRS), etc., have been developed, and are being used for improved POC. Complementary technologies, e.g., microfluidics, lab-on-a-chip technologies, system integration, device automation, and signal readout, are providing the desired impetus for continuous improvements in POC.[17]There is also a huge unmet need for quantitative and multiplex POC.

ASSURED Criteria	Detection methods			
	Culture	**Nucleic Acid**	**Fluoro/ Colorimetric**	**Antibody**
Affordable	No, requires laboratory equipment	No, Cepheid and Biomeriux sell point of care system but cost thousands of dollars.	No, an instrument costs thousand and the reagents are expensive.	Yes, however, cost varies. Typical cost is ~ 18-20 $ per test. e.g., Quidel Flu A&B test is 450 $ for a pack of 25. However, the cost of these tests is coming lower.
Sensitive	High	High	High	No, very low sensitivity (20-80%), especially at low concentrations.
Selective	High, can distinguish between live and dead virus.	High, however, requires the correct primers and cannot distinguish between dead and live virus	Medium/High but cannot distinguish between live and dead viruses.	High, > 90%, however, cannot distinguish between live and dead virus.
Rapid	No, requires days.	No, sample preparation takes hours, but newer systems are integrated to yield results in 1-2 hours.	60 minutes.	15 minutes
Robust	No, requires several reagents, which are not stable	Yes/No, some reagents may require refrigeration	No, requires refrigeration.	Yes/No, depends on antibody stability. May require refrigeration
User friendly	No, requires trained personnel.	Yes/No, newer systems are becoming simpler, but still, require trained personnel.	No, requires trained personnel.	Yes
Equipment free	No	No	No	Yes
Deliverable to end users	No, requires a laboratory.	No, requires space	No, requires space	Yes, small footprint, portable

Drug susceptibility	Yes, however, takes days	Yes, however, takes days	Yes, but requires hours	No

Table 2. *A comparison of different tests for influenza virus based on the ASSURED criteria.*

1.2.4.1 Lateral flow Assays

Lateral flow assays (LFA) are simple in-expensive POC devices that can detect the presence of a target analyte in a sample matrix. These are commonly used for at home testing. One of the most common and successful LFA is the pregnancy tests. Apart from the pregnancy tests, Lateral flow assays determine various different infectious pathogens like HIV, Malaria, Influenza. Some LFA based cardiac marker POC device was recently approved by the FDA.[53-55] The Lateral flow devices are very fast inexpensive and can be used in very low resource settings. These can detect biological analytes in urine, saliva, sweat serum, blood, plasma, etc.

The principle behind the Lateral flow assay is capillary action. The sample containing the target analyte moves through the test strip and interacts and binds at the site where the proteins are immobilized. The binding of the target analyte to the immobilized proteins can be detected optically.

The main components of a Lateral flow device are the following:

Sample application pad*:* The sample application pad consists of cellulose and/or glass fiber and sample is applied on this pad. The sample application pad is to ensure the smooth transport the sample to other components of the lateral flow test strip (LFTS). Sample pad should be capable of transportation of the sample in a smooth, continuous and homogenous manner.

***Conjugate pad*:** The conjugate pad contains the labeled biorecognition component. The conjugate pad releases the labeled when the solution moves through it. The conjugate pad is mainly made of glass fiber or cellulose.

***Nitrocellulose membrane*:** The nitrocellulose membrane is the most critical component of the lateral flow assay. The sensitivity of the LFA is determined by the nitrocellulose membrane. The control and the test lines are present on the LFA. The proteins are immobilized on the nitrocellulose membrane, and the pore size of the membrane should be chosen very carefully based upon what proteins need to be immobilized. The nitrocellulose membrane also should be treated properly to avoid any nonspecific binding. The sensitivity of the assay is affected by the wicking rate of the nitrocellulose membrane. Proper dispensing of bioreagents, drying and blocking play a role in improving the sensitivity of assay.

***Adsorbent pad*:** The adsorbent pad as the name suggests absorbs the excess solution from the analyte while maintaining the proper flow rate and preventing any backflow. It is usually made of cellulose.

All these components are fixed or mounted over a backing card. This backing card serves as a support and makes the strip easier to handle.[31]

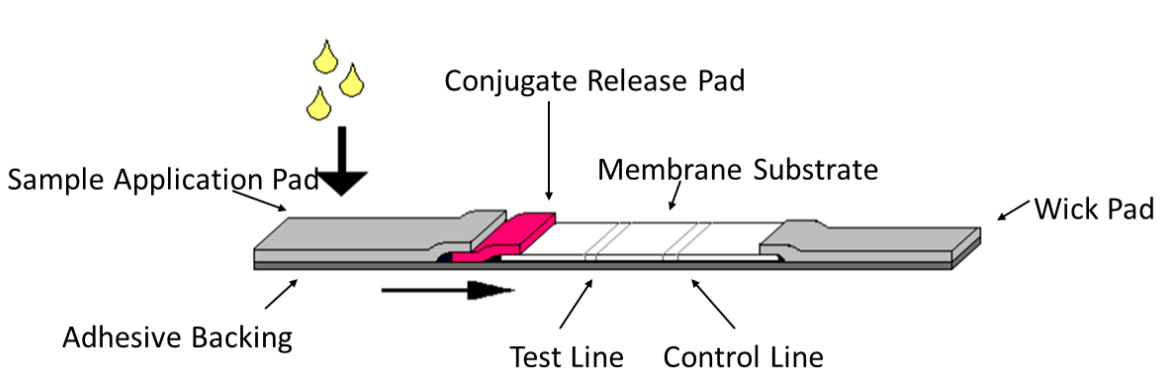

Figure 10. *Different parts of Lateral Flow Assay (LFA).*

(Reprinted with permission from MDPI Journal)[17]

The bio-recognition element of the LFA is either antibodies (lateral flow immunoassay; LFIA) or amplicons formed during the PCR (Nucleic acid lateral flow immunoassay; NALFA). The LFIA is an antibody-based technique, specificity and sensitivity may be affected by other chemicals with similar structures, leading to false positive results. The sensitivity of assays is limited by the κ_d (dissociation constant) of the antibody-antigen conjugate and by the colorimetric read-out. The colorimetric labels employed for LFIA are usually colloidal gold nanoparticles it can be prepared in the laboratory at low cost. It has an intense color and requires no extra steps for visualization. The stability of the gold nanoparticles are high in both liquid and dried forms. Another promising label is latex, it can be developed in multiple colors, and can be easily used in multiplexed format Latex based labels can also be tagged with a variety of detector reagents such as colored or fluorescent dyes, and magnetic or paramagnetic components. Fluorescent dyes or paramagnetic particles cannot be detected directly by the naked eye and requires fluorescent and magnetic strip readers. Quantum dots and carbon nanotubes have also shown potential as labels for LFA and has also exhibited 10-fold lower detection limit than that of gold-based techniques. In recent years, there have been major advances in LFA development.[17,29] This includes novel signal-amplification strategies, applications of new labels, improved quantification systems, and simultaneous detection. Some of the new strategies used to enhance the signal from the colloidal gold nanoparticles (GNPs) have adopted silver enhancement technology or combinations of GNPs with an enzyme (such as horseradish peroxidase), which results in catalytic amplification of the signal.[29]

1.2.4.2 Nucleic Acid-based assays:

Nucleic acid amplification is a precious molecular diagnostic tool for application-based fields, such as clinical prognosis, infectious diseases diagnosis, gene cloning, and industrial quality control. Polymerase chain reaction (PCR) was the first nucleic acid amplification method.

Further research led to the development of alternative nucleic acid amplification methods such as loop mediated isothermal amplification (LAMP), nucleic acid sequence-based amplification (NASBA), strand displacement amplification, multiple displacement amplification, rolling cycle amplification (RCA). Mostly all these methods do not require thermal cyclers and are isothermal based methods. In principle, they are much more complex and require several different primers than that of PCR, but are faster, more sensitivity and can be used under low resource setting compared to PCR.[10,31-33]

Parameter	PCR	LAMP	3SR	SDA	LCR	NASBA	RCA
High sensitivity	<10	<10	10	10	<10	10	<10
High specificity	+	+	+	+	+	+	+
Allow quantification	+	+	±	±	−	±	−
Live versus dead microorganisms	+	+	+	−	−	±	−
Commercial availability	+	−	±	±	−	−	−
Linear dynamic range	6-7	6	7	ND	ND	7	ND
Multiplexity	+	−	+	−	+	+	+
No. of enzymes	1	1	2-3	2	2	2-3	1
Primer design	Simple	Complex	Simple	Complex	Simple	Simple	Complex
Tolerance to biological compounds	−	+	−	−	−	−	−
Need to template denaturation	+	−	+	+	+	+	−
Denaturing agents	Heat	Betaine	Rnase H	Restriction enzymes; bumper primers	Helicase	Rnase H	Ø29 DNA polymerase
Product detection method	Gel electrophoresis, ELISA, real time	Gel electrophoresis, turbidity, real time	Gel electrophoresis, ELISA, real time, ECL	Gel electrophoresis, real time	Gel electrophoresis, real time	Gel electrophoresis, ELISA, real time, ECL	Gel electrophoresis, real time

PCR: Polymerase chain reaction, LAMP: Loop-mediated isothermal amplification, SR: Sequence replication, SDA: Strand displacement amplification, LCR: Ligase chain reaction, NASBA: Nucleic acid sequence based amplification, RCA: Rolling circle amplification, DNA: Deoxyribonucleic acid, ELISA: Enzyme-linked immunosorbent assay, ECL: Electrochemiluminescent

Figure 11. *Comparison of the different isothermal nucleic acid amplification methods.* Reprinted with permission.[10]

1.2.4.3 Electrochemical assays

Biosensors that use amperometric detection methods are gaining prominence since the development of the highly successful ubiquitous glucose meters. Amperometric biosensors involve the conjugation of enzymes and the electrochemical reaction for their output. Glucose, hydrogen peroxide, lactate levels can be determined by using the enzyme coupled electrochemical setup. The biggest success story of POC biosensors is glucose meters. Glucose biosensors account for about 80% of the biosensor market.[2]

Diabetes is a worldwide public health problem, and currently, the diabetes patients are still the leading driver of the POCD market. The diabetes patient needs to measure the blood glucose

concentration levels several time one day. Glucose meters play a very important role in this direction. The normal range of blood glucose is 80-120mg/dL. The insulin deficiency or hyperglycemia results in higher or lower levels of glucose in blood than normal levels. Home glucose monitoring of type 1 diabetes was first introduced in the late 1970s, and the first meters were marketed for home in the year 1981. The two most predominant models available in North America are Glucometer ones whose trademark is owned by Bayer and the Accu-chek meter owned by Roche. Current models reflect several decades of innovation since their introduction in the 1970s, both in terms of strip technology and in meter design. The overall goals have switched to make them easier to use, with less potential errors, and to minimize the effects of matrixs[9]. Of the many different types of strip that have been developed, all are electrochemical biosensors incorporating an enzyme such as glucose oxidase (GOx) and glucose dehydrogenase (GDH). They are often termed thick-film sensors because each strip is composed of several layers each with designated functions such as separation, spreading or support.

Figure 12. *Glucose meters for controlling and monitoring diabetes.*
Reprinted with permission[11]

1.2.4.4 Multiplexed POC devices or x-POCT:

Multiplexed point-of-care testing (xPOCT), involves simultaneous on-site detection of different analytes from a single specimen. In recent years xPOCT has gained increasing importance for clinical diagnostics, with ever requiring applications in resource-limited settings. There has been tremendous research towards the development of xPOCT devices for the detection of several diseases from one analyte, for point-of-care testing.[35]

It is highly desirable to screen various analytes simultaneously, enabling a rapid, low-cost, and reliable quantification. Therefore, in the last decade, multiplexing has become crucial in the POC testing. In this context, there is an unmet demand for xPOCT devices, which ensure the quality and also can meet the ASSURED criteria by WHO. This will in future pave the way for novel home health monitoring systems and add valuable information for personalized medicine.

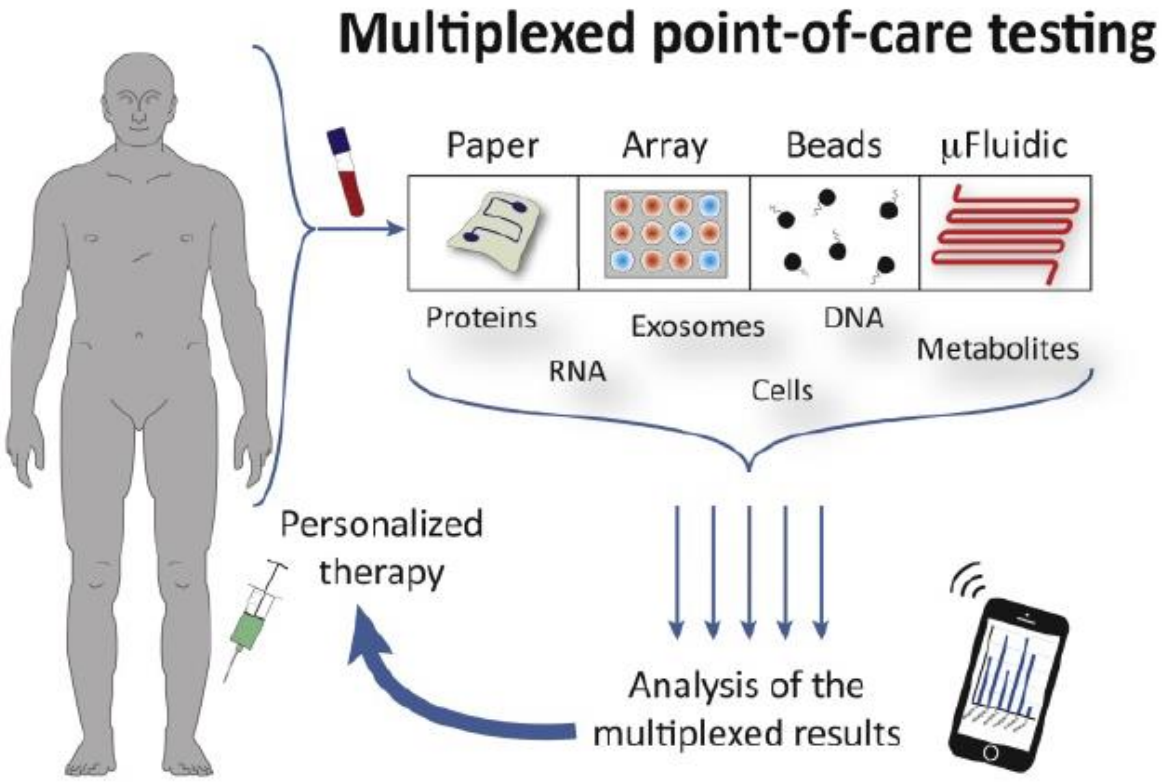

Figure 13*. Multiplexed Point of Care Testing (x-POCT).*
(Reprinted with permission from Sensors Journal)[35]

1.2.4.4.1 POC MDx devices available in market:

There exists a number of different commercial devices for the simultaneous detection of several clinical parameters, including blood gases, electrolytes, or immunoassays (e.g., Radiometer AQT90 Radiometer, or acute metabolites (e.g., Abbott i-STAT system, Abaxis Piccolo Xpress, or Nova Biomedical StatSensor), and Mitsubishi PATHFAST analyzer). Some other xPOCT devices are Atlas io system, Cobas Liat, Alere I, Alere q Analyzer, Genexpert Omni, Spartan RX, Spartan Cube, Film Array, PanNAT etc.[38]

A

B

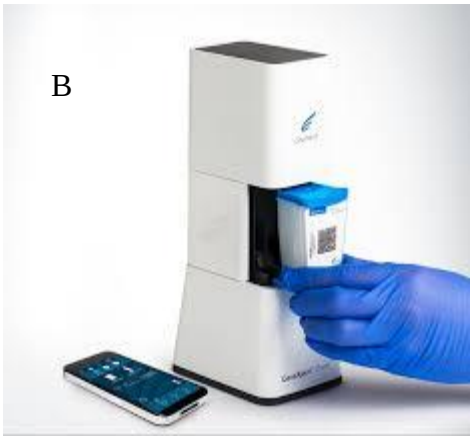

Figure 14*.Multiplexed POC devices available in market.*
Reprinted with permission[15]

A: Abbott i-STAT system; B: Cephid Genexpert Omni;

Some of the more relevant examples of POC biosensors are given in Table 3 and Table 4.

1.3 Summary

As described in this chapter, there are a number of biosensors available in the marketplace. Some of these biosensors are used primarily in a laboratory environment, and some are used at point of care settings. Despite a burgeoning market and major advances in the field, there is a growing need for more accurate, inexpensive and highly accurate biosensors. Biosensors for early detection of diseases and monitoring of diseases leading to personalized treatment is of paramount importance. Individualized drug dosing based on patient's response to drugs is more superior than the current "one shoe fits all" approach. This self-monitoring strategy had precedent and been very valuable for diabetic and pre-diabetic patients as daily testing leads to better glucose control compared to once-a-quarter Ha1C testing.[12] Similarly, monitoring several times in a day compared to weekly or biweekly hospital visits will allow physicians to modify the drug dose and improve personalized care. This type of personalized care also provides privacy which is critical for certain diseases.

The POC biosensors also reduce the morbidity related to a disease and allow the monitoring of disease progression, response to therapy and post-surveillance tracking for a number of clinically relevant enzymes, e.g. HIV viral load detection, oral anticoagulant therapy. etc. using glucose meters at the comfort of home.

The approaches presented in the next 3 chapters represents potential methods to achieve these goals.

Table 3. *Summary of Recent xPOCT systems*[38-43]

	Multiplexing capability	**Detection Technique**	**System flexibility**	**System complexity**	**On-site applicability**	**Commercially available**
	Paper-based systems					
μPADs	2 analytes, extendable	Colorimetric readout by naked eye	Low	Low	Yes	–
Triage	Up to 3 analytes	Lateral flow test with optical detection	Low	Low	Yes	Alere Inc.
	Array-based systems					
ElectraSense	Up to 12 544 analytes	Optical and electrochemical detection	High	Middle	Yes	CustomArray Inc.
	Bead-based systems					
xMAP	Up to 500 analytes	Flow cytometry	High	High	No	Luminex Corp.
GeneXpert Omni	Up to 6 analytes	Real-time PCR	Low	Low	Yes	Cepheid
	Microfluidic multiplexed systems					
MChip	Up to 5 analytes, extendable	Colorimetric detection	Low	Low	Yes	OPKO Diagnostics
DxBox	2 analytes, extendable	Colorimetric detection	Low	Middle	Yes	

	Multiplexing capability	Detection Technique	System flexibility	System complexity	On-site applicability	Commercially available
MultiLab	Up to 8 analytes, extendable	Amperometry combined with stop-flow protocols	High	Low	Yes	

1.4 Currently available POC, Tabulated list: (Table-4)

Company	Product Name	Disease	Format	Required Sample	Detection time	Sensitivity	Specificty	Approved
Alere, Inc.	Clearview HIV ½ STAT-PAK	HIV	Gold labelled Lateral Flow Assay	Whole blood/serum/plasma5µL	15-20 mins	99.7 (98.9-100)	99.9(99.6-100)	US FDA
Alere, Inc.	Clearview COMPLETE HIV ½	HIV	Gold labelled Lateral Flow Assay	Whole blood/serum/ plasma 2.5 µL	15 mins	99.7 (98.9-100)	99.9 (99.6-100)	
OraSure Technologies, Inc.	OraQuick ADVANCE HIV-1/2	HIV	Gold labelled Lateral Flow Assay	Oral fluid/whole blood/Plasma 5 µL	20 min	99.6 (98.9-99.8)	99.9 (99.6-99.9)	
Bio-Rad Laborotories, Inc.	Multispot HIV	HIV	Gold labelled Lateral Flow Assay	serum/plasma 30 µL	20 min	100 (99.9-100)	99.9 (99.8-100)	
MedMira, Inc.	Reveal G3 HIV-1	HIV	Fluorescence Lateral Flow immunoassay	serum/plasma 30 µL	<2 min	Serum-99.8 (99.2-100) Plasma-99.8 (99-100)	Serum-99.1 (98.8-99.4) Plasma-98.6 (98.4-98.8)	
Trinity Biotech PLC	Uni-Gold Recombigen HIV-1	HIV	Gold labelled Lateral Flow Assay	Whole blood/serum/plasma 50 µL	10 min	100 (99.5-100)	99.8 (99.3-100)	
ChemBio Diagnostic Systems, INC	Chembio DPP HIV 1/2	HIV	immunochromatographic, in vitro test for	Whole blood/serum/plasma or oral fluid swab 10 µL	10-25 min for blood samples 25-40 min for oral sample	99.9(99.4-99.9)	99.9 (99.7-99.9)	CLIA-waived

Company	Product Name	Disease	Format	Required Sample	Detection time	Sensitivity	Specificty	Approved
			the detection of antibodies					
Alere	Determine HIV 1/2 Ag/Ab Combo Test	HIV (HIV 1 & 2 antibodies and HIV-1 p24 antigen)		Serum/Plasma/whole blood 50 µL	20 min	99.9(99.4-100)	Serum: Low risk subjects 100 (99.6-100) High-risk subjects 98.9 (97.7-99.5) Plasma: Low risk subjects 100 (99.6-100) High-risk subjects 99.2 (98.2-99.7)	
Biolytical	INSTI HIV-1/HIV-2 Rapid Antibody Test	HIV		Plasma/whole blood 50 µL	< 2 min	99.9 (99.5-100)	100 (99.7-100)	
Hain Lifescience GmbH	GenoType MTBDRplus assay GenoType	Tuberculosis Detection of multidrug resistant TB	Line probe assay	Pulmonary blood sample (clinical) or cultured material (solid/liquid medium	5 h	"a limit of detection of 160 bacteria/ml was determined with both	100%	

Company	Product Name	Disease	Format	Required Sample	Detection time	Sensitivity	Specificty	Approved
						extraction methods”		
Cepheid, Inc.	Xpert MTB/RIF assay	Tuberculosis Detection of multidrug resistant TB	Automated cartridge based nucleic acid amplification test	Sputum sample	<2 h			
Cepheid, Inc.	Xpert MTB/RIF assay ULTRA	Tuberculosis Detection of multidrug resistant TB	Automated cartridge based nucleic acid amplification test		<80 min			
Unimed International	FirstSign MTB test	Tuberculosis	Serology based POC test					
Alere, Inc.	Determine TB-LAM Ag	Tuberculosis (in HIV+ patients)	Urine LAM test Lipoarabinomannan LFA	Urine	25 mins	Per CD4 cell count, sensitivity changes: >200 cells/µL 4% <200 cells 39.0% <150 cells 45.7% <100 cells 51.7%	>98%	

Company	Product Name	Disease	Format	Required Sample	Detection time	Sensitivity	Specificty	Approved
						<50 cells 66.7% ****		
Alere	BINAX NOW	Malaria Plasmodium Ag	LFA Invitro immunochromatographic assay	Whole blood (15 µL)	15 mins	P. falciparum 99.7% P. vivax 93.5%	P. falciparum 94.2% P. vivax 99.8%	
Alere	Panbio dengue Duo Cassette	Dengue Fever IgM and IgG (differentiation between primary and secondary infections)	Immunochromatography test (capture ELISA)	Serum, Plasma, Whole blood	3-5 days	Primary 85.1% Secondary 98.8%	91.6%	
Alere/Abbott	SD Dengue IgG capture ELISA	Dengue 1-4 (marker for secondary dengue infection)	ELISA			98.8%	99.2%	
Alere/Abbott	SD Dengue IgM capture ELISA	Dengue 1-4(early diagnosis of primary infection)	ELISA			96.4%	98.9%	
Orchid Biomedical Systems; India	Paracheck-Pf	Malaria	Immunochromatographic assay	Capillary Whole Blood (5 ul)	20 min			Not FDA approved

Company	Product Name	Disease	Format	Required Sample	Detection time	Sensitivity	Specificty	Approved
Becton Dickinson	ParaSight – F	Malaria	Immunochromatographic assay	Capillary Whole blood (50 ul) (detects >100 parasites/ul)				Not FDA approved
Amrad-ICT Diagnostics	ICT Malaria PF/pv	Malaria	Immunochromatographic assay	10 ul				Not FDA approved
ICT Diagnostics	ICT Malaria PF	Malaria	Immunochromatographic assay	Capillary whole blood or venous (5 ul)	15 min (>200 parasites/ul)			Not FDA approved
Accu-tell	Rapid Malaria Pf/Pv	Malaria		Capillary whole blood or venous (10 ul)	15 min			Not FDA approved
Access Bio	CareStart Malaria Pf/Pan	Malaria	Immunochromatographic assay	Capillary whole blood (5 ul)	20-30 min			Not FDA approved
Zephyr Biomedicals	Parabank	Malaria	Immunochromatographic assay	Capillary whole blood (5 ul)	20 min			Not FDA approved
Span Diagnostic Ltd	ParaHIT-F	Malaria	Immunochromatographic assay	Capillary whole blood (5 ul)	15 min			Not FDA approved
MACROmed Manufacturing LTD	MAKROmed Malaria Test	Malaria	Immunochromatographic assay	Capillary whole blood	<20 min			Not FDA approved
Omega Diagnostics LTD	Visitect Malaria Pf	Malaria	Immunochromatographic assay	Capillary whole blood or venous (5 ul)	15 min			Not FDA approved

Company	Product Name	Disease	Format	Required Sample	Detection time	Sensitivity	Specificty	Approved
Omega Diagnostics LTD	Visitect Malaria Combo Pan/Pf	Malaria	Immunochromatographic assay	Capillary whole or venous blood (5 ul)	15 min			Not FDA approved
BIO-RAD	DiaMed OptiMAL-IT	Malaria	Immunochromatographic assay	Capillary whole blood (10 ul)	20 min (>50-100 parasites/ul)			Not FDA approved
Cellabs	Malaria-Ag CELISA	Malaria	Enzyme-linked immunosorbent	Capillary, whole blood or serum (100 ul)	2 h			Not FDA approved
Zephry Biomedicals	Malascan	Malaria	Immunochromatographic assay	Capillary whole blood (5 ul)	20 min			Not FDA approved
PATH	PATH Falciparum Malaria IC test	Malaria	Immunochromatographic assay	Capillary whole blood (5 ul)				Not FDA approved
Abbott	Determine Malaria Pf	Malaria	Immunochromatographic assay	Capillary Whole blood (2 ul)	30 min			Not FDA approved
Acumen Diagnostics Inc	DiaSpot Malaria	Malaria	Immunochromatographic assay	Capillary whole blood (10 ul)	10 min			Not FDA approved
HUMAN Diagnostics	Hexagon Malaria	Malaria	Immunochromatographic assay	Capillary or venous whole blood (5 ul)	15 min			Not FDA approved
SD Diagnosics	SD Malaria Antigen Bioline	Malaria	Immunochromatographic assay	Capillary whole blood (5 ul)	15-30 min (>50/ul)			Not FDA approved

Company	Product Name	Disease	Format	Required Sample	Detection time	Sensitivity	Specificty	Approved
Zephyr Biomedical Systems	Parascreen Rapid Test for Malaria Pan/Pf	Malaria	Immunochromatographic assay	Capillary whole blood (5 ul)	20 min			Not FDA approved
Premier Medical Corporation	First Response Malaria (pLDH/HRP2combo test)	Malaria	Immunochromatographic assay	Whole blood (5 ul)	<20 min			Not FDA approved
Abbott Technologies	i-STAT analyzer (BNP)	Cardiac markers BNP	Immunienzymatic assay with electrochemical detection	whole blood or plasma (2-3 drops)	10 min			FDA cleared for professional use only
Alere Technologies	Triage BNP test	Cardiac markers BNP	Two site Fluorescence lateral flow immunoassay	whole blood or plasma or finger prick	15 mins			
Response Biomedical Corp	RAMP Myoglobin test	Cardiac markers NT-proBNP Acute Myocardial infraction	Two site Fluorescence lateral flow immunoassay	whole blood	10 min			Cleared for sale by FDA

Company	Product Name	Disease	Format	Required Sample	Detection time	Sensitivity	Specificty	Approved
Roche Diagnostics	Cardiac Reader or cobas h 232 system	Cardiac markers NT-proBNP	Portable/ two-site gold labelled lateral flow immunoassay	Heparinized whole blood or finger prick	8-12 min	60 – 9,000 pg/mL Cut-off values: <125 pg/mL = Exclusion of Non-acute heart failure, <300 pg/mL = Exclusion of acute heart failure		
LifeSign	StatusFirst CHF NT-pro BNP	Congestive Heart Failure	LFA			<75-year-old 92.1% >75 87.8%	<75-year-old 70.4% >75-year-old 86.5%	FDA approved for prescription use
BTNX, Inc.	Rapid response CK-MB test	Myocardial Infraction Creatine kinase MB(CKMB)	LFA	Whole Blood, Serum, Plasma	10 min	5 ng/ml	Creatinine Kinase MB	
BTNX, Inc	RAPID RESPONSE D-DIMER TEST	Venous Thromboembolism (VTE), D-Dimer	LFA	Whole Blood, Plasma	10 min	500 ng/ml	D-Dimer	

Company	Product Name	Disease	Format	Required Sample	Detection time	Sensitivity	Specificty	Approved
Boditech Med, Inc.	Ichroma CK-MB test	Myocardial Infraction Creatine kinase MB(CKMB)	LFA	Whole blood, Plasma, Serum (75 µL)	12 min			
Trinity Biotech.	Meritas Troponin	Myocardial Infarction Troponin I	LFA					Not FDA approved
American Screening Corp	Instant View Troponin	Acute Myocardial Infarction (AMI)	LFA	Whole Blood, Serum 160-200 µL	15-20 min	>98%	95-100%	
CTK Biotech	On Site PSA Rapid Test	Prostate Cancer Prostate Specific Antigen (PSA)	LFA	Whole Blood, Serum, Plasma				
Alere, Inc.	Alere NMP22 BladderChek	Bladder Cancer Nuclear Matrix Protein (NMP22)	Invitro immunoassay	Urine (4 drops)	30 min	99%	99%	FDA cleared for professional and prescription home use
Alere, Inc.	Clearview iFOBT	Colon Cancer Fecal Occult Blood	Antibody sandwich assay		5 min	93.6%	99.1%	

Company	Product Name	Disease	Format	Required Sample	Detection time	Sensitivity	Specificty	Approved
Arbor Vita Corp	OncoE6 Cervical Test	Cervical Cancer E6 Oncoproteins	Lateral flow	Cervical Swab	2.5 hours			
Quicking Biotech Co., Ltd	CA125 rapid test kit	Ovarian Cancer CA125 Ag	Lateral flow immunoassay	Serum	5 min			
Innovation Biotech	AFP Test	Hepatocellular Cancer Alpha fetoprotein Ag		Serum/Plasma				
Roche	CoaguChek XS Plus System	Coagulation monitoring						CLIA waived
Alere	Binax Now Influenza A and B test	Influenza A and B nucleoprotein antigen based	Lateral Flow Assay	Nasal Swab	10 min	Influenza A 93.8% Influenza B 77.4%	Influenza A 95.8% Influenza B 98%	CLIA waived
Becton Dickinson & Co	BD Veritor Flu A + B	influenza A or B Antigen based	chromatographic immunoassay	Nasal Swab, nasopharyngeal swab,	10-15 min			CLIA waved
Quidel Corp	Sofia Influenza A + B FIA	influenza A or B antigen based	Lateral Flow Assay	Nasal Swab, nasopharyngeal wash	3-15 min	A 90-99% B 88-90%	A 95-96% B 96-97%	CLIA waved
Quidel Corp	QuickVue Influenza A + B	influenza A or B antigen based		Nasopharyngeal swab, nasal swab	<10 min			CLIA waved

Company	Product Name	Disease	Format	Required Sample	Detection time	Sensitivity	Specificty	Approved
Princetone BioMeditech Corp	BioSign Flu A & B	influenza A or B antigen based	Lateral Flow Assay	Nasal Swab, nasopharyngeal swab	10-15 min			CLIA waved
Princetone BioMeditech Corp	LABSCO Advantage Flu A & B	influenza A or B nucleoprotein antigens		nasopharyngeal wash	10-15 min			CLIA waved
LifeSIgn LLC	Status Flu A & B	Influenza A or B nucleoprotein antigens	LFA	Nasal Swab, nasopharyngeal swab,	10-15 min			CLIA waved
OraSure	QuickFly Rapid Flu A + B test	influenza A or B antigen based	LFA	Nasal Swab, nasopharyngeal swab,	10-15 min	A = 97-98.4% B = 93.2-94.4%	A = 94.2-05.8% B = 93.5-100%	CLIA waved
Polymedco	Poly stat Flu A & B	influenza A or B nucleoprotein antigen based		Nasal Swab, nasopharyngeal swab,	10-15 min			CLIA waved
Sekisui Diagnostics	OSOM ULTRA Flu A & B	influenza A or B nucleoprotein antigens		Nasal Swab, nasopharyngeal swab, nasopharyngeal wash, nasopharyngeal wash	10-15 min			CLIA waved
Meridian BioScience	ImmunoCard STAT Flu A & B	influenza A or B	LFA	Nasal Swab, nasopharyngeal swab,	10-15 min			CLIA waved

Company	Product Name	Disease	Format	Required Sample	Detection time	Sensitivity	Specificty	Approved
		nucleoprotein antigens		nasopharyngeal wash, nasopharyngeal wash				
McKesson Consult Diagnostics	Influenza A & B Tests	influenza A or B nucleoprotein antigens	LFA	Nasal Swab, nasopharyngeal swab, nasopharyngeal wash, nasopharyngeal wash	10-15 min			CLIA waved
Remel/Thermo Fisher	XPECT Flu A & B	Influenza A or B viral antigens	LFA	Nasal Wash	10-15 min			
Roche	Cobas Liat PCR System	Influenza A/B RSV Strep A	RT-PCR		<20 min	Influenza A/B 100%Strep A 98.3% RSV = 97%	A = 96.8% B = 94.1% Strep A = 94.2% RSV = 98.7%	CLIA waved
ZeptiMetrix	ZeptoMetrix Respiratoryh Verification Panel	RUO panel (Influenza A/B, RSV, Adenovirus, Rotavirus, & negatives) via nucleic acids						
Alere	Binax NOW	Pneumonia S.pneumonia Ag		Urine/CSF	15 min	Urine 86% CSF 97%	Urine 94% CSF 99%	

Company	Product Name	Disease	Format	Required Sample	Detection time	Sensitivity	Specificty	Approved
Quidel Corp	Quick Vue RSV Test	Infantile Bronchitis Respiratory syncytial virus (RSV) Ag	Dipstick immunoassay	Nasopharyngeal Swab, nasopharyngeal aspirate, nasal/nasopharyngeal wash	15 min	Nasopharyngeal Swab 92%, nasopharyngeal aspirate 99%, nasal/nasopharyngeal wash 83%	Nasopharyngeal Swab 92%, nasopharyngeal aspirate 92%, nasal/nasopharyngeal wash 90%	
Quidel Corp	Sofia RSV FIA	Respiratory syncytial virus (RSV) nucleoprotein antigen	Fluorescent Immunoassay	Nasopharyngeal swab, aspirate/wash	3-15 min	86-92%	96-98%	
Thermofisher	Xpect RSV test	RSV antigen detection	LFA immunochromatographic sandwich assay	Nasopharyngeal specimen	15 min			
Alere, Inc.	Binax NOW Filariasis	Lymphatic filariasis Wucheria bancrofti		Whole Blood, Serum, Plasma (finger prick) (75 ul)	10 min			
IMMY	CrAg A	Cryptococcal meningitis C. neoformans C. gattii	LFA	CSF/Serum	10 min			FDA cleared

Company	Product Name	Disease	Format	Required Sample	Detection time	Sensitivity	Specificty	Approved
Trinity Biotech	Uni-Gold legionella urinary Antigen PLUS	Legionnarie's Disease Legionella Pneumophila serogroup1 Ag		Urine (4 drops)	15 min	82-91%	98-99%	

Table 4. *Tabulated list of current POC diagnostic on market.*[31-47,61-70]

1.5 References

1. G. B. M.-A. a. F. Global Biosensors Market - Analysis and Forecast (2018 -2027). *Report ID: 5381405,* April 2018.

2. Turner, A. P. Biosensors 2012. *Biosens Bioelectron* 2013, *40* (1), 1.

3. Citartan, M.; Gopinath, S. C.; Tominaga, J.; Tang, T. H. Label-free methods of reporting biomolecular interactions by optical biosensors. *Analyst* 2013, *138* (13), 3576.

4. Turner, A. P. 30th Anniversary issue of Biosensors and Bioelectronics. *Biosens Bioelectron* 2016, *76*, 1.

5. Cho, I. H.; Irudayaraj, J. In-situ immuno-gold nanoparticle network ELISA biosensors for pathogen detection. *Int J Food Microbiol* 2013, *164* (1), 70.

6. Damborsky, P.; Svitel, J.; Katrlik, J. Optical biosensors. *Essays Biochem* 2016, *60* (1), 91.

7. Darder, M.; Casero, E.; Pariente, F.; Lorenzo, E. Biosensors based on membrane-bound enzymes immobilized in a 5-(octyldithio)-2-nitrobenzoic acid layer on gold electrodes. *Anal Chem* 2000**,** *72* (16), 3784.

8. Monteiro, T.; Almeida, M. G. Electrochemical Enzyme Biosensors Revisited: Old Solutions for New Problems. *Crit Rev Anal Chem* 2018, DOI:10.1080/10408347.2018.1461552 10.1080/10408347.2018.1461552, 1.

9. Schuhmann, W.; Zimmermann, H.; Habermuller, K.; Laurinavicius, V. Electron-transfer pathways between redox enzymes and electrode surfaces: reagentless biosensors based on thiol-monolayer-bound and polypyrrole-entrapped enzymes. *Faraday Discuss* 2000**,** (116), 245.

10. Rocchitta, G.; Spanu, A.; Babudieri, S.; Latte, G.; Madeddu, G.; Galleri, G.; Nuvoli, S.; Bagella, P.; Demartis, M. I.; Fiore, V.et al. Enzyme Biosensors for Biomedical Applications: Strategies for Safeguarding Analytical Performances in Biological Fluids. *Sensors (Basel)* 2016, *16* (6).

11. Wilson, G. S.; Hu, Y. Enzyme-based biosensors for in vivo measurements. *Chem Rev* 2000, *100* (7), 2693.

12. Zeng, L.; Lie, P.; Fang, Z.; Xiao, Z. Lateral flow biosensors for the detection of nucleic acid. *Methods Mol Biol* 2013**,** *1039*, 161.

13. Du, Y.; Dong, S. Nucleic Acid Biosensors: Recent Advances and Perspectives. *Anal Chem* 2017, *89* (1), 189.

14. Li, D.; Tian, X.; Wang, A.; Guan, L.; Zheng, J.; Li, F.; Li, S.; Zhou, H.; Wu, J.; Tian, Y. Nucleic acid-selective light-up fluorescent biosensors for ratiometric two-photon imaging of the viscosity of live cells and tissues. *Chem Sci* 2016**,** *7* (3), 2257.

15. Palmisano, F.; Zambonin, P. G.; Centonze, D. Amperometric biosensors based on electrosynthesised polymeric films. *Fresenius J Anal Chem* 2000**,** *366* (6-7), 586.

16. Eshkenazi, I.; Sacks, V.; Neufeld, T.; Rishpon, J. Amperometric biosensors based on microflow injection system. *Appl Biochem Biotechnol* 2000, *89* (2-3), 217.

17. Gogol, E. V.; Evtugyn, G. A.; Marty, J. L.; Budnikov, H. C.; Winter, V. G. Amperometric biosensors based on nafion coated screen-printed electrodes for the determination of cholinesterase inhibitors. *Talanta* 2000, *53* (2), 379.

18. Stefan, R. I.; van Staden, J. K.; Aboul-Enein, H. Y. Amperometric biosensors/sequential injection analysis system for simultaneous determination of S- and R-captopril. *Biosens Bioelectron* 2000**,** *15* (1-2), 1.

19. Garjonyte, R.; Malinauskas, A. Amperometric glucose biosensors based on Prussian Blue- and polyaniline-glucose oxidase modified electrodes. *Biosens Bioelectron* 2000, *15* (9-10), 445.

20. Clark T.J. The triage cardiac panel. Point Care J. Near Patient Test. Technol. 2002; 1:42–46.

21. Ahmed S. Paper-based chemical and biological sensors: engineering aspects. Biosens. Bioelectron.2016;77:249–263.

22. Rolland J.P., Mourey D.A. Paper as a novel material platform for devices. MRS Bull. 2013; 38:299–305.

23. Yang Y. Paper-based microfluidic devices: emerging themes and applications. Anal. Chem. 2017; 89:71–017;

24. Pollock N.R. A paper-based multiplexed transaminase test for low-cost, point-of-care liver function testing. Sci. Transl. Med. 2012;4 152ra129–152ra129.

25. Vella S.J. Measuring markers of liver function using a micropatterned paper device designed for blood from a fingerstick. Anal. Chem. 2012; 84:2883–2891.

26. Dungchai W. Electrochemical detection for paper-based microfluidics. Anal. Chem. 2009; 81:5821–5826.

27. Ge L. Three-dimensional paper-based electrochemiluminescence immunodevice for multiplexed measurement of biomarkers and point-of-care testing. Biomaterials. 2012; 33:1024–1031.

28. Li X., Liu X. A microfluidic paper-based origami nano-biosensor for label-free, ultrasensitive

immunoassays. Adv. Healthc. Mater. 2016; 5:1326–1335.

29. Li W. Multiplex electrochemical origami immunodevice based on cuboid silver-paper electrode and metal ions tagged Nano porous silver origami immunodevice based on Cu 2014;56:167–173.
30. Wu Y. A paper-based microfluidic electrochemical immunodevice integrated with amplification-by polymerization for the ultrasensitive multiplexed detection of cancer biomarkers. Biosens. Bioelectron.2014;52:180–187.
31. Wu Y. Paper-based microfluidic electrochemical immunodevice integrated with nanobioprobes onto graphene film for ultrasensitive multiplexed detection of cancer biomarkers. Anal. Chem.2013; 85:8661–8668.
32. Zang D. Electrochemical immunoassay on a 3D microfluidic paper-based device. Chem. Commun. 2012; 48:4683.
33. Ling M.M. Multiplexing molecular diagnostics and immunoassays using emerging microarray technologies. Expert Rev. Mol. Diagn. 2007; 7:87–98.
34. Chandra P.E. Novel multiplex technology for diagnostic characterization of rheumatoid arthritis.Arthritis Res. Ther. 2011;13: R102.
35. Kadimisetty K. Automated multiplexed immunoassays for cancer biomarker proteins. Anal.Chem. 2015;87:4472–4478.
36. Chen P. Multiplex serum cytokine immunoassay using nanoplasmonic biosensor microarrays. ACS Nano. 2015; 9:4173–4181.
37. Masson J.-F. Surface plasmon resonance clinical biosensors for medical diagnostics. ACS Sens. 2017; 2:16–30.

38. Aćimović S.S. LSPR chip for parallel, rapid, and sensitive detection of cancer markers in serum. Nano Lett. 2014; 14:2636–2641.
39. Schumacher S. Highly-integrated lab-on-chip system for point-of-care multiparameter analysis. Lab Chip. 2012; 12:464–473.
40. Otieno B.A. Cancer diagnostics via ultrasensitive multiplexed detection of parathyroid hormone related peptides with a microfluidic immunoassay. Anal. Chem. 2016; 88:9269–9275.
41. Wilson M.S., Nie W. Multiplex measurement of seven tumor markers using an electrochemical protein chip. Anal. Chem. 2006; 78:6476–6483.
42. Díaz-González M. Diagnostics using multiplexed electrochemical readout devices. Electroanalysis. 2014; 26:1154–1170.
43. Wan Y. Development of electrochemical immunosensors towards point of care diagnostics. Biosens. Bioelectron. 2013; 47:1–11.
44. Ghindilis A.L. CombiMatrix oligonucleotide arrays: genotyping and gene expression assays employing electrochemical detection. Biosens. Bioelectron. 2007; 22:1853–1860.
45. Roth K.M. Electrochemical detection of short DNA oligomer hybridization using the CombiMatrixElectraSense Microarray reader. Electroanalysis. 2006; 18:1982–1988.
46. Dunbar S.A. Applications of Luminex® xMAP™ technology for rapid, high-throughput multiplexed nucleic acid detection. Clin. Chim. Acta. 2006; 363:71–82.
47. Feng L.-N. Ultrasensitive multianalyte electrochemical immunoassay based on metal ion functionalized titanium phosphate nanospheres. Anal. Chem. 2012; 84:7810–7815.
48. Tang J. Magneto-controlled graphene immunosensing platform for simultaneous multiplexed

electrochemical immunoassay using distinguishable signal tags. Anal. Chem. 2011; 83:5407–5414.

49. Kong F.-Y. Simultaneous electrochemical immunoassay using CdS/DNA and PbS/DNA nanochains as labels. Biosens. Bioelectron. 2013; 39:177–182.
50. Wang J. Electrochemical coding technology for simultaneous detection of multiple DNA targets. J. Am. Chem. Soc. 2003; 125:3214–3215.
51. Tang D. Multiplexed electrochemical immunoassay of biomarkers using metal sulfide quantum dot nanolabels and trifunctionalized magnetic beads. Biosens. Bioelectron. 2013; 46:37–43.
52. Sato K. Microchip-based immunoassay system with branching multichannels for simultaneous determination of interferon-γ Electrophoresis. 2002; 23:734–739.
53. Ko Y.-J. Microchip-based multiplex electro-immunosensing system for the detection of cancer biomarkers. Electrophoresis. 2008; 29:3466–3476.
54. Drain P.K., Garrett N.J. The arrival of a true point-of-care molecular assay – ready for global implementation Lancet Glob. Health. 2015;3: e663663enta55. Ateya D.A. The good, the bad, and the tiny: a review of microflow cytometry. Anal. Bioanal. Chem. 2008; 391:1485–1498.
56. Godin J. Microfluidics and photonics for Bio-System-on-a-Chip: a review of advancements in technology towards a microfluidic flow cytometry chip. J. Biophotonics. 2008; 1:355–376.
57. Dunbar S., Jacobson J.W. Parallel processing in microbiology: detection of infectious pathogens by Luminex xMAP multiplexed suspension array technology. Clin. Microbiol. News. 2007; 29:79–86.
58. Shriver-Lake L.C. Simultaneous assay for ten bacteria and toxins in spiked clinical samples using a microflow cytometer. Anal. Bioanal. Chem. 2013; 405:5611–5614.

59. Hashemi N. Optofluidic characterization of marine algae using a microflow cytometer. Biomicrofluidics. 2011; 5:32009.

60. Duncan P.N. Scaling of pneumatic digital logic circuits. Lab Chip. 2015; 15:1360–1365.

61. Araci I.E., Brisk P. Recent developments in microfluidic large-scale integration. Curr. Opin. Biotechnol. 2014; 25:60–68.

62. Shao H. Chip-based analysis of exosomal mRNA mediating drug resistance in glioblastoma. Nat. Commun. 2015; 6:6999.

63. Thorsen T. Microfluidic large-scale integration. Science. 2002; 298:580–584.

64. Wu A.R. High throughput automated chromatin immunoprecipitation as a platform for drug screening and antibody validation. Lab Chip. 2012; 12:2190–2198.

65. Piraino F. A digital–analog microfluidic platform for patient-centric multiplexed biomarker diagnostics of ultralow volume samples. ACS Nano. 2016; 10:1699–1710.

66. Wu X. In situ characterization of the mTORC1 during adipogenesis of human adult stem cells on chip. Proc. Natl. Acad. Sci. U. S. A. 2016;113: E4143E4143c. N67. Kalisky T., Quake S.R. Single-cell genomics. Nat. Methods. 2011; 8:311–314.

68. Chin C.D. Microfluidics-based diagnostics of infectious diseases in the developing world. Nat.Med. 2011;17:1015–1019.

69. Chin C.D. Mobile device for disease diagnosis and data tracking in resource-limited settings. Clin.Chem. 2013;59:629–640.

70. Lafleur L. Progress toward multiplexed sample-to-result detection in low resource settings using microfluidic immunoassay cards. Lab Chip. 2012; 12:1119.

71. Rossier J. GRAVI: robotized microfluidics for fast and automated immunoassays in low volume. J.Assoc. Lab. Autom. 2008; 13:322–329.

CHAPTER 2

* Most of the work described in this chapter has been published in the following publication and it is used in this chapter with permission from ACS and RSC:

- **Das, A.**; Cui, X.; Chivukula, V.; Iyer, S. S., Detection of Enzymes, viruses and bacteria using glucose meters. *Anal. Chem.*, **2018**, *90* (19), 11589-11598.
- Cui, X.; **Das, A.**; Dhawane, A.; Sweeney, J.; Zhang, X.; Chivukula, V.; Iyer, S. S., Highly specific and rapid glycan based amperometric detection of influenza viruses. ***Chem. Sci.***, 2017, **8**, 3628-3634

2 DETECTION OF VIRUSES, PATHOGENS ENZYMES USING GLUCOSE METERS

2.1 Introduction

A number of clinically relevant enzymes provide a snapshot of the human condition. For example, blood tests to ascertain liver enzyme activity is part of regular blood tests to determine the health of a patient. [1-3] The standard method for diagnosis proceeds from sample collection, shipping to a centralized laboratory and enzyme assays using fluorescent or chemiluminescent substrates. These methods, while clearly valuable, are time consuming and expensive. Translating biochemical assays performed in *resource rich* clinical or microbiological or biochemical laboratories by trained personnel to *resource poor* environments like primary clinics, remote locations and/or home by patients could arrest the spread of an emerging disease.[4] For example, rapid detection of influenza results in early administration of antiviral drugs, which leads to faster recovery.[5,6] Similarly, detection of environmentally harmful pathogens in food before the products are shipped to consumers is more valuable than expensive recalls of contaminated food. [7,8] Taken together, there is a urgent need to develop diagnostics that can be deployed in a variety of settings for the detection of infectious agents. As described in Chapter 1, these diagnostics should meet the ASSURED criteria. Hundreds of biosensors have been designed to detect different analytes, but very few meets all the ASSURED criteria as it is a very high bar to meet and often, there are trade-offs. For example, point of care PCR tests are extremely accurate, but the instruments are expensive, and the cost of reagents are expensive and should survive the supply chain. Indeed, the list price of Alere i Influenza A and B is ~ 9,000 $. Each test is also expensive, the list price at CVS minute clinic for the 2018 season is 70$, although some portion of the cost may be covered by the patient's insurance.[9] Despite these costs, the loss of productivity and other economic costs

far outweigh the cost of the test (especially in the case of emerging pandemics) and these tests are administered to patients suspected of influenza. If the costs are reduced from thousands of dollars to a few dollars, more people can avail themselves of the tests and the burden due to influenza can be decreased. Clearly, if a diagnostic meets the ASSURED criteria, the impact can be transformative. For example, devices like the glucose monitor, which meets the ASSURED criteria have assisted millions of type 1 and 2 diabetic patients take more control of their blood glucose levels, thereby decreasing morbidity and healthcare costs significantly.[10,11]

2.2 Purpose of the study

We and others have been promoting the use of glucose meters to detect non-glucose analytes. Liu and coworkers have used glucose meters to detect several analytes that include cocaine, adenosine, etc.[12,13] Their approach was to design assays that release invertase upon target binding, which converts sucrose to glucose. (**Figure 15 A**) On the other hand, we and others have developed substrates that release glucose when exposed to an enzyme.[14-17] (**Figure 15 B**) In both cases, the released glucose is oxidized by glucose oxidase or glucose hydrogenase, releasing electrons that can be recorded by a standard glucose meter. Thus, the concentration of the analyte such as cocaine or the activity of the enzyme such as influenza neuraminidase can be correlated to the pathogen concentration. Using this approach, we demonstrated the detection of influenza viruses and measured drug susceptibility for influenza viruses as Relenza and Tamiflu are enzyme inhibitors. Glucose is not released when the inhibitors are added to the sample containing susceptible strains. All these assays use glucose meter for the detection of glucose or galactose. Galactose is detected if the dehydrogenase enzyme is impregnated on the test strips. [18,19] Taken together, a glucose meter can be repurposed to detect analytes other than blood glucose. This strategy is expected to have a significant impact in the development of point of care biosensors for

a variety of ailments as millions of people have adopted glucose meters and there will be minimal training involved in using the same device for a new purpose. However, one potential concern in the use of the glucose meters and test strips for detection of analytes is the problem of background glucose in blood samples. In our previous work on influenza viruses, we used nasal swabs which is not as complex as blood and does not contain glucose unless the patient is suffering from an underlying condition.[21] Also, we compared the glucose (or galactose level) *before and after* adding the substrate; the difference between these two readings allowed us to accurately determine the presence of influenza virus.[15] While this strategy of measuring *before and after* addition of the substrate works well, background glucose levels can be an issue if the initial glucose reading is high especially when measuring blood samples from diabetic patients.[21] Glucose meters are typically calibrated to measure the normal range of blood present in humans (70 -120 mg/dl) and anything lower or higher beyond this range is met with an error or "low" or "high" message.[20] An alternate method that will overcome the problem of background glucose will allow us to adapt this strategy to detect analytes other than glucose, especially in blood and other matrices, where the background levels of glucose can be very high in people suffering from type 1 or type 2 diabetes.

In this chapter, we report novel assays wherein paracetamol or catechol bearing compounds, when exposed to their respective enzymes, release paracetamol or catechol. Paracetamol or catechol can be detected using standard glucose test strips and glucose meters. Paracetamol/catechol oxidation is a two electron and two proton process that has been described previously.[21,22] we demonstrate broad scope of the assays by detecting multiple enzymes and pathogens. We also demonstrate that strips without glucose oxidase or dehydrogenase can be used to detect paracetamol, suggesting that this method could be used to develop assays that can detect enzymes, viruses and bacteria in the presence of high levels of background glucose.

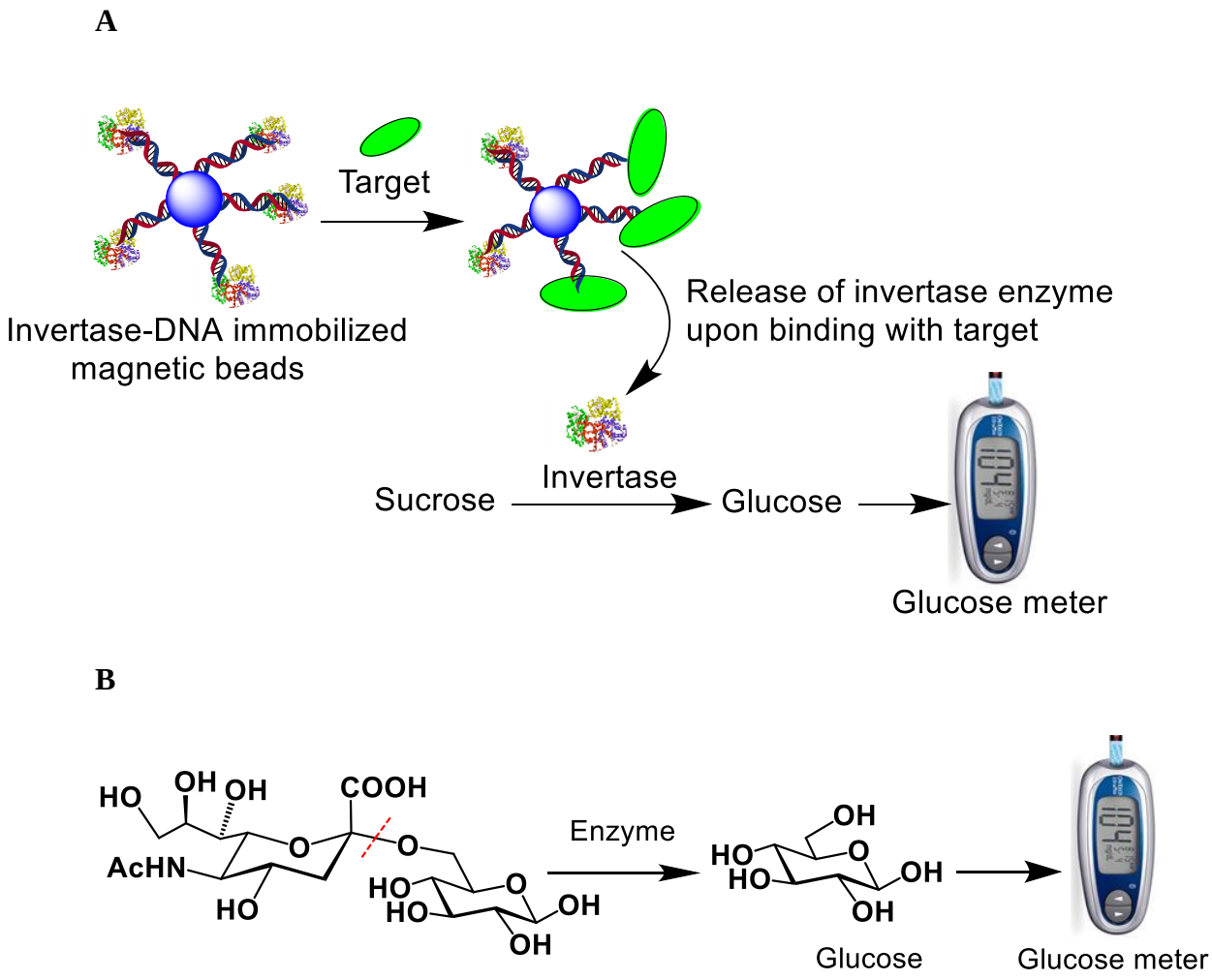

Figure 15*. Detection of non-glucose analytes using a glucose meter.*

15A. DNA-invertase conjugates are immobilized onto magnetic beads. The DNA strands respond to the target of interest releasing DNA-invertase conjugates from the beads. The released invertase catalyzes the conversion of sucrose to glucose which can be quantified using a glucose meter. Because the concentration of DNA-invertase conjugate is proportional to the concentration of target, the glucose meter reading can be used to quantify the target concentration.

15B. Cleavage of substrate-glucose into substrate and glucose by the target enzyme. The released glucose and enzyme can be quantified using a glucose meter

2.2.1 Mechanism of detection

General working of glucose strips and glucose meters. The glucose gets oxidized to gluconolactone in presence of FAD, which in turn gets converted to $FADH_2$ and oxygen is reduced to hydrogen peroxide. It also involves the presence of a mediator Prussian white which gets converted to Prussian blue and releases the electrons that are detected by the glucose meters and hence detecting glucose present in the analyte.

Paracetamol attached to specific substrate will be added to the sample containing the relevant enzymes/pathogens. Cleavage of the substrate with the enzyme/pathogen releases paracetamol which can be quantified using a glucose meter

A:

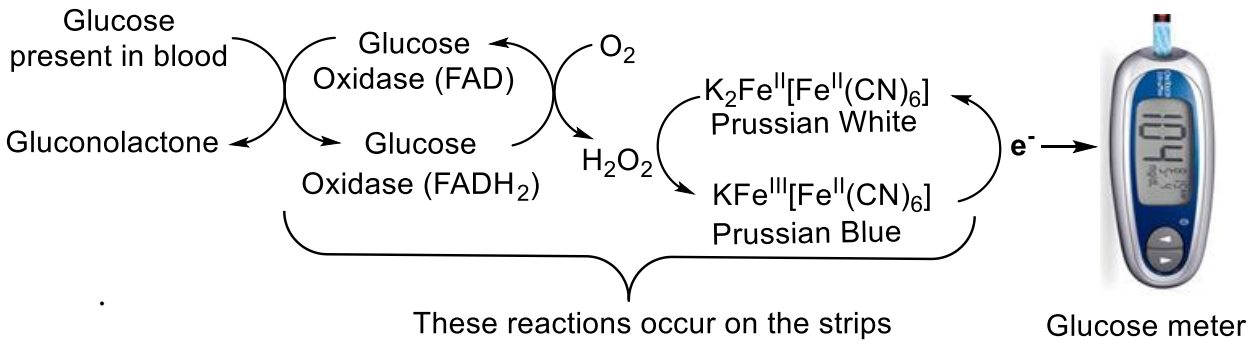

.

B:

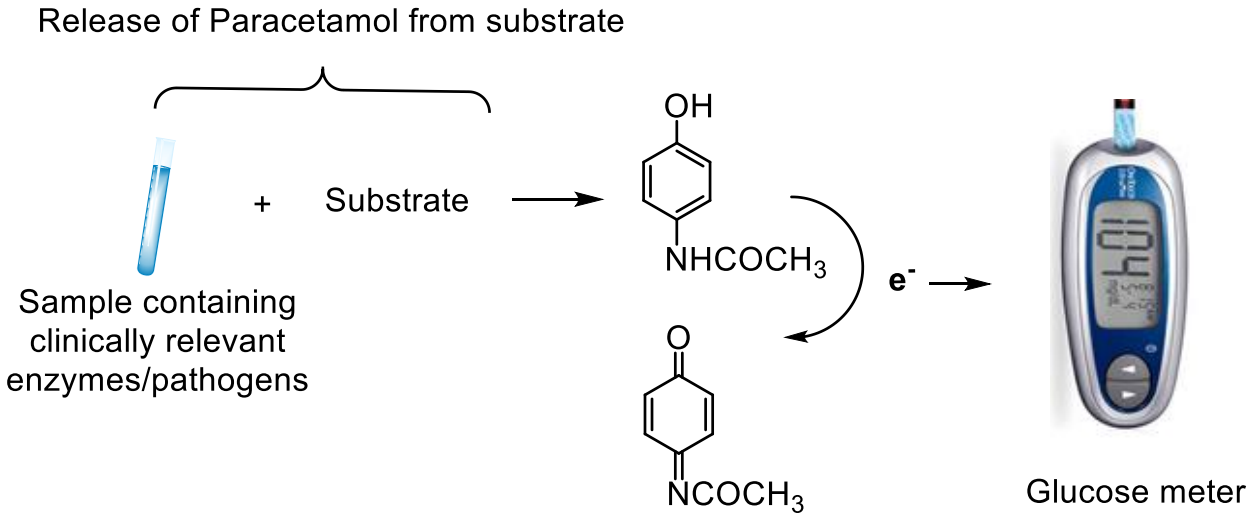

Figure 16*. General working Principle of glucose meters and strips and our strategy to detect paracetamol.*

16A. Glucose is detected by the strips containing the Glucose oxidase using the above shown mechanism. Glucose is oxidized to gluconolactone. In presence of the mediator Prussian blue-white the electrons released are detected by the glucose meter.

16B. The specific enzymes release paracetamol from the substrates and the releases paracetamol is directly oxidized on the surface of the electrodes releasing electrons which are captured by the glucose meter.

2.3 Results

Our first step was to demonstrate that paracetamol can be detected using a glucose meter. To this end, we used a Onetouch glucose meter and standard strips to generate a calibration curve (**Figure 17).** The calibration curve and linear range for paracetamol, which ranges from 0.1 mM to 5mM, demonstrates that it is possible to detect paracetamol using a glucose meter. Since we could detect paracetamol readily and rapidly using glucose meters, we generated several compounds that could release paracetamol when exposed to the enzyme or pathogen. The structures of the figures are given in **Figure 18** and the syntheses of the compounds are described in **Schemes 1-4**. For the synthesis of SP, the carboxylic acid of the sialic acid is converted to the methyl ester and then the per-acetylated methyl ester of sialic acid chloride was reacted with paracetamol to yield the α derivative in reasonably good yield. Deprotection of the acetate and the ester protecting groups resulted in the desired compound in high yield. For $SP(OMe)_2$, the methyl ester was treated with anhydrous acetone to protect the 8 and 9 hydroxyl groups as diacetone form and then the 4 and 7 hydroxyl groups were converted to methoxyl form using BaO, $Ba(OH)_2$ to generate the oxyanions and then methyl iodide was added to generate the 4,7 methoxy derivative. Next similar to SP, the 4,7 dimethoxymethyl ester of sialic acid chloride was reacted with paracetamol to again yield the α derivative in reasonably good yield. For both SP and $SP(OMe)_2$, the H-3 axial and H-3 equatorial protons resonated at 1.7 and 2.8 ppm in the ^{1}H NMR, respectively and the C-2 carbon resonated at 100.0 ppm in the ^{13}C NMR, indicating α isomer. Both GP and GC were synthesized by reacting the galactose imidate with paracetamol/catechol via glycosidic bond formation using TMSOTf conditions in reasonably high yield to produce the β isomer. Unlike syntheses that introduces glucose or galactose into the substrates as an output,[15] the syntheses of paracetamol bearing compounds is relatively straightforward.

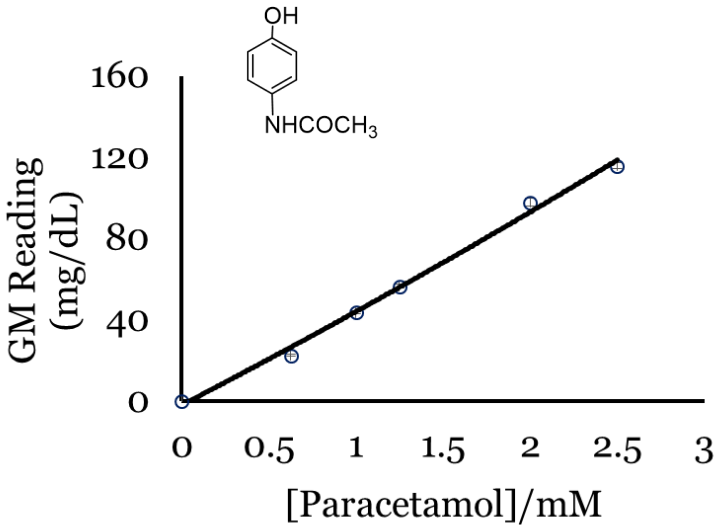

Figure 17*. Standard curve for Paracetamol.*

Calibration curve and linear range for paracetamol using Onetouch glucose meter and Unistrip strips.

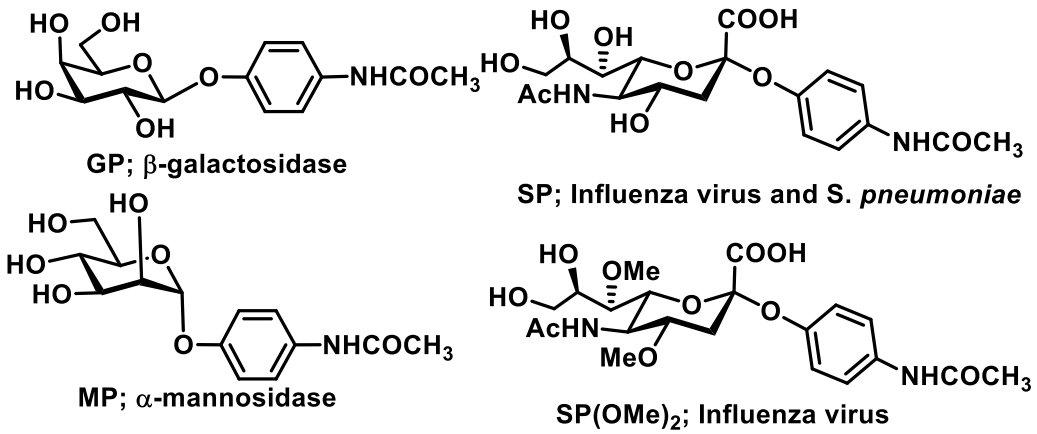

Figure 18*. Structure of various glycoconjugates used as substrates for different enzymes.*

GP, Galactose-paracetamol cleaved by β-galactosidase; **SP**, Sialic acid-paracetamol cleaved by Neuraminidase released by influenza virus and *S. pneumoniae*; **MP**, Mannose-paracetamol cleaved by α-mannosidase; **SP(OMe)$_2$** – 4,7 methoxy sialic acid-paracetamol cleaved by influenza virus neuraminidase and **GC**, Galactose-catechol cleaved by β-galactosidase.

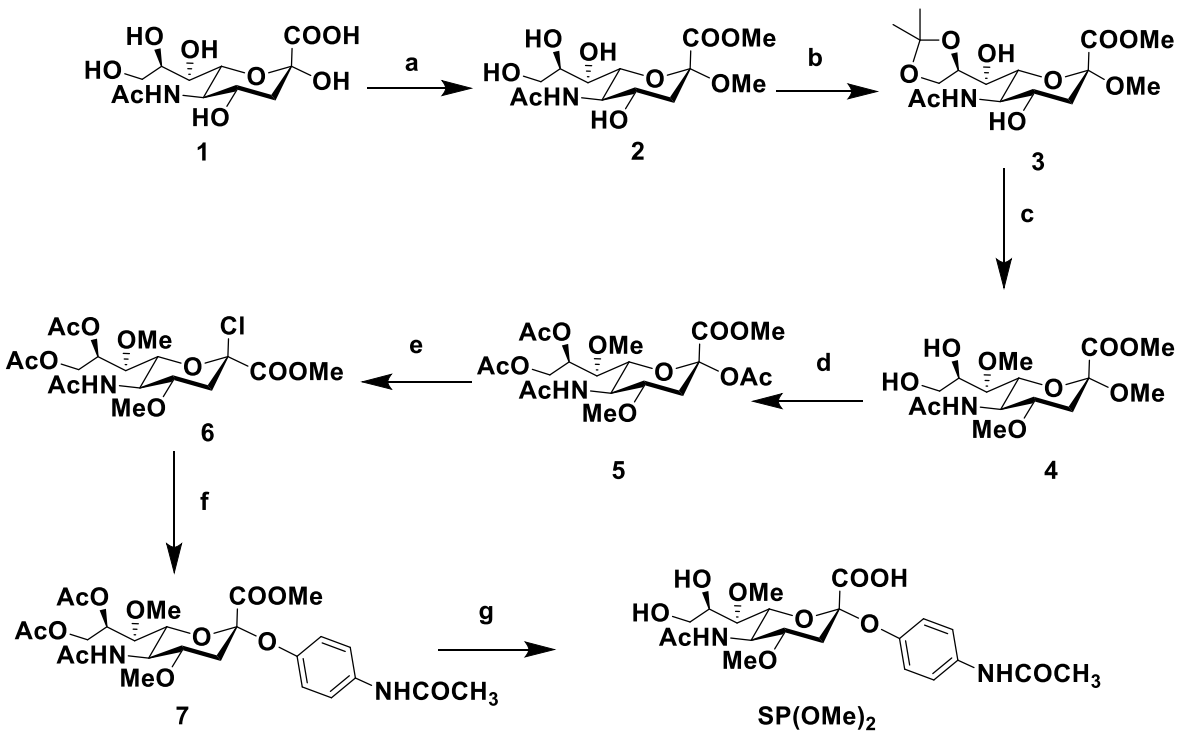

Scheme 1. Synthesis of SP(OMe)$_2$

Reagents and conditions: a) H^+ resin, anhydrous MeOH, reflux, 65^0C, 72h, 75%, b)Anhydrous Acetone, TsOH, pH=6.0, 3h, rt, 72%, c) $Ba(OH)_2$, BaO, CH_3I, DMF, 45h, rt,66% d)i)NaOMe, MeOH, 3h, rt, ii) HCl(l),H+ resin, MeOH, 5h, rt iii)Ac_2O, Pyridine, DMAP, 15h, rt, 66% (over 3 steps) e)HCl (g), AcCl, Anhydrous CH_2Cl_2 3h, rt, (crude, not purified) f) N-(4-hydroxyphenyl)acetamide, Na_2CO_3, TBHSO4, anhydrous EtOAc, rt, 3h, 63% b) i.NaOMe, MeOH, 2h; ii. aq. 0.05 N NaOH, rt, 2h, 92%.

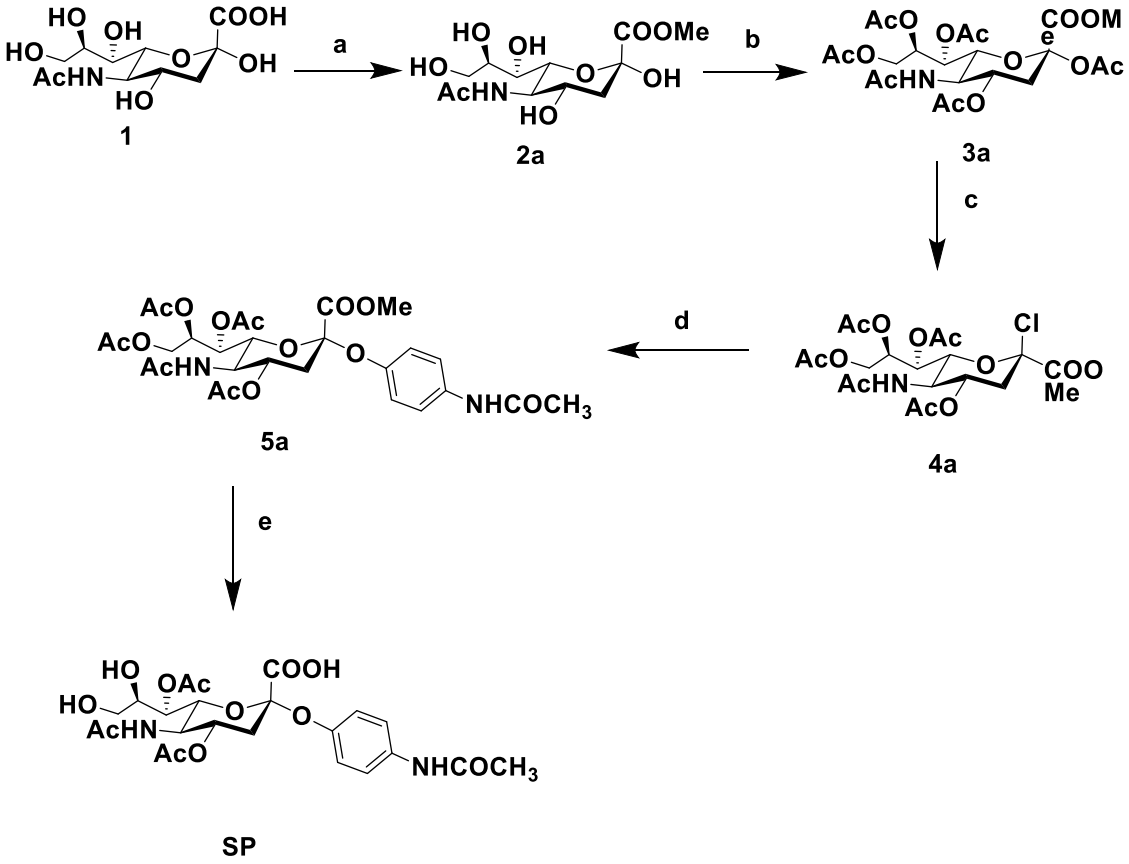

Scheme 2. Synthesis of SP

Reagents and conditions: a) H^+ resin, anhydrous MeOH, rt, 12h, 79%, b) Ac2O, Pyridine, DMAP, 15h, rt, 66% c) HCl (g), AcCl, Anhydrous CH_2Cl_2 3h, rt, (crude, not purified) d) N-(4-hydroxyphenyl) acetamide, Na_2CO_3, TBHSO4, anhydrous EtOAc, rt, 3h,58%. b) i. NaOMe, MeOH, 2h; ii. aq. 0.05 N NaOH, rt, 2h, 94%

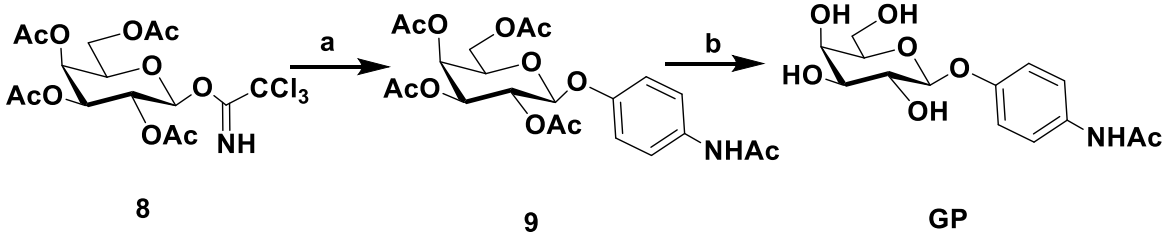

Scheme 3: Synthesis of GP:

Reagents and conditions: a) Acetaminophenol, TMSOTf, DCM, 0 ^{0}C, 2h, 76% b) i) NaOMe, MeOH rt 1h, ii) Pd $(OH)_2/C/H_2$, EtOH rt 12 h 1h, 95% (over two steps)

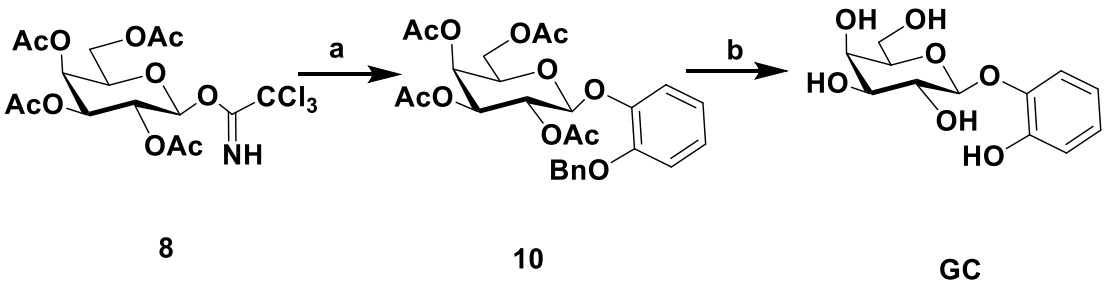

8 10 GC

Scheme 4:Synthesis of GC

Reagents and conditions a) 2-(benzyloxy) phenol, TMSOTf, DCM, 0 ^{0}C, 2h, 71% b) i) NaOMe, MeOH rt 1h, ii) Pd $(OH)_2/C/H_2$, EtOH rt 12 h 1h, 92% (over two steps)

To summarize the synthesis of the compounds, GP, MP, etc. were synthesized in high yield and in minimal number of steps. All compounds were characterized extensively with NMR and mass spectroscopies and were obtained in pure form for the biological assays.

2.3.1 Detection of Enzymes and E. coli

The first assay we developed was to detect enzymes such as β-galactosidase and α-mannosidase. We chose these glycosidases as they are commonly used in several biochemical assays to indicate the presence of microorganisms. **GP**[23] was introduced to different concentrations of β-galactosidase and after different times, a drop of the solution (μL) was used to measure the paracetamol concentration. When 100 U (1 unit (U) of β-galactosidase will hydrolyze 1umole of o-nitrophenyl-β-galactosidase to o-nitrophenol and β-D-galactose per minute at pH=7.3 at 37^{0}C) of the enzyme was used, paracetamol was released almost instantaneously, and the reaction was complete in 15 mins. We determined the limit to be 0.01 U of enzyme in 5 min, however, given a longer incubation time, the limit of detection can be decreased further as this is an enzyme-based

detection assay. To demonstrate that we can detect β-galactosidase in different matrices using this assay system, we spiked **GP** in different matrices and performed similar experiments. Matrix effects are not an issue. A similar result was obtained with **MP** [24] and α-mannosidase. These experiments demonstrate that we can reliably detect enzymes using paracetamol releasing substrates.

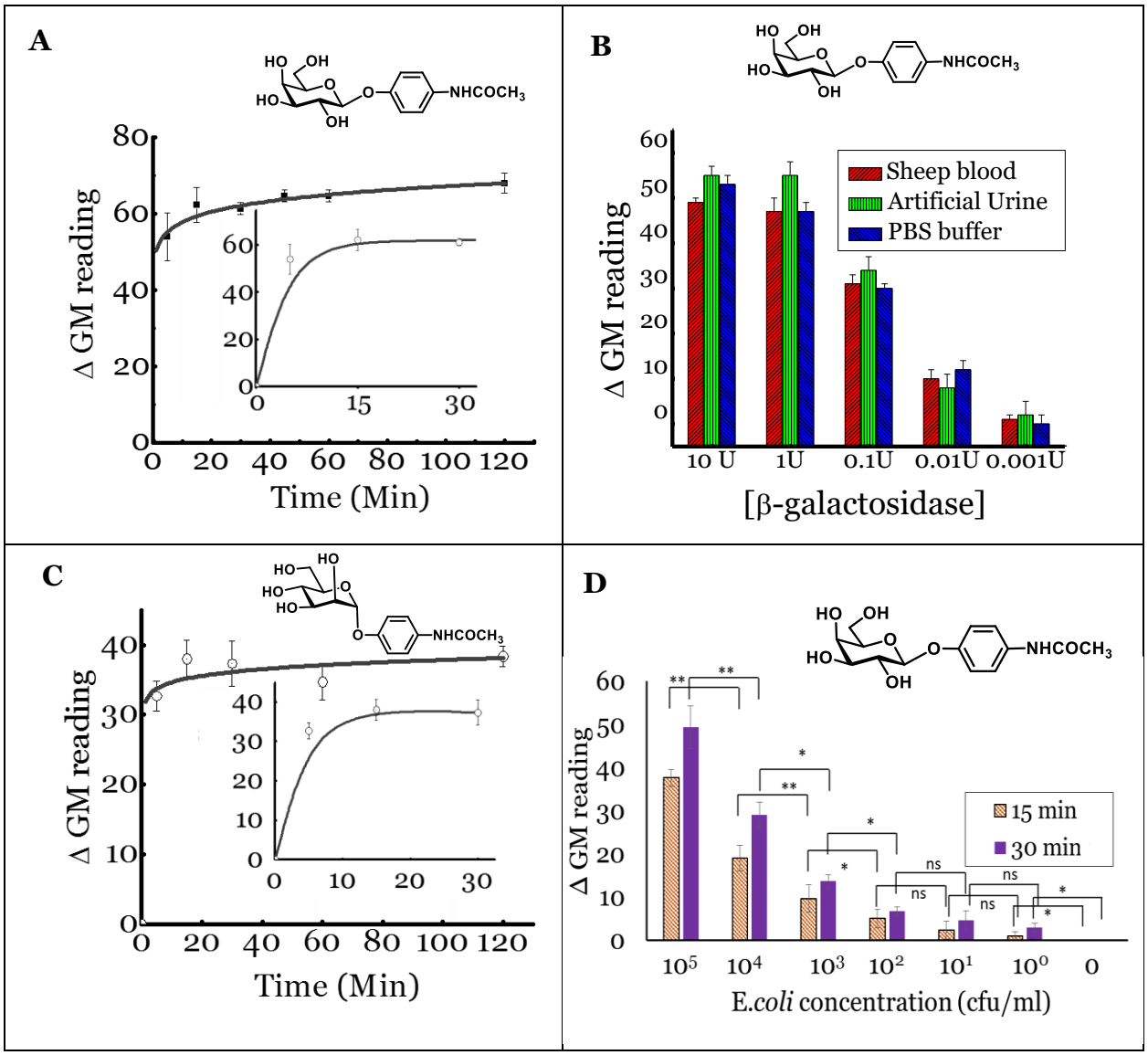

Figure 19*. Detection of enzymes and E. coli using Onetouch meters and Unistrips.*

A. Rapid detection of β-galactosidase: 1 mM of **GP** was incubated with 100 U of enzyme and monitored at different times. **B.** Rapid detection of β-galactosidase in various matrices: Various concentrations of β-galactosidase enzyme was added to artificial urine, defibrinated glucose-free sheep blood, and phosphate buffered saline (PBS) solutions and paracetamol was measured. **C**. Rapid detection of α-mannosidase: 1 mM of **MP** was incubated with 10 U of enzyme and monitored at different times. **D**. Rapid detection of *E. coli* and limit of detection studies: 1 mM of **GP** was incubated with different *E. coli* concentrations and paracetamol was measured at 15 and 30 min. The y axis, Δ glucose meter reading, represents the difference in current between the negative control (no enzyme or *E. coli*) and the sample. All experiments were performed in triplicate (*p<0.05, **p<0.01, ***p<0.001, ns>0.05).

Building on these results, we performed experiments to detect *Escherichia coli*. Detection of *E. coli* in recreational and drinking water is typically done by culture-based methods and the disadvantage of these methods is that it requires a microbiology laboratory, trained personnel and it is time consuming.[25-27] Colorimetric methods are available, but those tests rely on a visual color change, which might be subject to human error, especially when turbid or murky water samples are being tested.[25,28] The assays described here use an electronic output and therefore, are not subject to the same human errors. Since β-galactosidase is released by the bacteria, we introduced **GP** to different concentrations of *E. coli* and measured the response at 15 min and 30 min.). We could detect 10^2 CFU/ml in 15 min; however, a longer time of 1 h is required to obtain a better linear range because it is an enzyme-based detection method.

2.3.2 Detection of Influenza

The next set of experiments were designed to demonstrate broad scope and to detect and differentiate influenza viruses from *Streptococcus pneumoniae*. Briefly, influenza virus is a deadly respiratory pathogen that spreads rapidly. Early and accurate detection is important to reduce the disease burden. [29-31] Of importance is to differentiate between influenza and *S. pneumoniae* as this bacterium has been demonstrated to result in severe secondary illness after the initial attack by influenza viruses. [32-35] Previously, we reported the rapid and specific electrochemical detection and differentiation of influenza viruses in 15 minutes after sample processing using glucose and galactose bearing substrates. [15]

Here, we use paracetamol bearing substrates to rapidly and specifically detect influenza viruses. When **SP** was exposed to a H3N2 strain of influenza virus (A/Aichi/2/1968) or *S. pneumoniae* (serotype 1, ATCC 6301), paracetamol was released as evidenced by the increase in the glucose meter readings, with *S. pneumoniae* producing a higher value. This is anticipated as the compound represents the natural substrate present on the termini of the glycocalyx of mammalian cells and all neuraminidases, viral, bacterial and human, cleave the natural substrate.[36-39] However, when **SP(OMe)$_2$** was used, only influenza virus cleaves the substrate and not the bacteria because the methoxy groups interferes with the smaller binding pocket of the bacterial neuraminidase.[15,40-42] Therefore, this compound can be used to specifically detect influenza viruses. The limit of detection studies with two different strains of influenza viruses, a H1N1 (A/SolomonIslands/3/2006) and a H3N2 (A/Aichi/2/1968) strain indicate that we can detect 10^1 pfu/sample of influenza viruses rapidly. The range of detection for both strains can be improved if a longer time is used as these are enzyme-based assays. We also note that different strains could potentially be differentiated using this technique using continuous glucose meters; standard curves

as a function of time for each strain could be developed and data from an unknown sample can be fitted to these curves to identify the specific strain.

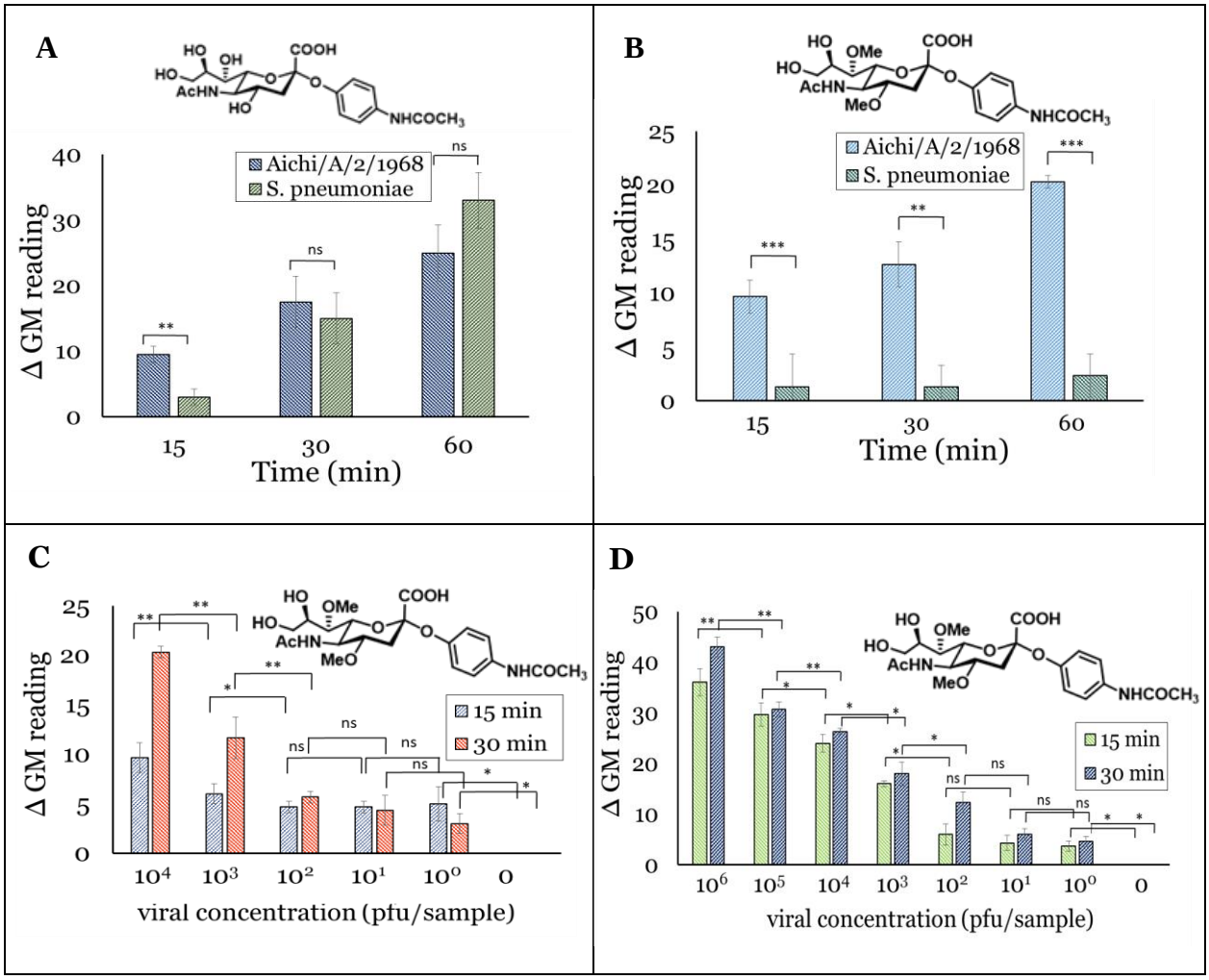

***Figure 20**. Rapid detection of influenza virus and S. pneumoniae.*

A. 1 mM of substrate **SP** was incubated with 100 µL of 10^4 pfu/sample of influenza *A/Aichi/2/1968(*H3N2) or 10^6 CFU/ml *S. pneumoniae*. Readings were taken at 15, 30- and 60-min. **B**. 1 mM of substrate **SP(OMe)$_2$** was incubated with 100 µL of 10^4 pfu/sample of influenza *A/Aichi/2/1968 (*H3N2) or 10^6 CFU/ml of *S. pneumoniae.* Readings were taken at 15, 30- and 60-min. **C.** Limit of detection of influenza virus *A/Aichi/2/1968(*H3N2): 1 mM of substrate **SP(OMe)$_2$** was incubated with different concentrations of *A/Aichi/2/1968(*H3N2) at 37 °C for 1 h. Readings

were taken at 15 and 30 min. **D**. Limit of detection of influenza virus *A/Solomon Islands/3/2006 (*H1N1): 1 mM of substrate **SP(OMe)$_2$** was incubated with different concentrations of *A/Solomon Islands/3/2006 (*H1N1) at 37 °C for 1 h. Readings were taken at 15 and 30 min. The y axis, Δ glucose meter reading, represents the difference in current between the negative control (no virus*)* and the sample. All experiments were performed in triplicate (**p*<0.05, ***p*<0.01, ****p*<0.001, ns>0.05).

2.3.3 Matrix effects

To demonstrate that background glucose does not affect the readings, we purchased commercial screen-printed electrodes without any enzyme imprinted on them. Next, the strips were connected to a portable potentiostat and the current was measured when exposed to PBS buffer, which served as our negative control. As expected, there was no current generated as there is no analyte in solution. (**Table 5**) When exposed to 2 mM glucose solution, no current was generated as the enzyme required to convert glucose to gluconolactone is not present. Next, the strips were exposed to 2 mM paracetamol solution. We observed an increase in the current since paracetamol is directly oxidized on the surface of the electrodes. Finally, a mixture of 2mM glucose and 2 mM paracetamol was exposed to the strips. The increase in current was equal to the increase observed when only 2 mM paracetamol was used. The 2 mM glucose present in the solution that contained the mixture of 2 mM glucose and 2 mM paracetamol did not affect the reading, indicating that background glucose is not a problem. We repeated these experiments in different matrices, such as simulated urine and sheep blood that did not contain glucose to demonstrate there were no matrix effects. Briefly, either paracetamol or glucose or a mixture of paracetamol and glucose were spiked into these samples and the readings were taken using strips

without any glucose oxidase. As seen in **Table 5**, there are no matrix effects and background glucose are not an issue when we are detecting paracetamol.

Test solution	**Current output from i-t curve (I/ X 10^{-8} A)**		
	Strips coated with 0.5 % Chitosan (in 2% Acetic Acid)		
	PBS buffer	**Urine**	**Sheep Blood**
Control (no paracetamol or Glucose).	0.7±0.1	1.0±0.4	0.8±0.1
2mM Glucose solution added to control.	0.6±0.1	0.7±0.3	0.7±0.1
2mM paracetamol solution added to control.	141.0±6.8	133.1±11.6	135.4±4.3
2mM paracetamol + 2mM Glucose solution added to control.	138.3±7.0	134.6±14.1	135.3±5.0

Table 5. *Studies demonstrating that background glucose is not a problem when glucose oxidase or dehydrogenase enzyme is absent.*

2.3.4 Use of catechol to as an alternate electrochemical signal

The final set of experiments was designed to broaden the scope of the output, i.e., replacing paracetamol by catechol. This would allow more options for detection if paracetamol bearing substrates are more complicated to synthesize or the sample contains high levels of paracetamol. First, we generated a standard curve for catechol. Next, we synthesized a catechol bearing substrate **GC** and exposed it to 100 U of β-galactosidase enzyme. The enzyme was detected within 5 mins, indicating that catechol or paracetamol bearing substrates could be used for the rapid detection of enzymes and pathogens using a personal glucose meter.

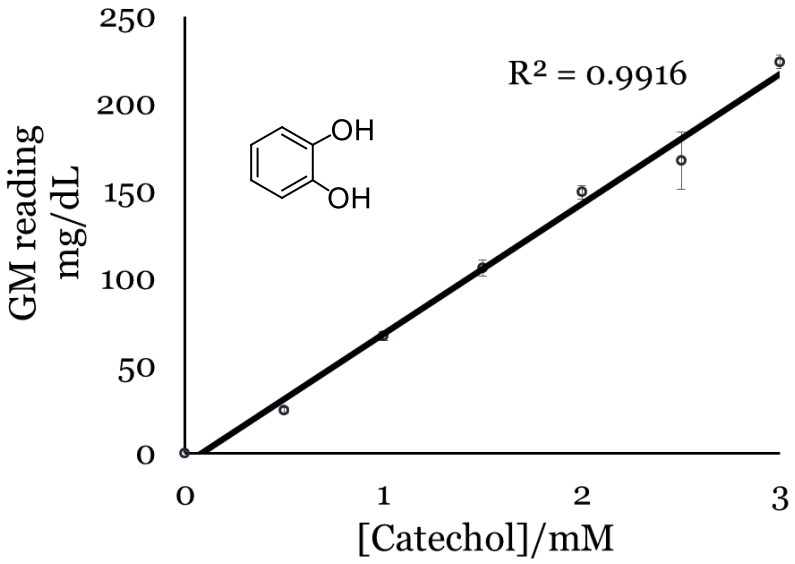

Figure 21. *Calibration curve for catechol using Onetouch glucose meter and unistrip test strips.*

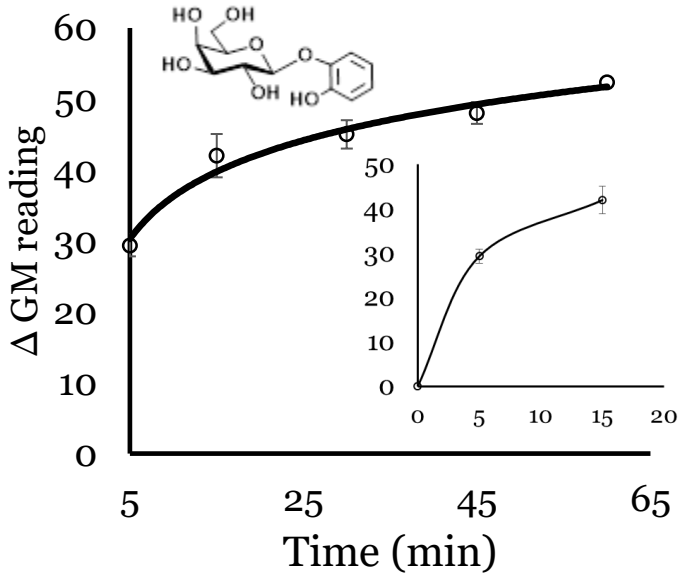

Figure 22. *Rapid detection of β-galactosidase using GC.*

2.4 Experimental Details

2.4.1 General

Glycosylation reactions were performed under argon with solvents dried using a solvent purification system (Innovative Technology Inc., Amesbury, MA, USA). Other chemical reagents were of analytical grade, used as supplied, without further purification unless indicated. The acidic ion exchange resin used was Amberlite® IR-120 (H+) resin. Analytical thin layer chromatography (TLC) was performed on silica gel 230-400 mesh (Silicycle, Quebec City, Canada). Plates were visualized under UV light, and/or by staining with acidic CeH8Mo3N2O12, followed by heating. 1H and 13C NMR spectra were recorded on Bruker 400 MHz spectrometer. Chemical shifts are reported in δ (ppm) units using 13C and residual 1 H signals from deuterated solvents as references. Spectra were analyzed with MNova® (Mestrelab Research, Escondido, CA, USA). Electrospray ionization mass spectra were recorded on a Micromass QT 2 (Waters) and data were analyzed with MassLynx® 4.0 (Waters, Milford, MA, USA) software. Reported yields refer to spectroscopically and chromatographically pure compounds that were dried under high vacuum (10^{-2} mbar) before analytical characterization, unless otherwise specified. **GP** and **MP** were synthesized as described previously.[23,24]

2.4.2 Synthesis and characterization

The synthesis of some of the compounds was performed as described in the literature with some changes. Therefore, the experimental details are described to reflect these changes.[18,23]

Methyl (5-acetamido-3,5-dideoxy-D-*glycero*- β-D-*galacto*-2-nonulopyranosidonate) (2).

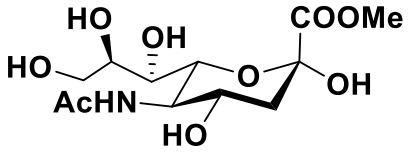

A suspension of *N*-acetylneuraminic acid (**1)** (10.0 g, 32.4 mmol) was treated with the Bio-Rad (H^+) resin (5.0 g) in anhydrous methanol (400 mL) at room temperature with vigorous stirring for 12 h. The resin was filtered off and washed with methanol, and then the filtrate was concentrated and kept at -20 ^oC overnight for crystallization. The crystals were collected and washed with cold ethyl acetate: methanol (6:1) to provide white powder **2a** (8.2 g, 75%). The NMR data matched reported literature values [18]

^{1}H NMR (400 MHz, CD_3OD) δ 1.68 (dd, 1H, *J* = 12.7, 11.4 Hz), 2.38 (dd, 1H, *J*=12.0, 4.9 Hz), 3.31 (s, 3H), 3.54 (d, 1H, *J*=9.1 Hz), 3.69 (dd, 1H, *J* = 12.0, 6.0 Hz), 3.82-3.90 (m, 7H), 4.02-4.06 (m, 1H).

^{13}C NMR (100 MHz, CD_3OD) δ 23.17, 52.06, 53.58, 54.20, 65.72, 68.13, 70.60, 71.82, 72.71, 100.81, 171.29, 175.25. MS (m/z): 338.1 $[M+H]^-$. Anal. Calcd for $C_{13}H_{23}NO_9$: C, 46.29; H, 6.87; N, 4.15. Found: C, 46.13; H, 6.81; N, 4.23.

Methyl (5-acetamido-2,8,9-tri-O-acetyl-3,5-dideoxy-4,7-di-O-methyl- D-*glycero*-α,β-D-*galacto*-2-nonulopyranosidonate) (3a).

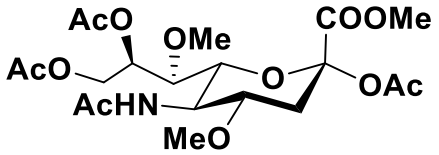

To the suspension of **2a**, Ac_2O (5 mL, 52.9 mmol), pyridine (5 mL) and DMAP (0.2 g) was added and the reaction mixture was stirred at room temperature for 15 h. The liquids were evaporated off and the residue was purified by chromatography on silica gel. The column was washed with mixtures of hexane and ethyl acetate in the ratio 2: 1 and 1 : 1 respectively, and then the product was eluted with ethyl acetate to afford **3a** (1.5 g, 66%) as a white powder.

^{1}H NMR (400 MHz, CD_3OD) δ 1.76 (dd, 1H, *J* = 13.2, 11.3 Hz), 2.08 (s, 3H), 2.12 (s, 3H), 2.12 (s, 3H), 2.20 (s, 3H), 2.66 (dd, 1H, *J* = 13.3, 4.7 Hz), 3.45 (s, 3H), 3.57 (s, 3H), 3.63 (dd, 1H, *J* = 5.5, 1.3 Hz), 3.75 (td, 1H, *J* = 10.8, 4.7 Hz), 3.83 (s, 3H), 3.95 (dd, 1H, *J* = 10.5, 1.0 Hz), 4.11 (t, 1H, *J* = 10.2 Hz), 4.25 (dd, 1H, *J* = 12.4, 6.4 Hz), 4.75 (dd, 1H, *J* = 12.4, 2.3 Hz), 5.09 (td, 1H, *J* = 6.2, 2.3 Hz).

^{13}C NMR (100 MHz, CD_3OD) δ 20.90, 20.95, 21.25, 23.28, 36.98, 51.53, 53.70, 57.65, 61.74, 63.98, 74.34, 74.81, 77.40, 79.00, 99.32, 169.13, 170.32, 171.99, 172.76, 173.68. MS (m/z): 478.2 $[M+H]^-$. Anal. Calcd for $C_{20}H_{31}NO_{12}$: C, 50.31; H, 6.54; N, 2.93. Found: C, 50.43; H, 6.48; N, 2.89.

Methyl (5-acetamido-8,9-di-O-acetyl-3,5-dideoxy-4,7-di-O- methyl-D-*glycero*-β-D-*galacto*-2-nonulopyranosyl chloride)onate (4a).

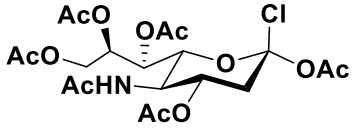

A mixture of AcCl (1.4 mL, 20 mmol) and anhydrous CH_2Cl_2 (10 mL) containing **3a** (1.2 g, 2.6 mmol) was saturated with dry HCl (g) at room temperature, which was continuously stirred for 3 h as observed by TLC, resulting in a complete reaction (R_f = 0.49 in CH_2Cl_2 :

CH_3OH = 92 : 8). Then the reaction mixture was evaporated to dryness in vacuum. The crude **4a** was provided as a white powder which was not further purified and used at once in the next reaction.

Methyl [4-N-acetamidophenyl-(5-acetamido-8,9-di-*O*-acetyl-3,5-dideoxy-D-glycero-α-D-galacto-2-ulopyranosyl)] onate (5a)

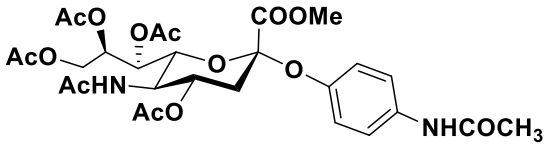

To the stirring, solution of **4a** (0.30 g, 0.64 mmol) in EA, paracetamol (0.12 g, 0.77 mmol) was added. TBHSO4 (0.33 g, 0.96 mmol), was dissolved in 1M solution of Na_2CO_3 and was added dropwise. The biphasic reaction was stirred vigorously for 3 h. The reaction was monitored with TLC. On completion of the reaction, it was diluted with 20 ml of EA; washed with saturated Na2CO3 solution. (X2) The organic layers were collected and dried over Na_2SO_4 and concentrated under reduced pressure. The residue was subjected to flash silica gel column chromatography eluting with *EA*, to afford **5a** (0.25 g, 63%) as white solid.

^{1}H NMR (400 MHz, CDCl3): δ 8.12 (s, 1H), 7.40 (d, *J* = 8Hz, 2H), 6.97 (d, *J* = 8Hz, 2H), 5.92 (d, J = 8Hz, 1H), 5.34-5.34 (m, 2H), 4.93-4.87 (m, 2H), 4.36-4.28 (m, 2H), 4.15-4.05 (m, 2H), 3.59 (s, 3H), 2.67 (dd, J = 20Hz, 8Hz, 1H), 2.10 (s, 3H), 2.09 (s, 3H), 2.07 (s, 3H), 2.01 (s, 3H), 1.99 (s, 3H), 1.85 (s, 3H).

^{13}C NMR (100 MHz, $CDCl_3$): δ 170.8, 170.5, 170.2, 168.6,167.9, 149.8, 134.5, 120.8, 100.2, 73.2, 69.3,68.9, 67.4, 62.0, 52.9, 49.2, 38.0, 24.3, 23.1, 21.0. **ESI-MS:** $[M+Na]^+$: Calcd for $C_{28}H_{36}N_2O_{14}Na$: 647.2167; obtained 647.1951.

4-N-acetamidophenyl-(5-acetamido-3,5-dideoxy-D-glycero-α-D-galacto-2-ulopyranoside)onic acid: (SP)

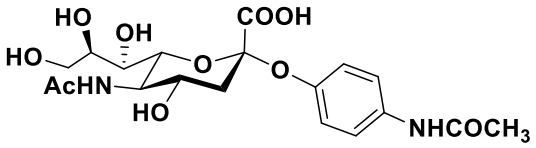

Compound **2** (0.05 g, 0.080 mmol) was dissolved in 1 ml of MeOH and treated with 30% NaOMe in MeOH ((100 µL) and stirred at rt for 1 h. The solution was neutralized with Amberlite IR 120(H^+) resin, filtered and concentrated under reduced pressure. The residue was treated with aqueous 0.05 N NaOH and stirred at rt for 2 h. The reaction was monitored by TLC, the mixture was neutralized with Amberlite IR 120(H^+) resin, filtered and concentrated under reduced pressure and subjected to P2 column to obtain pure compound **SP** (0.034 g, 94%).

^{1}H NMR (400 MHz, D2O): δ 7.24 (d, J = 12 Hz, 2H), 7.07 (d, J = 12 Hz, 2H), 3.83-3.75 (m, 6H), 3.71-3.65 (m, 2H), 3.57-3.49 (m, 4H), 2.79 (dd, J = 20 Hz, 8 Hz, 1H), 2.65 (s, 3H), 1.95 (s, 3H), 1.85 (t, J = 16 Hz, 1H).

^{13}C NMR (100 MHz, D_2O): δ 175.0, 172.9, 171.8, 150.5, 124.6, 123.2, 122.0, 115.7, 101.6, 73.5, 71.3, 68.1, 67.6, 62.8, 51.6, 40.1, 22.6, 22.0. **ESI-MS m/z:** $[M-H]^-$: Calcd for $C_{19}H_{25}N_2O_{10}$: 441.1587; obtained 441.1443.

Methyl (methyl 5-acetamido-3,5-dideoxy-D-*glycero*- β-D-*galacto*-2-nonulopyranosidonate) (2).

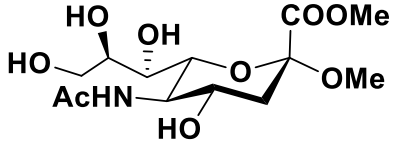

The suspension of *N*-acetylneuraminic acid (**1)** (10.0 g, 32.4 mmol) was treated with the Bio-Rad (H^+) resin (5.0 g) in anhydrous methanol (400 mL) and refluxed with vigorous stirring for 72 h at 65^{o}C. The resin was filtered off and washed with methanol, and then the filtrate was concentrated and kept at -20 ^{o}C overnight for crystallization. The crystals were collected and washed with cold ethyl acetate: methanol (6 **:** 1) to provide white powder **2** (8.2 g, 75%).

^{1}H NMR (400 MHz, CD_3OD) δ 1.68 (dd, 1H, *J* = 12.7, 11.4 Hz), 2.05 (s, 3H), 2.38 (dd, 1H, *J*=12.0, 4.9 Hz), 3.31 (s, 3H), 3.54 (d, 1H, *J*=9.1 Hz), 3.69 (dd, 1H, *J* = 12.0, 6.0 Hz), 3.82-3.90 (m, 7H), 4.02-4.06 (m, 1H).

^{13}C NMR (100 MHz, CD_3OD) δ 23.17, 42.00, 52.06, 53.58, 54.20, 65.72, 68.13, 70.60, 71.82, 72.71, 100.81, 171.29, 175.25. MS (m/z): 338.1 $[M+H]^-$. Anal. Calcd for $C_{13}H_{23}NO_9$: C, 46.29; H, 6.87; N, 4.15. Found: C, 46.13; H, 6.81; N, 4.23.

Methyl (methyl 5-acetamido-3,5-dideoxy-8,9-O-isopropylidene-D-*glycero*-β- D-*galacto*-2-nonulopyranosidonate) (3).

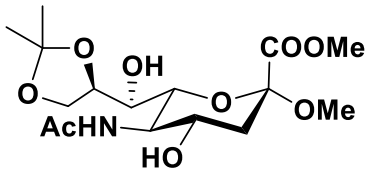

A mixture of **2** (7.0 g, 20.8 mmol) and $TsOH \cdot H_2O$ (0.2 g) in dry anhydrous acetone (100 mL) was stirred at room temperature for 3 h, then neutralized with TEA to pH = 6-7. The solution was evaporated to dryness. The solid was triturated and washed with ether, then purified by chromatography (CH_2Cl_2: CH_3OH: TEA = 95: 5 : 0.1) to afford **3** (5.6 g, 72%) as a white powder.

^{1}H NMR (400 MHz, CD_3OD) δ 1.34 (s, 3H), 1.40 (s, 3H), 1.69 (dd, 1H, *J* = 12.6, 11.6 Hz), 2.06 (s, 3H), 2.39 (dd, 1H, *J* = 13.0, 4.9 Hz), 3.29 (s, 3H), 3.52 (d, 1H, *J* = 8.3 Hz), 3.75 (dd, 1H, *J* = 10.0, 0.5 Hz), 3.85-3.88 (m, 4H), 4.00 (dd, 1H, *J* = 8.4, 5.5 Hz), 4.04 (td, 1H, *J* = 10.6, 4.9 Hz), 4.16 (dd, 1H, *J* = 8.4, 6.3 Hz), 4.29-4.33 (m, 1H).

^{13}C NMR (100 MHz, CD_3OD) δ 22.85, 25.78, 27.42, 41.72, 51.65, 53.31, 53.83, 67.67, 68.81, 71.68, 72.85, 75.98, 100.55, 110.41, 170.81, 174.90. MS (m/z): 378.1 $[M+H]^-$. Anal. Calcd for $C_{16}H_{27}NO_9$: C, 50.92; H, 7.21; N, 3.71. Found: C, 50.94; H, 7.31; N, 3.68.

Methyl (methyl 5-acetamido-3,5-dideoxy-4,7-di-O-methyl-8,9-O- isopropylidene-D-*glycero*-β-D-*galacto*-2-nonulopyranosidonate) (4).

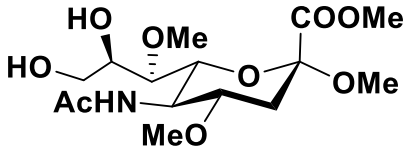

A mixture of **3** (4.0 g, 10.6 mmol) was treated with BaO (5.8 g, 37.7 mmol) and $Ba(OH)_2 \cdot 8H_2O$ (0.7 g, 2.2 mmol) in dry DMF (36 mL). After 20 min, CH_3I (10 mL, 197.3 mmol) was added. The reaction suspension was kept stirring for 45 h at room temperature. The solids were filtered off and washed exhaustively with ethyl acetate. The filtrate was concentrated to about 30 mL by evaporation under diminished pressure, further extracted with ethyl acetate (60 mL) and 5% NaCl solution (30 mL). The organic phase was separated, and the aqueous phase was extracted with ethyl acetate (60 mL) again. The collected organic phase was dried over anhydrous Na_2SO_4, then evaporated to 5 mL under reduced pressure and kept at -20 ^{o}C with 20 mL ether overnight to give the product **4** as a white powder (2.8 g, 66%).

^{1}H NMR (400 MHz, CD_3OD) δ 1.35 (s, 3H), 1.44 (s, 3H), 1.57 (dd, 1H, *J* = 12.9, 11.4 Hz), 2.04 (s, 3H), 2.51 (dd, 1H, *J* = 12.9 , 4.8 Hz), 3.26 (s, 3H), 3.38 (s, 3H), 3.54 (s, 4H), 3.66 (td, 1H, *J* = 10.8, 4.8 Hz), 3.79 (dd, 1H, *J* = 10.7, 0.9 Hz), 3.83 (s, 3H), 4.03-4.09 (m, 2H), 4.16 (dd, 1H, *J* = 8.5, 6.3 Hz), 4.30 (dd, 1H, *J* = 12.1, 6.4 Hz).

^{13}C NMR (100 MHz, CD_3OD) δ 23.12, 25.67, 27.04, 37.86, 51.38, 51.64, 53.11, 57.31, 61.90, 67.49, 73.48, 77.84, 78.20, 80.00, 100.46, 109.55, 169.84, 173.41. MS (m/z): 406.2 $[M+H]^-$. Anal. Calcd for $C_{18}H_{31}NO_9$: C, 53.32; H, 7.71; N, 3.45. Found: C, 53.43; H, 7.61; N, 3.49.

Methyl (5-acetamido-2,8,9-tri-O-acetyl-3,5-dideoxy-4,7-di-O-methyl- D-*glycero*-α,β-D-*galacto*-2-nonulopyranosidonate) (5).

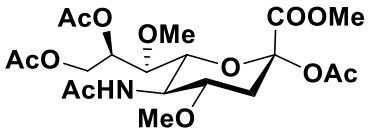

The product **4** (2.0 g, 4.9 mmol) was suspended in mixture of methanol/water (1 : 1, 20 mL). 1 M NaOH (10 mL) was added and the reaction mixture was stirred for 3 h, the reaction was neutralized by adding Bio-Rad (H^+) resin to pH = 7.0. The resin was filtered off, washed with methanol and the washing was evaporated to dryness. HCl (30 mM, 33 mL) was added to residue as well as Bio-Rad resin (2.0 g), then the resulting mixture was heated at 70 ^{o}C for 16 h. The resin was filtered off and washed with water. The solvent was evaporated off and the residue was dissolved in dry methanol (26 mL). Bio-Rad resin (1.7 g, dried over P_2O_5) was added and the reaction mixture was stirred for 5 h at room temperature. The resin was filtered off and the methanol was evaporated with the addition of 0.5 mL pyridine. The residue was dried under high

vacuum for 15 h over P_2O_5. It was then treated with Ac_2O (5 mL, 52.9 mmol), pyridine (5 mL) and DMAP (0.2 g) for 15 h at room temperature. The liquids were evaporated off and the residue was purified by chromatography on silica gel. The column was washed with mixtures of hexane and ethyl acetate in the ratio 2: 1 and 1 : 1 respectively, and then the product was eluted with ethyl acetate to afford **5** (1.5 g, 66%) as a white powder.

^{1}H NMR (400 MHz, CD_3OD) δ 1.76 (dd, 1H, *J* = 13.2, 11.3 Hz), 2.08 (s, 3H), 2.12 (s, 3H), 2.12 (s, 3H), 2.20 (s, 3H), 2.66 (dd, 1H, *J* = 13.3, 4.7 Hz), 3.45 (s, 3H), 3.57 (s, 3H), 3.63 (dd, 1H, *J* = 5.5, 1.3 Hz), 3.75 (td, 1H, *J* = 10.8, 4.7 Hz), 3.83 (s, 3H), 3.95 (dd, 1H, *J* = 10.5, 1.0 Hz), 4.11 (t, 1H, *J* = 10.2 Hz), 4.25 (dd, 1H, *J* = 12.4, 6.4 Hz), 4.75 (dd, 1H, *J* = 12.4, 2.3 Hz), 5.09 (td, 1H, *J* = 6.2, 2.3 Hz).

^{13}C NMR (100 MHz, CD_3OD) δ 20.90, 20.95, 21.25, 23.28, 36.98, 51.53, 53.70, 57.65, 61.74, 63.98, 74.34, 74.81, 77.40, 79.00, 99.32, 169.13, 170.32, 171.99, 172.76, 173.68. MS (m/z): 478.2 $[M+H]^-$. Anal. Calcd for $C_{20}H_{31}NO_{12}$: C, 50.31; H, 6.54; N, 2.93. Found: C, 50.43; H, 6.48; N, 2.89.

Methyl (5-acetamido-8,9-di-O-acetyl-3,5-dideoxy-4,7-di-O- methyl-D-*glycero*-β-D-*galacto*-2-nonulopyranosyl chloride)onate (6).

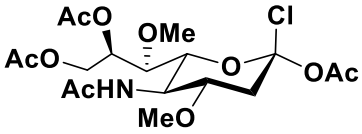

A mixture of AcCl (1.4 mL, 20 mmol) and anhydrous CH_2Cl_2 (10 mL) containing **5** (1.2 g, 2.6 mmol) was saturated with dry HCl (g) at room temperature, which was continuously stirred for 3 h as observed by TLC, resulting in a complete reaction (R_f = 0.49 in CH_2Cl_2 : CH_3OH = 92 :

8). Then the reaction mixture was evaporated to dryness in vacuum. The crude **6** was provided as a white powder which was not further purified and used at once in the next reaction.

Methyl [4-N-acetamidophenyl-(5-acetamido-8,9-di-*O*-acetyl- 3,5-dideoxy-4,7-di-*O*-methyl D-glycero-α-D-galacto-2-ulopyranosyl)] onate (7):

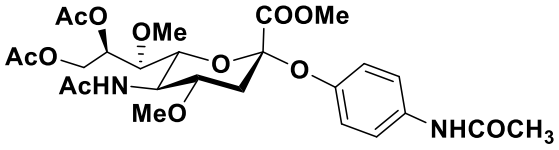

To a solution of **6** (0.40 g, 0.88 mmol) in EA, paracetamol (0.16 g, 1.1 mmol) was added. $TBHSO_4$ (0.45 g, 1.3 mmol) was dissolved in 1M solution of Na_2CO_3 in H_2O and was added dropwise to the above stirring solution. The bi-phasic reaction was stirred vigorously for 3 h. The reaction was monitored with TLC. On completion of the reaction, it was diluted with 20 ml of EA; washed with saturated Na2CO3 solution. (X2) The organic layers were collected and dried over Na_2SO_4 and concentrated under reduced pressure. The residue was subjected to flash silica gel column chromatography eluting with *EA*, to afford **7** (0.29 g, 58%) as white solid.

^{1}H NMR (400 MHz, CDCl3): δ 7.57 (s, 1H), 7.37 (d, *J* = 8Hz, 2H), 7.01 (d, *J* = 8 Hz, 2H), 5.56-5.54 (m, 1H), 5.36-5.26 (m, 2H), 4.62-4.59 (m, 1H), 4.25-4.09 (m, 4H), 3.63 (s, 3H), 3.52 (s, 3H), 3.34 (s, 3H), 2.81 (dd, J = 16 Hz, 8 Hz, 1H), 2.14 (s, 3H), 2.10 (s, 3H), 2.08 (s, 3H), 2.05 (s, 3H), 1.95 (t, J= 12 Hz, 1H).

^{13}C NMR (100 MHz, $CDCl_3$) δ 170.7, 170.6, 170.2, 168.4, 150.2, 134.1, 121.1, 100.7, 73.7, 70.9, 63.1, 61.4, 56.4, 53.5, 50.3, 37.7, 24.8, 23.4, 21.1, 13.9. **ESI-MS m/z:** $[M+K]^+$: Calcd for $C_{26}H_{36}N_2O_{12}$ K: 607.2268; obtained 607.2259.

4-N-acetamidophenyl-(5-acetamido-3,5-dideoxy-4,7-di-*O*-methyl D-glycero-α-D-galacto-2-ulopyranoside)onic acid: SP(OMe)$_2$

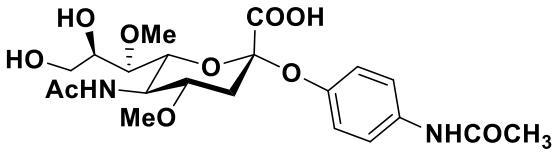

Compound **7** (0.03 g, 0.05 mmol) was dissolved in 1 ml of MeOH and treated with 30% NaOMe in MeOH (100 µL) and stirred at rt for 1 h. The solution was neutralized with Amberlite IR 120(H^+) resin, filtered and concentrated under reduced pressure. The residue was then treated with aqueous 0.05 N NaOH and stirred at rt for 2h. The reaction was monitored by TLC, the mixture was neutralized with Amberlite IR 120(H^+) resin, filtered and concentrated under reduced pressure and subjected to P2 column to obtain pure compound **SP(OMe)$_2$** (0.022 g, 98%).

^{1}H NMR (400 MHz, D$_2$O): δ 7.25 (d, *J* = 8 Hz, 2H), 7.05 (d, *J* = 8 Hz, 2H), 3.93-3.80 (m, 2H), 3.79-3.57 (m, 2H), 3.46 (s, 2H), 3.45-3.38 (m, 2H), 3.36-3.34 (m, 1H), 3.33 (s, 3H), 3.33 (s, 3H), 3.28-3.26 (m, 1H), 2.91 (dd, *J* = 12.5, 4.4 Hz, 1H), 2.06 (s, 3H), 1.96 (s, 3H), 1.73 (t, J = 12 Hz, 1H)

^{13}C NMR (100 MHz, D$_2$O): δ 174.1, 172.9, 172.5, 171.0, 165.9, 151.1, 123.3, 122.1, 102.9, 78.3, 78.0, 73.1, 71.4, 69.6, 62.2, 60.2, 56.7, 49.8, 37.4, 22.6, 22.2. **ESI-MS m/z:** [M-H]$^-$: Calc. for $C_{21}H_{29}N_2O_{10}$: 469.1900; obtained 469.1828.

2-benzyloxyphenyl 2,3,4,6-tetra-*O*-acetyl-β-D-galactopyranoside (4):

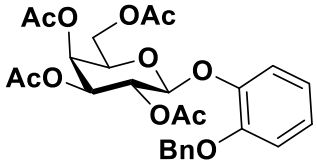

To the stirring solution of galactose imidate **3** (0.20g, 0.40 mmol) in DCM, 2-(benzyloxy) phenol (0.10g, 0.54 mmol) was added. TMSOTf (1 ml, 0.04 mmol solution in DCM) was added dropwise at 0 ^{0}C. The reaction was monitored using TLC. Et_3N was added to quench the reaction and warmed to rt. The reaction mixture was diluted with DCM, washed with Na_2CO_3 (X2) and brine solution (X2). The organic layers were collected and dried over Na_2SO_4 and concentrated under reduced pressure. The residue was subjected to flash silica gel column chromatography eluting with hexane: EA (40:60) to afford **4** (0.15 g, 71%) as white solid.

^{1}H NMR (400 MHz, CDCl3): δ 7.46-7.39 (m, 4H), 7.35-7.34 (m, 1H), 7.19-7.17 (m, 1H), 7.05-7.03 (m, 1H), 6.99-6.90 (m, 2H), 5.58-5.54 (m, 1H), 5.45 (d, J=4Hz, 1H), 5.11-5.08 (m, 2H), 5.01 (d, J=8Hz, 1H), 4.26-4.13 (m, 3H), 4.00-3.97 (m, 1H), 2.20 (s, 3H), 2.06 (s, 3H), 2.02 (s, 3H), 1.82 (s, 3H)

^{13}C NMR (100 MHz, D_2O): δ 136.9, 128.5, 128.0, 127.4, 121.4, 120.2, 114.9, 101.0, 92.4, 85.4, 72.0, 70.9, 68.7, 66.2, 61.2, 29.7, 29.4, 20.6, 20.4, 17.4, 13.4. **ESI-MS m/z:** $[M+K]^-$: Calc for $C_{27}H_{30}O_{11}K$: 569.1830; obtained 569.3121

2-hydroxyphenyl β-D-galactopyranoside (GC):

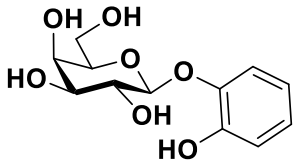

Compound **4** (0.05 g, 0.09 mmol) was dissolved in 1 ml of MeOH and treated with a 30% solution of NaOMe in MeOH (70 µL) and stirred at rt for 1 h. The solution was neutralized with Amberlite® IR 120 (H^+) resin, filtered and concentrated to dryness. The dried compound was treated with Pd (OH)2/C (0.01 g) in absolute EtOH, was stirred for 12h at rt under H2 at 1 atmosphere. After completion of reaction as monitored by TLC, reaction mixture was filtered

using celite pad, washed with EtOH and combined solvent was concentrated to dryness and subjected to P-2 gel column to furnish **GC** (0.023 g, 92%).

^{1}H NMR (400 MHz, D_2O): δ 7.12 (d, J=8 Hz, 1H), 6.98-6.94 (m, 1H), 6.91-6.83 (m, 2H), 4.94 (d, J=8Hz, 1H), 3.97 (s, 1H), 3.92 (d, J= 4Hz, 1H), 3.80-3.68 (m, 4H), 3.58-3.54 (m, 1H), 3.49-3.45 (m, 1H).

^{13}C NMR (100 MHz, D_2O): δ 144.9, 124.1, 120.6, 116.8, 101.8, 75.4, 72.5, 70.5, 68.5, 62.5, 60.7. **ESI-MS m/z:** $[M-2H]^-$: Calc for $C1_2H_{14}O_7$: 270.2530; obtained 270.1854.

2.4.3 Biological Assays

2.4.3.1 Materials:

β-galactosidase from Escherichia coli and α-Mannosidase from Canavalia ensiformis (Jack Bean) were purchased from Sigma Aldrich, St. Louis, MO, USA. H3N2 (A/Aichi/2/1968), H1N1 (A/Brisbane/59/2007) were obtained from Beiresources (NIAID). *S. pneumoniae* ATCC 6301 and *E. coli* B (ATCC 11303) were obtained from American Type Culture Collection (ATCC). Glucose meter One Touch Ultra 2 and Unistrip-1 generic blood glucose strips were purchased from Amazon. Defibrinated sheep blood was purchased from ThermoFisher Scientific (Waltham, MA) and treated with hexokinase to remove residual glucose. Artificial urine without glucose was purchased from Carolina Biologicals (Burlington, NC).

Generation and growth of pathogens:

***E. coli* bacterial growth**: The *E. coli* B (ATCC 11303) samples were grown in Luria-Bertani (LB) broth for 24 h at 37^0C, supplemented with a final concentration of 1 mM isopropyl β -D-thiogalactopyranoside (IPTG) for the induction of β-galactosidase enzyme. The cells were harvested by centrifuging them at 2500 rpm for 5 min and re-suspended in sterile PBS buffer. 1% Triton was added to the *E. coli* cells to lyse and release the β - galactosidase enzyme.

***S. pneumoniae* bacterial growth**: *S. pneumoniae* (ATCC 6301) was inoculated in Brain Heart Infusion (BHI) broth which was augmented with 0.16g/L of sialic acid to enhance NA production by the bacteria. Bacterial concentration was determined as 1.2 X 106 CFU/ml using colony count method. 100 µL of bacterial solution was lysed using 0.01% SDS and 20µl of chloroform was added to it. The sample was then lysed by vortexing for 30 sec and incubating at a temperature of 28^0C for 5 min.

2.4.4 Detection of different pathogens

For all measurements, since the range of glucose meters has been set for testing normal blood glucose levels, low concentrations of glucose or paracetamol are recorded as "error". Since we are detecting low concentrations of paracetamol, a known concentration of paracetamol is added to all solutions to establish a baseline number, which is subtracted from the assay readings.

Detection of enzymes or *E. coli*: 100 µL of different concentrations of β-galactosidase or α-mannosidase or lysed *E. coli* was mixed with 100 ul of substrate **GP** or **GC** (3 mM) and 100 µl of paracetamol (3 mM) in PBS or citrate buffer at 37^0C for 1 h. 2 µL of the solution was used to measure the release of paracetamol using the Onetouch meter and Unistrips.

Detection of influenza virus or *S. pneumoniae*: 100 µL of different concentrations of lysed H3N2 (A/Aichi/2/1968), H1N1 (A/Brisbane/59/2007) or *S. pneumoniae* was mixed with 100 µL of substrate **SP** or **SP(OMe)$_2$** (3 mM) and 100 µl of paracetamol (3 mM) in PBS buffer at 37^0C for 1 h. 2 µL of the solution was used to measure the release of paracetamol from the substrate.

2.5 Discussion

We have been developing point of care diagnostics using glucose meters for the past several years. Our previous detection strategy involved the development of glucose or galactose-based

substrates. Exposure of these substrates to enzymes or pathogens released glucose or galactose, which was readily detected using a personal glucose meter. However, improvements to this strategy are required for several reasons. First, glucose is present in blood and in urine and other body fluids for diabetic and prediabetic patients. High background levels of glucose could cause a problem in the detection strategy. Second, detecting bacteria using glucose or galactose is problematic because the released glucose or galactose is used as a food source by *E.coli*, making it difficult to detect.[43]

In our investigations, we discovered that there are a few interfering chemical compounds that can perturb the glucose meter reading.[44] One such compound is acetaminophen or paracetamol, which can directly get oxidized at the electrode surface, which made us realize that we could incorporate paracetamol into the substrate. Cleavage of the substrate will release paracetamol, which can be detected by the glucose meter. Therefore, we have introduced paracetamol or catechol as an alternate output molecule and demonstrated that this strategy can be used to detect enzymes, viruses and bacteria. An advantage is the ease of synthesis of these derivatives compared to more complex synthesis using glucose; the latter has five hydroxyl groups compared to one hydroxyl group present in paracetamol. A second advantage is that paracetamol and catechol have higher sensitivity than glucose, the limit of detection for paracetamol is 0.5 mM. In contrast, the limit of detection of glucose is 2 mM as measured using a Onetouch glucose meter. Thus, the detection limits of the enzyme in question can be decreased. A third advantage is the strips without glucose oxidase or dehydrogenase can be used to detect paracetamol. (**Figure 16A, B**). Thus, background glucose or galactose will no longer be an issue if glucose oxidase or dehydrogenase is removed. The cost of producing the strips will also be reduced and the robustness of the strips will

be increased as glucose oxidase or dehydrogenase is not required. One concern that could potentially arise is the presence of high levels of paracetamol in the blood or other body fluids. While paracetamol is not present in bodily fluids such as urine, blood or saliva, paracetamol is a pain medication. Fortunately, the peak plasma concentration reaches a maximum of ~ 20 microgram, which is too low for detection by a glucose meter. [45-47] The concentration in peripheral blood is negligible and after a few hours, the drug is metabolized and excreted through urine as predominantly acetaminophen glucuronide.[48] Thus, we are not overly concerned with background paracetamol levels and furthermore, catechol can be used instead of paracetamol. The assays described here compare very well with other established assays. For influenza viruses, the diagnostic tests available in the marketplace are rapid influenza antigen detection tests (RIDTs), direct fluorescent-antibody assays (DFAs) and nucleic acid amplification tests (NAAT). The commercially available RIDTs for clinical samples provide a qualitative yes/no answer within 15-30 mins. However, their sensitivity varies between 60-70% and can be lower, depending on the sample.[49,50] DFAs are more sensitive compared to the RIDTs, but require around 2-3 h and skilled personnel to analyze the results. NAATs, e.g. Alere-i are highly sensitive and have a low detection limit of 10^1 to 10^3 pfu/ml and can be detected within 15-30 mins but are very expensive.[51] The electrochemical assay described here is inexpensive, user-friendly and can detect 10^1 pfu/sample of influenza rapidly. This assay also compares very well for *E. coli* with established assays. Fluorescent based enzyme assays for *E. coli* focuses on the release of 4- Methylumbelliferyl-β-D-glucuronide (MUG) substrate. The hydrolysis of MUG releases fluorescent 4-methylumbelliferone (4-MU) and the intensity of the measured fluorescent signal is proportional to the amount of *E. coli* present in the sample. Using this method it is possible to detect 10-10^8 CFU/ml of *E. coli* in 20-120 mins, depending on the bacterial count.[52] A hydrogel based, *E. coli* detection system using

a plunger-tube assembly, involving a colorimetric substrate can detect 10^5-10^6 CFU/ml of *E.coli* in 5 mins.[53] The assay reported here can detect 10^2 CFU/ml in 15 mins.

To summarize, we anticipate that this technique will be widely used for the rapid detection of several clinically relevant enzymes to report acute/chronic infections and human disorders as the technique meets the ASSURED criteria.

2.6 Summary and Future work

This study demonstrated that we can use reporters other than glucose to detect enzymes. This is an important advance because, until now, clinically relevant enzymes could not be easily detected in blood, serum and other matrices using glucose meters because of high background levels of glucose. In future studies, the Iyer group will be developing assays that can detect a wide variety of clinically relevant enzymes present in blood or serum for disease diagnosis using repurposed glucose meters and test strips that do not contain glucose oxidase or glucose dehydrogenase.

2.7 References

(1) Limdi, J. K.; Hyde, G. M. Postgraduate medical journal 2003, 79, 307-312.

(2) Hie-Won Hann , S. W., Ronald E. Myers, Richard S. Hann, Jinliang Xing, Bicui Chen, Hushan Yang. Plos ONE 7 2012, 10.

(3) Kwo, P. Y.; Cohen, S. M.; Lim, J. K. Am J Gastroenterol 2017, 112, 18-35.

(4) G Wu, M. Z. SciELO Public Health 2012, 90, 914–920.

(5) Falsey, A. R.; Murata, Y.; Walsh, E. E. Archives of internal medicine 2007, 167, 354-360.

(6) Nelson, R. E.; Stockmann, C.; Hersh, A. L.; Pavia, A. T.; Korgenksi, K.; Daly, J. A.; Couturier, M. R.; Ampofo, K.; Thorell, E. A.; Doby, E. H.; Robison, J. A.; Blaschke, A. J. Pediatr Infect Dis J 2015, 34, 577-582.

(7) Hoffmann, S.; Batz, M. B.; Morris, J. G., Jr. Journal of food protection 2012, 75, 1292-1302.

(8) Cho, I. H.; Ku, S. International journal of molecular sciences 2017, 18.

(9) Mabey, D.; Peeling, R. W.; Ustianowski, A.; Perkins, M. D. Nat Rev Micro 2004, 2, 231-240.

(10) Schnell, O.; Erbach, M.; Wintergerst, E. J Diabetes Sci Technol 2013, 7, 904-912.

(11) Diabetes Care 2016, 39 Suppl 1, S107-108.

(12) Xiang, Y.; Lu, Y. Nature chemistry 2011, 3, 697-703.

(13) Lan, T.; Zhang, J.; Lu, Y. Biotechnol Adv 2016, 34, 331-341.

(14) Zhang, X.; Dhawane, A. N.; Sweeney, J.; He, Y.; Vasireddi, M.; Iyer, S. S. Angewandte Chemie International Edition 2015, 54, 5929-5932.

(15) Cui, X.; Das, A.; Dhawane, A. N.; Sweeney, J.; Zhang, X.; Chivukula, V.; Iyer, S. S. Chemical Science 2017, 8, 3628 – 3634.

(16) Mohapatra, H.; Phillips, S. T. Chem Commun (Camb) 2013, 49, 6134-6136.

(17) Gurale, B. P.; Dhawane, A. N.; Cui, X.; Das, A.; Zhang, X.; Iyer, S. S. Analytical Chemistry 2016, 88, 4248-4253.

(18) Dimeski, G.; Jones, B. W.; Tilley, V.; Greenslade, M. N.; Russell, A. W. Ann Clin Biochem 2010, 47, 358-365.

(19) Ceriotti, F.; Kaczmarek, E.; Guerra, E.; Mastrantonio, F.; Lucarelli, F.; Valgimigli, F.; Mosca, A. Journal of Diabetes Science and Technology 2015, 9, 268-277.

(20) Tonyushkina, K.; Nichols, J. H. Journal of diabetes science and technology (Online) 2009, 3, 971-980.

(21) Engin, C.; Yilmaz, S.; Saglikoglu, G.; Yagmur, S.; Sadikoglu, M. Int J Electrochem Sc 2015, 10, 1916-1926.

(22) Lin, Q. Q.; Li, Q.; Batchelor-McAuley, C.; Compton, R. G. J Phys Chem C 2015, 119, 1489-1495.

(23) Mizuma, T.; Nagamine, Y.; Dobashi, A.; Awazu, S. Bba-Gen Subjects 1998, 1381, 340-346.

(24) Han, Z. F.; Pinkner, J. S.; Ford, B.; Obermann, R.; Nolan, W.; Wildman, S. A.; Hobbs, D.; Ellenberger, T.; Cusumano, C. K.; Hultgren, S. J.; Janetka, J. W. J Med Chem 2010, 53, 4779-4792.

(25) Fiksdal, L.; Tryland, I. Current opinion in biotechnology 2008, 19, 289-294.

(26) Sicard, C.; Shek, N.; White, D.; Bowers, R. J.; Brown, R. S.; Brennan, J. D. Anal Bioanal Chem 2014, 406, 5395-5403.

(27) Maheux, A. F.; Dion-Dupont, V.; Bouchard, S.; Bisson, M. A.; Bergeron, M. G.; Rodriguez, M. J. J Water Health 2015, 13, 340-352.

(28) Deshmukh, R. A.; Joshi, K.; Bhand, S.; Roy, U. MicrobiologyOpen 2016, 5, 901-922.

(29) Heron, M. Natl Vital Stat Rep 2016, 65, 1-95.

(30) Short, K. R.; Habets, M. N.; Hermans, P. W. M.; Diavatopoulos, D. A. Future Microbiology 2012, 7, 609-624.

(31) New influenza A (H1N1) virus: WHO guidance on public health measures, J. Wkly Epidemiol Rec 2009, 84, 261-264.

(32) Mitchell, A. M.; Mitchell, T. J. Clin Microbiol Infect 2010, 16, 411-418.

(33) Krivan, H. C.; Roberts, D. D.; Ginsburg, V. Proc Natl Acad Sci U S A 1988, 85, 6157-6161.

(34) Linder, T. E.; Daniels, R. L.; Lim, D. J.; DeMaria, T. F. Microb Pathog 1994, 16, 435-441.

(35) Tong, H. H.; Blue, L. E.; James, M. A.; DeMaria, T. F. Infect Immun 2000, 68, 921-924.

(36) Varghese, J. N.; Smith, P. W.; Sollis, S. L.; Blick, T. J.; Sahasrabudhe, A.; McKimm-Breschkin, J. L.; Colman, P. M. Structure 1998, 6, 735-746.

(37) Varghese, J. N.; McKimm-Breschkin, J. L.; Caldwell, J. B.; Kortt, A. A.; Colman, P. M. Proteins 1992, 14, 327-332.

(38) Varghese, J. N.; Laver, W. G.; Colman, P. M. Nature 1983, 303, 35-40.

(39) Gut, H.; Xu, G.; Taylor, G. L.; Walsh, M. A. J Mol Biol 2011, 409, 496-503.

(40) Liav, A.; Hansjergen, J. A.; Achyuthan, K. E.; Shimasaki, C. D. Carbohydr Res 1999, 317, 198-203.

(41) Shimasaki, C. D.; Achyuthan, K. E.; Hansjergen, J. A.; Appleman, J. R. Philos Trans R Soc Lond B Biol Sci 2001, 356, 1925-1931.

(42) Achyuthan, K. E.; Pence, L. M.; Appleman, J. R.; Shimasaki, C. D. Luminescence 2003, 18, 131-139.

(43) Chavali, R.; Gunda, N. S. K.; Naicker, S.; Mitra, S. K. Anal Methods-Uk 2014, 6, 6223-6227.

(44) Tang, Z.; Du, X.; Louie, R. F.; Kost, G. J. Am J Clin Pathol 2000, 113, 75-86.

(45) Bannwarth, B.; Netter, P.; Lapicque, F.; Gillet, P.; Péré, P.; Boccard, E.; J Royer, R.; Gaucher, A. Plasma and cerebrospinal fluid concentrations of paracetamol after a single dose of propacetamol, 1992; Vol. 34, p 79-81.

(46) Nielsen, J. C.; Bjerring, P.; Arendt-Nielsen, L.; Petterson, K.-J. European Journal of Clinical Pharmacology 1992, 42, 261-264.

(47) Singla, N. K.; Parulan, C.; Samson, R.; Hutchinson, J.; Bushnell, R.; Beja, E. G.; Ang, R.; Royal, M. A. Pain Pract 2012, 12, 523-532.

(48) Prescott, L. F. British Journal of Clinical Pharmacology 1980, 10, 291S-298S.

(49) Beck, E.; Fan, J.; Hendrickson, K.; Kumar, S.; Shively, R.; Kramp, W.; Villanueva, J.; Jernigan, D.; Klimov, A.; Chen, L.-M.; Donis, R.; Williams, T.; Pirkle, J.; Barr, J. MMWR Morb Mortal Wkly Rep, Centers for Disease Control and Prevention, 2012, 61, 873-876.

(50) Balish, A.; Warnes, C. M.; Wu, K.; Barnes, N.; Emery, S.; Berman, L.; Shu, B.; Lindstrom, S.; Xu, X.; Uyeki, T.; Shaw, M.; Klimov, A.; Villanueva, J. MMWR Wkly Rep 2009, 58, 826-829.

(51) Nie, S.; Roth, R. B.; Stiles, J.; Mikhlina, A.; Lu, X.; Tang, Y.-W.; Babady, N. E. Journal of clinical microbiology 2014, 52, 3339-3344.

(52) Hesari, N.; Alum, A.; Elzein, M.; Abbaszadegan, M. Enzyme Microb Technol 2016, 83, 22-28.

(53) Gunda, N. S.; Chavali, R.; Mitra, S. K. Analyst 2016, 141, 2920-2929.

CHAPTER 3.

* Most of the work described in this chapter has been published in the following publication and it is used in this chapter with permission from Heterocyclic Communication journal:

- **Das, A.;** Gurale, B.; Dhawane, A.; Iyer, S. S., Synthesis of biotinylated bivalent zanamivir analogues as probes for influenza viruses. Heterocycl. Commun. **2017**; 23(3): 181–186.

3 DETECTION OF INFLUENZA VIRUS

3.1 Introduction

Influenza virus is a deadly pathogen which affects the upper and lower respiratory tract and may cause severe illness in infants and old people. The symptoms of the influenza infection can vary from mild to very severe and mostly include fever, runny nose, coughing, sore throat, headaches and muscular pain.[1] The symptoms of the influenza viral infection starts to arise usually after 2-3 days after the exposure and typically last around a week. In severe cases the influenza viral infection is accompanied with viral pneumonia, secondary bacterial pneumonia, trouble with breathing, finally leading to heart failure, causing death in many cases. The major risk groups for influenza infection are children under five years, older people and other immune-compromised individuals.[2] It causes widespread annual epidemics and pandemics every 20 to 30 years. According to World Health Organization (WHO), it severely affects approximately 3 to 5 million people per annum and resulting in 250,000 to 500,000 deaths globally.[1] The influenza virus is a highly contagious virus and spreads very rapidly; an infected individual can spread the infection one day before the onset of the symptoms and 5-7 days after it. Sneezing and coughing during the viral infection create tiny droplets or aerosols of viruses, which facilitates the spread of the virus. Close contact or touching a person who has influenza infection can also spread the virus.[7] Rapid and accurate detection is key to mitigate the spread of virus. Consequently, a rapid point of care kit which can detect the virus accurately is essential. The current U.S. Food and Drug Administration (FDA) approved method for detection of influenza virus, involves polymerase chain reaction (rt-PCR). It is considered as the gold standard for detection of influenza virus.[3] PCR involves long hours and qualified personnel with lab expertise. There are several antibody based

rapid point of care kits that are available in the market, but they are not very sensitive.[4] There is a significant need for a rapid, accurate and sensitive detection method for influenza virus.

3.1.1 History

The first documented use of the word influenza was found in an article in Rome in 1743, to describe a disease which was similar to the plague and caused a huge economic burden on people. The word came from the Latin word *influentia* and the meaning connotes as a disease, caused due to astrological phenomenon.[6] Smith, Andrewes, and Laidlaw were the first to isolate influenza A virus in 1933, later Francis isolated influenza B virus in 1936, followed by Taylor who isolated the influenza C virus in 1950.[7] The first influenza virus was grown in embryonated hens' eggs in 1936 by Burnet. This paved the way for the study and characterization of the virus and the development of inactivated vaccines.[12] The first live attenuated influenza vaccine was licensed in 2003.[12] There are currently two types of FDA approved anti-viral drugs for influenza virus. The first type is, M-2 channel inhibitors, Amantadine and Rimantadine. The others are Neuraminidase inhibitors Zanamivir and Oseltamivir.[5]

3.1.2 Classification and nomenclature

Influenza virus is part of the family orthomyxoviridae. Influenza virus can be classified into three genus; *Influenza virus A*, *Influenza virus B*, *Influenza virus C*. The Influenza virus classification is based mainly on antigenic differences.[8, 10] The three main influenza virus antigens are nuclear protein, hemagglutinin and Neuraminidase. The classification of the Influenza types A, B and C are based on the internal proteins.[10] The influenza virus A is further classified into different strains based on the surface antigens, Hemagglutinin and Neuraminidase.[5] There are three major types of Hemagglutinin (H1, H2, H3) and two major types of Neuraminidase (N1, N2) that

cause significant pathogenicity in humans.[5,9] All the different types of influenza viruses are characterized by a segmented negative single stranded RNA genome encapsulated in a viral capsid. The major differences in the different viruses are given in the following **Table 6**. Comparison of characteristics of Influenza Virus A, B, C.

	Influenza A	**Influenza B**	**Influenza C**
Genome	8 segments	8 segments	7 segments
Structure	11 viral proteins	11 viral proteins	9 viral proteins
Host Range	Mammals, Birds and Pigs	Humans and seals	Humans only
Mechanisms of Mutations	Both Antigenic shift and drift	Antigenic drift only	Antigenic drift only
Clinical features	Causes widespread pandemics. Highest mortality among the three genera. Causes severe illness in young and old people.	Do not cause pandemics due to absence of antigenic shift. Mutations occurring are low. Causes illness in very young and old people.	Causes mild illness, most cases are sub clinical. Causes illness in children

Table 6*. Comparison of characteristics of Influenza Virus A, B, C*

The nomenclature of the different isolated human Influenza virus strains are articulated according to the following standardized order: 1) virus type, 2) geographic origin where it was first isolated, 3) strain number, 4) year of isolation, and 5) virus subtype. eg: A/California/7/2009 (H1N1).[8]

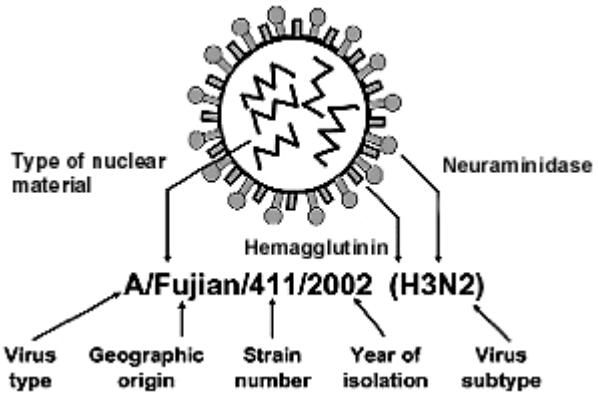

Figure 23. Nomenclature of Influenza virus.

3.1.3 Characteristics of Influenza virus

The influenza virus is a segmented negative polarity single stranded RNA virus from the family orthomyxoviridae. The influenza virus is an encapsulated virus that can be both filamentous (20 nm in diameter and 200- 3000 nm long) or spherical (80 to 120 nm in diameter). The influenza virus isolated from clinical samples are usually filamentous or rod shaped while the viruses which are cultured in embryonic egg or cells are spherical. It is assumed that the shape of the virus is directly related to its transmissibility. The filamentous virions are adept at infecting adjacent cells while the spherical ones are suitable for host transmission through aerosol.[9]

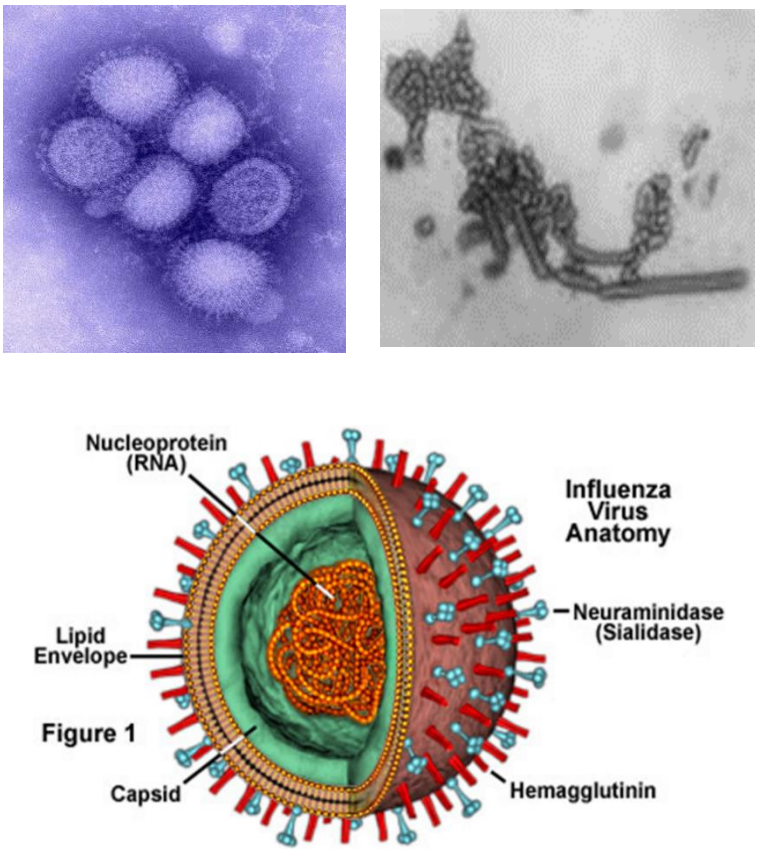

Figure 24. Images and Structure of Influenza virus.

A. Colorized micrograph showing the spherical morphology of influenza (Image taken from Public Health Image library (PHIL) at www.cdc.gov, Image ID- 11214, C Goldsmith and A Balish (2009)).

B. Micrograph showing the filamentous morphology of influenza-A H1N1, (Image taken from Public Health Image library (PHIL) at www.cdc.gov, Image ID- 7814.).

C. Anatomy of influenza virus. (Image taken from Kulkarni *et al*., *Medicinal Chemistry Reviews*, **2010**, *30*, 327-393).

The influenza virion consists of 8 segments of viral RNA. Each linear segment is made of approximately 2000-2500 nucleotides. In total each virion consists of 14000-15000 nucleotides.[9] They contain all the genetic material to produce all the viral proteins. The influenza viral RNA segments are of negative polarity 3'-5' and needs to be converted to the complimentary positive polarity 5'-3' before the genetic material can be translated to make a protein. Upon entering the host cell the negative polarity RNA sequence is converted to the complimentary positive polarity RNA using RNA polymerase enzyme present within the virus. These mRNA serve as a template for the production of the different viral proteins of the influenza virus. Influenza A, B, C contains 7 linear segmented RNA sequences, which encodes for the viral proteins HA, NA, RNA polymerase, ribonucleoprotein and M1 matrix protein. The 8th segment in influenza A encodes for M2 ion channel protein and in influenza B encodes for NB membrane protein. The influenza virus C only consists of 7 linear segmented RNA strands.[11] The re-assortment of the influenza virus is facilitated by the segmented genome which leads to the development of new strains through antigenic shift. This re-assortment of the genes causes the pandemics every 20-30 years.

There are two major proteins present on the surface of the influenza virus. The hemagglutinin (HA) and the neuraminidase (NA). Each viron contains around 300-400 HA which are evenly distributed over the surface of the virion. There are 40-50 copies of NA which are present as clusters over the surface of the virion.[12] There are approximately 16 different types of HA and 10 different types of NA, but only H1, H2, H3 of HA and N1, N2 are predominant among humans.[9] After every seasonal outbreak of the influenza virus these two surface proteins accumulate point mutations (antigenic drift) so that lasting immunity to the virus can never be achieved. Every 20 to 30 years there is a re-assortment of the genes between the different hosts of

the influenza virus e.g humans and pigs, resulting in a completely new strain of the influenza virus (antigenic shift) this strain is usually highly virulent and causes wide spread pandemics.[14]

3.1.4 Epidemic and Pandemic Spread

The influenza virus infection occurs every season during the cold and temperate climate in every hemisphere. It affects mainly children and older individuals. The seasonal outbreaks are caused by strains which have acquired point mutations and are able to escape the acquired immunity from the past season. Every year it causes approximately 250,000 to 500,000 deaths globally.[1] It also causes widespread illness or pandemics with even higher mortality rates. These pandemics are associated with the emergence of new strains, to which the population has no immunity or pre-exposure. So, the vaccines have no effect and thus have very high mortality rates.[17] There are four recorded pandemics till date. The earliest recorded pandemic was the Spanish Influenza A/H1N1 in 1918. Followed by the Asian flu A/H2N2 in 1957, the Hong Kong flu A/H3N2 in 1977. The most recent one being the 2009 Mexican flu.[14, 18]

3.1.4.1 Antigenic drift

The influenza virus undergoes point mutations during every replication. These point mutations accumulate and evolve into newer strains and finally it is able to escape the acquired immunity from the pre-existing strain. These acquired mutations render the strain unrecognizable to the T-lymphocytes and are unable to neutralize it. This is known as antigenic drift.[16] The antigenic drift causes mutations in the amino acid sequence of the surface proteins HA and NA. The HA of the Influenza virus is mostly affected. The NA of the influenza virus is mostly conserved.[13] These point mutations occur while replication of the virus during the imprecise RNA polymerase activity.[17] Due to change of the amino acids in the HA or the NA the antibodies and the vaccines that were developed for the older strain and previously effective are rendered futile

against the newer strain. They need to be developed against the newer strain to be effective. The point mutations are more predominant in the HA as compared to the NA.[13] The antigenic drift is more prevalent in influenza A than influenza B. Influenza C undergoes a minor amount of Antigenic drift.[13, 17]

3.1.4.2 Antigenic Shift

The influenza virus also undergoes abrupt and vast changes in its genome resulting in a completely new virus with a completely different HA or NA from the previous strains. The emergence of these new strains cause pandemics as the population has no or little protection from the virus. This type of a rapid and vast changes occurs due to re-assortment of the influenza virus genomes between two completely different strains originating from different hosts.[5, 14] The new strain has little or no similarity to the original virus surface antigens. This antigenic shift usually results when there is a re-assortment of genes between human and avian strains to produce a virus strain whose surface antigens are completely new.[5] H3N2 from humans and H5N1 from avian flu after re-assortment may result in H5N2. These new strains are highly dangerous and have a high mortality as the affected population has no previous exposure to this new strain and hence there is no immunity for it.[16] The latest pandemic in 2009 was caused when a previous triple re-assorted virus from the pig, bird and humans underwent another re-assortment of genes with an Eurasian pig flu strain.[18] The 2009 Mexican flu spread very rapidly but the mortality rate was not as high as previous pandemics.[19]

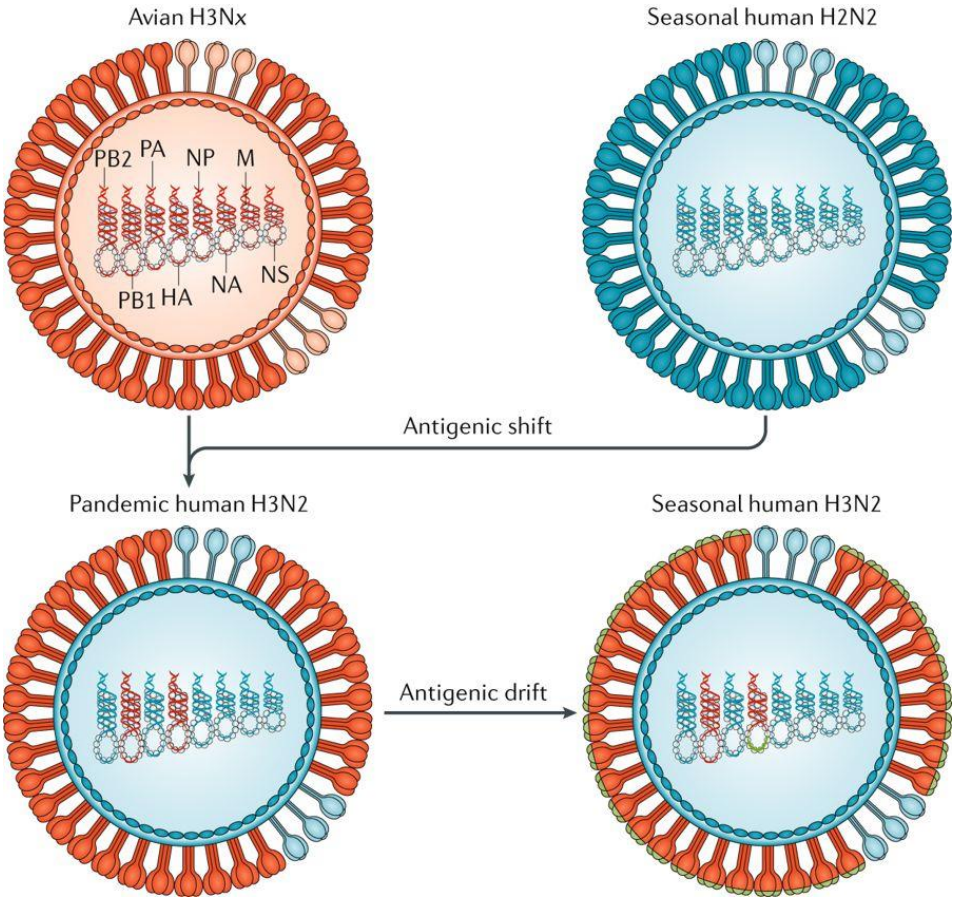

Figure 25. *Antigenic shift and drift.*
(Reprinted with permission[20])

Antigenic drift and Shift: Antigenic drift creates influenza viruses with slightly modified antigens, thus the antibodies developed against the original strain become ineffective. Antigenic shift results after the re-assortment of the genes from different strains to generate a novel strain with surface antigens HA and NA which have little or no resemblance to the surface antigens of the original strain.

3.1.5 Influenza virus proteins

The influenza A virus has in total16 viral proteins. But not all the Influenza viruses have 16 proteins. The major two surface antigens are hemagglutinin HA and Neuraminidase NA. The other viral proteins include the three different polymerases (PA, PB1 and PB2), matrix protein M1, M2 ion channel protein, nuclear protein NP and two nonstructural proteins NS1 and NS2 and some newly identified proteins PB1-F2, N40, PA-X, PA-N155, PAN182 and M42.[19]

3.1.5.1. Hemagglutinnin (HA)

The HA is one of the major surface antigens present on the surface of Influenza virus. It is present in a trimeric form.[17] It has two parts HA1 and HA2. The major function of the hemagglutinin is receptor binding, it binds to the receptor Sialic acid present on the surface of the host cell. It also catalyzes the fusion process with endosomal membrane, when suitably triggered by proton binding at low pH. Another major function of the HA is that it undergoes point mutations or variations without compromising the main functions of the antigen and can evolve to escape the immune response. The HA is presented all over the surface of the virus and each virion contains around 300-400 copies of the HA on its surface.[5] The HA is synthesized as a precursor HAO which is cleaved into HA1 and HA2, the active forms of the HA. HA1 part of the HA folds into a globular domain and this contains the receptor binding site for Sialic Acid. This part of the HA is a much conserved feature of a highly antigenically variable protein.[19] The HA2 forms the stalk of the protein that projects it outward from the surface of the virus. The transmembrane segment present near the C-terminal end anchors the protein to the viral membrane. The N-terminal end has the hydrophobic peptide called the fusion peptide. This fusion peptide is hidden inside the HA protein and at lower pH due to proton binding it undergoes a major unfolding and allows the fusion peptide

to interact with the target membrane and undergo fusion with the endosomal membrane.[20] The sialic acid utilize two types of glycolipids to enter the host cell. The avain Influenza prefers α-2,3-sialic acid-galactose linkages, while the human shows preference to α -2,6 sialic acid –galactose linkages.[21, 22]

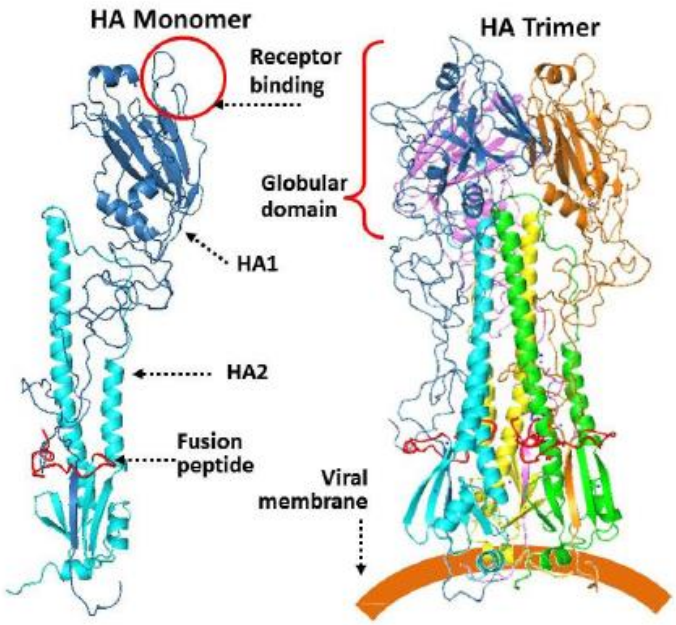

Figure 26*. Structure of Influenza HA.*

The HA monomer (A) and trimer (B). The image was generated using Pymol and Protein Data Bank, code 3HMG.

3.1.5.2. Neuraminidase (NA)

NA is the second major surface glycoprotein present on both Influenza A and B viruses. NA is a tetrameric protein, that consist of four identical subunits with the molecular weight of approximately 240kD.[23] The Neuraminidase (NA) facilitates the release of the viral progeny by cleavage of the virus-sialic acid association, prompting further infection.[24] NA catalyzes the

enzymatic cleavage of NeuAα-2-3, and NeuAα 2-6 glycosidic bonds. NA allows viral particles to move through mucin by cleaving sialic acid from host cells, allowing the efficient spread of influenza virus progeny from one host cell to the other host cell.[12,13] NA can remove both sialic acid from cellular glycoproteins, glycolipids, and even from both virus surface proteins. Thus, preventing newly formed viruses from aggregating.[25] If NA activity is inhibited, infection is limited to one round of replication and viral particles are prevented from invading the upper respiratory airway and spread to other host cell to initiate another round of infection. There is no amplification of the virus and the infection does not spread any further. [13, 27]

There are 10 serologically different subtypes of influenza NA, isolated thus far.[26] Influenza A contains (N1-N9) and one belongs to influenza B viruses (type B NA). Classification of the subtypes are based on the interaction of NA with the antibodies. The subtypes of NA that illicit a similar response with antibodies of the same type are classified together to the same subtype.[12] The subtypes N1 and N2 can infect humans. There are two phylogenetically and structurally distinct groups among neuraminidase. Group-1 contains N1, N4, N5 and N8; while group-2 contains N2, N3, N6, N7 and N9.[13, 25, 28] The structure of group-2 NA of influenza A virus was used to model and design current drugs (e.g. oseltamivir and zanamivir) using the conserved structure of the NA active site.[5]

The active site analysis of neuraminidase shows that it is highly conserved. The highly conserved nature of Neuraminidase led to it being chosen as a drug target for Influenza virus. The conserved residues in the catalytic sites that directly bind to the substrate are: Arg118, Asp151, Arg152, Arg224, Glu276, Arg292, Arg371, and Tyr406. The residues that support the catalytic residues are Glu119, Arg156, Trp178, Ser179, Asp/Asn198, Ile222, Glu227, His274, Glu277, Asn294, and Glu425.[29-32] The three arginine residues, (Arg118, Arg292 and Arg371) in the active

site of the Influenza A NA, directly bind to the substrate carboxylate group (Figure 1.5.3). Glu276 and Glu277 forms hydrogen bonds with two hydroxyl groups at carbon 8 and 9 of the NeuAc. Arg 152 interacts directly with the acetamido group of NeuAc. [29, 30] Calcium ion coordinates amino acids near the substrate binding and it is believed to maintain substrate binding conformation.[13]

NA is considered an exo-glycohydrolase; it hydrolyzes terminal sialic acid (SA) residues from glycoproteins and glycoconjugates.[33] Cleavage of terminal SA initiate with the binding of SA the active sites of NA. The stable chair conformation is forced into a less stable boat conformer due to the highly conserved tri-arginyl cluster (Arg-118, Arg-292, and Arg-371).[35] Conformational changes facilitate the departure of aglycon residue through the formation of an oxocarbocation ion intermediate (sialosyl cation)[34,36] The sialosyl cation undergoes a nucleophilic attack to form a glycosyl-enzyme intermediate. The glycosyl-enzyme intermediate breaks to form a sialosyl cation, where it goes under another stereo-selective nucleophilic attack by a water molecule to form α-Neu5aAc as the first product to release for the active site. The α-Neu5Ac product is further isomerize into β-Neu5Ac, the more thermodynamically favored product.[36]

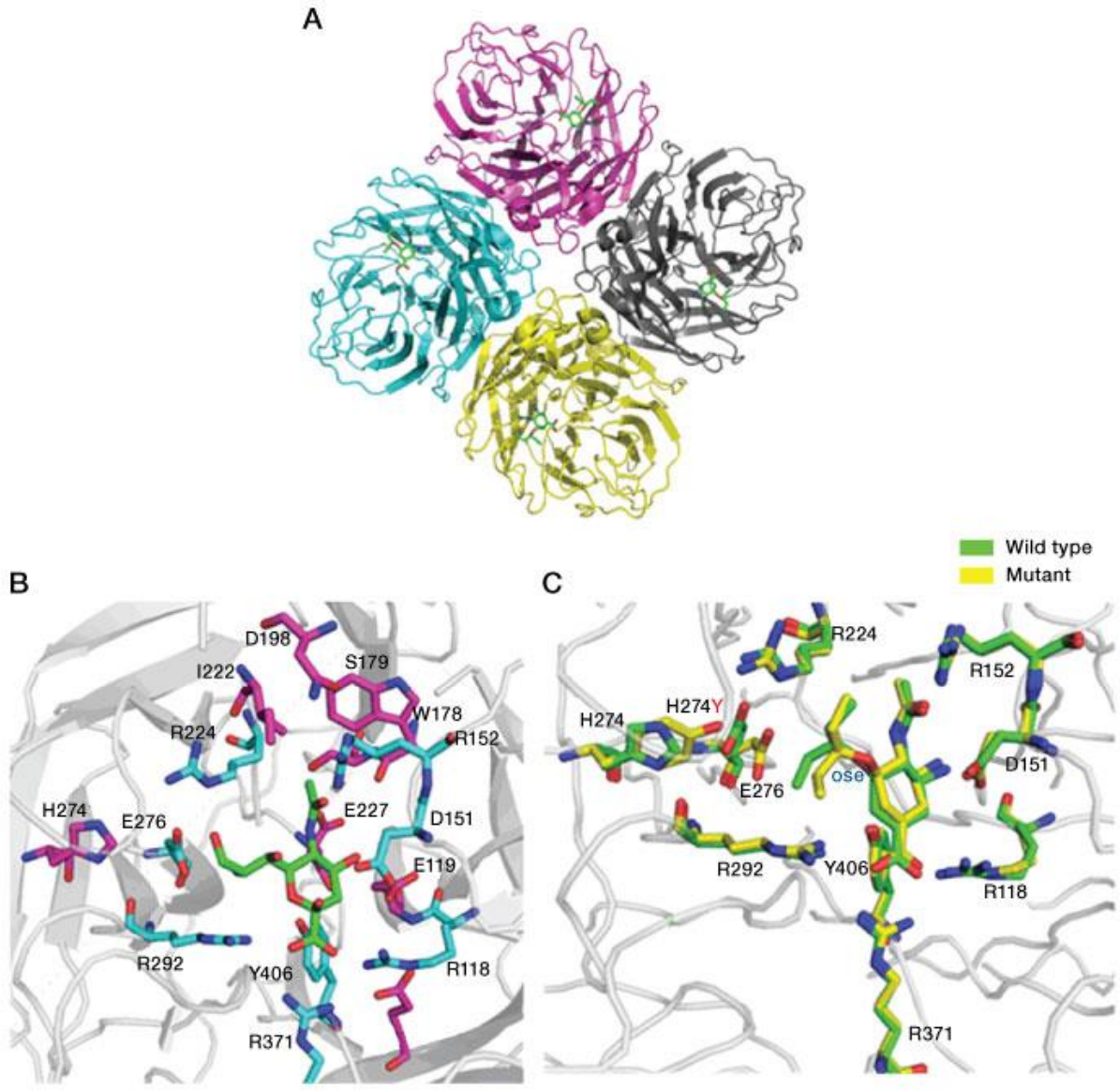

Figure 27*. Visualization of the neuraminidase structure in complex with ligands*

(A) Tetramer form of N1 neuraminidase (NA). (The image was generated using Protein Data Bank [PDB] code 2HU4)

(**B)** The active site structure of NA, in complex with *N*-Acetylneuraminic acid (Neu5Ac). (The image was generated using Protein Data Bank [PDB] code 2C4L)

(C) Comparison of the N1 NA active site of the wild-type and of H274Y substitution in complex with oseltamivir. (The image was generated using Protein Data Bank [PDB] codes 2HU0 and 2HU4) Active site residues are displayed in stick form and the backbone is in ribbon form.

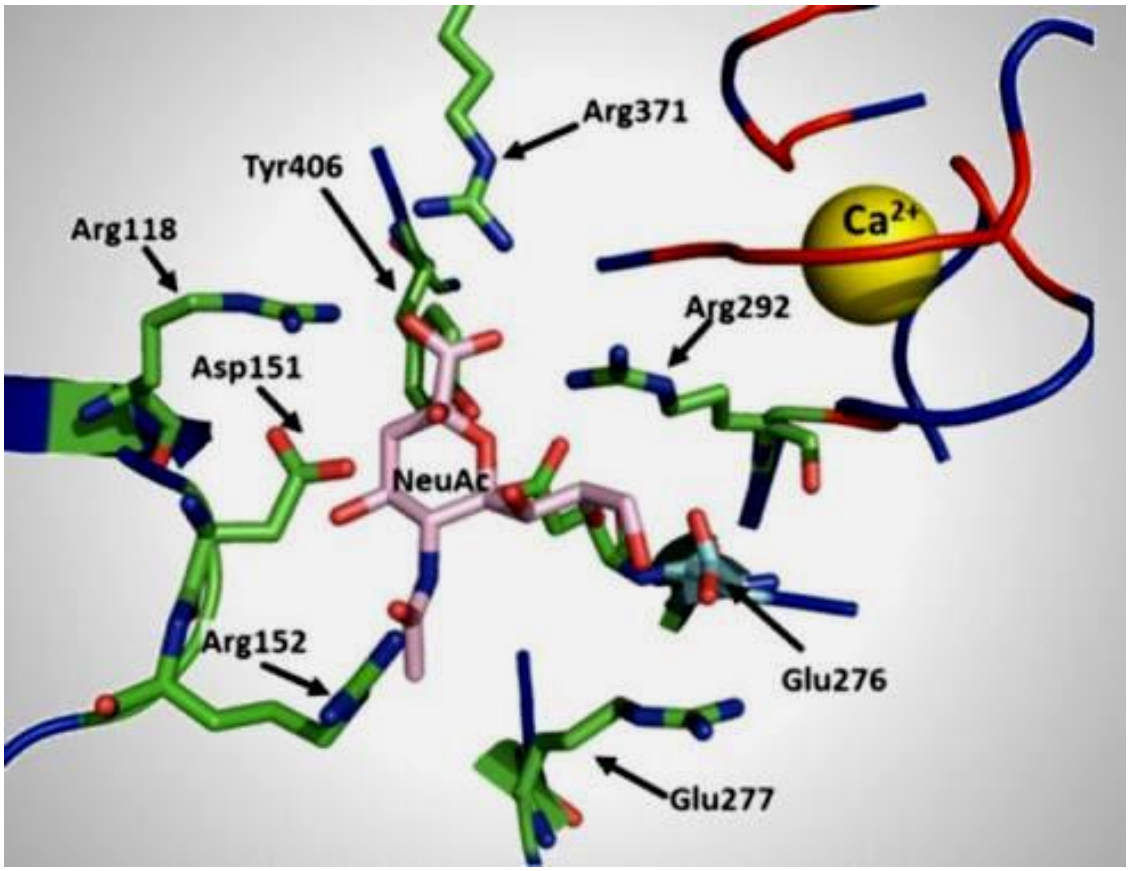

Figure 28*. Active site structure of NA bound to Sialic Acid.*
(The image was generated using Protein Data Bank [PDB] codes 2HU0 and 2HU4)

Residues that bind to the substrate are highlighted in green. Sialic acid (NeuAc) is shown in pink. Ca^{2+} binding site is close to the substrate binding site. The Ca^{2+} ion is shown as a yellow sphere. Figure generated using PyMol software (**Figure 28**).

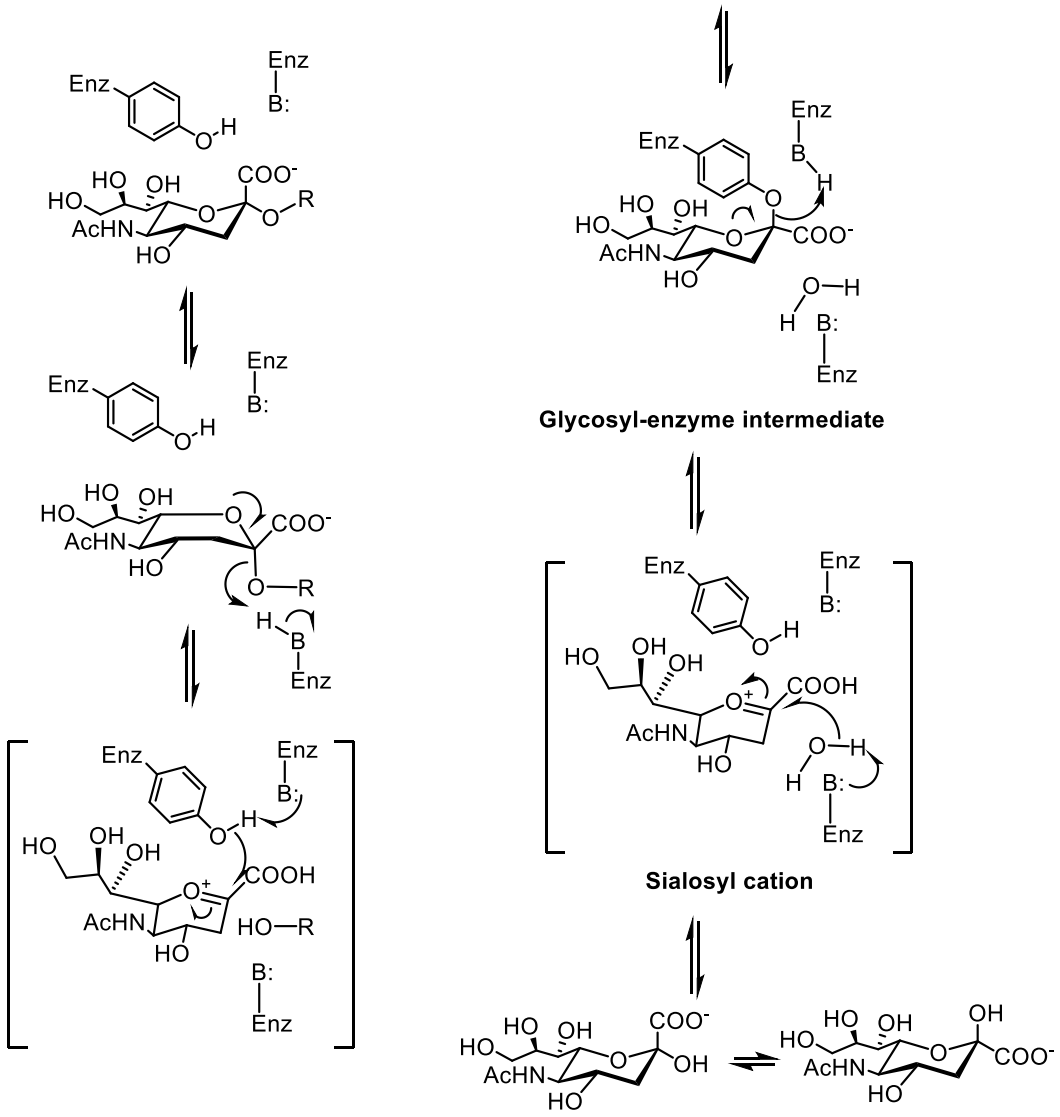

Figure 29*. Mechanism of enzymatic cleavage by NA.*

Mechanism showing the cleavage of terminal sialic acids by influenza viral neuraminidase.[36]

3.1.5.3 Influenza viral polymerase

Influenza polymerase is a heterotrimer, which is composed of three subunits call PA, PB1, and PB2with the molecular weight of approximately 250k Da.[37] All three subunits are required for the transcription and replications of viral RNA. Each unit has a distinct role in the transcription process. The initiation step for viral RNA transcription is where the PB2 subunit recognizes cap structure of host pre-mRNA in the nucleus.[38] The short capped oligomers (10-13 nucleotides) [39] is cleaved by an endonuclease subunit of PA and is used to prime viral mRNA by the subunit of PB1.[40] The transcription process ends when the polymerase recognizes the polyadenylation signal, a oglio-U sequence located near the 5' end.[38] Cusack et. al. was successful in obtaining X-ray crystals of the complete structure of influenza A and B polymerase including PA, PB1, PB2 and viral RNA promoter.[41, 42]

3.1.5.4. M2 Proton Channel

M2 protein of type A and B influenza virus are homotetrameric, type III integral membrane proteins that are important to the life cycle of the influenza virus.[43, 44] M2 proteins are responsible for the dissociation of the viral particles to release RNA materials. At the later stage of replication, M2 is responsible for maintaining the high pH of the trans-Golgi network to prevent premature folding of HA. M2 works as a proton gate where they have an open and close mechanism. Researchers believe that the open and close mechanism is based on a single trans-membrane domain residue of tryptophan (Trp [41]).[43]

3.1.6 Life Cycle of Influenza Virus

The Influenza virus replication cycle is very rapid. It takes approximately 6 hours[29] for the viral replication cycle to complete and release new viral progeny to infect new cells. The replication cycle starts with the HA binding to the receptor sialic acid on the host cell surface. The host cell surface has N-glycans which have sialic acid. The globular part of the HA1 binds to the sialic acid and initiates the endocytosis process of the virus. The exact mechanism for the virus internalization process is unclear. The major pathways for the endocytosis are Clathrin-dependent endocytosis, caveolae-mediated, clathrin- and caveolin-independent pathway and/or micropinocytosis.[38]

After the virus is internalized the low pH within the endosomal membrane, facilitates a conformation change in the HA2 domain of the HA. This conformation change projects the otherwise hidden hydrophobic fusion peptide at the N-terminal end of HA2 towards the endosomal membrane.[45] This fusion peptide then binds to the endosomal membrane. After the binding is complete the lower part of the stalk of the HA2 starts to contract bringing together the viral and the host membranes together.[47] This contraction leads to the folding of the stalk of the HA2. The folding is complete with the fusion of the viral and the endosomal host membrane.[46, 48] The low pH inside the endosome also activates the M2 ion channel. The M2 ion channel, facilitates the entry of protons into the virus bilayer and starts the dissociation of the viral capsid releasing the viral RNPs, consisting of the viral genome and RNA-dependent viral RNA polymerase and the nucleoprotein which coats the viral RNA.[43] The viral genome and the RNA dependent RNA polymerase are then imported into the host cell nucleus. Inside the nucleus RNA transcription occurs. The polymerase acidic component of the RNA dependent RNA polymerase cleaves the cap of a host pre-cellular m RNA and starts off the RNA replication process. This is called cap

snatching.[49] The viral genome is a negative sense RNA, which gets converted to its complementary positive sense strand. These complementary positive sense strands are exported outside to the host cell cytoplasm where they use the host ribosomes to produce the different viral proteins. When a certain concentration of the viral proteins is achieved. The complimentary positive sense RNA starts replicating inside the host nucleus to make copies of the negative sense viral genome. After enough copies of the viral genome is produced the assembly and the nuclear export of RNP occurs. The viral genome is packaged into RNP complexes, consisting of the viral RNA, NP and polymerase complex.[47] M1 matrix protein is responsible for export of the whole complex from the nucleus. Simultaneously after production of the viral proteins in the host cell cytoplasm they go into the endoplasmic reticulum to undergo proper folding, glycosylation and polymerization. The M2 ion channel at this stage increases the pH, inside the acidic Golgi network to prevent the activation of the fusion peptide of the HA.[40]

After all the viral proteins, viral capsid are packaged, the budding process is initiated by the M1 matrix protein and M2 facilitates the cell membrane split to release the viral progeny.[45, 51] After the budding out process of the viral progeny from the infected cell the sialic acid is still bound to the HA. This HA-sialic acid association is then cleaved by NA to finally release the viral progeny to infect other cells.[47, 52] This cleavage of the sialic acid HA, completes the viral replication cycle.

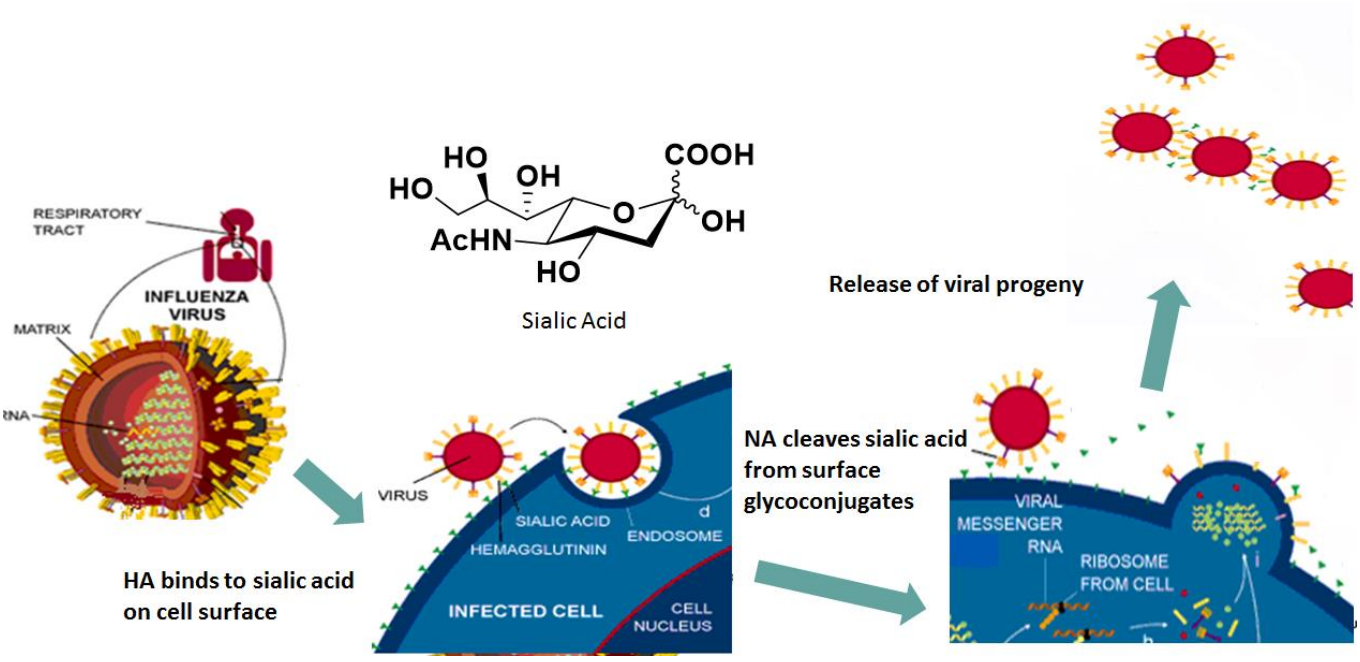

Figure 30. *Life Cycle of Influenza Virus.*

3.2 Controlling the transmission of influenza viruses

Influenza virus is a lethal pathogen and therefore a number of methods have been employed to mitigate the spread of this disease. These include proper hygiene, vaccinations, antivirals and rapid diagnostic tests for appropriate countermeasures. In combination, these different methods have been shown to arrest the spread of the disease, however as it mutates very rapidly, some of these methods become in-effective within a very short span and need to be re-evaluated and regenerated.

3.2.1 Vaccines

Influenza affects millions annually and thus the need for preventions are in high demand. Antiviral drugs assist in treating the infected cells, and also arrest the spread of the viruses. However, the excessive use of one kind of antiviral (Oseltamivir) has resulted in a number of resistant virus strains.[50] Annual vaccinations against the influenza virus is a good method to control

the spread.[53] Vaccination generates antibodies that mainly targets HA surface glycoproteins. As influenza antibodies mainly recognized specific regions on the globular head of the HA surface proteins, their efficiency relies on the similarities between the HA of the vaccines and the HA of the currently seasonal strains. If the point mutations caused due to antigenic drift has caused the virus to escape the acquired immunity the viruses are no longer effective.[55]

3.2.2 Current Anti-Influenza Drugs

There are currently two types of FDA approved antiviral drugs available against the Influenza virus. M2 ion inhibitors and NA inhibitors.

3.2.2.1 M2 ion inhibitors

The M2 ion channel is responsible for transporting protons to facilitate the dissociation of viral particle and the release of viral genome.[56] This process is crucial for viral infections and therefore, was among one of the first proteins targeted for production of antiviral drugs. Amantadine and Rimantidine are FDA approved M2 ion channel inhibitor Influenza antiviral drugs. 24 The antivirals work by direct pore-blocking mechanism.[43] However, as the influenza virus mutates, these older antiviral drugs has proven to be ineffective. Over 90% of the influenza viral A strains has shown resistance to this class of antivirals. A more recent strain of H1N1, 2009 outbreak, have also shown to be resistant to the adamantane-based drugs.[55, 56]

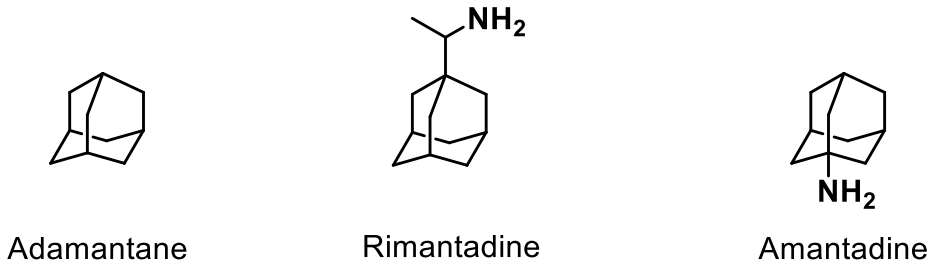

Figure 31. *Structure of M2 Inhibitors.*

Stucture of adamantane based antiviral drugs used against the influenza virus. These class of inhibitors inhibit the M2 channel present on the influenza virus.

3.2.2.2. NA Inhibitors

FDA approved, anti-Influenza drugs Zanamivir and Oseltamivir, are based on inhibition of Neuraminidase protein. It is possible to restrict the spread of the infection by stopping the cleavage of the virus-sialic acid association. The restriction of the virus-sialic acid cleavage prevents the spread of the influenza virus. [59]

These antivirals are more effective as they target a more conserved NA and are less likely to develop resistantance. Current FDA approved Zanamivir and Oseltamivir are transition state analog inhibitors of NA. Zanamivir is a sialic acid analog (2-deoxy-α-D-Nacetylneuraminc acid) that has a guanidine functionality at the 4th position of 2-deoxy-α-D-Nacetylneuraminc acid. Oseltamivir© is a cyclohexene derivative that contains an amino functionality at the 4th position of the cyclohexene ring.[35] But unfortunately, Oseltamivir resistant strains have been isolated from patients.[57,58] But those strains have not yet developed resistance to Zanamivir.[59, 60]

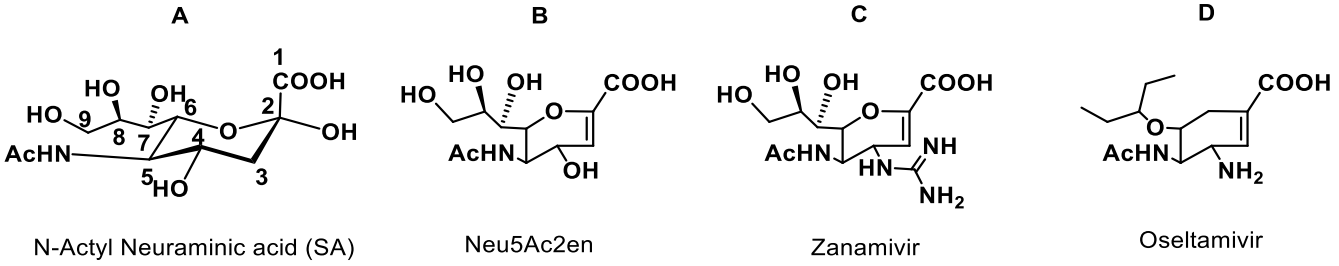

Figure 32*. Structures of NA inhibitors.*

A) Native sialic acid with numeric system for assigning carbon.

B) Deoxy form of sialic acid with hydroxy group at the 4th position.

C) Zanamivir© is a deoxy form of sialic acid with a guanidine functional group at the 4th position.

D) Oseltamivir© derivative of clycohexane that mimics the transition state of sialic acid with an amino functional group on the 4th position.

Peramivir a new NA inhibitor drug was approved recently for the treatment of influenza virus, in 2014. Peramivir (Rapiacta®, Peramiflu®, BioCryst Pharmaceuticals, Research Triangle Park, North Carolina, USA) is among one of the drugs that was in phase III clinical trials and was approved for used during the 2009 H1N1 influenza outbreak under the Emergency Investigational New Drug (eIND) regulations.[61] Peramivir, unlike traditional NA inhibitors, it has a unique structure differ from known NA inhibitors. This NA inhibitor exhibits high binding affinity that last up to 24 hours and has a slow rate of dissociation.[62]Premavir has been approved for the treatment of influenza in both Japan and South Korea.[61] Unlike Zanamivir and Oseltamivir, Peramivir is administered through IV injections.

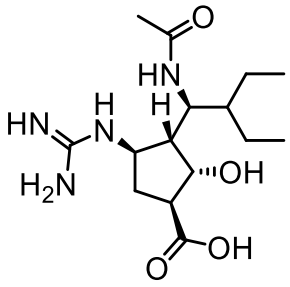

Peramivir

Figure 33*. Structure of Permavir.*

Neuraminidase inhibitor Peramivir was recently approved by the Food and Drug Administration (FDA) in 2014.

3.3 Detection of Influenza virus using glycan microarray

Hemagglutinnin (HA) binds to a nine carbon glycan, N-acetylneuraminic acid or sialic acid, present on the termini of glycolipids and glycoproteins of the epithelial cells of the respiratory tract.[53-54] This is followed by cell entry and infection of the host cell. After utilizing the host cell machinery for virus propagation, the progeny escapes the host cell to infect neighboring cells and tissues. Interestingly, sialic acid present on the infected host cell prevents the viral progeny from escaping. Mucins containing sialic acid also inhibit the virus from propagating.[55] Neuraminidase (NA), an enzyme cleaves sialic acid on the infected host cell and mucins are freeing viral progeny to infect other cells. We choose to target these glycoproteins for three reasons. (i) They are vital proteins of the virus and require sialic acids to bind. (ii) There are approximately 300-400 copies of HA and 50-100 copies of NA on a single viral particle. Hemagglutinnin (HA) exists as a trimer and NA as a tetramer, and a large number of copies on a single virion provides an adequate amount of protein targets for synthetic or natural sialic acids to capture.[56-57] (iii) This receptor-based approach is unique in comparison to antibody-based diagnostics. All strains of the influenza virus are expected to bind to sialic acid analogs and each strain would yield a "fingerprint" pattern of recognition that can be used to detect the virus.[58-59] In previous studies, we developed microarrays comprised on synthetic sialic acid analogs that could bind to HA and/or NA. After exposure of the focused microarray to different virus strains, a fluorescently labeled antibody was used as the readout.[58-59] (**Figure 34A**) These studies were important to establish proof of principle that sialic acid analogs could be used to detect influenza viruses; however, a limitation of the studies was that antibody based reporters were required. Following a report by Wong and coworkers,[60] we report the synthesis, characterization and initial binding studies of an "universal" glycan based

reporter molecule that could bind to all virus strains. Since the capture and reporter molecules are made of glycans, antibodies are not required. (**Figure 34 B**)

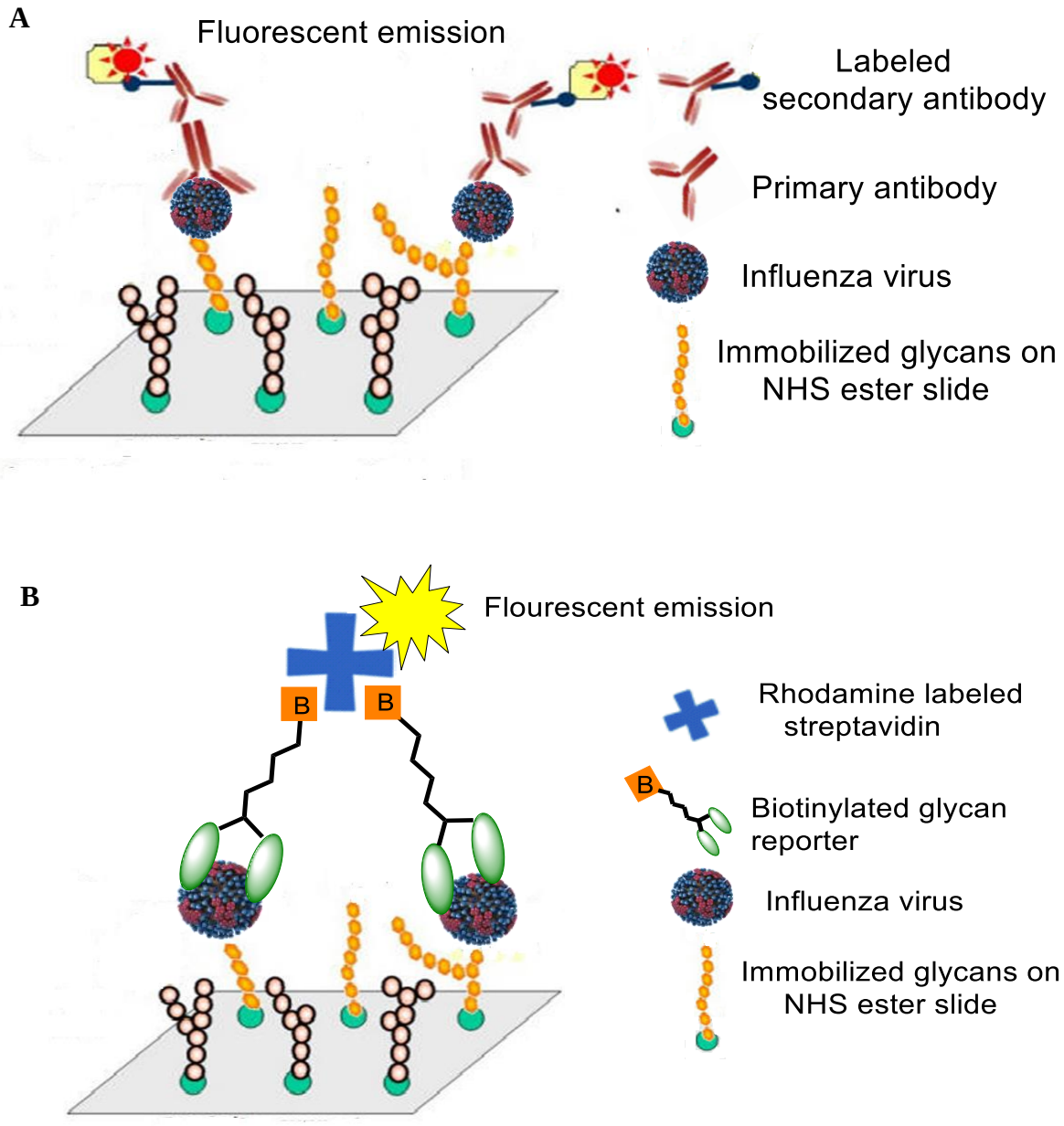

***Figure 34**. Sandwich ELISA assay for detection of Influenza virus.*

A. Cartoon representation of the sandwich assay using glycans as capture and labeled antibody as reporters. **B.** Cartoon representation of the sandwich assay using glycans as capture and biotinylated glycan-labeled streptavidin as reporters

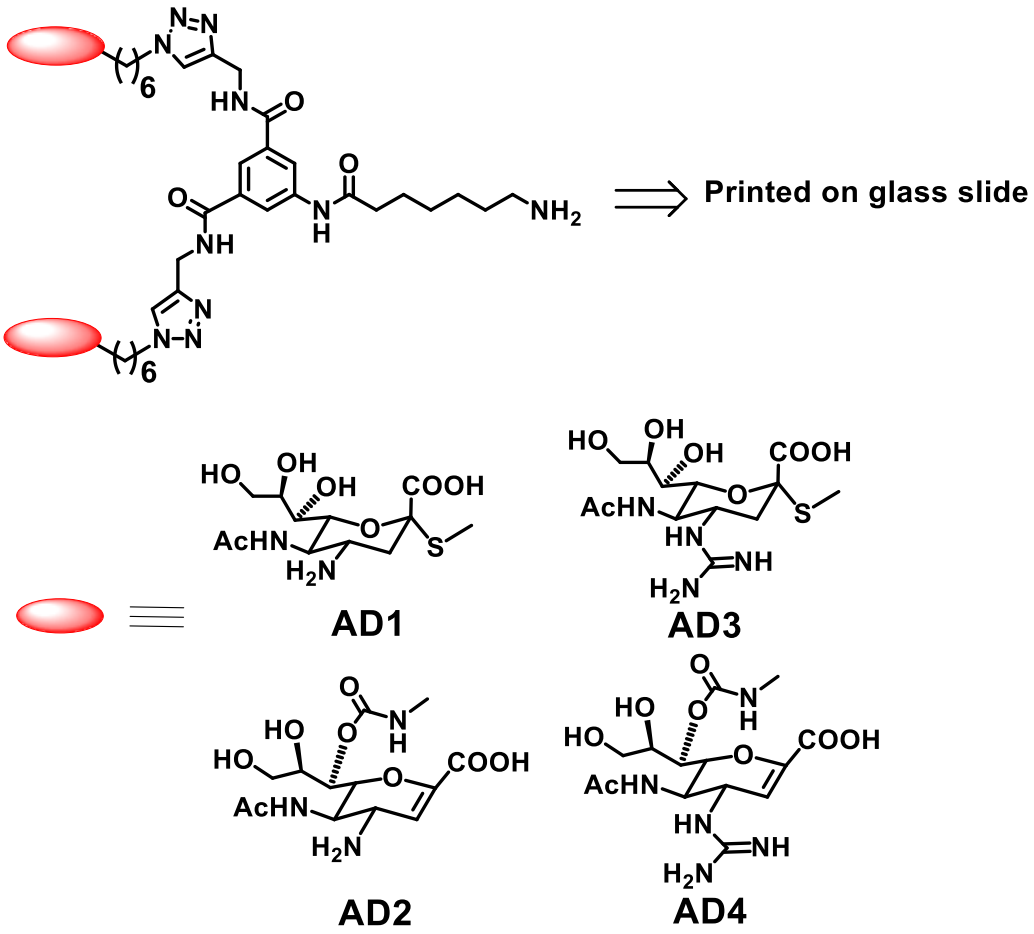

Figure 35*. Structures of the four glycans immobilized on glass slides for capturing influenza virus.*

3.4 Results

The design and synthesis of the universal reporter is shown in **Scheme 5** and it follows our previous publications.[58] We choose to use Zanamivir analogs as the glycan headgroups as the binding affinity of Zanamivir to NA is in the nanomolar range. The active site of influenza NA is also highly conserved and furthermore, resistance to Zanamivir is not as high as Oseltamivir. In fact, very few cases of Zanamivir resistance has been reported.[61] We also choose to develop a dimeric scaffold as dimers improve the avidity effect dimers; [62]we designed the molecule such that the two Zanamivir analogs moieties fit into two active sites of a NA tetramer or two adjacent NA tetramers.[63] We attached biotin at the opposite end of the scaffold because biotin can bind to

fluorescently labeled avidin yielding our desired reporter. The final construct is expected to possess eight zanamivir analogs moieties as one avidin binds to four biotin molecules. The azido compound **1** and the scaffold **2** were synthesized as described previously. 1,3 Dipolar cycloaddition[64] reaction under standard conditions was performed to yield the biotinylated bivalent compound. Deprotection of the tert-butyloxycarbonyl and methyl ester groups resulted in the desired reporter molecule **AD-R** in 60% yield**.** This compound was purified using size exclusion Biogel P2 columns to yield a foamy solid. All intermediates and the final compound were characterized using NMR and mass spectroscopies.

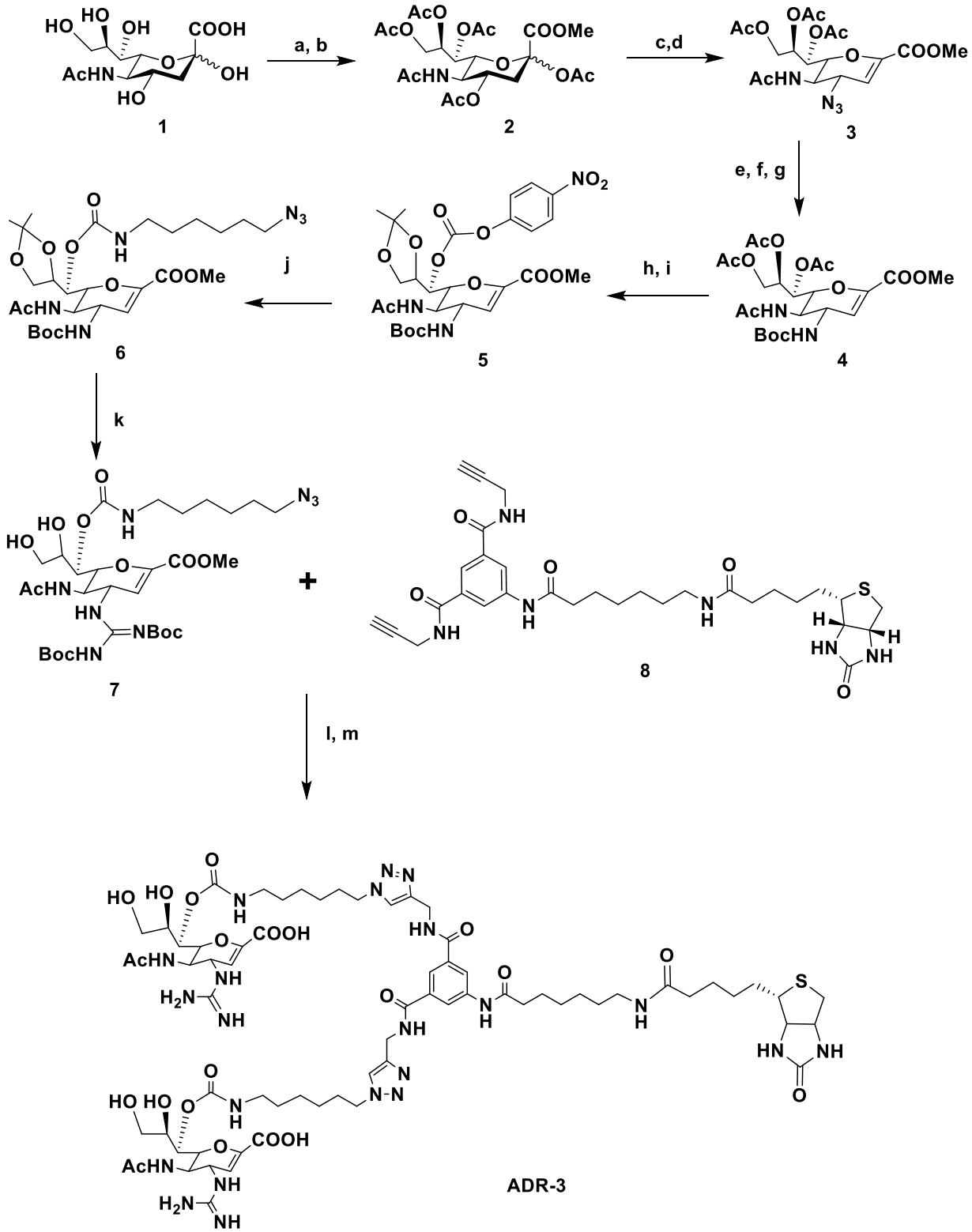

Scheme 5 Synthesis of the Reporter molecule.

Reagents and conditions: a) H^+ resin, MeOH, rt, overnight 99%. **b)** Ac_2O, py, rt, overnight, 99%. **c)**TMSOTf, EtOAc (anhydrous), 50^0C, 3h. **d)** $TMSN_3$, t-BuOH, reflux, overnight, 60% (over two steps). **e)** PPh_3, THF: H2O (1:1), rt, 4h, 60%. **f)** Boc_2O, Et_3N, THF, cat DMAP, rt, overnight, 90%. **g)** NaOMe, MeOH, rt, 2 h , **h)** H^+ resin, CH_3COCH_3, rt, 5 h, 80% (over two steps). **i)** 4-nitrophenylchloroformate, py, DMAP, rt, 16h, 80%. **j)** 6-azidohex-1-amine, NEt_3, DCM, (pH=8.5), rt, overnight, 70%. **k)** DCM: TFA (1:1), rt, 2h, 1,3-Bis(tert-butoxycarbonyl)-2-methyl-2thiopseudourea, $HgCl_2$, NEt_3, DCM, rt, overnight, 50%. **l)** t-BuOH: H_2O (7:3), $CuSO_4$, L-ascorbate, rt, 12h, 70%. **m)**TFA: DCM (1:1), rt, 1 h, NaOMe, MeOH, rt, 1 h, 60% (over two steps)

Next, we used the biotinylated compound as a reporter in microarray studies. We printed four bivalent compounds on glass slides for these exploratory studies. [58-59] (**Figure 35**) These compounds have been shown in our previous studies to capture different strains of influenza viruses. [58] After incubating with Influenza A H1N1, A/Brisbane/59/2007 virus at rt for 1 hour, the slides were washed extensively, and exposed to **AD-R**. This step was followed by extensive washing and addition of labeled streptavidin. While we choose a two step procedure of adding the biotinylated compound followed by the labeled streptavidin, an alternate method of premixing the avidin with the biotin could also be used with the caveat that the latter method requires purification of the avidin-biotin complex. The slides were scanned using a Genepix400B scanner at 557 nm. It was gratifying to observe that all four printed compounds capture the virus when the labeled streptavidin-**AD-R** conjugate is used as the reporter; non-specific binding to PEG is negligible. (**Figure 36**) The increase in Relative Fluorescence Units (RFU) from background is not as high in comparison with antibody based reporters, [58] presumably because we are using capture and reporter ligands that primarily bind to NA. The number of NAs on a single virion is not as high as the number of HAs. [56-57] Secondly, NAs have been shown to be present in clusters or scattered on the

virus surface, [56-57] which may limit the number of available sites for the reporter to bind when the virus is captured by the glycans on the glass slides. This may lead to a lower RFU. We plan to develop the use of ligands that capture HA, which should give us a higher RFU. We also determined the limit of detection of this virus to be 10^4 PFU (plaque forming units).

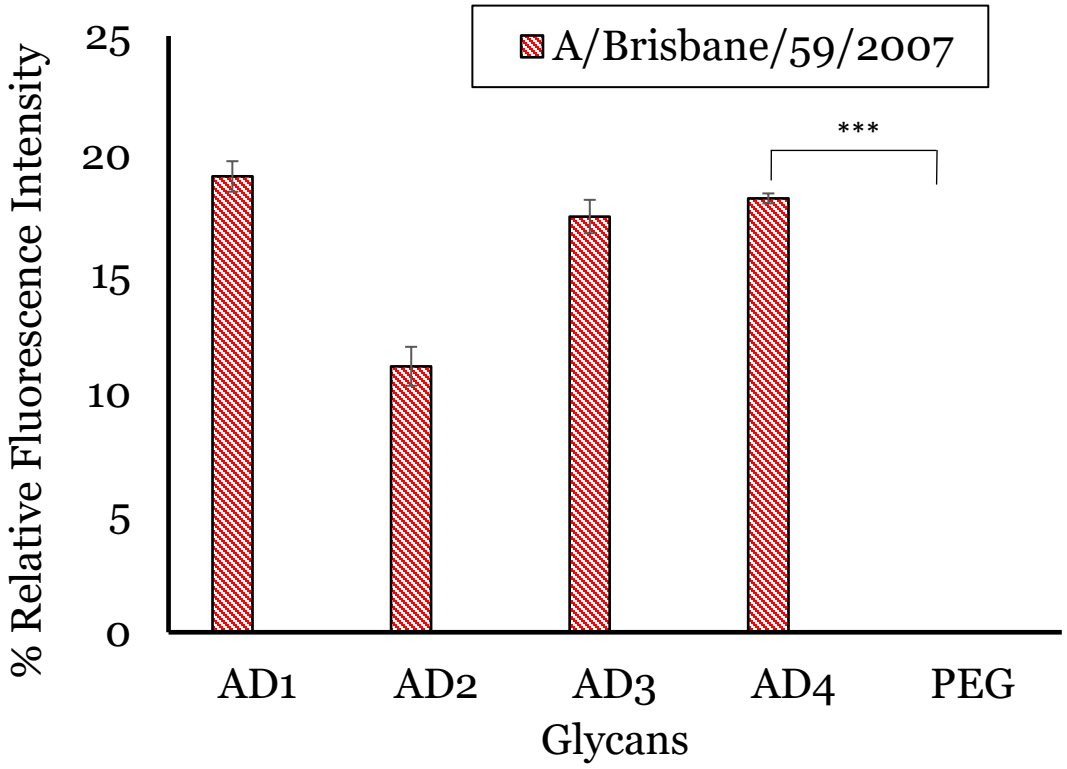

Figure 36. Influenza virus (A/Brisbane/59/2007) binding studies.

Fluorescence detection of H1N1 (A/Brisbane/59/2007) influenza A virus using synthetic glycans as capture and biotinylated glycan-label streptavidin as reporter. Glycans and PEG (negative control) were printed at 200 μM. Virus concentration was 10^5 PFU. Fluorescence intensity was measured by the Genepix400B scanner using tetramethylrhodamine (TRITC) labeled streptavidin and scanned at 557 nm. All experiments were performed in triplicate (*$p<0.05$, **$p<0.01$, ***$p<0.001$, ns>0.05)

3.5 Experimental section

3.5.1 General

All reagents and solvents were reagent grade or were purified by standard methods before use. All reactions were performed under argon with solvents dried using a solvent purification system (Innovative Technology). All chemical reagents were of analytical grade, used as supplied without further purification unless indicated. Tetramethylrhodamine (TRITC) labeled streptavidin was purchased from Thermo Scientific as a lyophilized powder. Compounds AD1-4 were synthesized as described previously.[58] The acidic ion exchange resin used was Amberlite® IR 120 (H^+) resin. Analytical thin layer chromatography (TLC) was performed on silica gel 230-400 mesh (Sicicycle). Plates were visualized under UV light, and/or by staining with acidic $CeH_8Mo_3N_2O_{12}$ followed by heating. Column chromatography was performed on silica gel (230-400 mesh). ^1H and ^{13}C NMR spectra were recorded on Bruker 400MHz spectrometer. Chemical shifts are reported in δ (ppm) units using ^{13}C and residual ^1H signals from deuterated solvents as references. Spectra were analyzed with MestreNova® (Mestrelab Research). Electrospray ionization mass spectra were recorded on a Micromass Q \T 2 (Waters) and data were analyzed with MassLynx® 4.0 (Waters) software. Reported yields refer to spectroscopically and chromatographically pure compounds that were dried under high vacuum (10^{-2} mbar) before analytical characterization, unless otherwise specified.

3.5.2 Synthesis and Characterization

(1S,2R)-1-((1R,2S,3S)-2-acetamido-3,5-diacetoxy-5-(methoxycarbonyl)cyclohexyl)propane-1,2,3-triyl triacetate (2).

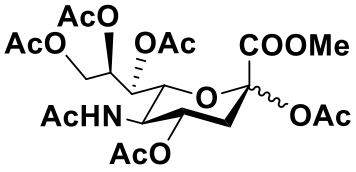

Compound **1** (10.0 g, 32 mmol) was dissolved in 300.0 mL of methanol and 1.0 g of H^+ DOWEX 50WX8-200 ion-exchange resin was added. The reaction mixture allowed to stir overnight. The resin was filtered, and the filtrate was concentrated under reduced pressure to give a white solid (10.2 g, 99% yield). The white solid was dried under vacuum. The dried solid (10.0 g, 31 mmol) was dissolved in 300 mL of anhydrous pyridine, acetic anhydride was added dropwise (35 ml) at 0°C. Reaction mixture was allowed to stir overnight. The reaction mixture was washed with excess of 1.0 M hydrochloric acid solution and extracted with DCM (50ml, 3x), organic layers were collected and further washed with saturated $NaHCO_3$, extracted with DCM, dried over Na_2SO_4 and concentrated under reduced pressure to yield a white foam **2** (16.5g, 99% yield). NMR obtained was similar to the literature.

(1S,2R)-1-((2R,4S)-3-acetamido-4-azido-6-(methoxycarbonyl)-3,4-dihydro-2H-pyran-2-yl)propane-1,2,3-triyl triacetate (3).

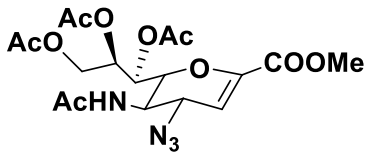

To a solution of compound **2** (11.0 g, 20 mmol) in anhydrous EtOAc at 50°C, TMSOTf (11ml, 61 mmol) was added dropwise. The reaction mixture was allowed to stir at 50°C for 3 h. The reaction was washed with saturated $NaHCO_3$ solution, in small portions (50 ml, 3x). Organic layers were collected and dried with Na_2SO_4 and concentrated under reduced pressure, to give a solid (8g, 75% yield). The solid was dried under reduced pressure and used immediately for the successive reaction without purification. The resulting solid (7g, 16 mmol) was dissolved in 50 mL of t-BuOH, $TMSN_3$ (3ml, 26 mmol) was added dropwise and allowed to stir overnight at 80^0

C. The reaction mixture was concentrated under reduced pressure. The crude product was purified using column chromatography with n-hexane: acetone (2:1) to yield a pale golden solid (5.4g, 60% overall yield for 2 steps).

^{1}H NMR (400 MHz, $CDCl_3$): δ ppm 6.21 (d, *J* = 8.8 Hz, 1H), 5.97 (s, 1H), 5.47 (d, *J* = 2.0 Hz, 1H), 5.32 (s, 1H), 4.67 (d, *J* = 12.4 Hz,1H), 4.50 (d, *J* = 10 Hz, 1H), 4.42 (d, *J* = 8.8 Hz, 1H), 4.20 (dd, *J* = 6.4, 12.2 Hz, 2H), 3.81 (s, 3H), 2.13 (s, 3H), 2.06 (s, 3H), 2.05 (s, 3H), 2.00 (s, 3H).

5-Acetylamino-4- N-tert-butyloxycarbonyl-6- (1,2,3-triacetoxy-propyl) -5,6-dihydro-4H-pyran-2-carboxylic acid methyl ester (4).

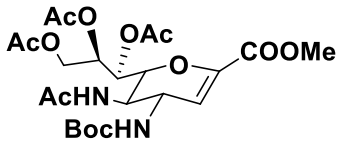

Compound **3** (5g, 10 mmol) was dissolved in a mixture of THF: H_2O (5ml, 1:1), PPh_3 (4.3g, 16 mmol) was added and reaction was allowed to stir at 40^0C for 12 hours. Tetrahydrofuran (THF) was removed under reduced pressure and the crude product was purified by column chromatography to obtain the intermediate amine as an oil. The purified amine intermediate was immediately used for the subsequent reaction. To the amine intermediate (2.3g, 0.53 mmol) in THF (10.0 ml), Et_3N (1.86 ml 13 mmol), was added and the reaction mixture was allowed to stir for 30 min at rt. Boc_2O (4.0 g, 18 mmol) was added and the reaction was allowed to stir for 12 h at rt. THF was removed under reduced pressure and the crude was washed with HCl (1M, 50 ml), extracted with DCM (50 ml 3X). The organic layers were combined and washed with $NaHCO_3$ solution and dried over Na_2SO_4. Product was purified by column chromatography with hexane: acetone (3:1), to yield a white solid. (3.18g, 60% yield over two steps).

^{1}H NMR (400 MHz, $CDCl_3$): δ 6.46 (d, *J* = 9.0 Hz, 1H), 5.94 (s, 1H), 5.43 (s, 1H), 5.27 (s, 1H), 4.63 (d, *J* = 12.4 Hz, 1H), 4.44 (d, *J* = 10.0 Hz, 1H), 4.35 (d, *J* = 8.9 Hz, 1H), 4.15 (dd, *J* = 12.3, 7.1 Hz, 1H), 3.95 (d, *J* = 9.2 Hz, 1H), 3.77 (s, 3H), 2.14 (s, 9H), 2.10 (s, 3H), 2.03 (s, 3H), 2.02 (s, 3H), 1.95 (s, 3H).

^{13}C NMR (100 MHz, $CDCl_3$): δ 170.9, 170.6, 170.3, 170.0, 161.8, 156.2, 144.6, 111.0, 80.2, 71.4, 67.8, 62.2, 60.4, 52.4, 50.1, 47.3, 28.2, 23.1, 21.0, 20.9, 20.8.

HRMS(ESI): Calculated for $C_{20}H_{32}N_2O_9$: 444.2108; Found: 445.2180 (M+H).

5-Acetylamino-4-N-tert-butyloxycarbonyl-6- [(2,2-dimethyl-[1,3] dioxolan-4-yl)- (4-nitro-phenoxycarbonyloxy)-methyl]-5,6-dihydro-4H-pyran-2-carboxylic acid methyl ester (5).

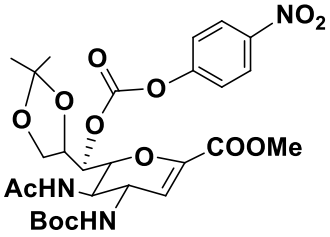

The compound **4** (0.6g, 1.3 mmol) was dissolved in MeOH and NaOMe (0.05 eq) was added and the reaction was allowed to stir at rt for 2h. The reaction was monitored by TLC. After completion the reaction mixture was neutralized with H^+ DOWEX 50WX8-200 ion-exchange resin to pH 7. The resin was filtered, and the filtrate was concentrated and dried under reduced pressure to give a colorless solid. The dried solid was then dissolved in dry acetone and the H^+ resin was added to the reaction mixture to adjust the pH to 4. The reaction mixture was stirred overnight at rt. The reaction was filtered and then the filtrate was washed with saturated $NaHCO_3$ solution and extracted with DCM (20 ml, 3X). The organic phases were combined and dried over Na_2SO_4. The crude product was purified by column chromatography with hexane: acetone (4:1) to give a white solid. The solid (0.5 g, 0.11 mmol) was then dissolved in pyridine (10 ml) and

DMAP (0.68g, 0.56 mmol) was added. The reaction mixture was allowed to stir at rt for 30 min. 4-nitrochloroformate (0.7g, 3.3 mmol) was added to the reaction mixture and it was allowed to stir for 16 h at rt. The reaction was monitored by TLC and upon completion, the reaction mixture was washed with HCl (1M, 30 ml) and extracted with DCM (30 ml, 3X). The combined organic layers were washed with saturated $NaHCO_3$ and dried over Na_2SO_4. The crude was purified by column chromatography with hexane: acetone (3:1) to give **5** (0.4 g, 60% overall yield for 2 steps).

^{1}H NMR (400 MHz, $CDCl_3$): δ 8.27 (d, *J* = 8.9 Hz, 2H), 7.50 (d, *J* = 8.9 Hz, 2H), 5.97 (d, *J* = 9.6 Hz, 1H), 5.90 (s, 1H), 5.31 (t, *J* = 5.7 Hz, 1H), 4.81 (d, *J* = 9.6 Hz, 1H), 4.54 (t, *J* = 9.7 Hz, 1H), 4.47 – 4.29 (m, 2H), 4.24 (dd, *J* = 8.9, 5.7 Hz, 2H), 4.17 – 4.05 (m, 1H), 3.79 (s, 3H), 1.95 (s, 3H), 1.42 (s, 9H), 1.41 (s, 3H), 1.38 (s, 3H).

^{13}C NMR (100 MHz, $CDCl_3$): δ 171.3, 161.6, 156.4, 155.7, 152.5, 145.6, 144.8, 125.2, 122.3, 110.5, 108.9, 80.6, 75.1, 74.2, 65.5, 52.5, 49.5, 48.1, 28.2, 26.4, 25.5, 23.2.

HRMS(ESI): Calculated for $C_{27}H_{35}N_3O_{13}$: 609.2170; Found: 632.2057 (M+Na).

5-Acetylamino-4-N-tert-butyloxycarbonyl-6-[(6-azido-hexylcarbamoyloxy) -(2,2-dimethyl-[1,3] dioxolan-4-yl)-methyl]-5,6-dihydro-4H-pyran-2-carboxylic acid methyl ester (6).

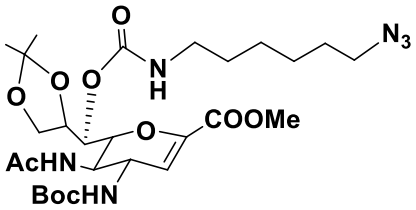

To a solution of 6-azidohex-1-amine (0.55g, 0.39 mmol) in CH_3CN (20 ml), Et_3N (0.4 ml, 0.29 mmol) was added and the reaction mixture was allowed to stir for 30 min at rt. Solution of **5** (0.6 g, 0.98 mmol) in CH_3CN was added to the reaction mixture and stirred at rt for 3h. The reaction was monitored by TLC. Upon completion CH_3CN was removed under reduced pressure and the crude was washed with HCl (1M, 30 ml) and extracted with DCM (30 ml, 3X). The organic layers

were collected and washed with saturated $NaHCO_3$ solution and dried over Na_2SO_4. The product was purified by column chromatography with hexane: EtOAc (1:1) to give **6** (0.42g, 70%).

^{1}H NMR (400 MHz, $CDCl_3$): δ 6.15 (d, *J* = 9.4 Hz, 1H), 5.90 (s, 1H), 5.24 (d, *J* = 3.7 Hz, 1H), 5.01 – 4.83 (m, 2H), 4.51 (t, *J* = 8.9 Hz, 1H), 4.33 (dd, *J* = 13.6, 7.8 Hz, 2H), 4.19 – 4.04 (m, 2H), 4.04 – 3.92 (m, 2H), 3.76 (s, 3H), 3.73(s, 1H) 3.24 (t, *J* = 6.9 Hz, 2H), 3.11 (m, 2H), 1.93 (s, 3H), 1.66 – 1.53 (m, 2H), 1.48 (m, 2H), 1.41 (m, 2H), 1.39 (s, 9H), 1.34(s, 3H), 1.23(s, 3H).

^{13}C NMR (100 MHz, $CDCl_3$): δ 170.8, 162.1, 156.2, 155.5, 144.4, 111.4, 108.9, 80.1, 74.9, 69.7, 65.9, 52.4, 51.3, 50.0, 47.6, 41.1, 29.6, 28.7, 28.3, 26.4, 26.3, 25.4, 23.2.

HRMS(ESI): Calculated for $C_{27}H_{44}N_6O_{10}$: 612.3119; Found: 635.3006 (M+Na).

5-Acetylamino-4-[2,3-bis(tert-butoxycarbonyl)guanidine]-6-[(6-azido-hexyl carbamoyloxy)-2,3 dihydroxy propyl]-5,6-dihydro-4H-pyran-2-carboxylic acid methyl ester (7).

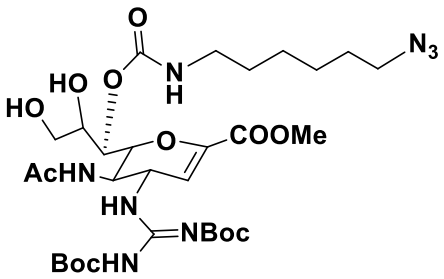

To a solution of compound **6** (0.1g, 0.16 mmol) in DCM (3.0 ml), TFA (3.0 ml) was added. The reaction mixture was stirred at rt for 1 h. DCM was removed, and the crude product was dried under reduced pressure. The dried compound was dissolved in DCM and Et_3N (68 µl, 0.48 mmol) was added. The solution was stirred at rt for 30 min. $HgCl_2$ (0.06g, 0.24 mmol) and 1,3-Bis(tert-butoxycarbonyl)-2-methyl-2-thiopseudourea (0.07g, 0.24 mmol) was added. The reaction mixture

was allowed to stir at rt for 12 h. The reaction was monitored by TLC. Upon completion the reaction mixture was washed with HCl (1M, 25ml) and extracted with DCM (20 ml, 3X). The organic layers were collected and washed with saturated $NaHCO_3$ and dried over Na_2SO_4. The product was purified by column chromatography with DCM: MeOH (25:1) to give the product **7** (0.058g, 50%).

^{1}H NMR (400 MHz, $CDCl_3$): δ 11.40 (s, 1H), 8.54 (d, *J* = 8.7 Hz, 1H), 7.39 (s, 1H), 7.28 (s, 1H), 6.85 (s, 1H), 5.89 (s, 1H), 5.32 (s, 1H), 5.20 (t, *J* = 9.5 Hz, 1H), 5.03 (t, *J* = 5.7 Hz, 1H), 4.82 (d, *J* = 9.4 Hz, 1H), 4.49 (d, *J* = 10.5 Hz, 1H), 4.37 (m, 1H), 4.14 (dd, *J* = 14.2, 7.1 Hz, 1H), 4.05 (d, *J* = 9.2 Hz, 1H), 3.80 (s, 3H), 3.68 (m, 1H), 3.27 (t, *J* = 6.8 Hz, 2H), 3.17 (m, 2H), 1.95 (d, *J* = 10.0 Hz, 3H), 1.60 (dd, *J* = 13.8, 6.8 Hz, 2H), 1.50 (s, 18H), 1.38 (m, 4H), 1.27 (dd, *J* = 7.7, 6.5 Hz, 2H).

^{13}C NMR (100 MHz, $CDCl_3$): δ 171.0, 162.8, 162.4, 162.2, 162.1, 157.1, 152.5, 144.9, 110.5, 83.7, 79.7, 69.4, 68.7, 62.4, 53.5, 52.31, 51.26, 49.4, 47.1, 45.7, 41.2, 29.4, S-14 28.7, 28.3, 28.2, 28.1, 27.9, 26.3, 26.2, 22.7.

HRMS(ESI): Calculated for $C_{30}H_{50}N_8O_{12}$: 714.3548; Found: 715.3627 (M+H).

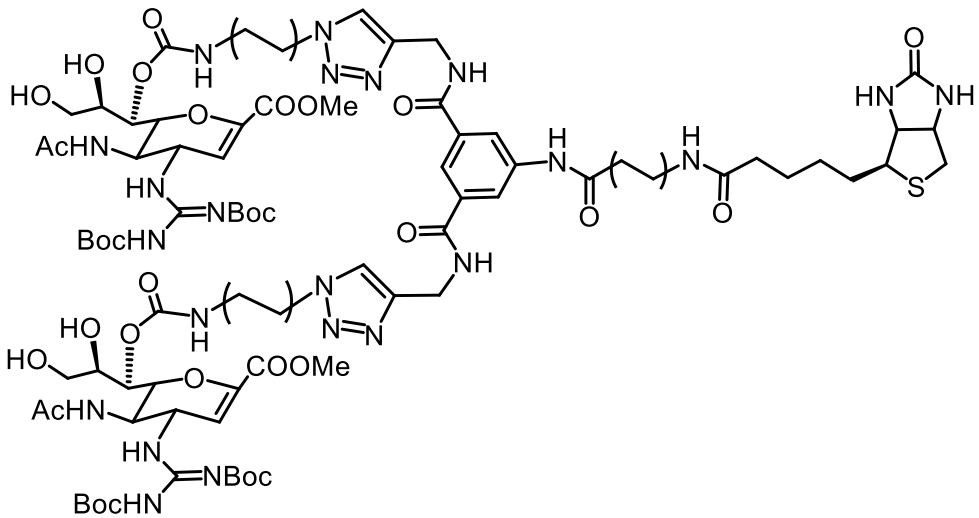

Compound 3: 7 (0.03g, 0.05 mmol) was dissolved in t-BuOH/ H_2O (1.0 ml, 7:3) and **8** (0.01g, 0.02 mmol) were added. $CuSO_4$ (0.004g, 4.6 mg, 0.03 mmol) and sodium L-ascorbate (0.007g, 7.3 mg, 0.02 mmol) was added to the reaction mixture and stirred at rt for 12 h. Reaction was monitored by TLC. Upon completion, solvent was removed under reduced pressure and product was purified by column chromatography with DCM: MeOH (10:1) to yield **3** (0.06g, 60% yield).

^{1}H NMR (400 MHz, $CDCl_3$): δ 11.40 (s, 2H), 8.62 (S, 1H), 8.62 (s,1H), 8.48 (d, *J* = 4.0 Hz, 2H), 8.20 (s, 1H), 8.05 (s, 1H), 7.80 (s, 1H), 7.39 (s, 2H), 6.90 (s, 1H), 6.52 (m, 3H), 5.90 (s, 2H), 5.42-5.33 (m, 3H), 5.14 (s, 1H), 5.10-5.08 (m, 1H), 5.02-4.99 (m, 1H), 4.75-4.51 (m, 9H), 4.38- 4.22 (m, 10H), 4.03-4.01 (m, 3H), 3.77 (s, 6H), 3.70-3.66 (m, 3H), 3.58-3.50 (m, 3H), 3.37 (s, 1H), 3.20-3.05 (m, 6H), 2.99-2.84 (m, 5H), 2.33-2.15 (m, 16 H), 1.92-1.78 (m, 10H), 1.66-1.59 (m, 8H), 1.47 (s, 18H), 1.27 (s, 18H).

^{13}C NMR (101 MHz, $CDCl_3$): δ 170.9, 166.9, 164.2, 164.2, 163.0, 162.5, 156.9, 152.6, 144.9, 139.4, 122.9, 110.6, 100.1, 83.6, 79.6, 73.9, 73.0, 71.7, 69.9, 68.6, 62.6, 60.4, 55.9, 52.5, 50.1, 46.9, 31.9, 29.7, 29.7, 29.8, 29.6, 29.4, 29.1, 28.9, 28.3, 28.0, 25.6, 25.6, 25.5, 22.9, 22.7, 14.1, 1.0.

HRMS (ESI): Calculated for $C_{91}H_{140}N_{22}O_{29}S$: 2038.29; Found: 1020.00 (m/z; m = M+2H; z=2).

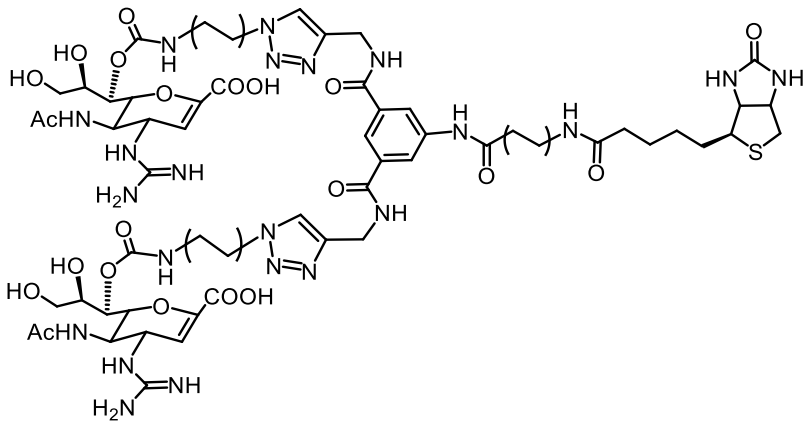

AD-R: **3** (0.01g, 0.004 mmol) was dissolved in DCM: TFA (1ml, 1:1) and stirred at rt for 1 h. The reaction mixture was neutralized with H^+ DOWEX 50WX8-200 ion-exchange resin to pH 7. The resin was filtered and washed with MeOH and the product was concentrated under reduced pressure. The solid was re-dissolved in MeOH and NaOH (50 mM, 1 ml) was added and the reaction mixture was allowed to stir at rt for 2 h. The reaction was neutralized to pH 7 with H^+ DOWEX 50WX8-200 ion-exchange resin. The resin was filtered, and the product was purified with Bio-Gel P-2 Gel with DI water to give **AD-R** (0.005g, 5.2 mg, yield 80%).

^{1}H NMR (400 MHz, D_2O): δ 7.91-7.85 (m, 5H), 5.55-5.51 (m, 2H), 4.79-4.77 (m, 4H), 4.57 (s, 3H), 4.41-4.40 (m, 1H), 4.39 (d, *J* = 8Hz, 1H), 4.36-4.35 (m, 1H), 4.31-4.28 (m, 5H), 4.03-3.90 (m, 4H), 3.61 (s, 3H), 3.54-3.44 (m, 3H), 3.36-3.34 (m, 1H), 3.08-2.99 (m,3H), 2.88-2.86 (m, 3H), 2.63 (s, 1H), 2.30-2.26 (m, 2H), 2.12-2.06 (m, 2H), 2.01-1.99 (m, 1H) 1.90 (s, 1H), 1.84 (s, 6H), 1.77-1.73 (m, 2H), 1.67-1.64 (m, 2H), 1.55-1.53 (m, 2H), 1.48-1.45 (m, 2H), 1.39-1.37 (m, 2H), 1.31-1.29 (m, 4H), 1.23-1.20 (m, 6H), 1.15-1.12 (m, 6H), 0.80-0.78 (m,2H).

^{13}C NMR (100 MHz, D_2O): 175.8, 171.2, 168.4, 163.5, 163.2, 162.9, 156.2, 135.8, 134.9, 129.3, 123.9, 122.5, 115.3, 110.0, 104.8, 100.0, 78.7, 75.2, 71.9, 69.6, 68.5, 62.5, 51.8, 50.0,47.3, 35.0, 29.1, 28.4, 28.0, 27.8, 27.5, 26.0, 25.6, 25.1, 21.8, 20.0.

HRMS (ESI): Calculated for $C_{69}H_{104}N_{22}O_{21}S$: 1609.7639; Found: 1610.7600 (M+H).

3.5.3 Biological Assays

A. Immobilization of Glycans: Synthetic glycans were covalently immobilized onto Nexterion NHS slides using a DIGILAB OmniGrid Micro printer in 300 mM phosphate buffer with 0.005% Tween-20 at pH 8.5.[58] Each glycan was printed 20 times in quintuplicate at 200 μM concentration. Following printing, the glycans were allowed to react for 30 min at 60% humidity. After overnight desiccation, the slides were blocked for 60 min with 50 mM

ethanolamine in 50 mM boric acid buffer (pH 9.5), washed 3 times with deionized (DI) water, dried and stored at −20 °C.

B. Binding studies: A serial 10-fold dilution of A/Brisbane/59/2007, starting with a concentration of 2.4 X 10^6 plaque forming units (PFU) was prepared in a buffer consisting of PBS, 2% BSA and 0.05% Tween-20. 200 μL of this solution was applied to the microarray for 60 min. Following virus incubation and wash (three times with PBS and 0.05% Tween-20 and two times with PBS), 200 μL of 20 mM of AD-Reporter was applied to the microarray for 60 min in the same buffer. TRITC labelled streptavidin (1mg) was re-suspended into 1 ml of the buffer. A 20,000-fold dilution of the fluorescently labelled streptavidin was applied to the microarray after the slides were washed as extensively and incubated for 60 min. The slides were washed as described followed by a rinse with DI water (three times). The slides were dried and scanned using GenePix4000B scanner at a wavelength of 557 nm. All experiments were performed in triplicate.

3.6 Discussion

Influenza virus affect millions worldwide annually. Therefore, it has been extensively studied and still being studied for more effective diagnostics and treatments. It is well known that influenza viruses has several surface proteins that are good targets for therapeutics. The adamantane based antiviral drugs, which block M2 protons pump proteins have been rendered inadequate in the recent years. The viruses mutated and have shown total resistance to these adamantine based drugs for both influenza A and B viruses. The NA inhibitors, as a result of overuse of Oseltamivir, several strains of Oseltamivir resistant influenza virus has been isolated. Thus, there is a need for both effective and less resistant antivirals. Surveillances of influenza viruses are required for a more effective treatment and arrest the spread of this deadly disease. However, detections methods currently on the market haveom poor sensitivity and low accuracy. The gold standard for influenza

detections are PCR which require expensive requirement and lab expertise. The limitation for the PCR is the lack of availability of specific primers and probes and the inability to use this method in low resourse setting. Methods of detection involving cell cultures require long turnaround time (4-7 days) and cannot differentiate types of influenza viruses. Therefore, it is not useful for doctors to use as a diagnostic methodology to prescribe anti-viral medications. Antiviral medications have an effectiveness window of 24-48 hours after onset of infection, therefore diagnostic tools must have fast turnaround times with accurate diagnosis that can be used by doctors to prescribe medications. Thus, there is an urgent need to develop both diagnostic tools which are highly accurate and time sensitive along with antiviral drugs which are effective and less likely to develop antiviral resistance.

3.7 Summary

In summary, we have synthesized a biotinylated bivalent Zanamivir analog for the specific capture of influenza viruses. We used this molecule as a reporter in our microarray studies and demonstrated that this compound could be used as a reporter in a sandwich assay with an influenza A H1N1 virus strain. While we used it as a reporter in our assay, the biotinylated molecule could be used as probes to capture influenza viruses as the biotin can readily be attached to streptavidin coated magnetic beads,[65] nanoparticles[66] or surfaces.[62] This technology will become very useful to detect high volume of samples in less amount of time.

3.8 References

1. WHO, Media Centre of World Health Organization. Fact sheet N°211 Influenza, April **2009**, World Health Organization: Geneva, Switzerland.
2. Wagner, R.; Matrosovich, M.; Klenk, H. D., Functional balance between haemagglutinin and neuraminidase in influenza virus infections. *Rev Med Virol* **2002,** *12* (3), 159-166.
3. Bass, C.; A comparism of rapid point of care tests for the detection of Avian Influenza A(H7N9 virus. *European Survellience,* **2013**, 18 (21).
4. Chi Hyun Cho, D. Evaluation of five rapid diagnostic kits for influenza A/B virus. *Journal of Virological Methods,* **2013**, 187, 51-56.
5. Islam, T.; von Itzstein, M., Anti-influenza drug discovery: are we ready for the next pandemic? *Advances in carbohydrate chemistry and biochemistry* **2007,** *61*, 293-352.
6. Creighton, Charles., *A History of Epidemics In Britain, With Additional Material* By D.E.C. Eversley **1965.**
7. Hannoun, C., The evolving history of influenza viruses and influenza vaccines. *Expert Rev Vaccines* **2013**, 1085-94. doi: 10.1586/14760584.2013.824709.
8. Cunha, B.A., Influenza: historical aspects of epidemics and pandemics. *Infectious disease clinics of North America*, **2004**, 18(1): p. 141-155.
9. Ryan, K., et al., *Sherris Medical Microbiology*, **2010,** McGraw-Hill: New York.
10. Hay, A; Gregory V; Douglas A; Lin Y., "The evolution of human influenza viruses. *Philosophical Transactions of the Royal Society B*, 2001, 356**,** (1416): 1861–70.
11. Nayak, D.P., Influenza virus morphogenesis and budding *Virus Research*, **2009**. 143(2): p.147.

12. Mubareka, S. and P. Palese, "Influenza virus: the biology of a changing virus," in Influenza Vaccines for the Future, eds Giudice G. D., Rappuoli R., editors. *Advances to infectious diseases*. **2011**, Springer Basel. p. 3-26.
13. Air. G.M., Influenza Neuraminidase. *Influenza and Other Respiratory Viruses,* **2012,** 6(4), 245–256.
14. Treanor, J., *Influenza viruses, including avian influence and swine influenza.*, *Principles and Practice of Infectious Diseases*, G. Mandell, J. Bennett, and R. Dolin, Editors. **2009**, Elsevier Churchill Livingstone: Philadelphia.
15. Gamblin, S. J.; Skehel, J. J., Influenza hemagglutinin and neuraminidase membrane glycoproteins. *The Journal of biological chemistry* **2010,** *285* (37), 28403-9.
16. Yewdell, J., Viva la revolución: rethinking influenza A virus antigenic drift, *Current Opinion in Virology*, **2011**, 1(3): p. 177-183.
17. Wolf, Yuri I. Viboud, C. Holmes, EC. Koonin, EV. Lipman, DJ., Long intervals of stasis punctuated by bursts of positive selection in the seasonal evolution of influenza A virus *Biol Direct.* **2006**, 1 (1): 34. doi- 10.1186/1745-6150-1-34.
18. Vladimir, T. Hossein, K. Raul R., Geographic Dependence, Surveillance, and Origins of the 2009 Influenza A (H1N1) Virus. *New England Journal of Medicine*. **2009**, 361 (2): 115–119. doi:10.1056/NEJMp0904572.
19. Shi, Y. Wu, Y. Zhang, W. Qi, J. Gao, G.F., Enabling the 'host jump': structural determinants of receptor-binding specificity in influenza A viruses. *Nature reviews microbiology*. **2014**, 12, 822-83.
20. Wiley, D. C.; Skehel, J. J., The Structure and Function of the Hemagglutinin Membrane Glycoprotein of Influenza Virus. *Annual review of biochemistry* **1987**, *56*, 365-94.

21. Wilson, I.A. Skehel, J.J. Wiley, D.C., Structure of the influenza virus haemagglutinin complexed with its receptor, sialic acid, *Nature*, **1981**, 289 (81), 366-373.

22. Hirst, G.K., Adsorption of Influenza hemagglutinins by Virus and red blood cells. *Journal of experimental medicine*, **1942**, 76 (2), 195-209.

23. Baum, L. G.; Paulson, J. C., Sialyloligosaccharides of the respiratory epithelium in the selection of human influenza virus receptor specificity.*Acta histochemica. Supplementband* **1990,** *40*, 35-8.

24. Gong, J.; Xu, W.; Zhang, J., Structure and Functions of Influenza Virus Neuraminidase, *Current medicinal chemistry* **2007**, *14* (1), 113-22.

25. Kerry, P. S.; Mohan, S.; Russell, R. J.; Bance, N.; Niikura, M.; Pinto, B. M., Structural basis for a class of nanomolar influenza A neuraminidase inhibitors. *Scientific reports* **2013,** *3*, 2871

26. Nobusawa, E.; Aoyama, T.; Kato, H.; Suzuki, Y.; Tateno, Y.; Nakajima, K., Comparison of complete amino acid sequences and receptor-binding properties among 13 serotypes of hemagglutinins of influenza A viruses. *Virology* **1991**, *182* (2), 475-85.

27. Kulkarni, A. Weiss, A. Iyer, S.S., Glycan-Based High-Afnity Ligands for Toxins and Pathogen Receptors *Medicinal Chemistry Reviews*, **2010**, *30*, 327-393.

28. Schrauwen, E. Fouchier, R. AM., Host adaptation and transmission of influenza A viruses in mammals. *Emerging Microbes and Infection*, **2014**, 3, e9; doi:10.1038/emi.2014.9

29. Moscona, A., Medical Management of Influenza Infection. Annual review of medicine, **2008**. 59(1): p. 397-413.

30. Yen, H.L., Importance of Neuraminidase Active-Site Residues to the Neuraminidase Inhibitor Resistance of Influenza Viruses. Journal of virology, **2006**. 80(17): p. 8787-8795. 123.
31. Taylor, N.R. and M. von Itzstein, Molecular Modeling Studies on Ligand Binding to Sialidase from Influenza Virus and the Mechanism of Catalysis. Journal of Medicinal Chemistry, **1994**. 37(5): p. 616-624. 124.
32. Burmeister, W.P., The 2.2 A resolution crystal structure of influenza B neuraminidase and its complex with sialic acid. The EMBO journal, **1992**. 11(1): p. 49.
33. Barchi, J. J., Jr., Emerging roles of carbohydrates and glycomimetics in anticancer drug design. *Current pharmaceutical design* **2000,** *6* (4), 485-501.
34. Burmeister, W. P.; Henrissat, B.; Bosso, C.; Cusack, S.; Ruigrok, R. W., Influenza B virus neuraminidase can synthesize its own inhibitor. *Structure* **1993,** *1* (1), 19-26.
35. Chong, A. K.; Pegg, M. S.; Taylor, N. R.; von Itzstein, M., Evidence for a sialosyl cation transition-state complex in the reaction of sialidase from influenza virus. *European journal of biochemistry / FEBS* **1992,** *207* (1), 335-43.
36. von Itzstein, M., The war against influenza: discovery and development of sialidase inhibitors. *Nature reviews. Drug discovery* **2007,** *6* (12), 967-74.
37. Reich, S.; Guilligay, D.; Pflug, A.; Malet, H.; Berger, I.; Crepin, T.; Hart, D.; Lunardi, T.; Nanao, M.; Ruigrok, R. W.; Cusack, S., Structural insight into cap-snatching and RNA synthesis by influenza polymerase. *Nature* **2014,** *516* (7531), 361-6.
38. Jorba, N.; Coloma, R.; Ortin, J., Genetic trans-complementation establishes a new model for influenza virus RNA transcription and replication. *PLoS pathogens* **2009,** *5* (5), e1000462.

39. Dias, A.; Bouvier, D.; Crepin, T.; McCarthy, A. A.; Hart, D. J.; Baudin, F.; Cusack, S.; Ruigrok, R. W., The cap-snatching endonuclease of influenza virus polymerase resides in the PA subunit. *Nature,* **2009,** *458* (7240), 914-8.
40. Resa-Infante, P.; Jorba, N.; Coloma, R.; Ortin, J., The influenza virus RNA synthesis machine: advances in its structure and function. *RNA biology* **2011,** *8* (2), 207-15.
41. Pflug, A.; Guilligay, D.; Reich, S.; Cusack, S., Structure of influenza A polymerase bound to the viral RNA promoter. *Nature* **2014,** *516* (7531), 355-60.
42. Chu, C.; Fan, S.; Li, C.; Macken, C.; Kim, J. H.; Hatta, M.; Neumann, G.; Kawaoka, Y., Functional analysis of conserved motifs in influenza virus PB1 protein. *Plos One* **2012,** *7* (5), e36113.
43. Pielak, R. M.; Schnell, J. R.; Chou, J. J., Mechanism of drug inhibition and drug resistance of influenza A M2 channel. *Proceedings of the National Academy of Sciences of the United States of America* **2009,** *106* (18), 7379-84.
44. Cady, S. D.; Mishanina, T. V.; Hong, M., Structure of amantadine-bound M2 transmembrane peptide of influenza A in lipid bilayers from magic-angle-spinning solid-state NMR: the role of Ser31 in amantadine binding. *Journal of molecular biology* **2009,** *385* (4), 1127-41.
45. Pinto, L. H.; Lamb, R. A., The M2 proton channels of influenza A and B viruses. *The Journal of biological chemistry,* **2006,** *281* (14), 8997-9000.
46. Lakadamyali, M., M.J. Rust, and X. Zhuang, Endocytosis of influenza viruses. *Microbes and infection*, **2004**, 6(10): p. 929-936.
47. Han, X., Membrane structure and fusion-triggering conformational change of the fusion domain from influenza hemagglutinin. *Nature structural biology*, **2001**, 8(8): p. 715-720.

48. Harrison, S.C., Viral membrane fusion. *Nature structural & molecular biology*, **2008**, 15(7): p. 690.

49. Reich, S.; Guilligay, D.; Pflug, A.; Malet, H.; Berger, I.; Crepin, T.; Hart, D.; Lunardi, T.; Nanao, M.; Ruigrok, R. W.; Cusack, S., Structural insight into cap-snatching and RNA synthesis by influenza polymerase. *Nature* **2014,** *516* (7531), 361-6.

50. Whittaker, G., Intracellular trafficking of influenza virus: clinical implications for molecular medicine. *Expert reviews in molecular medicine*, **2001**, 2001: p. 1-13.

51. Betakova, T., M2 Protein-A Proton Channel of Influenza A Virus. *Current Pharmaceutical Design*, **2007**, 13(31): p. 3231-3235.

52. Rossman, J.S., et al., Influenza Virus M2 Protein Mediates ESCRT-Independent Membrane Scission. *Cell*, **2010**, 142(6): p. 902-913.

53. Gamblin, S. J.; Skehel, J. J., Influenza hemagglutinin and neuraminidase membrane glycoproteins. *The Journal of biological chemistry* **2010,** *285* (37), 28403-9.

54. Yamashita, M.; Tomozawa, T.; Kakuta, M.; Tokumitsu, A.; Nasu, H.; Kubo, S., CS-8958, a prodrug of the new neuraminidase inhibitor R-125489, shows long-acting anti-influenza virus activity. *Antimicrobial agents and chemotherapy* **2009,** *53* (1), 186-92.

55. Webster, R. G.; Govorkova, E. A., Continuing challenges in influenza. *Annals of the New York Academy of Sciences* **2014,** *1323*, 115-39.

56. Bright, R. A.; Shay, D. K.; Shu, B.; Cox, N. J.; Klimov, A. I., Adamantane resistance among influenza A viruses isolated early during the 2005-2006 influenza season in the United States. *Jama* **2006,** *295* (8), 891-4.

57. Collins, P.J., Crystal structures of oseltamivir-resistant influenza virus neuraminidase mutants. *Nature* (London), **2008**. 453(7199): p. 1258-1261.

58. Tramontana AR, et al., Oseltamivir resistance in adult oncology and hematology patients infected with pandemic (H1N1) 2009 virus, *Australia. Emerg Infect Dis*, **2010**. 16(7): p. 1068-1075.

59. Kerry, P. S.; Mohan, S.; Russell, R. J.; Bance, N.; Niikura, M.; Pinto, B. M., Structural basis for a class of nanomolar influenza A neuraminidase inhibitors. *Scientific reports* **2013,** *3*, 2871.

60. Samson, M.; Abed, Y.; Desrochers, F. M.; Hamilton, S.; Luttick, A.; Tucker, S. P.; Pryor, M. J.; Boivin, G., Characterization of drug-resistant influenza virus A(H1N1) and A(H3N2) variants selected in vitro with laninamivir. *Antimicrobial agents and chemotherapy* **2014,** *58* (9), 5220-8.

61. Hernandez, J. E.; Adiga, R.; Armstrong, R.; Bazan, J.; Bonilla, H.; Bradley, J.; Dretler, R.; Ison, M. G.; Mangino, J. E.; Maroushek, S.; Shetty, A. K.; Wald, A.; Ziebold, C.; Elder, J.; Hollister, A. S.; Sheridan, W.; e, I. N. D. P. I., Clinical experience in adults and children treated with intravenous peramivir for 2009 influenza A (H1N1) under an Emergency IND program in the United States. *Clinical infectious diseases : an official publication of the Infectious Diseases Society of America* **2011,** *52* (6), 695-706.

62. Bantia, S.; Arnold, C. S.; Parker, C. D.; Upshaw, R.; Chand, P., Anti-influenza virus activity of peramivir in mice with single intramuscular injection. *Antiviral research* **2006,** *69* (1), 39-45.

CHAPTER 4

* Most of the work described in this chapter will be published in a manuscript that in under preparation.

Das, A., Dinh, H., Howard, J, H., Iyer, S. Electrochemical monitoring of Thrombin, Factor VIII, and Factor Xa using repurposed glucose meters. (Manuscript under preparation)

4 TOWARDS POC DETECTION OF THROMBIN

4.1 Introduction

Detection of pathogens in bodily fluids using glucose meters has always been challenging due to the high background interference from glucose. To overcome this problem, as described in chapter 2 we have devised new strips which can detect paracetamol in the presence of high background glucose. Using this method, we have successfully detected pathogens in blood and urine. Building on these results we wanted to detect thrombin in blood. Thrombin is a very important enzyme of hemostasis and is essential for blood coagulation.[1]

4.2 Blood coagulation cascade

The blood coagulation occurs through two pathways, the extrinsic and intrinsic pathway. The **intrinsic pathway** is activated when blood reaches the sub-endothelial connective tissues due to tissue damage. Quantitatively it produces or activates more thrombin of the two pathways but acts much slower compared to the extrinsic pathway. The Factor XII (*Hageman factor)*, Factor XI, prekallikrein, and High molecular weight *kininogen* (HMWK) are involved in this pathway of activation.[2-5]

Activation leads to the cleavage of the native Hageman factor into two subunits (50 and 28 KDa). The smaller subunit forms the activated Hageman factor (factor XIIa). Once triggered this pathway is self-amplifying. This factor XIIa then activates prekallikrein to *kallikrein.* This kallikrein further activates the activation of factor XII to factor XIIa. Presence of Ca^{2+} ions is essential for this step. HMWK, binds to factor XI and aids in the coagulation cascade.

The common pathway starts with the formation of Factor X. Factor X is formed by the complex of molecules consisting of activated factor IX, factor VIII, calcium, and phospholipid. The factor X is also synthesized from the extrinsic pathway.[5]

The **extrinsic pathway** activated instantaneously in response to injury and produces activated factor X in seconds compared to an intrinsic pathway which requires minutes. The primary function of the extrinsic pathway is to augment the intrinsic pathway as mentioned earlier the intrinsic pathway is self amplifying once triggered, so the extrinsic pathway helps in triggering the intrinsic pathway. Once there is an injury to the endothelium, tissue factor is released. The activated tissue factor then binds to factor VII. This complex containing the activated tissue factor, factor VII, calcium and phospholipid forms the activated factor X.[6]

Activated factor X then converts the prothrombin to Thrombin. The thrombin then converts the soluble fibrinogen to insoluble fibrin and ultimately together with aggregated platelets forms a clot. This is known as the **common pathway.**[6]

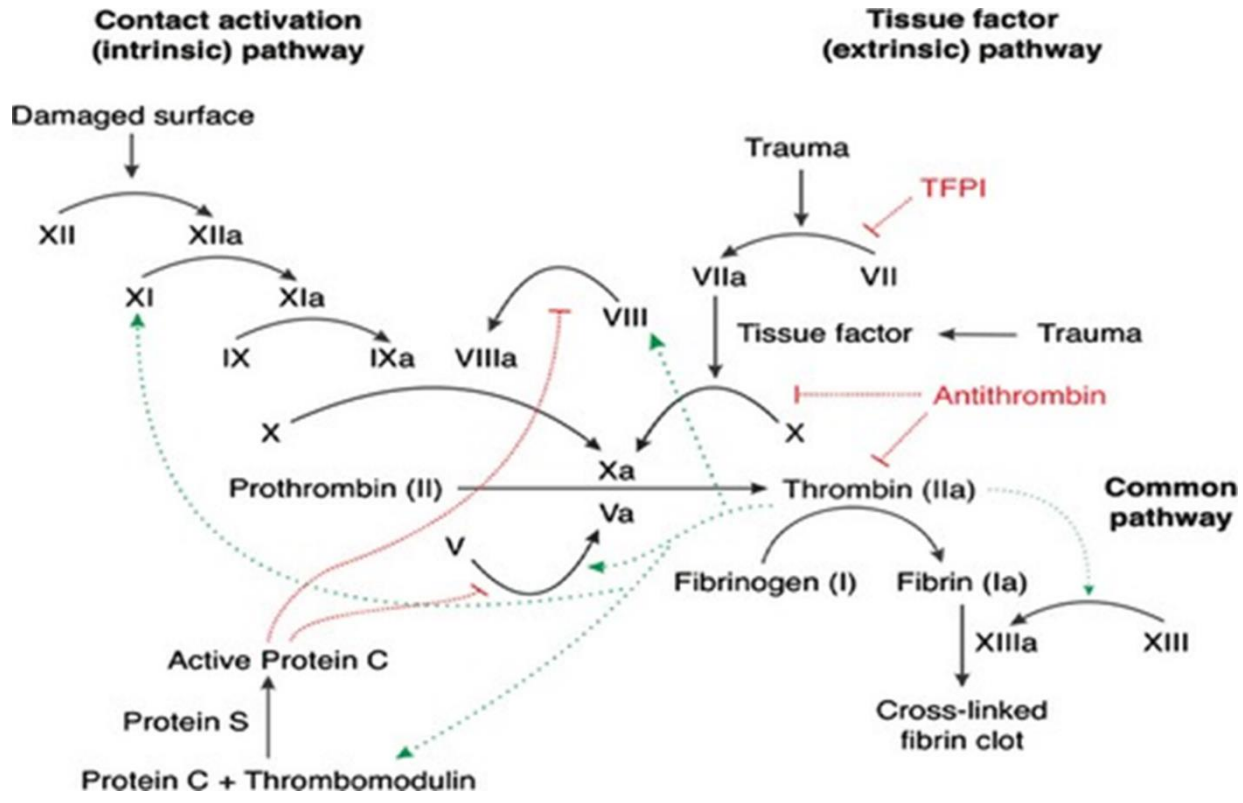

Figure 37*. Coagulation cascade.*
Reprinted with permission[6]

4.3 Background on Thrombin

Thrombin or blood coagulation factor IIa, is a serine protease that is encoded by the F2 gene and plays a pivotal role in the blood clotting cascade to promote hemostasis following an injury to the endothelium.[7] The word Thrombin comes from the greek word *thrombus* meaning clot. Thrombin is synthesized by the liver as inactive zymogen prothrombin in the blood. Prothrombin or coagulation factor II is proteolytically cleaved to form the active enzyme thrombin only at the site of vascular injury following an upstream activation of the coagulation pathway. Prothrombin is activated by Factor Xa, Factor V, phospholipid, and calcium to form the thrombin enzyme, which in turn converts the soluble plasma glycoprotein, fibrinogen, to insoluble fibrin, forming the clot.[1-2] Thrombin in the presence of calcium activates factor XIII, which promotes the cross-linking of fibrin polymers. The cross-linked fibrin then acts a hemostatic plug to stop blood loss. The thrombin plays the crucial role in the coagulation cascade by activating the platelets, Factor V, Factor VIII and also by the conversion of fibrinogen to fibrin. At the site of vascular damage, the coagulation cascade is activated by the binding of tissue factor (TF) to factor VII. The complex of TF-FVIIa initiates a complex cascade reaction which leads to the formation of prothrombinase complex consisting of FVa, FXa, calcium and phospholipid ions, which aid to the proteolytic cleavage of prothrombin to release Thrombin.[8-10]

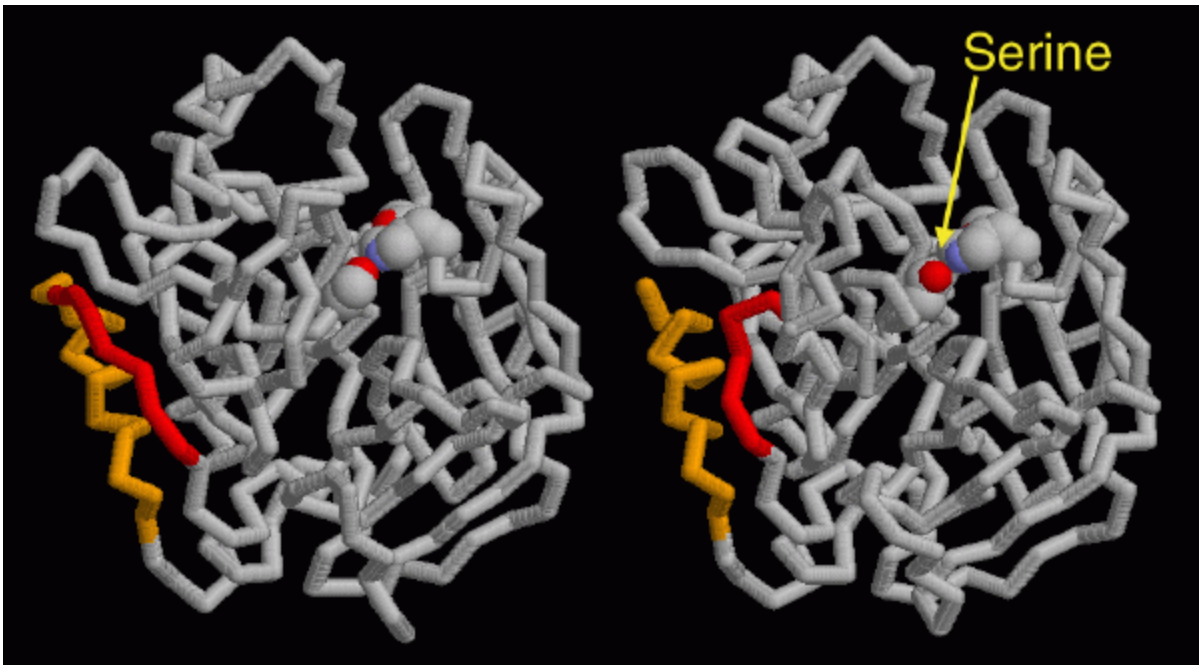

Figure 38*. Active and Inactive forms of Thrombin generated using PDB.*

The inactive form of the protein is depicted on the left. To generate the active form of the protein the strand between the yellow and the red strands must be cleaved. After this cleavage, the two ends separate and undergoes relaxation and produces the active form of the enzyme depicted on the right. In the active form, the key catalytic residue containing the serine amino acid (bright red depicts the oxygen atom of serine) is facing outwards unlike the inactive form.

4.4 Drugs to modulate coagulation

Anti-coagulant drugs are used to maintain the balance between hemostasis and bleeding. The targets of anti-coagulants are mainly the different clotting factors in the coagulation cascade they were first introduced in 1930. Heparin was the first anticoagulant to be approved by FDA.[11]

The anticoagulant drugs can be classified as follows:

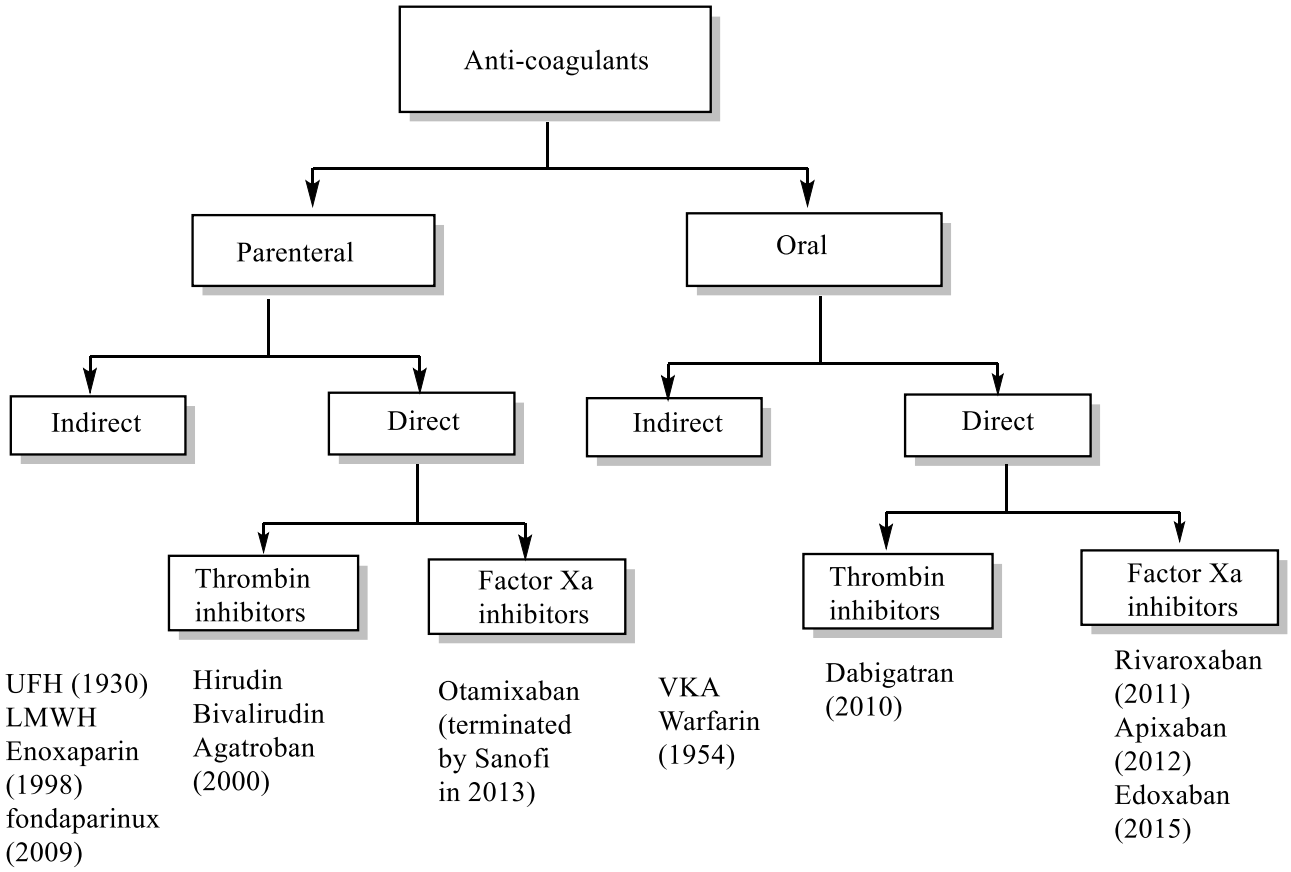

Figure 39*. Classification of anti-coagulants along with FDA approval times in parenthesis.*[11-13]

The oldest anti-coagulants in clinical use are the heparins, [unfractionated heparin (UFH) and low molecular weight heparin (LMWH)] and vitamin K antagonists (VKA) like warfarin. The heparins are parenteral or injectables while warfarin is an oral anticoagulant. Unfractionated heparin catalyzes the inhibition of Thrombin by the natural anti-coagulant antithrombin (AT). By catalyzing AT, it inhibits the activation of FIXa, FXa, FXIa, FXIIa along with Thrombin. The LMWH heparins inhibit FXa to a greater extent than thrombin. VKA inactivates the vitamin K dependent coagulation factors II, VII, IX, and X. they also inhibit the activation of anticoagulants

protein C and S.[9] The drug targets for the classical anti-coagulants (heparins and VKAs)are depicted in the following **Figure 40**.

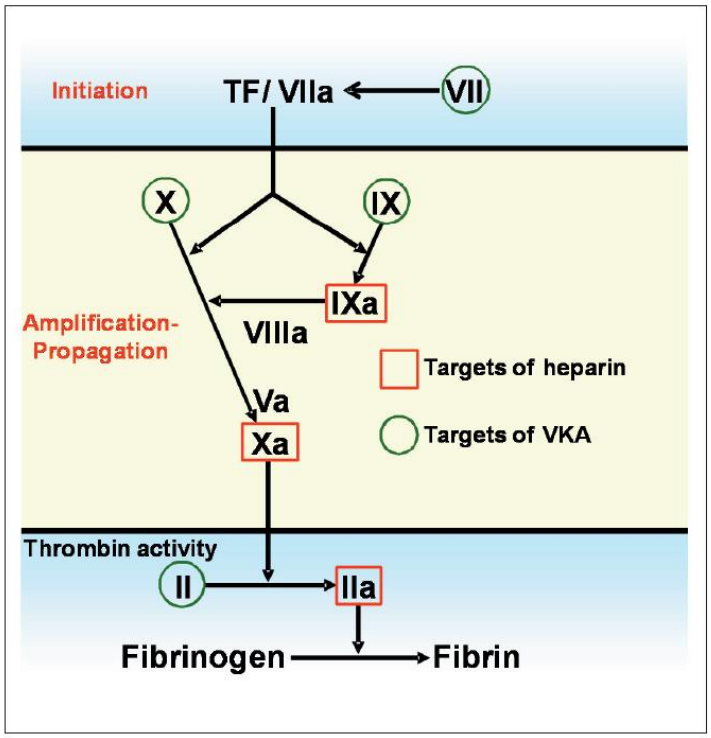

Figure 40. *Drug targets of the classical anti-coagulants Heparin and Vitamin-K antagonists.* Reprinted with permission[9]

Recently, a new class of direct oral anticoagulants (DOAC) were approved by FDA; these include the direct thrombin or direct Factor Xa inhibitors. In 2010, Dabigatran a direct thrombin inhibitor, (Pradaxa, Boehringer Ingelheim), and in 2011, rivaroxaban, direct factor Xa inhibitor (Xarelto, Johnson and Johnson, and Bayer Healthcare AG) were approved. Followed by, apixaban (Eliquis, Bristol-Meyers Squibb and Pfizer Inc) in 2012 and edoxaban (Savaysa/Lixiana, Daiichi Sankyo) in 2015. Both apixaban and edoxaban are direct factor Xa inhibitors. These directly inhibit the function of thrombin, thereby preventing the formation of fibrin and activation of platelets.[16]

These oral anticoagulants are much easier to take than the injectables like heparin and has proven to be safer than oral warfarin with fewer bleeding episodes and as of 2016, the DOAC prescriptions exceeded than those of warfarin.[33]

DOAC	Mechanism	Typical doses	Renal Elimination (%)	Half-life (h)	Reversal agent
Dabigatran	Direct Thrombin inhibitor	110, 150, 75 mg	80	12-14	Idarucizumab 5g dose (dose can be repeated)
Rivaroxaban	Factor Xa inhibitor	2.5, 5 mg	25	8-15	Andexanet.alfa
Apixaban	Factor Xa inhibitor	10, 15, 20 mg	33	9-13	Andexanet.alfa
Edoxaban	Factor Xa inhibitor	30, 60 mg	35	8-10	No

***Table 7**. Summary of new DOACC and their doses and available reversal agents.*[12]

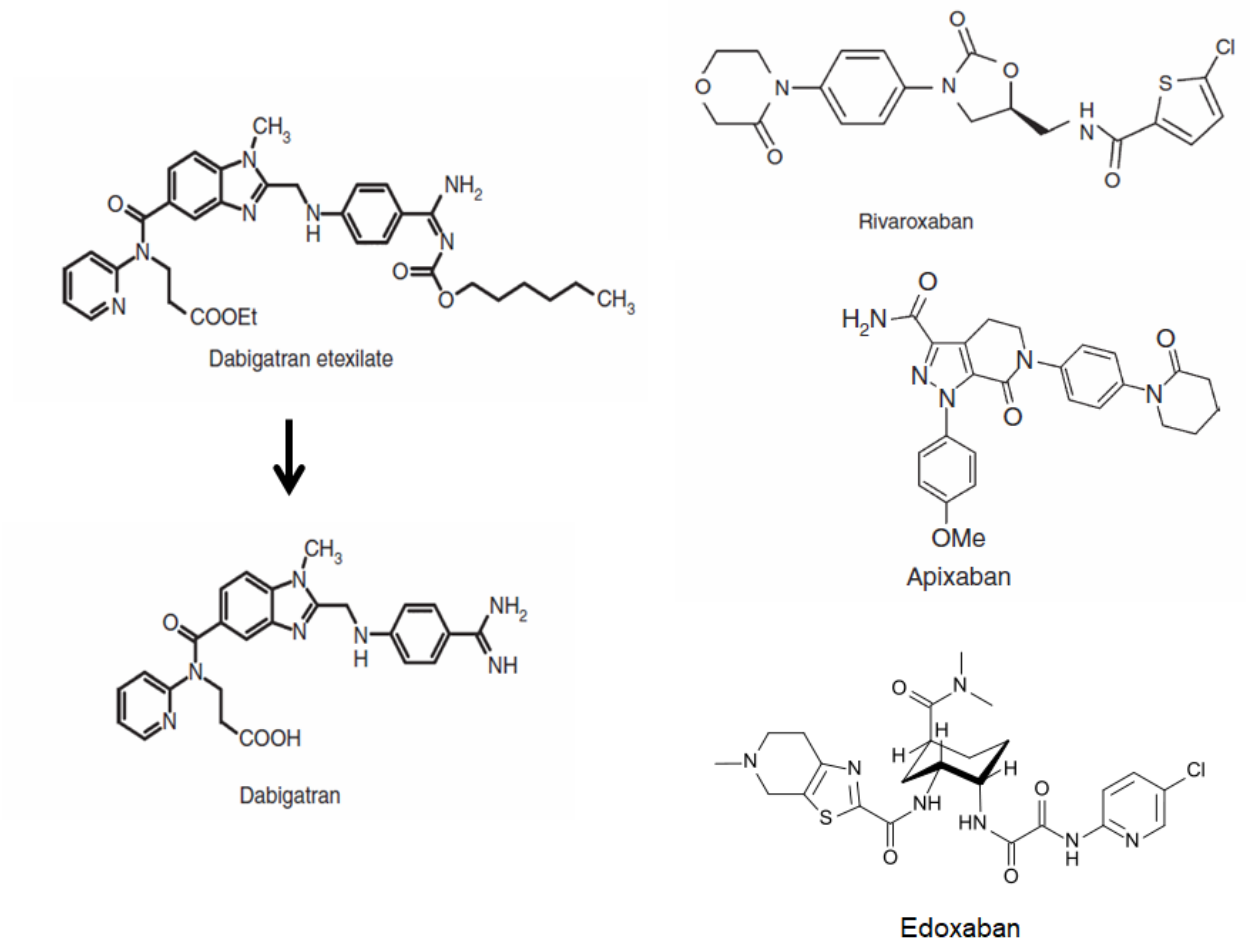

Figure 41. *FDA approved direct oral anti-coagulant drugs (DOAC).*

These new age DOAC cannot be monitored using the routine coagulation assays like prothrombin time (PT) and activated thromboplastin time (aPTT). There are no FDA approved methods to reliably monitor the DOACs. [33-34]

Unlike the widely available reversal agents for heparin (Protamine), warfarin (4-factor PCC) there is currently only one FDA approved reversal agent for Dabigatran (Idarucizumab) and for the reversal agents for FXa, Andexanet.alfa (Andexxa) was recently approved by FDA in May 2018, while another reversal agent for FXa, Ciraparantag is still under clinical trials.[33]

Thus, there is a huge need to monitor the level of thrombin in blood for the people who are prescribed with these new age anti-coagulants.

4.5 Need for monitoring oral-anti-coagulants

Thrombin plays an important part in the coagulation pathway. It is related to a number of blood clotting disorders. Some of these disorders are hereditary like hemophilia, von Willebrand disease, etc. and other cardiovascular diseases like Deep Vein Thrombosis, arteriosclerosis, hemorrhage etc.[4,9] Thrombin enzyme is a key component in thrombus formation, and maintains the finer balance in coagulation, anticoagulation and fibrinolysis. Anti-thrombotic treatment relies on the prevention of thrombosis while maintaining hemostasis.[7] It is very critical to maintain this balance otherwise there is a very high risk of either bleeding out or formation of clots that can cause thrombosis or embolism. Thrombin generation is dramatically reduced in patients with bleeding tendencies, while it is increased in patients with risk of venous thromboembolism. It is therefore used as a marker for deep vein thrombosis. Thrombin inhibitors like warfarin etc. are used to treat and prevent various diseases such as venous thrombosis and stroke. Excessive thrombin production can also lead to Disseminated intravascular coagulation (DIC). This causes the formation of huge lumps of clot throughout the body, resulting in depletion of clotting factors and platelets. This leads to bleeding in other areas, and the body is overwhelmed and is unable to stop the bleeding.[6,8]

Some of these anti-coagulant drugs have very high renal elimination rates. Dabigatran has a renal elimination rate of 80%.[33] This issue is further aggravated with patients with kidney failure, as they are taking these drugs and they are eliminated in the whole dose, making it very difficult to measure the amount of active drug in blood. Since there are no FDA approved ways to detect

the level of drug in blood coupled with the failure of PT and aPTT time to correctly detect the level of these DOAC drugs, it becomes essential to detect the amount of thrombin in blood.

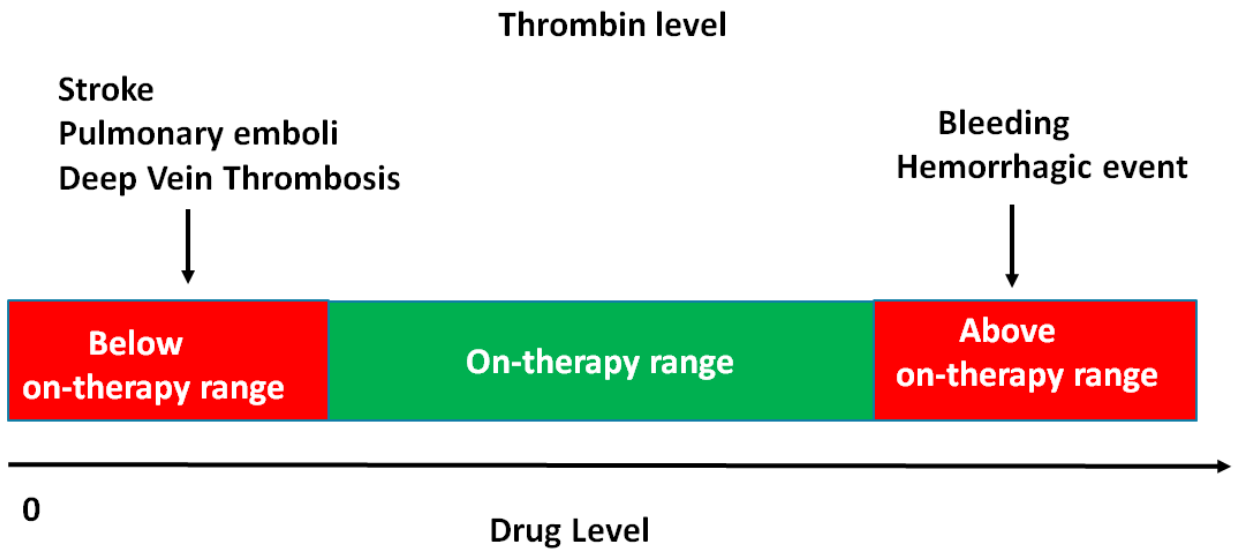

Figure 42*. Anti-coagulation therapy.*

4.6 Current detection methods of Thrombin

Thrombin is undoubtedly a pivotal component in multiple disease conditions as the enzyme directly affects blood circulation. Therefore, the ability to monitor thrombin activity in whole blood and in real time will allow researchers to elucidate the relationship between the thrombin and disease further. Current platforms to detect Coagulation activity Current methods to assess thrombin levels and coagulation activity include prothrombin time (PT), activated partial thromboplastin time (PTT), thrombin clotting time (TCT), bleeding time, platelet count, platelet function testing, aptamer-based assays, immunoassays.[15-18] The prothrombin time assay strictly looks at the extrinsic and common pathways of coagulation. Blood is drawn into a vacuum tube loaded with citrate (1:9 anticoagulant: blood), which chelates to the calcium ions in the sample. The blood is then centrifuged to separate the plasma from the red blood cells.[1,2,12, 24] Excess

amounts of calcium is introduced into the plasma sample to help in coagulation. Tissue factor II is added and the clotting time is measured optically. The prothrombin time (PT) falls within a range of 10-13 seconds.[10,24] The activated partial thromboplastin time (aPTT) assay strictly evaluates the intrinsic and common pathways of coagulation. Again, the blood sample is drawn into a vacuum tube loaded with citrate (1:9 anticoagulant: blood) phospholipids, silica activator, and calcium, which activates the intrinsic pathway. Thrombus formation time is then measured. In the presence of coagulation factors, I, II, V, VIII, IX, X, XI, and XII will normal PTT times range from 25 to 39 seconds.[24]

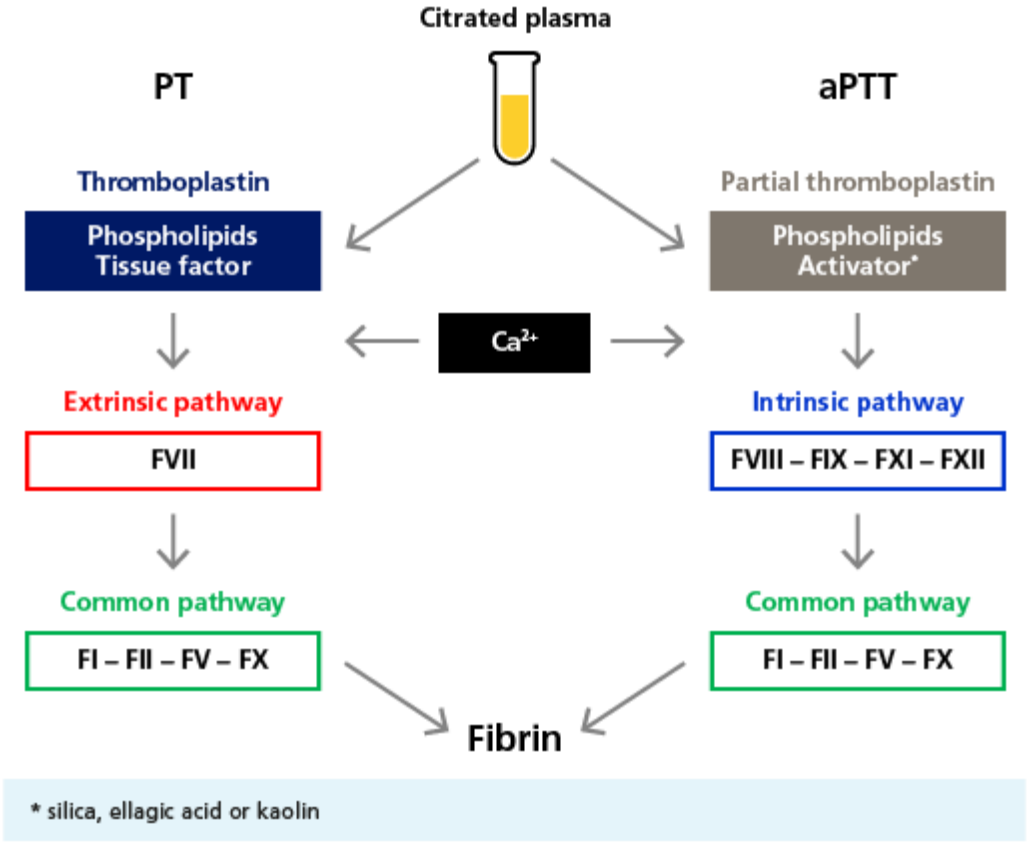

Figure 43. *Mechanism for measuring prothrombin time (PT) and activated partial thromboplastin time (aPTT).*
Reprinted with permission [12]

	Prothrombin time (PT)	***Activated Partial Thromboplastin time (aPTT)***
Normal	*11-13 seconds*	*25-30 seconds*

Table 8*. Detection methods of coagulation.*[3]

4.7 Chromogenic/Fluorogenic substrates for detection of Thrombin

There are several other chromogenic and fluorogenic substrates for direct detection of Thrombin. There are several chromogenic substrates that are available. These substrates contain a specific peptide sequence attached to o-nitrophenol (chromogenic) or resorufin (fluorogenic). The thrombin cleaves the peptide to release either, a chromogenic substrate o-nitrophenol (absorbs at 405nm)[11], or fluorogenic substrates like resorufin (E_{ex}/E_{em}=573-582 nm)[12] and 7-Amino-4-methyl coumarin (AMC) (E_{ex}/E_{em}=480-550 nm)[23] to indicate the presence of Thrombin. Several substrates that currently used for the detection of Thrombin are given in **Table 8.**

But these assays are qualitative in nature and does not quantify the amount of Thrombin present in the blood. Detection using chromogenic substrates is difficult because of the dark color of blood which makes it difficult to observe any color change. The fluorogenic substrate requires a fluorescent reader. Thus, the test can no longer be done at home or in a POC setting. Thus, there is a huge unmet need for quantitative detection of Thrombin in a POC setting. We were interested in developing an electrochemical assay that would use existing, ubiquitous glucose meters for the rapid detection of protease activity. Amperometric approaches are not subject to visual change in color but detect electron released upon oxidation of the electroactive substance (glucose, paracetamol, catechol, etc.). The use of glucose meters is very attractive for point of care diagnostics because glucose meters meet the ASSURED (Affordable, Sensitive, Selective, User-

friendly, Rapid and robust, Equipment free and Deliverable to end users) guidelines, established by the World Health Organization. Glucose meters are very affordable as the meters are a onetime cost and the disposable strips are inexpensive.

We thus devised the use of substrates that can be detected using a glucose meter. Out of the substrates available in the market we choose the tripeptide sequence with the highest Kcat/Km value (**Entry-6, Table-8**) and then coupled it with catechol. Catechol is absent in blood and can be detected with glucose meters in blood with a high background interference of glucose, (demonstrated in Chapter-2) making it the perfect candidate for detection of thrombin using glucose meters.

Entry	**Substrate**	**Km(mM)**	**Kcat (S^{-1})**	**Kcat/Km(S^{-1}/mM) X 10^{-3}**
1	Fibrinogen[11] (Natural substrate for FIIa)	0.012	71	6.5
2	Phe-Pip-Arg-pNA (Chromogenic substrate S-2238)	0.007	180	26
3	PyroGlu-Pro-Arg-pNA (Chromogenic substrate S-2366)	0.15	330	2.2
4	H-β-Ala-Gly-Arg-pNA (marketed by Siemens healthcare)	1.95	1.91	0.98
5	Gly-Gly-Arg-AMC (marketed by Technoclone)	0.31	1.86	6
6	H-D-Phe-Pro-Arg-Resorufin[12]	0.001	29	29

***Table 9**. Commercially available substrates for Thrombin or Factor IIa.*[11,21-22]

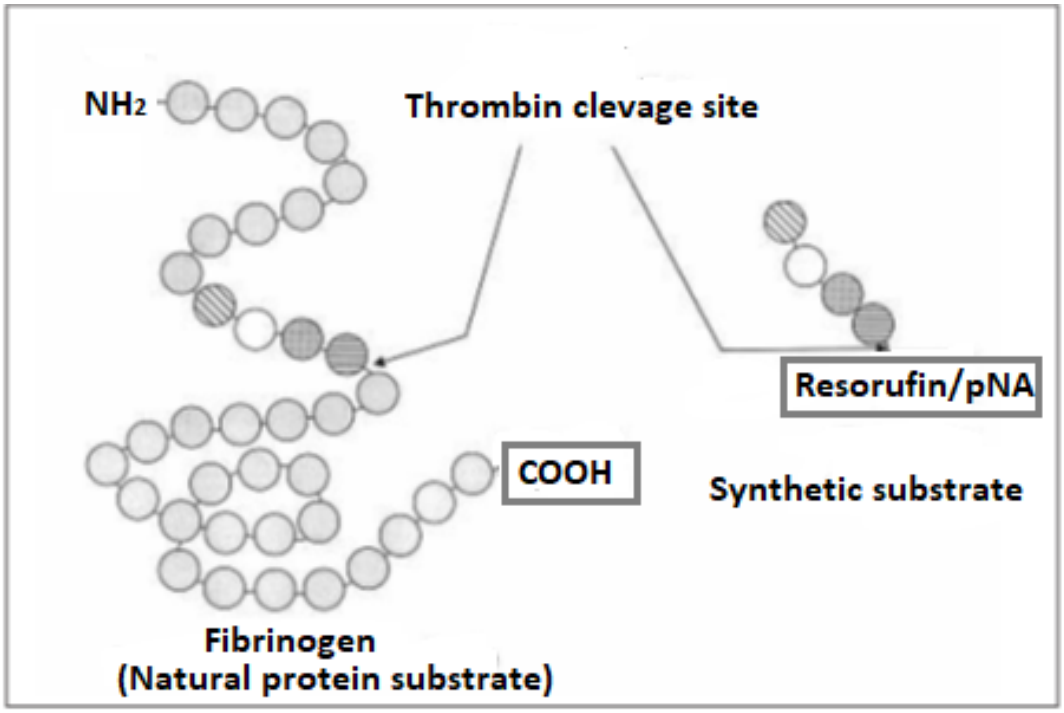

Figure 44*. Strategy for detection of thrombin using chromogenic/Fluorogenic substrates.*

4.8 Strategy to detection of Thrombin (FIIa)

The Factor IIa and Factor Xa are both serine proteases, and they cleave the substrate at specific sites to convert the zymogen to the activated form.[10] We have designed a tripeptide sequence that can be cleaved by the Factor IIa to release a unit of catechol that can be detected using a glucose meter. Successful probes for biomolecular applications need to fulfill several requirements: increase in cleavage efficiency, upon reaction with the enzyme, efficiency, and stability. We chose the model of a self-cleavable linker as a spacer between peptide substrate and the catechol. Katzenellenbogen reported for the first time the prodrug linker p-aminobenzyl alcohol (PABA).[19] The use of the spacer PABA made is very easy to conjugate peptides to catechol. The spacer is also beneficial to prevent steric hindrance around the cleavage site. We synthesized the prodrug-inspired substrate for thrombin (D-Phe-Pro-Arg-PABA-catechol) and will evaluate their effectiveness in the presence of thrombin (**Figure 45**). The synthesis of the building block 6,

started from NHFmoc-D-Arg (Pbf)- OH (**Scheme 6**). It coupled to PABA under standard conditions, affording the benzylic alcohol **2** in almost quantitative yield. The bromination of the alcohol was carried out by the PBr_3 under CH_2Cl_2 conditions to produce **3**, which was then coupled to catechol to give the first building block. As shown in **Scheme 6,** the synthesis of the second building block started with the coupling of NHFmoc-D-Phe-OH with H-Pro-OMe to provide the methyl ester **6** in good yield. The ester was hydrolyzed in THF/H2O mixture with AcOH under refluxing conditions, providing the free dipeptide **8** in good yield. The coupling of dipeptide **8** and building block **6** worked better with HATU as activator than with other agents. The reaction afforded better yields, and the product could be easily isolated from the byproducts. The Pbf and Fmoc deprotection with TFA/DCM mixture and C18 silica chromatography afforded D-Phe-Pro-Arg-PABA-catechol as TFA in good yields.

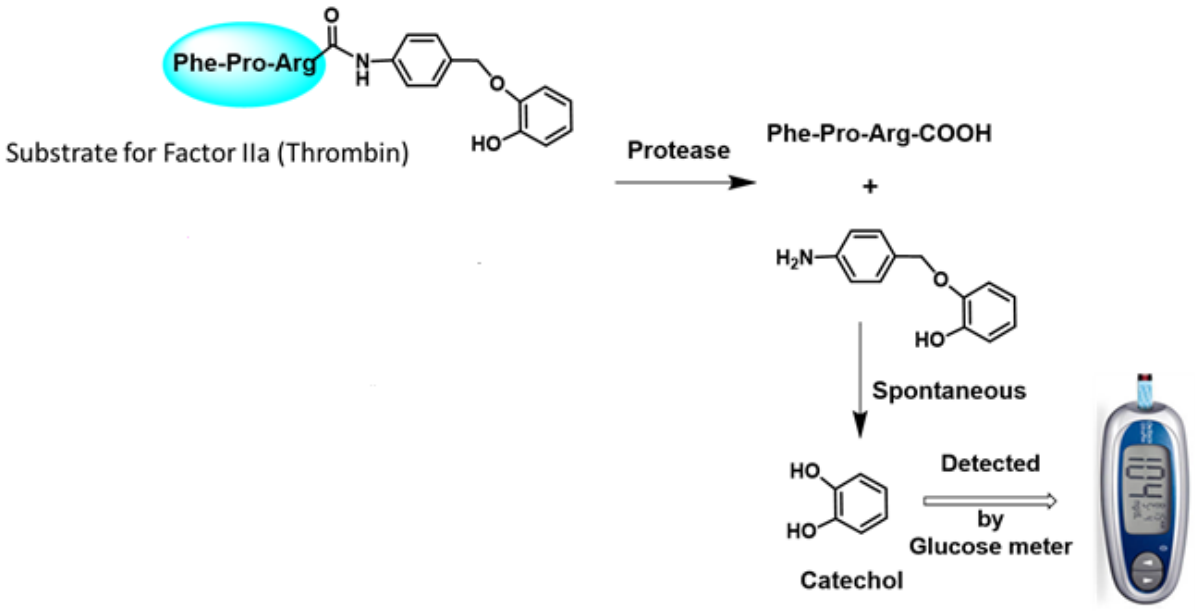

***Figure 45**. Design strategy for the substrate for detection of Thrombin.*

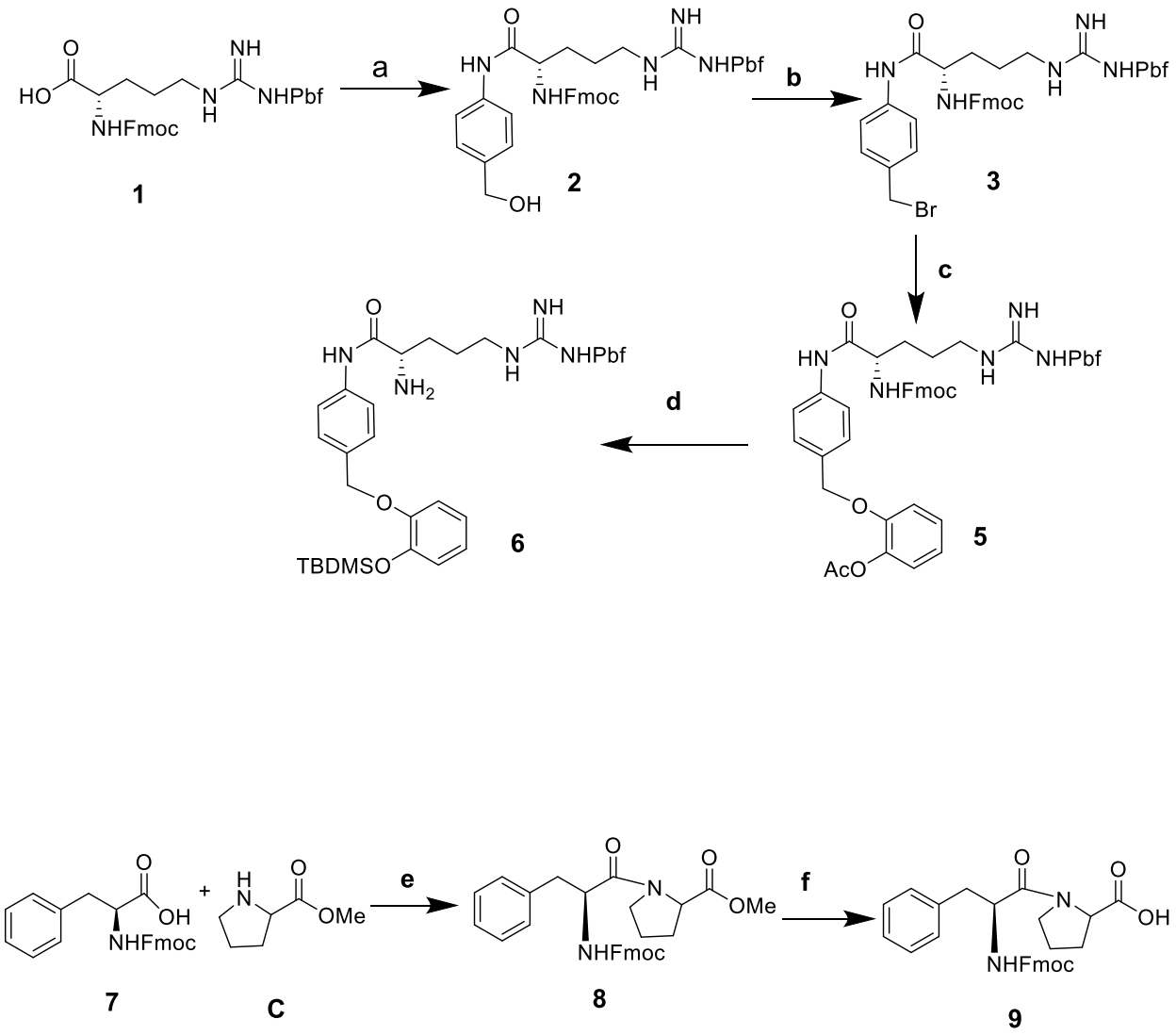

Scheme 6 *Synthesis of Phe-Pro-Arg-PABA -catechol*

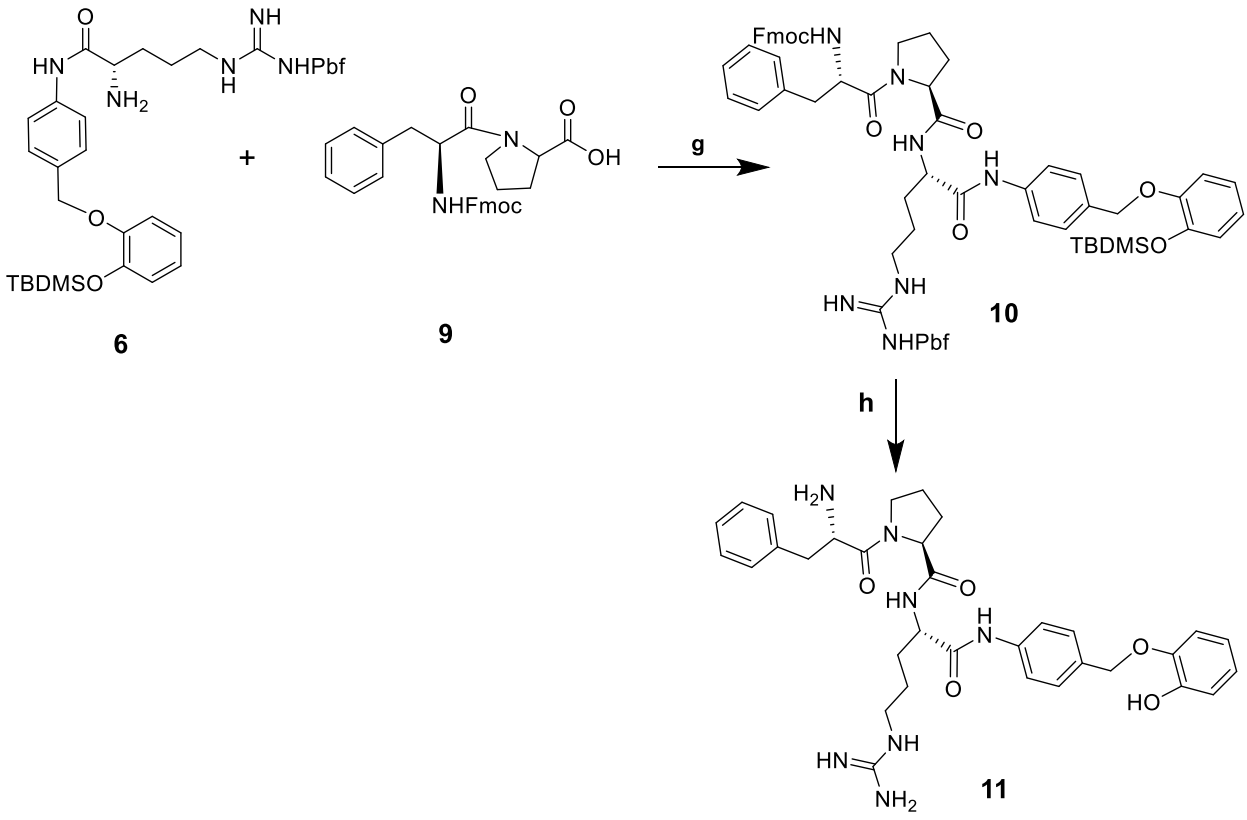

Phe-Pro-Arg-PABA-catechol

Scheme 6 *Synthesis of Phe-Pro-Arg-PABA-catechol*

Reagents and conditions: a) p-amino-benzyl alcohol, HATU, DIEPA, DMF 0^0C, 12 h, 78% b) PBr_3, CH_2Cl_2, 0^0C, 45 mins. c) **4**, K_2CO_3, Acetone, 12 h, rt, 68% (two steps). d)20% Piperidene, DMF, 0^0C, 45 mins, 85% e) HATU, DIEPA, DMF, 0^0C, 12 h, 71% f) TFA:DCM (1:2), 0^0C, 2 h, 87% g) HATU, DIEPA, DMF 0^0C, 12 h, 65% h) i)20% Piperidine, DMF, 0^0C, 45 mins ii)TFA (92.5%) Isopropyl silane (2.5%) H2O (5%),0^0C, 3h iii) NaOMe, MeOH, rt, 2h (72%, over three steps).

4.9 Experimental section

4.9.1 General

All reagents and solvents were reagent grade or were purified by standard methods before use. All reactions were performed under argon with solvents dried using a solvent purification system (Innovative Technology). All chemical reagents were of analytical grade, used as supplied without further purification unless indicated. The acidic ion exchange resin used was Amberlite® IR 120 (H^+) resin. Analytical thin layer chromatography (TLC) was performed on silica gel 230-400 mesh (Sicicycle). Plates were visualized under UV light, and/or by staining with acidic $CeH_8Mo_3N_2O_{12}$ followed by heating. Column chromatography was performed on silica gel (230-400 mesh). ^1H and ^{13}C NMR spectra were recorded on Bruker 400MHz spectrometer. Chemical shifts are reported in δ (ppm) units using ^{13}C and residual ^1H signals from deuterated solvents as references. Spectra were analyzed with MestreNova® (Mestrelab Research). Electrospray ionization mass spectra were recorded on a Micromass Q \T 2 (Waters) and data were analyzed with MassLynx® 4.0 (Waters) software. Reported yields refer to spectroscopically and chromatographically pure compounds that were dried under high vacuum (10^{-2} mbar) before analytical characterization unless otherwise specified.

4.9.2 Synthesis and Characterization

Compound 2:

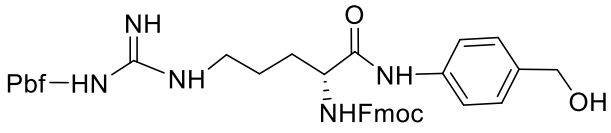

Add **1** (400 mg, 0.66 mmoles) and HATU (300mg, 0.78 mmoles) and dissolve in 10 ml of DMF (dry) at 0^0C and stir for 30 mins. Next add B (76 mg, 0.66 mmoles) to the above mixture and then

add DIEPA (0.128 ml, 0.74 mmoles) dropwise. The reaction mixture was allowed to stir at room temperature for 12 h. DMF is removed under reduced pressure and then the compound is purified by column chromatography. Pure compound 3(388mg, 78%) elutes at hex: EA (10: 90).

^{1}H NMR (CDCl3, 400 MHz): δ ^{1}H NMR (400 MHz, $CDCl_3$) δ 7.72 (d, *J* = 6.8 Hz, 2H), 7.51 (d, *J* = 10.9 Hz, 4H), 7.34 (s, 2H), 7.18 (d, *J* = 8.1 Hz, 4H), 6.19 (s, 3H), 4.54 (s, 2H), 4.33 (d, *J* = 5.8 Hz, 2H), 3.18 (d, *J* = 5.1 Hz, 2H), 2.87 (s, 2H), 2.56 (s, 3H), 2.48 (s, 3H), 2.07 (s, 3H), 2.04 (s, 2H), 1.85 (s, 1H), 1.66 (s, 2H), 1.54 (s, 1H), 1.41 (s, 4H).

Compound 7:

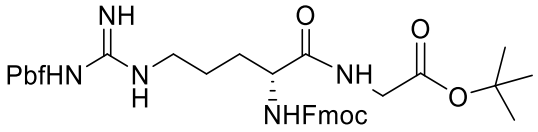

Add **C** (200 mg, 0.30 mmoles) and HATU (136 mg, 0.36 mmoles) and dissolve in 10 ml of DMF (dry) at 0^0C and stir for 30 mins. Next add **C** (62 mg, 0.36 mmoles) to the above mixture and then add DIEPA (0.26ml, 1.5 mmoles) dropwise. The reaction mixture was allowed to stir at room temperature for 12 h. DMF is removed under reduced pressure and then the compound is purified by column chromatography. Pure compound **7** (170 mg, 74%) elutes at hex: EA (30: 70).

^{1}H NMR (CDCl3, 400 MHz): δ ^{1}H NMR (400 MHz, D_2O) δ 7.89 – 7.86 (m, 1H), 7.52 (s, 2H), 7.35 (s, 2H), 7.15 (s, 4H), 5.78 (s, 2H), 5.49 (s, 2H), 4.16 (s, 3H), 3.88 – 3.80 (m, 1H), 3.56 (s, 2H), 2.68 (d, *J* = 22.5 Hz, 3H), 2.35 (s, 2H), 2.29 (s, 3H), 1.85 (s, 3H), 1.22 (s, 9H), 0.58 (s, 7H).

Compound 8

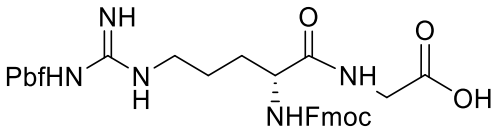

Compound 7 (120 mg, 0.14 mmoles) was dissolved in 20 ml of a mixture of DCM: TFA (2:1) at 0^0C. The reaction was allowed to stir for 2h. TLC was done to check completion of the reaction.

After completion, the reaction was concentrated under reduced pressure and dried under vacuum. The compound **8** was used in the next step without purification.

Compound 5

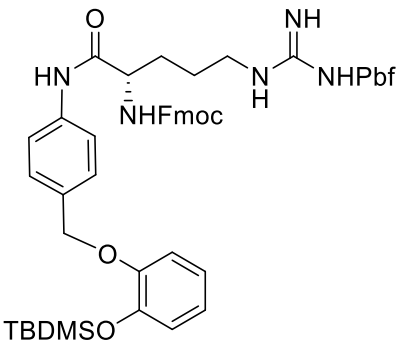

Dissolve **2** (130mg, 0.17 moles) in 10 ml of DCM (dry) and add PBr_3 (0.008ml, 0.08mmoles) at 0^0C. The reaction mixture was allowed to stir for 45 mins. Then TLC was checked to determine the completion of reaction. After completion, the reaction was concentrated under reduced pressure and dried under vacuum. The compound 3 was then dissolved in 20 ml of acetone dry (with $CaCl_2$) and then K_2CO_3 (141 mg, 1.0 mmoles) (dried in oven overnight) was added and then allowed to stir for 30 minutes. Next **4** (46 mg, 0.20 mmoles) was added to the reaction mixture. TBAI (5.4 mg, 0.017 mmoles) was added and the reaction was allowed to stir overnight at room temperature. The reaction mixture was filtered to remove K_2CO_3 and then concentrated under reduced pressure and then the compound is purified by column chromatography. Pure compound elutes at hex: EA (20: 80) to give **5** (84 mg, 52%).

^{1}H NMR (400 MHz, $CDCl_3$) δ 7.75 (d, *J* = 7.4 Hz, 2H), 7.61 (dd, *J* = 29.3, 7.7 Hz, 4H), 7.40 – 7.32 (m, 3H), 7.25 (s, 4H), 6.91 – 6.75 (m, 5H), 6.24 (s, 2H), 6.07 (d, *J* = 7.5 Hz, 1H), 5.14 (s, 1H), 4.98 (s, 2H), 4.38 (d, *J* = 6.9 Hz, 2H), 4.20 – 4.11 (m, 1H), 3.37 (s, 2H), 2.91 (s, 2H), 2.59 (s,

3H), 2.51 (s, 3H), 2.07 (s, 3H), 1.96 (s, 1H), 1.73 (s, 3H), 1.63 (s, 1H), 1.44 (s, 6H), 0.97 (s, 9H), 0.11 (s, 6H).

Compound 6

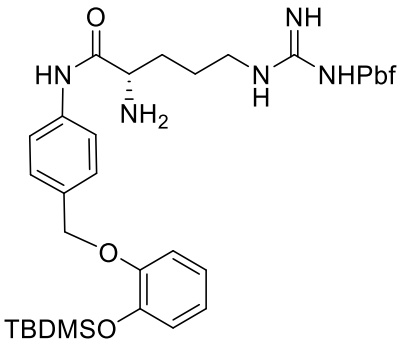

Compound **5** (150mg, 0.16 mmoles) was dissolved in 10 ml of DMF and 20% Piperidene in DMF was added to it at 0^0C and reaction mixture was allowed to stir for 45 minutes. TLC was done to check completion of the reaction. After completion, the reaction was concentrated under reduced pressure and dried under vacuum to give crude 6(100mg, 89%). The compound **6** was used in the next step without purification.

Compound 8:

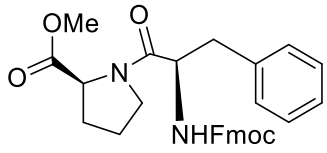

Add **7**(100 mg, 0.26 mmoles) and HATU (117mg, 0.30 mmoles) and dissolve in 10 ml of DMF (dry) at 0^0C and stir for 30 mins. Next add **C** (50 mg, 0.30 mmoles) to the above mixture and then add DIEPA (0.08 ml, 0.64 mmoles) dropwise. The reaction mixture was allowed to stir at room temperature for 12 h. DMF is removed under reduced pressure and then the compound is purified by column chromatography. Pure compound 3(91 mg, 71%) elutes at DCM: MeOH (90: 10).

^{1}H NMR (400 MHz, $CDCl_3$) δ 7.78 (s, 1H), 7.57 (d, *J* = 8.7 Hz, 2H), 7.40 (d, *J* = 7.3 Hz, 2H), 7.36 – 7.31 (m, 6H), 6.02 (d, *J* = 8.7 Hz, 1H), 4.79 (d, *J* = 8.6 Hz, 1H), 4.58 – 4.50 (m, 1H), 4.41 – 4.10 (m, 4H), 3.78 (s, 4H), 3.31 – 3.14 (m, 2H), 3.05 (dd, *J* = 13.7, 6.6 Hz, 1H), 2.20 – 2.10 (m, 1H), 1.93 (dd, *J* = 10.1, 4.6 Hz, 4H), 1.29 (d, *J* = 7.2 Hz, 1H).

Compound 9

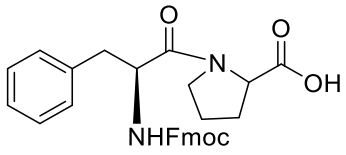

Compound **8** (120 mg, 0.14 mmoles) was dissolved in 10 ml of a mixture of 10% HCl in ACN and refluxed for 5h at 75^0C. TLC was done to check completion of the reaction. After completion, the reaction was concentrated under reduced pressure and dried under vacuum. The compound **9** was used in the next step without purification.

Compound 10

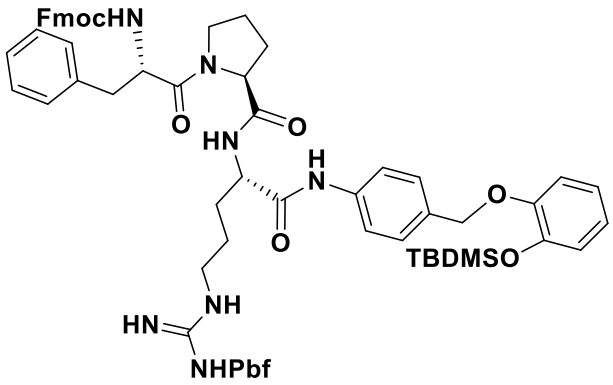

Add **9** (80mg, 0.14 mmoles) and HATU (67 mg, 0.17mmoles) and dissolve in 10 ml of DMF (dry) at 0^0C and stir for 30 mins. Next add **6** (70mg, 0.18 mmoles) to the above mixture and then add

DIEPA (3 eq) dropwise. The reaction mixture was allowed to stir at room temperature for 12 h. DMF is removed under reduced pressure and then the compound is purified by column chromatography. Pure compound elutes at DCM: MeOH (90:10) to give **10** (35mg, 65%).

NMR (400 MHz, $CDCl_3$) δ 7.75 (d, *J* = 7.4 Hz, 2H), 7.61 (dd, *J* = 29.3, 7.7 Hz, 4H), 7.40 – 7.32 (m, 3H), 7.25 (s, 4H), 6.91 – 6.75 (m, 5H), 5.93 (s, 2H), 5.80 (d, *J* = 7.5 Hz, 1H), 5.02 (s, 1H), 4.85 (s, 2H), 4.38 (d, *J* = 6.9 Hz, 2H), 4.20 – 4.11 (m, 1H), 3.37 (s, 2H), 2.91 (s, 2H), 2.59 (s, 3H), 2.51 (s, 3H), 2.07 (s, 6H), 1.80 (m, 3H), 1.73 (s, 3H), 1.63 (s, 1H), 1.48 (s, 6H), 0.97 (s, 9H), 0.13 (s, 6H).

Phe-Pro-Arg-PABA-catechol:

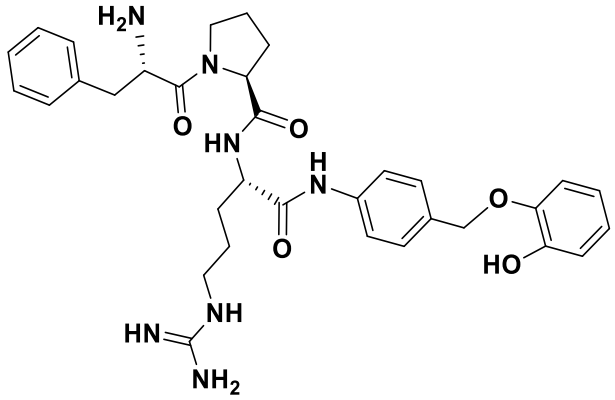

Compound **10**: (15 mg, 0.02 mmoles) was dissolved in 10 ml of DMF and 20% Piperidene in DMF was added to it at 0^0C and reaction mixture was allowed to stir for 45 minutes. TLC was done to check completion of the reaction. After completion, the reaction was concentrated under reduced pressure and dried under vacuum. The compound was used in the next step without purification. The dried compound was dissolved in a mixture of 5 ml of TFA: Isopropyl silane: H_2O (92.5: 2.5:5) and allowed to stir at 0^0C for 3h. TLC was done to check completion of the reaction. After completion, the reaction was concentrated under reduced pressure and dried under

vacuum. The compound was used in the next step without purification. The dried compound was then dissolved in MeOH (dry) and then NaOMe (0.5 eq) was added to it at room temperature and reaction mixture was allowed to stir for 2h. TLC was done to check completion of the reaction. The compound was purified using HPLC to get pure compound 10 (5mg, 65%).

^{1}H NMR (400 MHz, MeOD) δ 8.00 (s, 1H), 7.91 (d, *J* = 7.6 Hz, 2H), 7.74 (dd, *J* = 5.6, 3.0 Hz, 3H), 7.64 (dd, *J* = 5.7, 3.3 Hz, 2H), 7.50 (d, *J* = 7.3 Hz, 2H), 7.44 (t, *J* = 7.1 Hz, 2H), 6.76 (dd, *J* = 5.8, 3.6 Hz, 1H), 6.66 (dd, *J* = 5.9, 3.6 Hz, 1H), 4.51 (t, *J* = 5.2 Hz, 1H), 4.27 – 4.20 (m, 3H), 3.85 (d, *J* = 5.5 Hz, 2H), 3.66 (d, *J* = 3.0 Hz, 2H), 3.15 (d, *J* = 5.7 Hz, 7H), 3.01 (s, 2H), 2.88 (s, 2H), 1.80 (d, *J* = 5.4 Hz, 8H), 1.72 (d, *J* = 4.8 Hz, 5H), 0.94 – 0.90 (m, 11H).

HPLC purification:

HPLC elution. The elution solvents were pumped through the column at a flow rate of 1.5 ml/min using a Waters X Bridge Prep C18 5um column. Solution A was H_20/0.1% TFA, solution B was CH_3 CN/ 0.1% TFA at a max pressure of 400 mbar. Before each HPLC run the column was equilibrated with water containing 0.1% TFA (H_20/0.1% TFA) at a flow rate of 1.5 ml/min until the absorbance of the column effluent was constant, which usually took -30 min. The compound was eluted at a gradient where the starting polarity is 100% A to 95% B in 15 mins. The desired compound elutes at 11mins. At the end of each HPLC run, the column was flushed for 15 min with 100% acetonitrile to remove any residual TFA. The column was then stored in 100% acetonitrile.

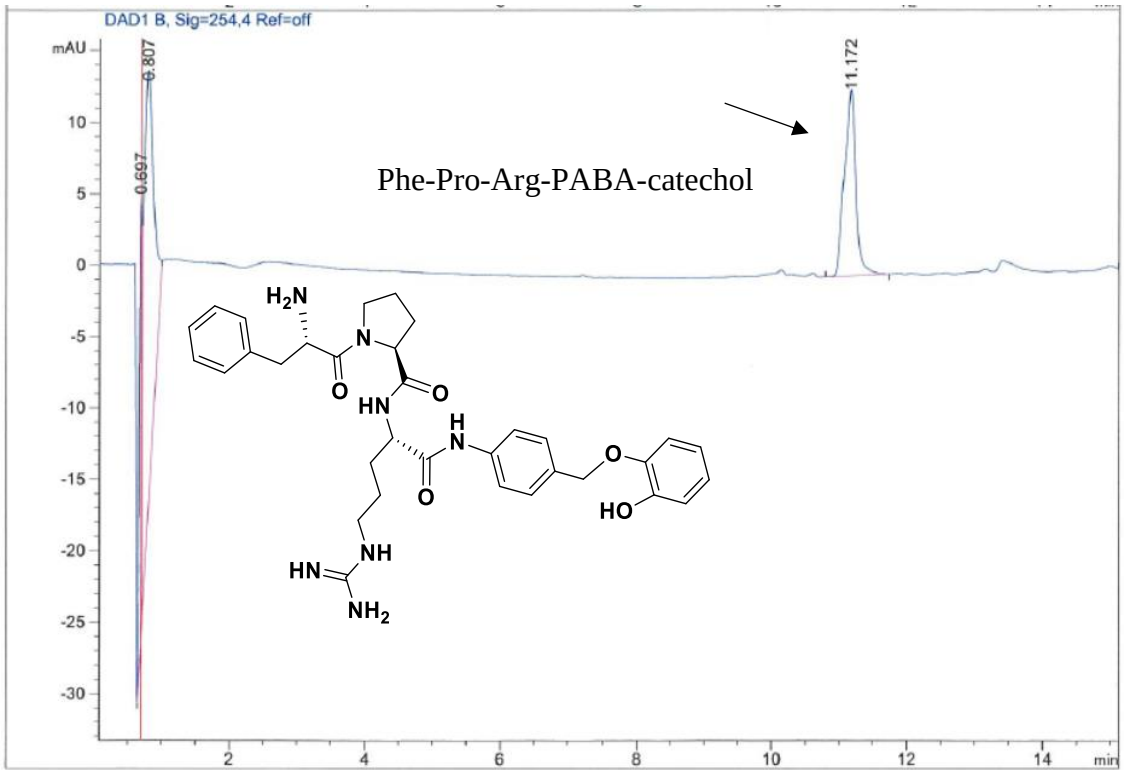

Figure 46*. HPLC trace for Phe-Pro-Arg-PABA-Catechol.*

4.10 Summary and Future work

In summary, we identified a need for the detection of thrombin in point of care setting and have successfully designed and synthesized and characterized a substrate for Thrombin detection. This substrate can be used to directly detect and quantify the amount of thrombin in blood using a repurposed glucose meter in a POC setting. Using this approach, it would be possible to monitor and accurately detect the level of thrombin in blood and modulate the level of anti-coagulants prescribed to a patient. For the new direct oral anti-coagulant (DOAC), there are currently no FDA approved test to regulate and monitor the level of drugs prescribed. Future work on this project will be towards developing assays that can be used to monitor the levels of these DOAC drugs using the synthesized substrate in a POC setting.

4.11 References:

1.Periayah, M. H.; Halim, A. S.; Mat Saad, A. Z. Mechanism Action of Platelets and Crucial Blood Coagulation Pathways in Hemostasis. *Int J Hematol Oncol Stem Cell Res* **2017,** *11* (4), 319.

2.Malyszko, J. S.; Malyszko, J.; Mysliwiec, M. [Tissue factor and inhibitor of the blood coagulation pathway in nephrotic syndrome]. *Pol Arch Med Wewn* **1999,** *101* (4), 301.

3. Cian, R. E.; Garzon, A. G.; Martinez-Augustin, O.; Botto, C. C.; Drago, S. R. Antithrombotic Activity of Brewers' Spent Grain Peptides and their Effects on Blood Coagulation Pathways. *Plant Foods Hum Nutr* **2018**, DOI:10.1007/s11130-018-0682-1 10.1007/s11130-018-0682-1.

4. Schousboe, I. beta 2-Glycoprotein I: a plasma inhibitor of the contact activation of the intrinsic blood coagulation pathway. *Blood* **1985,** *66* (5), 1086.

5.Tsang, V. C.; Damian, R. T. Demonstration and mode of action of an inhibitor for activated Hageman factor (factor XIIa) of the intrinsic blood coagulation pathway from Schistosoma mansoni. *Blood* **1977,** *49* (4), 619.

6. Stankowska, K.; Gadomska, G.; Boinska, J.; Michalska, M.; Bartoszewska-Kubiak, A.; Rosc, D. Extrinsic blood coagulation pathway and risk factors for thrombotic events in patients with essential thrombocythemia. *Pol Arch Med Wewn* **2016,** *126* (5), 340.

7. Adcock DM, Kressin DC, Marlar RA. Effect of 3.2% vs 3.8% sodium citrate concentration on routine coagulation testing. *Am J Clin Pathol.* 1997 Jan; 107(1):105-110.

8. Reneke J, Etzell J, Leslie S, Ng VL, Gottfried EL. Prolonged prothrombin time and activated partial thromboplastin time due to underfilled specimen tubes with 109 mmol/L (3.2%) citrate anticoagulant. Am J Clin Pathol. 1998 Jun; 109(6):754-757.

9. National Committee for Clinical Laboratory Standardization. Collection, Transport, and Processing of Blood Specimens for Coagulation Testing and General Performance of Coagulation Assays; Approved Guideline. 5th ed. Villanova, Pa: NCCLS; 2008. Document H21-A5:28(5).

10. Gottfried EL, Adachi MM. Prothrombin time and activated partial thromboplastin time can be performed on the first tube. Am J Clin Pathol. 1997; 107(6):681-683.

11. McGlasson DL, More L, Best HA, Norris WL, Doe RH, Ray H. Drawing specimens for coagulation testing: Is a second tube necessary, Clin Lab Sci. 1999 May-Jun; 12(3):137-139.

12. Arian, D., Harenberg, J., Kramer, R. A chromogenic and fluorogenic peptide substrate for the highly sensitive detection of proteases in biological matrices. *J. Med. Chem.*, **2016**, *59* (16), pp 7576–7583.

13. Adcock DM, Bethel MA, Macy PA. Coagulation Handbook. Aurora, Colo: Esoterix−Colorado Coagulation; 2006.

14. Dimichele D. Inhibitors: Resolving diagnostic and therapeutic dilemmas. Haemophilia. 2002 May; 8(3):280-287.

15. Boggio LN, Green D. Acquired hemophilia. Rev Clin Exp Hematol. 2001 Dec; 5(4):389-404.

16. Chandler WL, Rodgers GM, Sprouse JT, et al. Elevated hemostatic factor levels as potential risk factors for thrombosis. Arch Pathol Lab Med. 2002 Nov; 126(11):1405-1414.

17. Cohen AJ, Kessler CM. Hemophilia A and B. In: Kitchens CS, Alving BM, Kessler CM, eds. Consultative Hemostasis and Thrombosis.Philadelphia, Pa: WB Saunders Co;2002:43-56.

18. Lakich D, Kazazian HH, Antonarakis SE, Gitschier J. Inversions disrupting the factor VIII gene are a common cause of severe haemophilia A. Nat Genet. 1993 Nov; 5(3):236-241.

19. Kamphuisen PW, Eikenboom JC, Rosendaal FR, et al. High factor VIII antigen levels increase the risk of venous thrombosis but are not associated with polymorphisms in the von Willebrand factor and factor VIII gene. Br J Haematol. 2001 Oct; 115(1):156-158.

20. Cristina L, Benilde C, Michela C, Mirella F, Giuliana G, Gualtiero P. High plasma levels of factor VIII and risk of recurrence of venous thromboembolism. Br J Haematol. 2004 Feb; 124(4):504-510.

21. Ginsburg D, Nichols WC, Zivelin A, Kaufman RJ, Seligsohn U. Combined factors V and VIII deficiency−The solution. Haemophilia.1998 Jul; 4(4):677-682.

22. Wysocka, M.; Lesner, A. Future of protease activity assays. Curr. Pharm. Des. 2012, 19 (6), 1062−1067.

23. Marguerre, A. K.; Kramer, R. Lanthanide-based fluorogenic peptide substrate for the highly sensitive detection of thermolysin. Bioorg. Med. Chem. Lett. 2009, 19 (19), 5757−5759.

24. Chelyapov, N. Allosteric aptamers controlling a signal amplification cascade allow visual detection of molecules at picomolar concentrations. Biochemistry 2006, 45 (7), 2461−2466.

25. Pavlov, V.; Zorn, M.; Kramer, R. Probing single-stranded DNA and its biomolecular interactions through direct catalytic activation of factor XII, a protease of the blood coagulation cascade. Biochem. Biophys. Res. Commun. 2006, 349 (3), 1011−1015.

26. Li, X.; Gao, X.; Shi, W.; Ma, H. Design strategies for watersoluble small molecular chromogenic and fluorogenic probes. Chem. Rev. 2014, 114 (1), 590−659.

27. Miller, E. W.; Chang, C. J. Fluorescent probes for nitric oxide and hydrogen peroxide in cell signaling. Curr. Opin. Chem. Biol. 2007, 11 (6), 620−625.

28. Choi, M. G.; Hwang, J.; Eor, S.; Chang, S. K. Chromogenic and fluorogenic signaling of sulfite by selective deprotection of resorufin levulinate. Org. Lett. 2010, 12 (24), 5624−5627.

29. Zhang, Y.; Shi, W.; Li, X.; Ma, H. Sensitive detection of ozone by a practical resorufin-based spectroscopic probe with extremely low background signal. Sci. Rep. 2013, 3, 2830.

30. Arian, D.; Kovbasyuk, L.; Mokhir, A. 1,9-Dialkoxyanthracene as a(1)O2-sensitive linker. J. Am. Chem. Soc. 2011, 133 (11), 3972−3980.

31. Marmuse, L.; Asther, M.; Fabre, E.; Navarro, D.; LesageMeessen, L.; Asther, M.; O'Donohue, M.; Fort, S.; Driguez, H. New chromogenic substrates for feruloyl esterases. Org. Biomol. Chem. 2008, 6 (7), 1208−1214.

32. Zhang, Y.; Chen, W.; Feng, D.; Shi, W.; Li, X.; Ma, H. A spectroscopic off-on probe for simple and sensitive detection of carboxylesterase activity and its application to cell imaging. Analyst 2012, 137 (3), 716−721.

33. Bottcher, S.; Hederos, M.; Champion, E.; Dekany, G.; Thiem, J. Novel efficient routes to indoxyl glycosides for monitoring glycosidase activities. Org. Lett. 2013, 15 (14), 3766−3769. (14) Richard, J. A.; Meyer, Y.; Jolivel, V.; Massonneau, M.; Dumeunier, R.; Vaudry, D.; Vaudry, H.; Renard, P. Y.; Romieu, A. Latent fluorophores based on a self-immolative linker strategy and suitable for protease sensing. Bioconjugate Chem. 2008, 19 (8), 1707− 1718.

34. Witmer, M. R.; Falcomer, C. M.; Weiner, M. P.; Kay, M. S.; Begley, T. P.; Ganem, B.; Scheraga, H. A. U-3′-BCIP: a chromogenic substrate for the detection of RNase A in recombinant DNA expression systems. Nucleic Acids Res. 1991, 19 (1), 1−4.

35. Hakamata, W.; Machida, A.; Oku, T.; Nishio, T. Design and synthesis of an ER-specific fluorescent probe based on carboxylesterase activity with quinone methide cleavage process. Bioorg. Med. Chem. Lett. 2011, 21 (11), 3206−3209.

36. Harenberg, J.; Du, S.; Kramer, S.; Weiss, C.; Kramer, R.; Wehling, M. Patients' serum and urine as easily accessible samples for the measurement of non-vitamin k antagonist oral anticoagulants. Semin. Thromb. Hemostasis 2015, 41 (2), 228−236.

37. Joppa, S. A,Salcicciolli, J. Adamski, J. Apractical review of the emerging Direct Anti-coagulants, Laboratory monitoring, reversal agents. J. Clin. Med. 2018,7, 29.

38.Chowdhury, M. A.; Moya, I. A.; Bhilocha, S.; McMillan, C. C.; Vigliarolo, B. G.; Zehbe, I.; Phenix, C. P. Prodrug-inspired probes selective to cathepsin B over other cysteine cathepsins. J. Med. Chem. 2014, 57 (14), 6092−6104.

APPENDICES

Appendix A. NMR spectra

2, ^{1}H NMR, 400 MHz, $CDCl_3$,

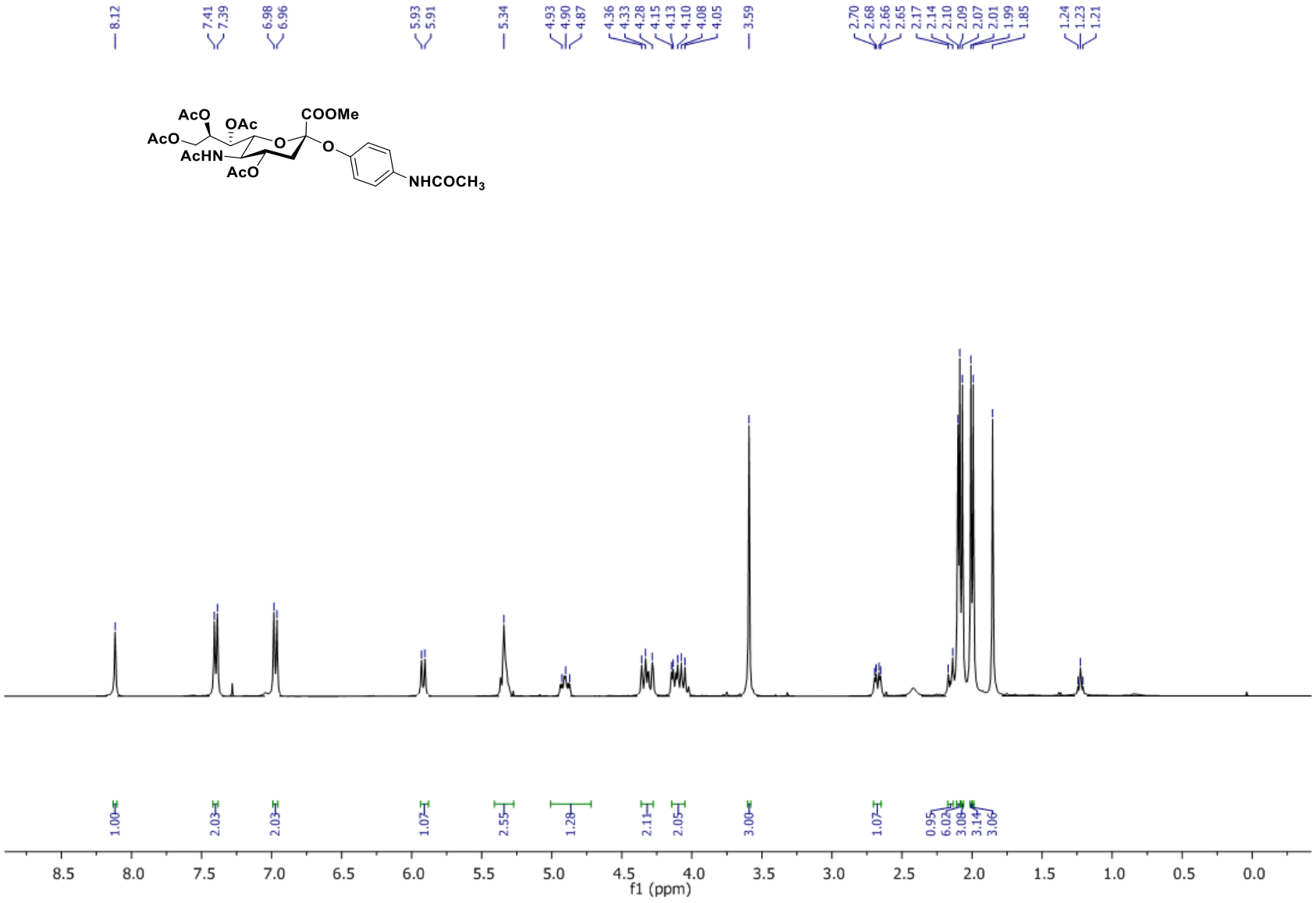

2, ^{13}C NMR, 100 MHz,

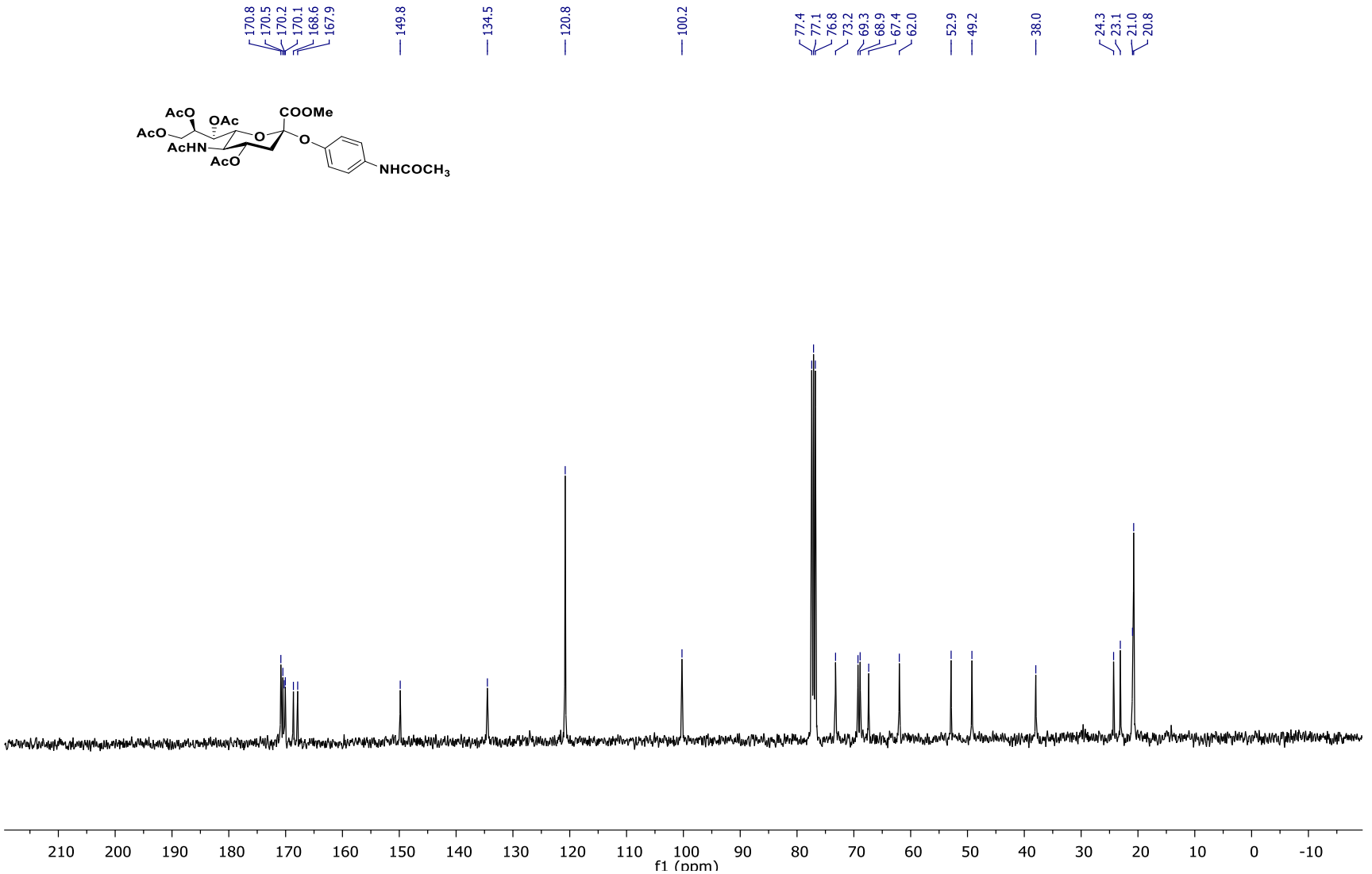

2 ,COSY, 400 MHz, $CDCl_3$

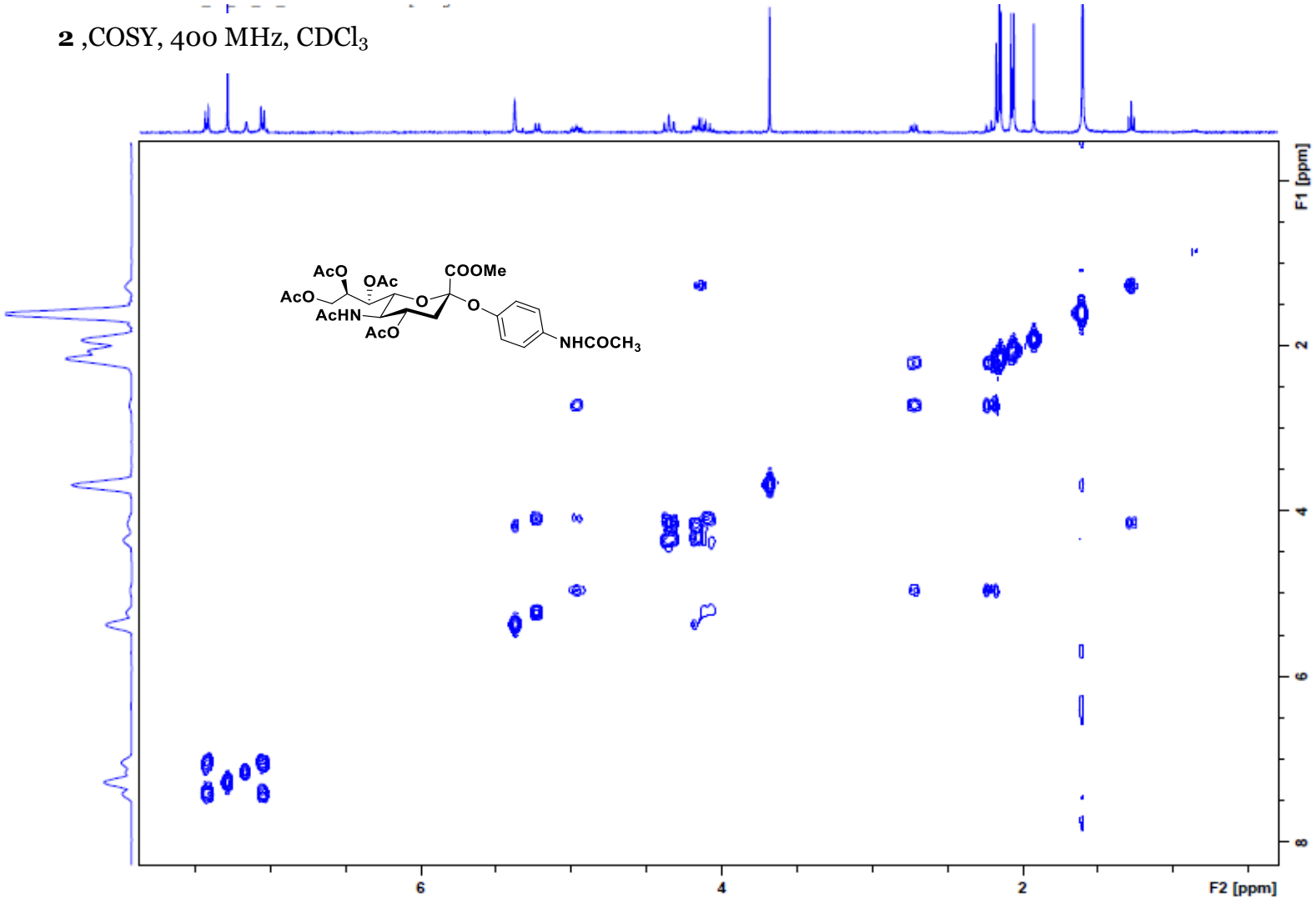

2, HSQC 400 MHz, $CDCl_3$,

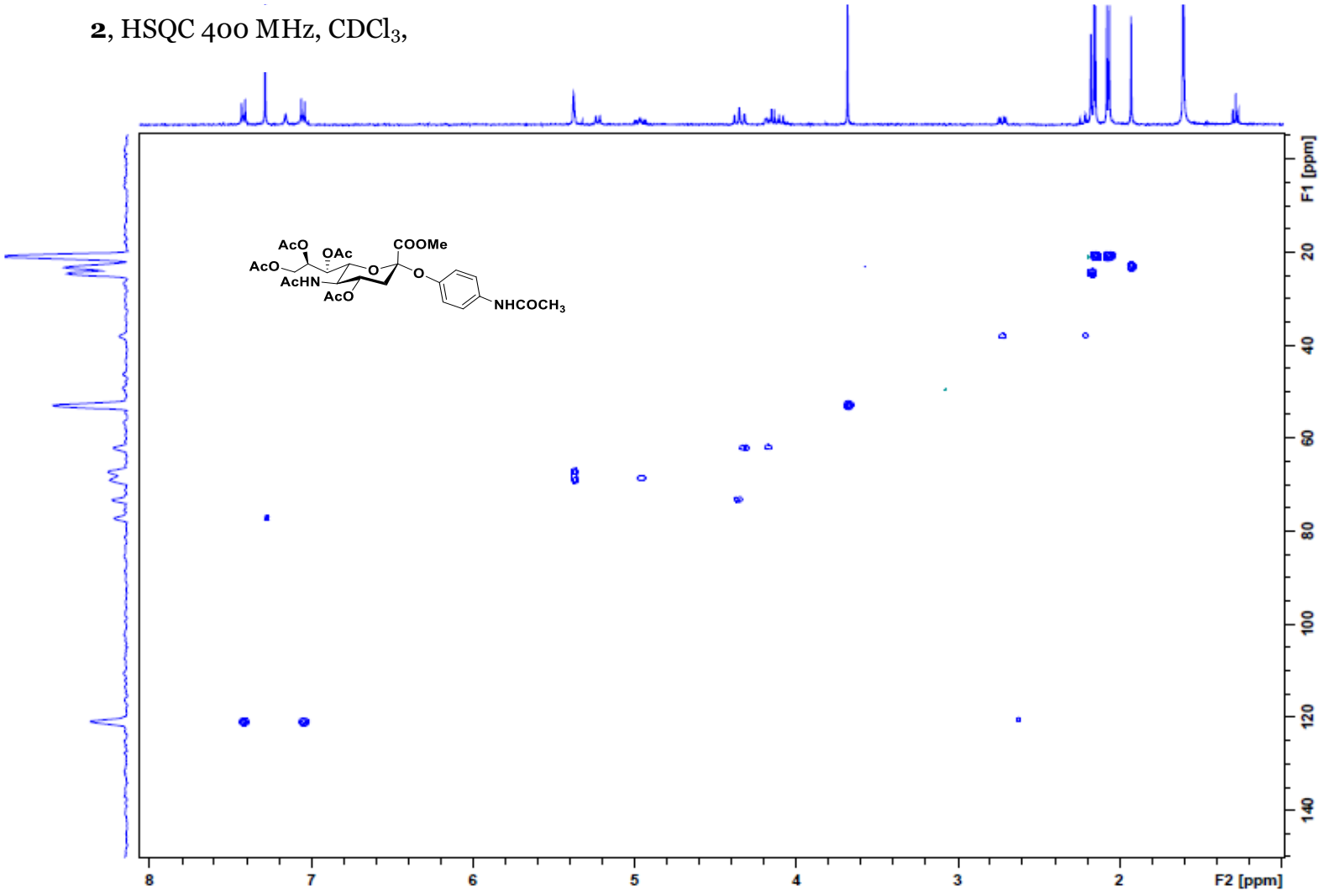

SP, ^{1}H NMR, 400 MHz, D2O,

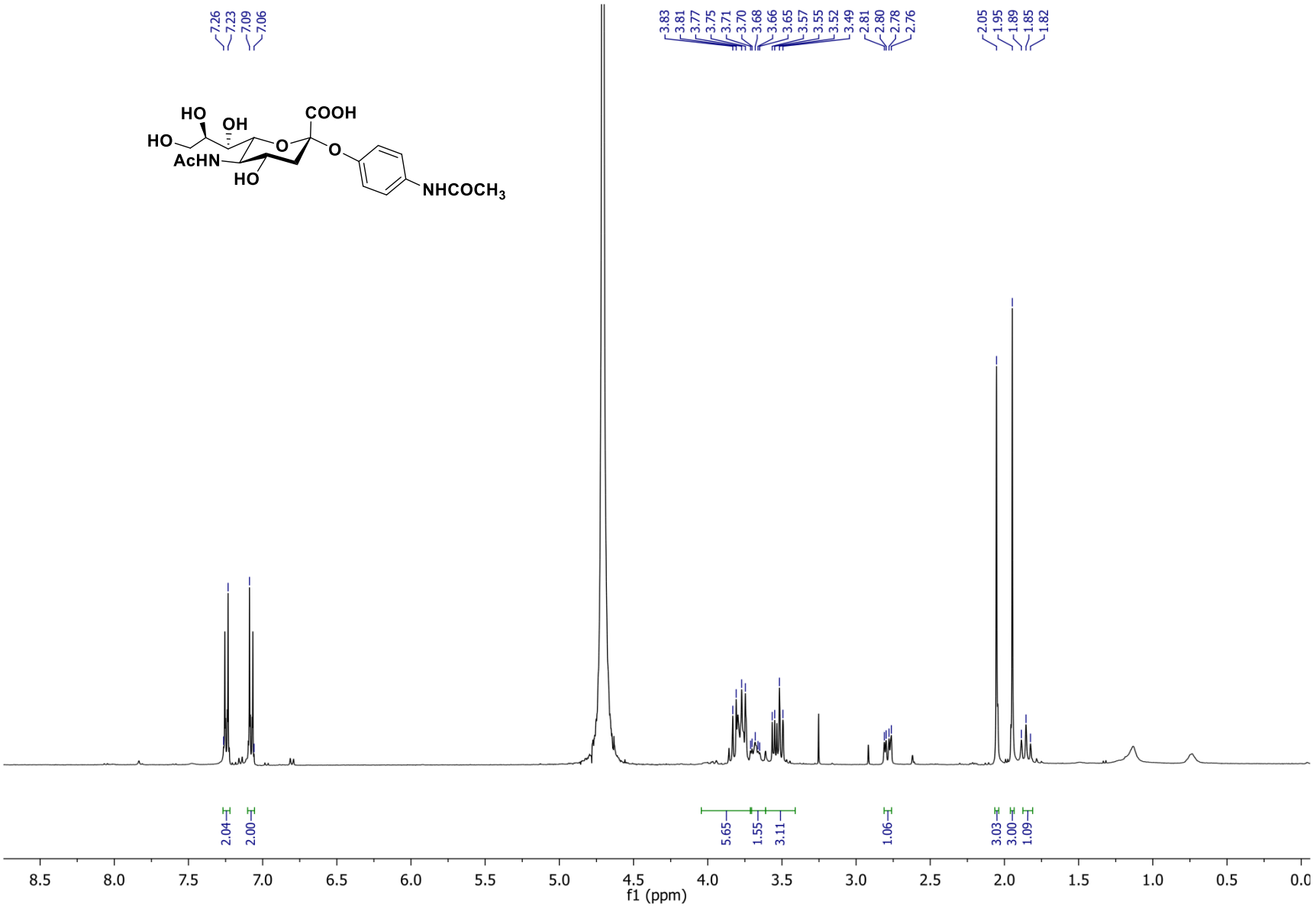

SP, ^{13}C NMR, 100 MHz,

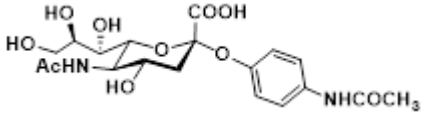

124.6
123.2
122.0
115.7
101.6
73.5
71.3
68.1
67.6
62.8
51.6
40.1
22.6
22.0

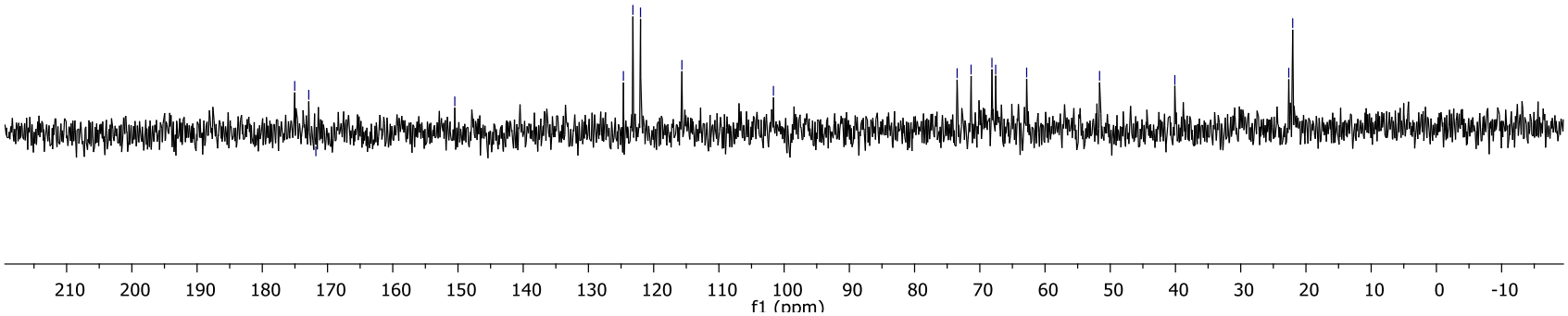

SP, COSY, 400 MHz, D_2O

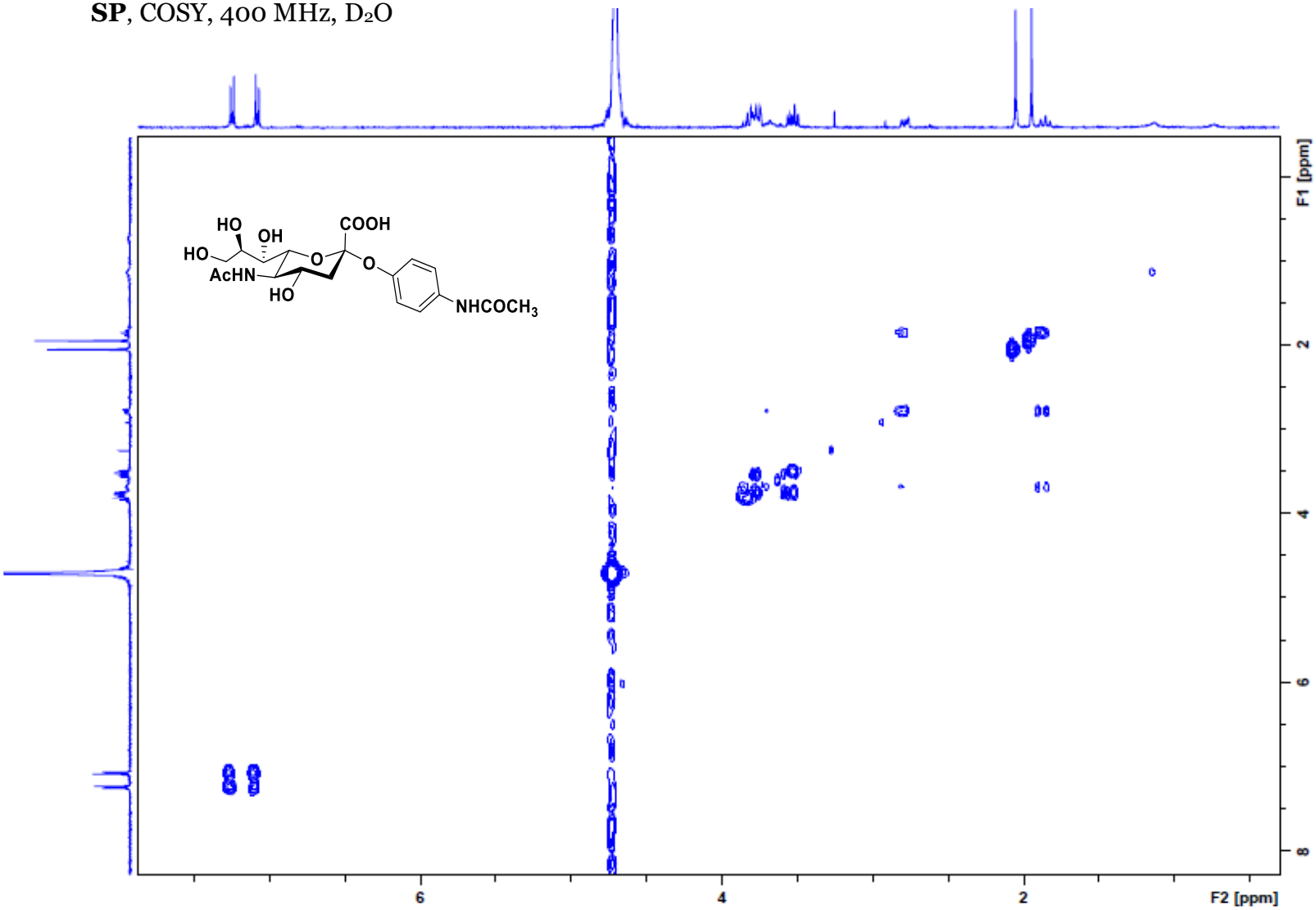

SP, HSQC, 400 MHz, D_2O

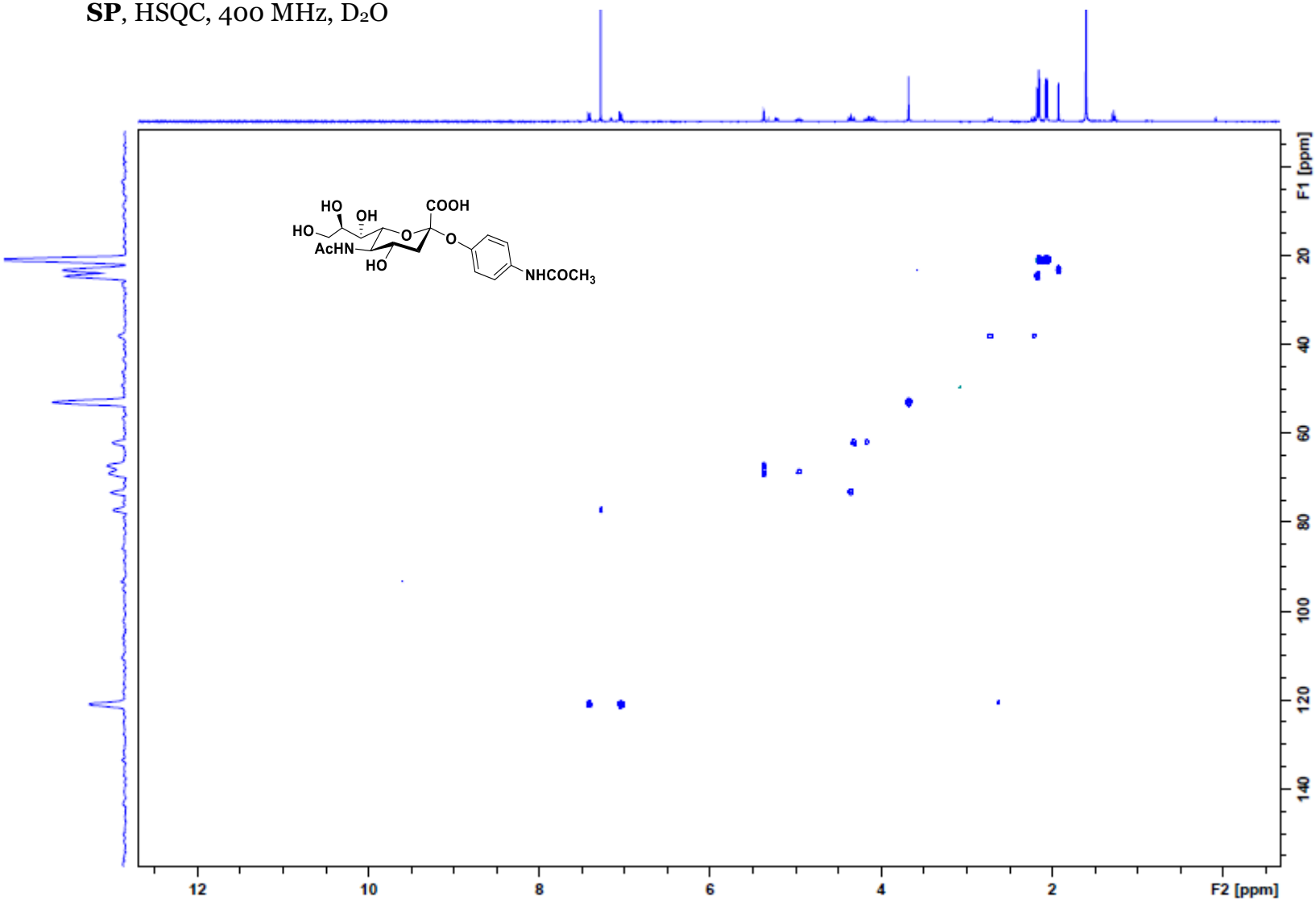

2a, ^{1}H NMR, $CDCl_3$,400 MHz,

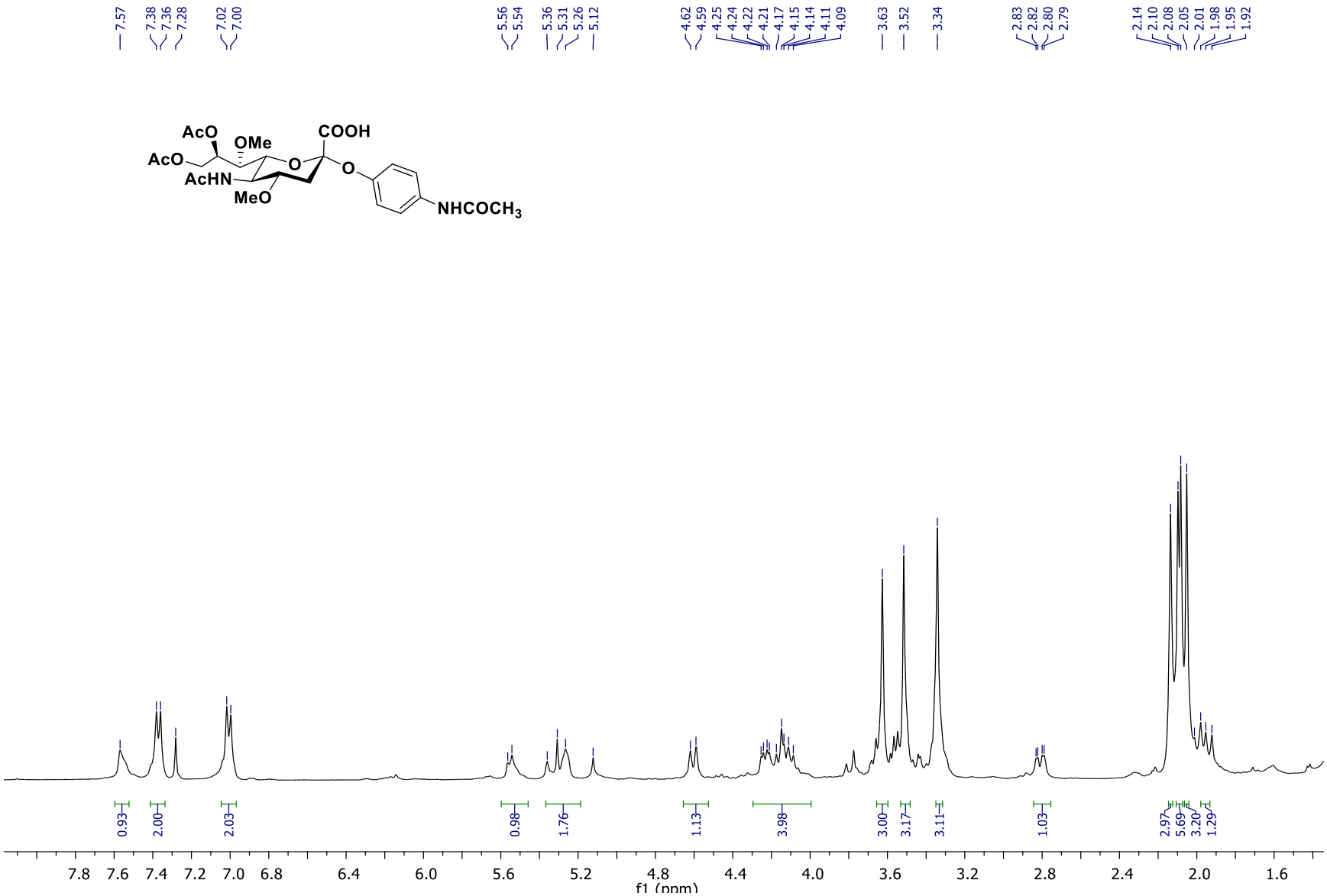

2a, ^{13}C NMR, CDCl3,100 MHz,

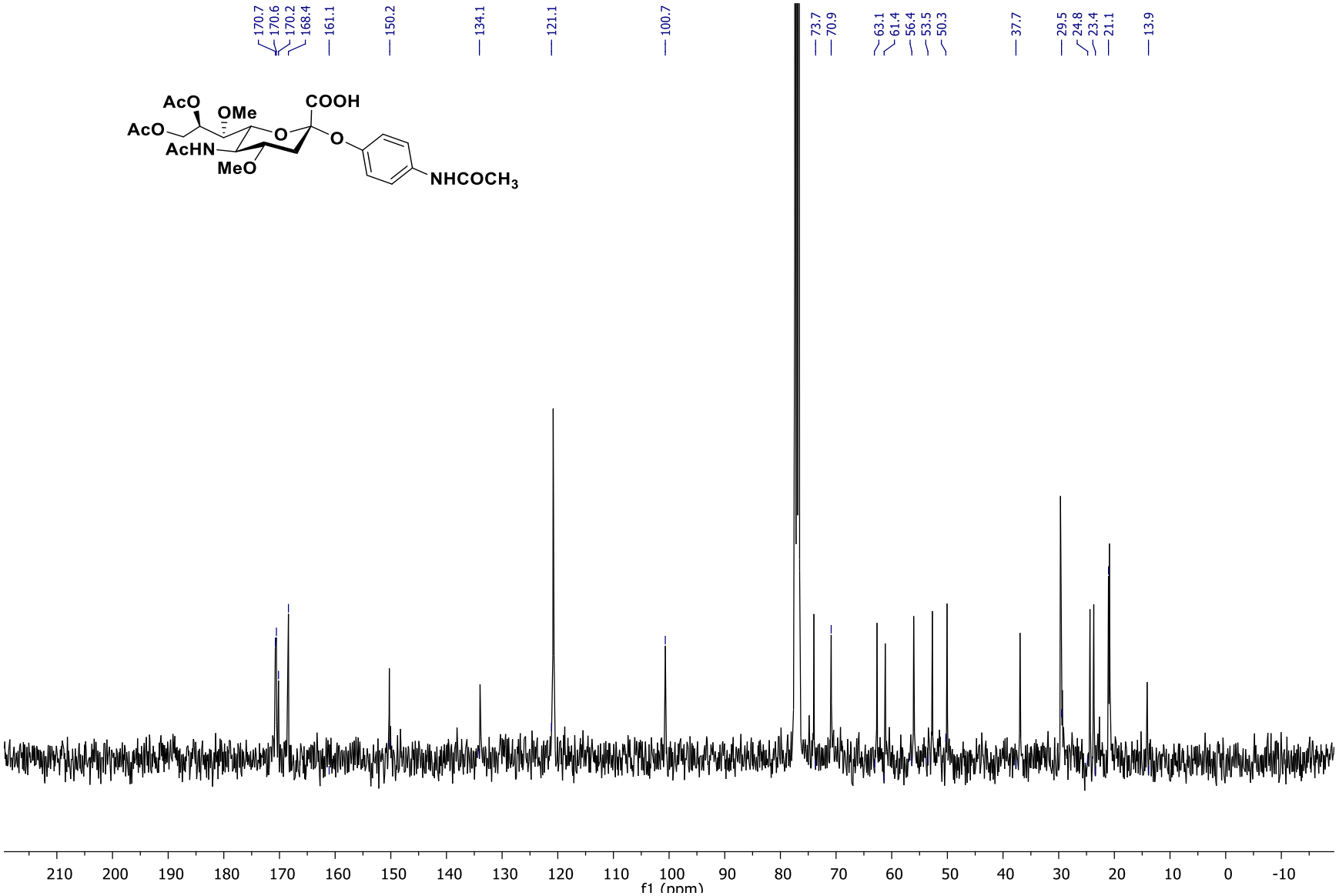

2a, COSY, $CDCl_3$, 400 MHz,

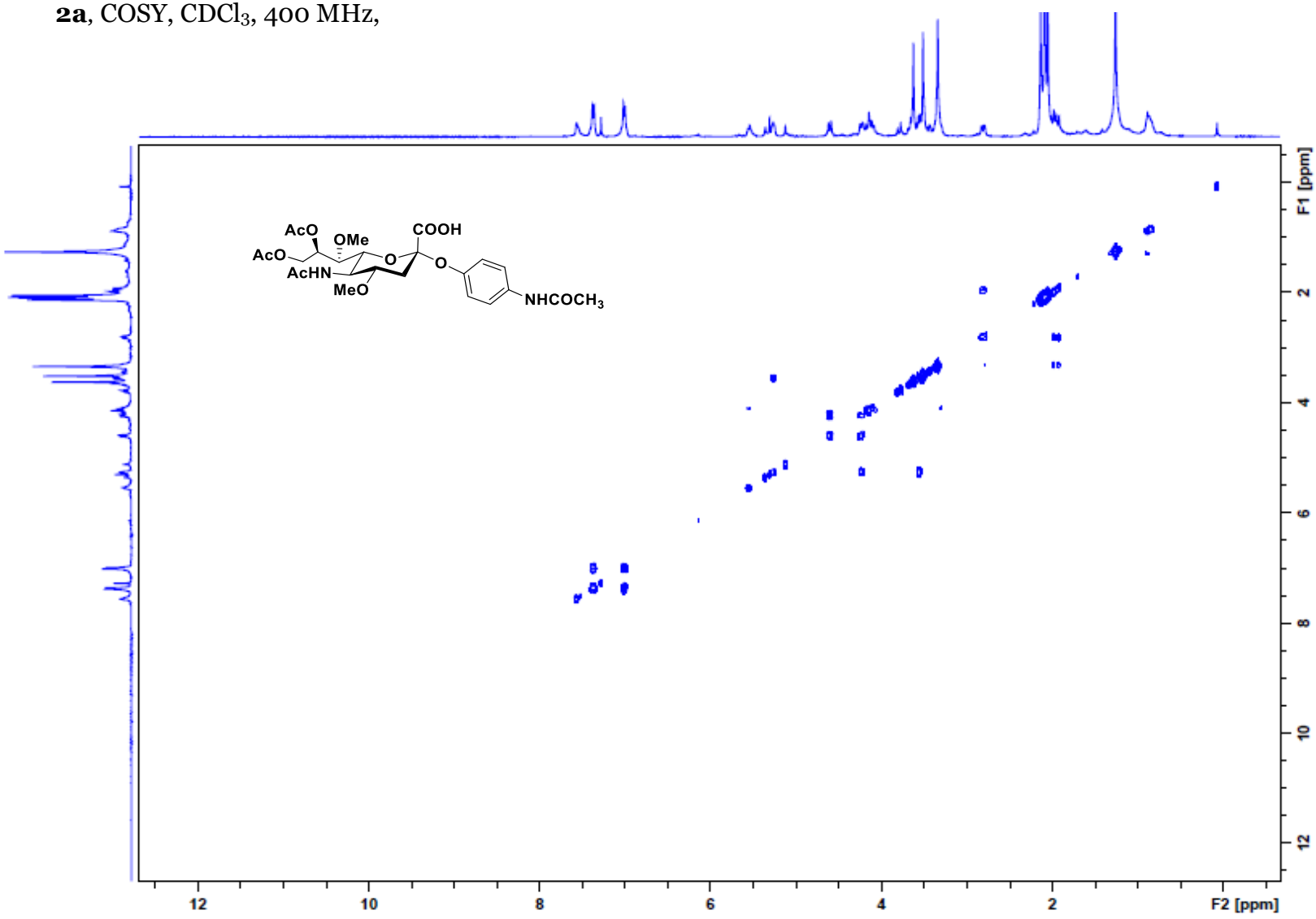

2a, HSQC, $CDCl_3$, 400 MHz,

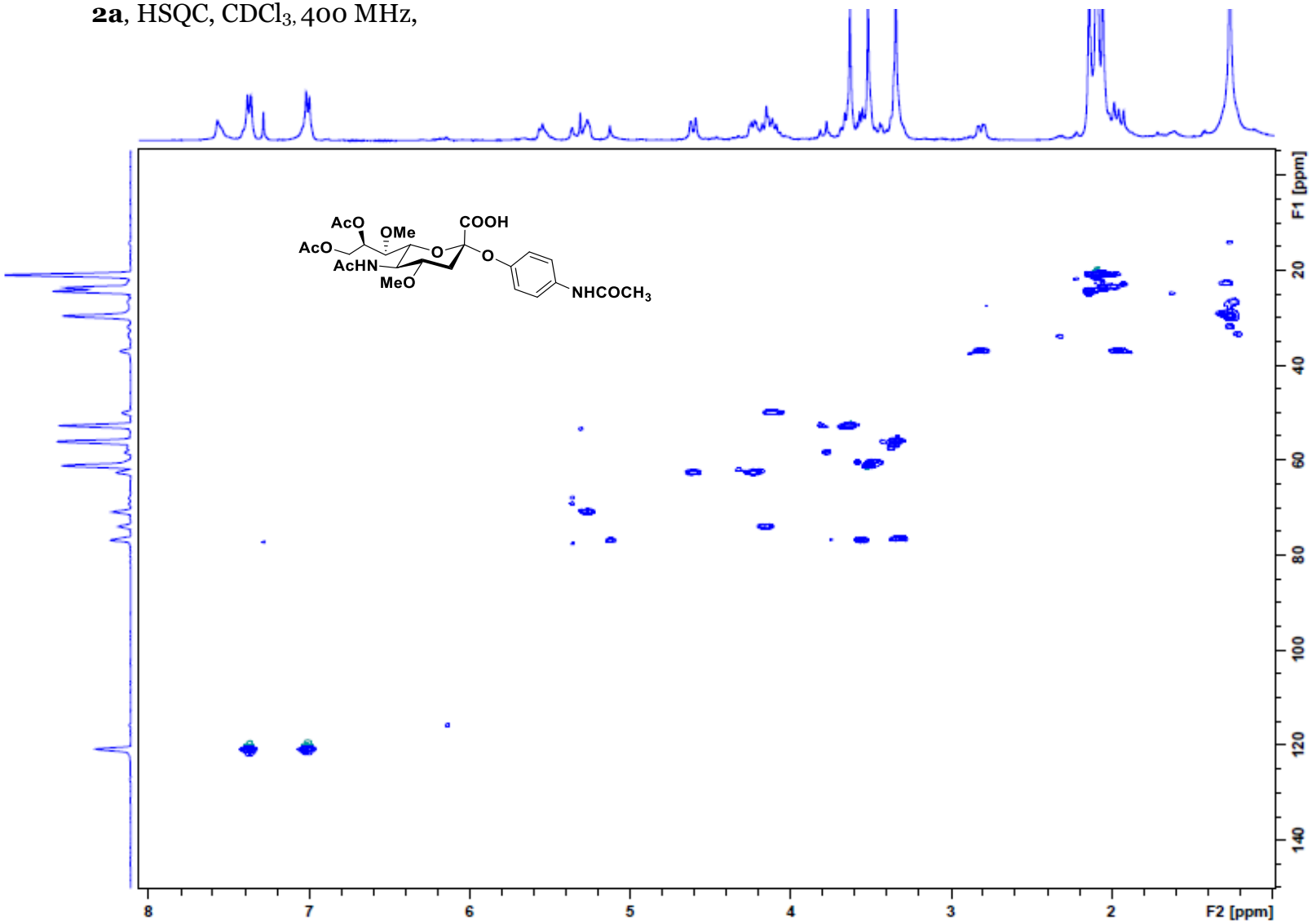

SP(OMe)$_2$, ^{1}H NMR, D_2O, 400 MHz,

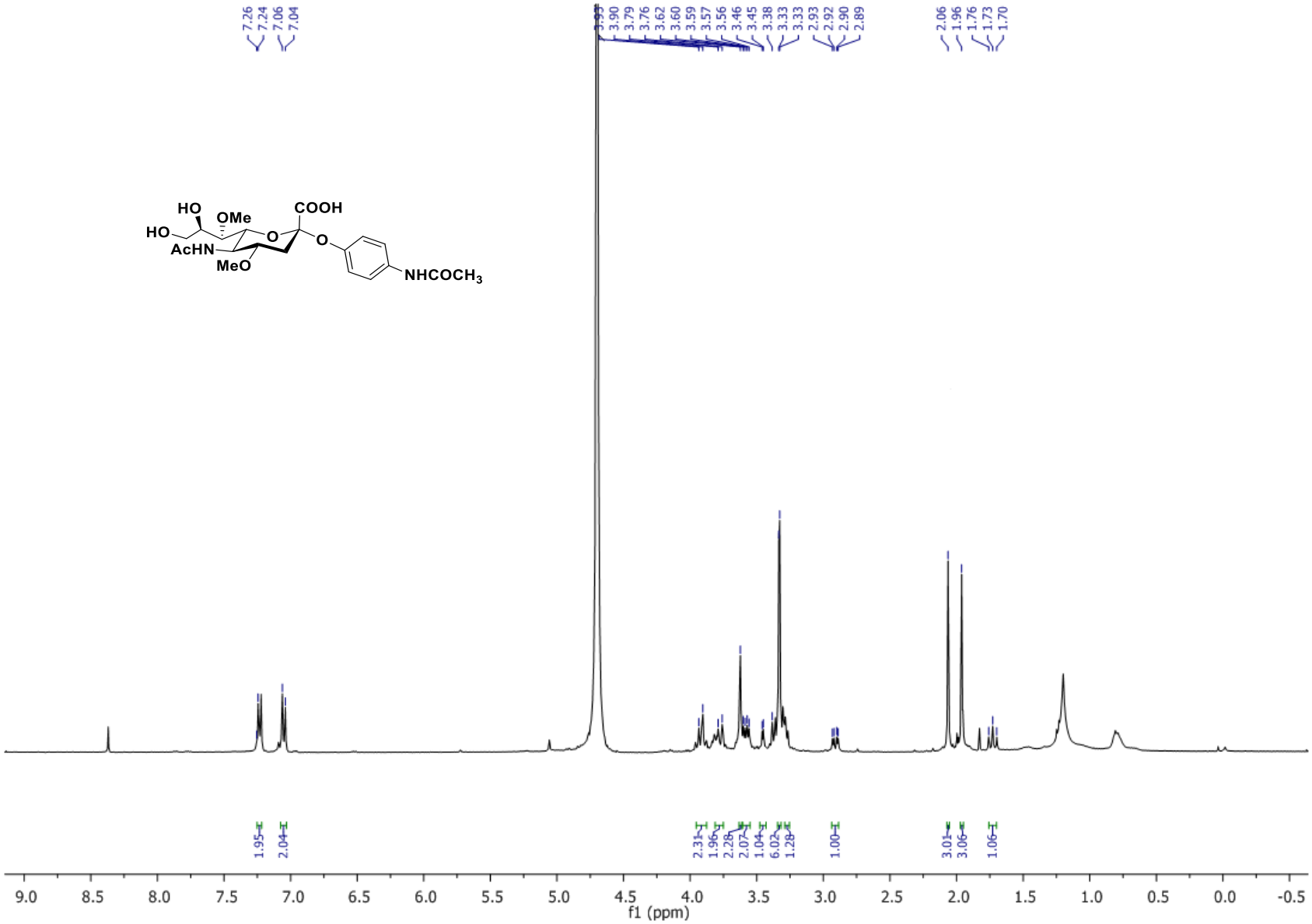

SP(OMe)$_2$, ^{13}C NMR, D_2O ,100 MHz,

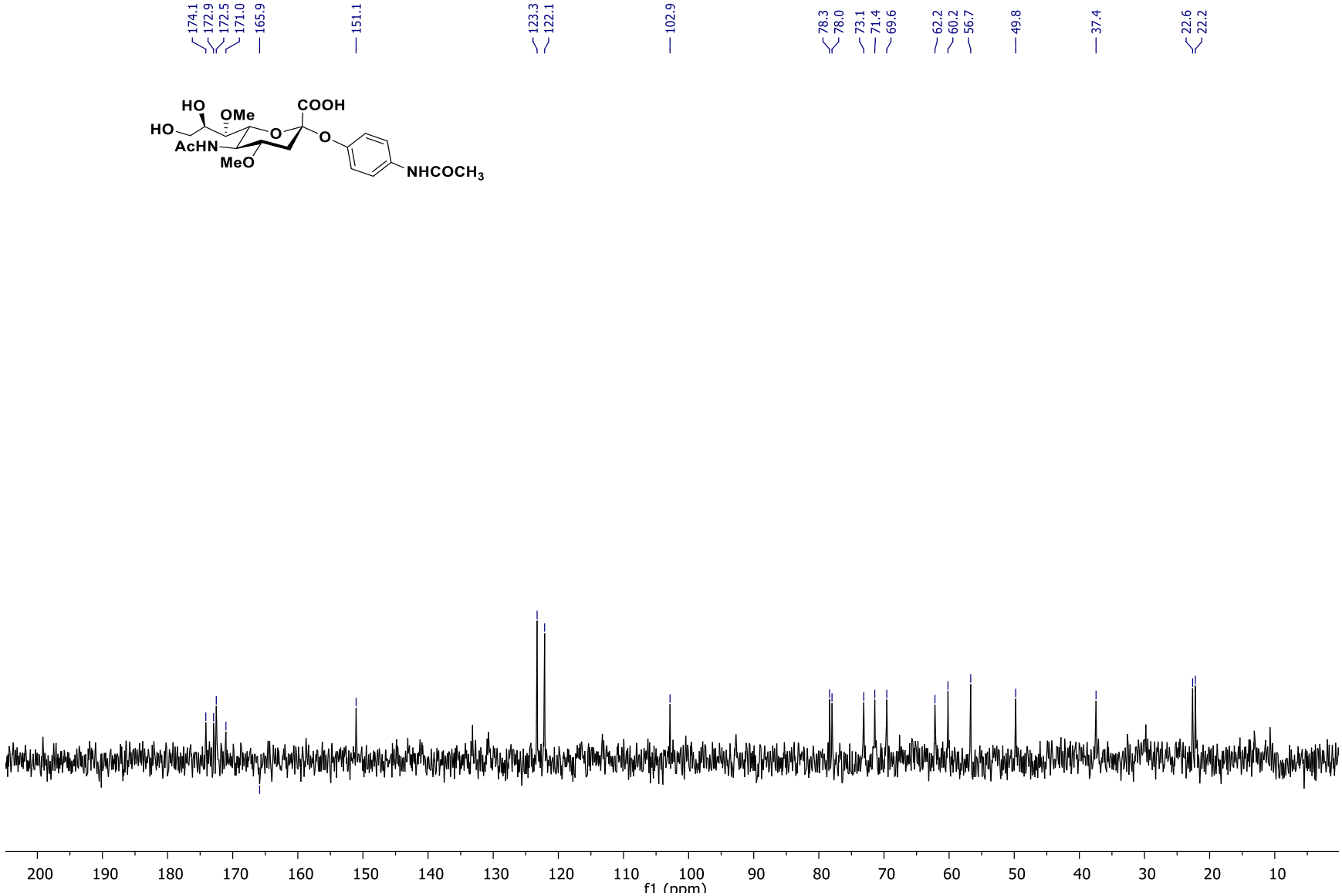

SP(OMe)$_2$, COSY ,D_2O, 400 MHz,

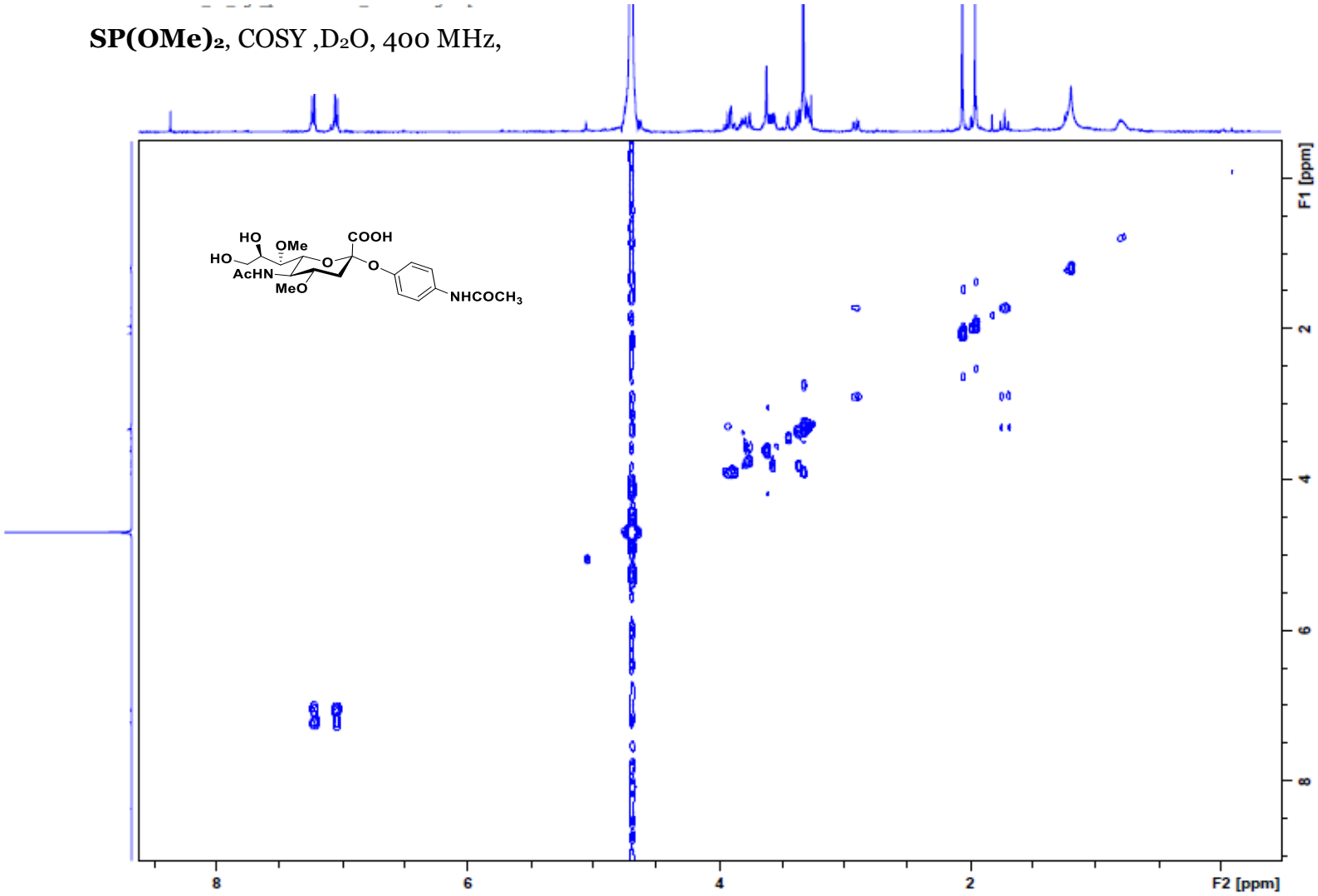

SP(OMe)$_2$, HSQC ,D_2O, 400 MHz,

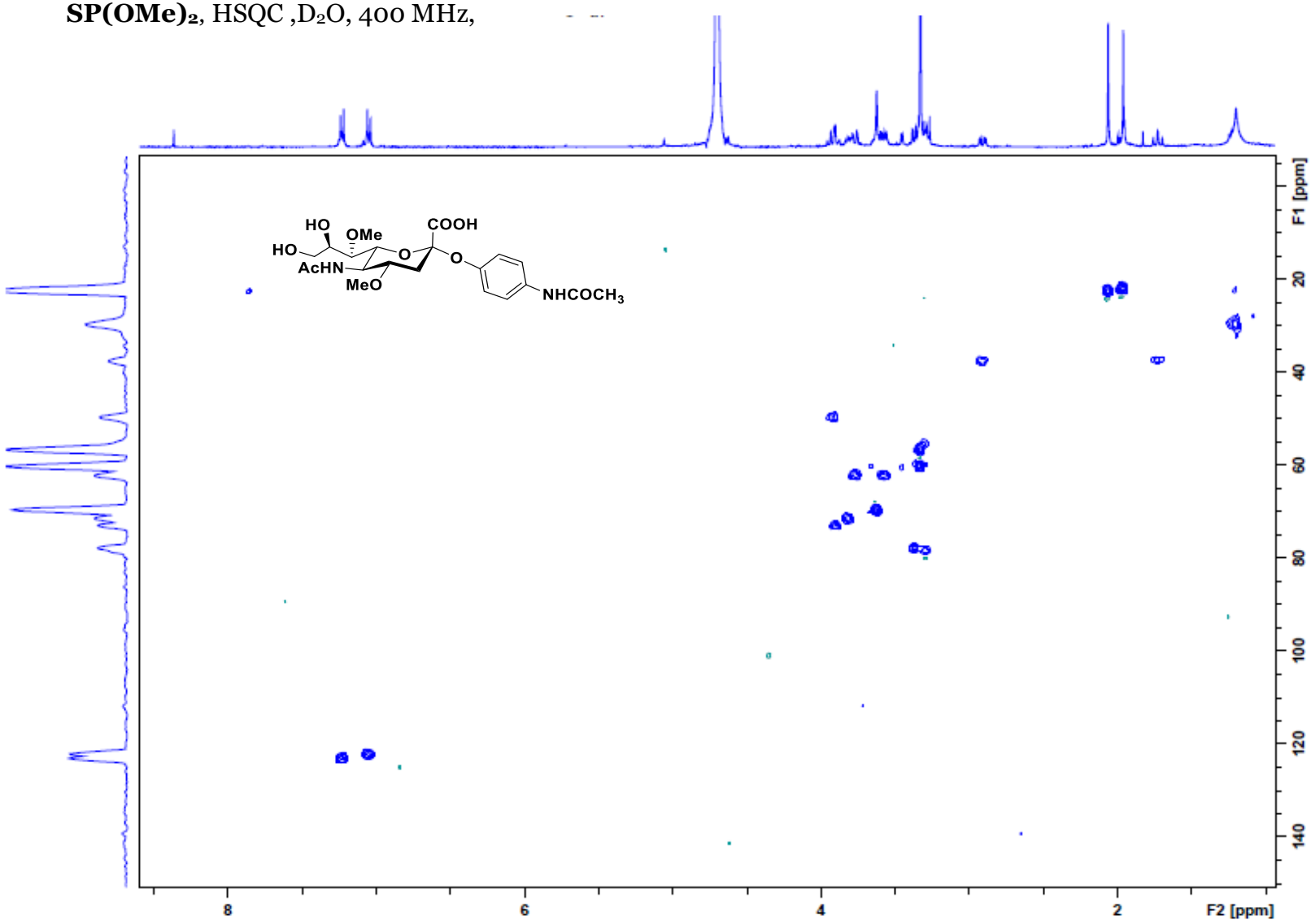

4, ^{1}H NMR, CDCl3,400 MHz,

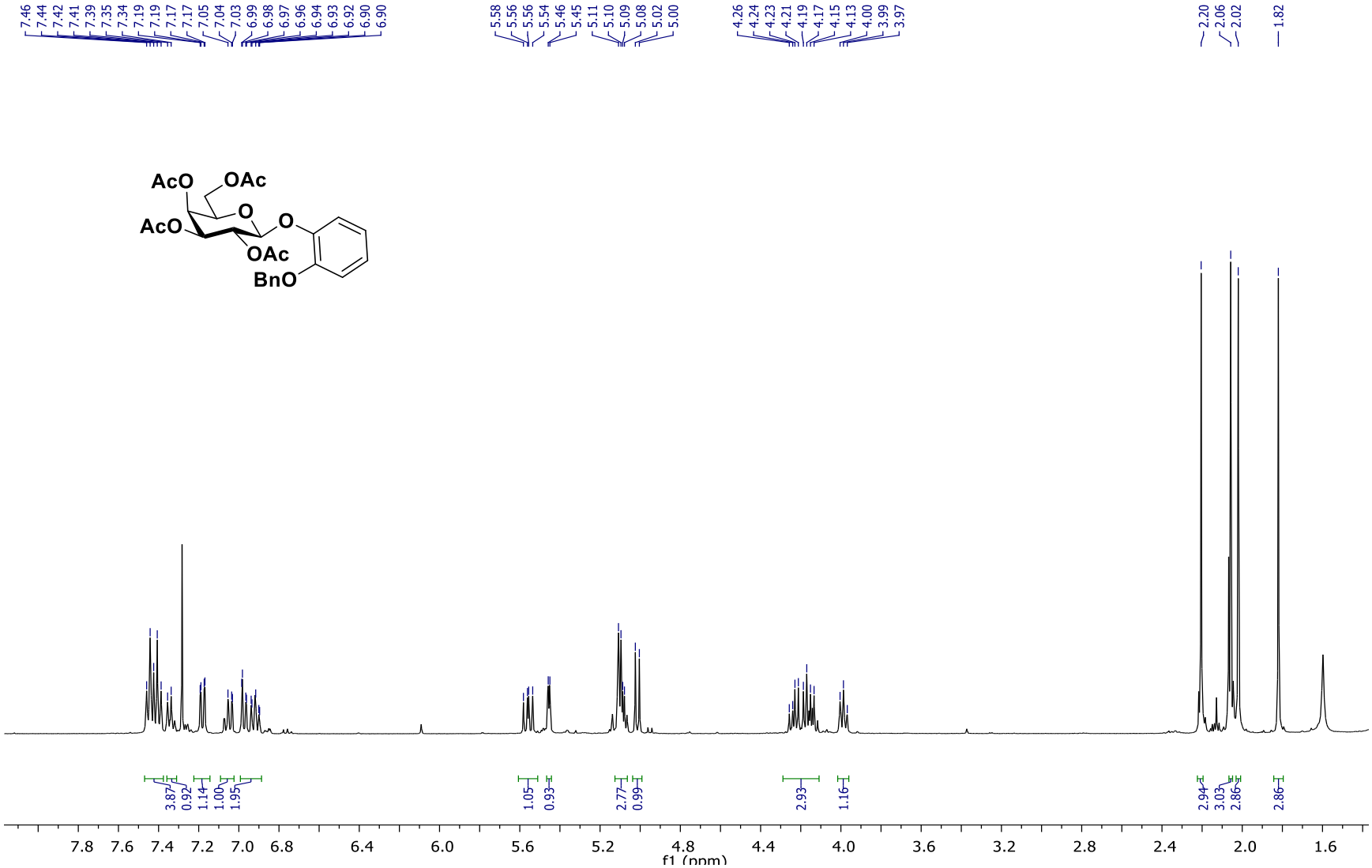

4, ^{13}C NMR, CDCl3,100 MHz,

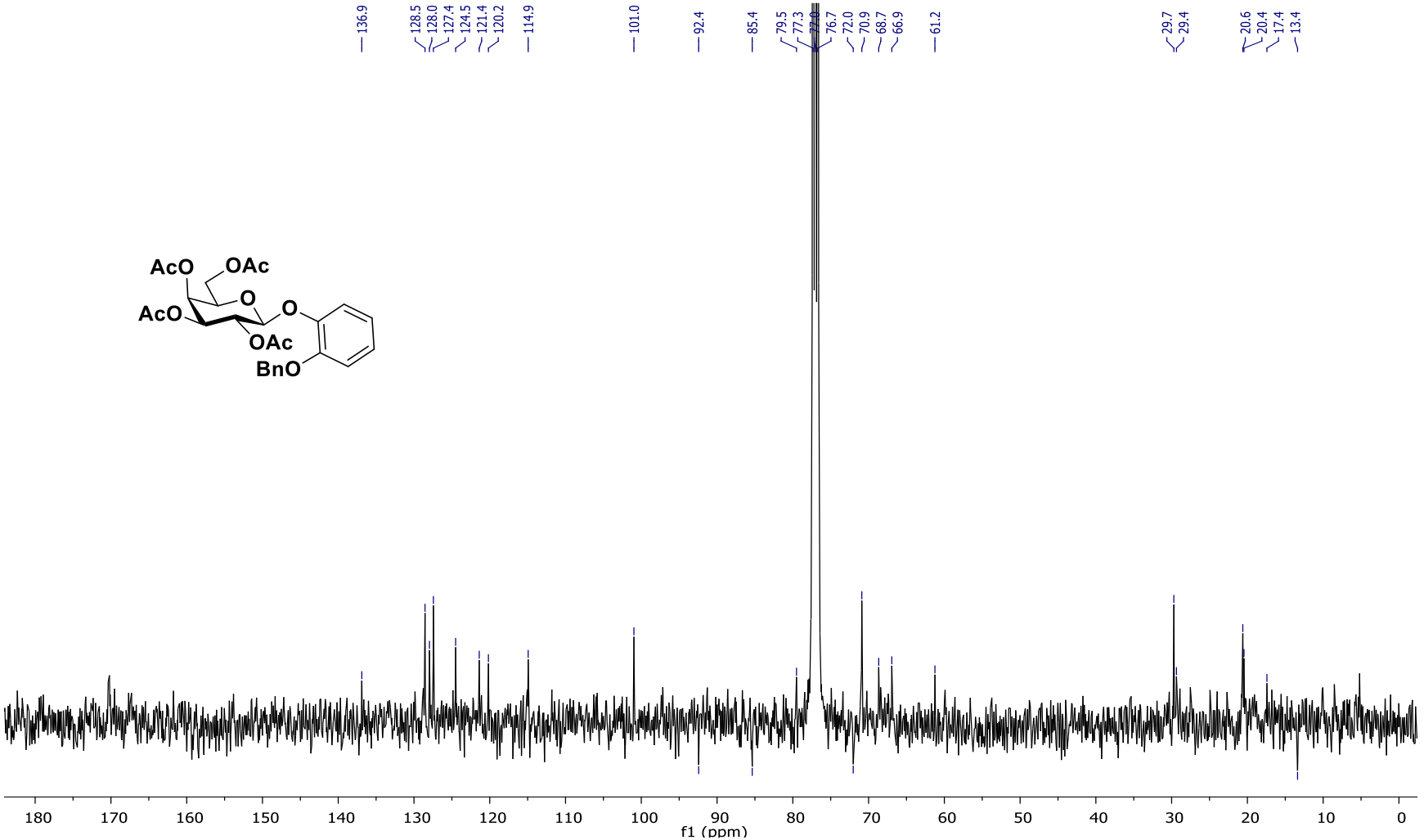

4, COSY, CDCl3, 400 MHz,

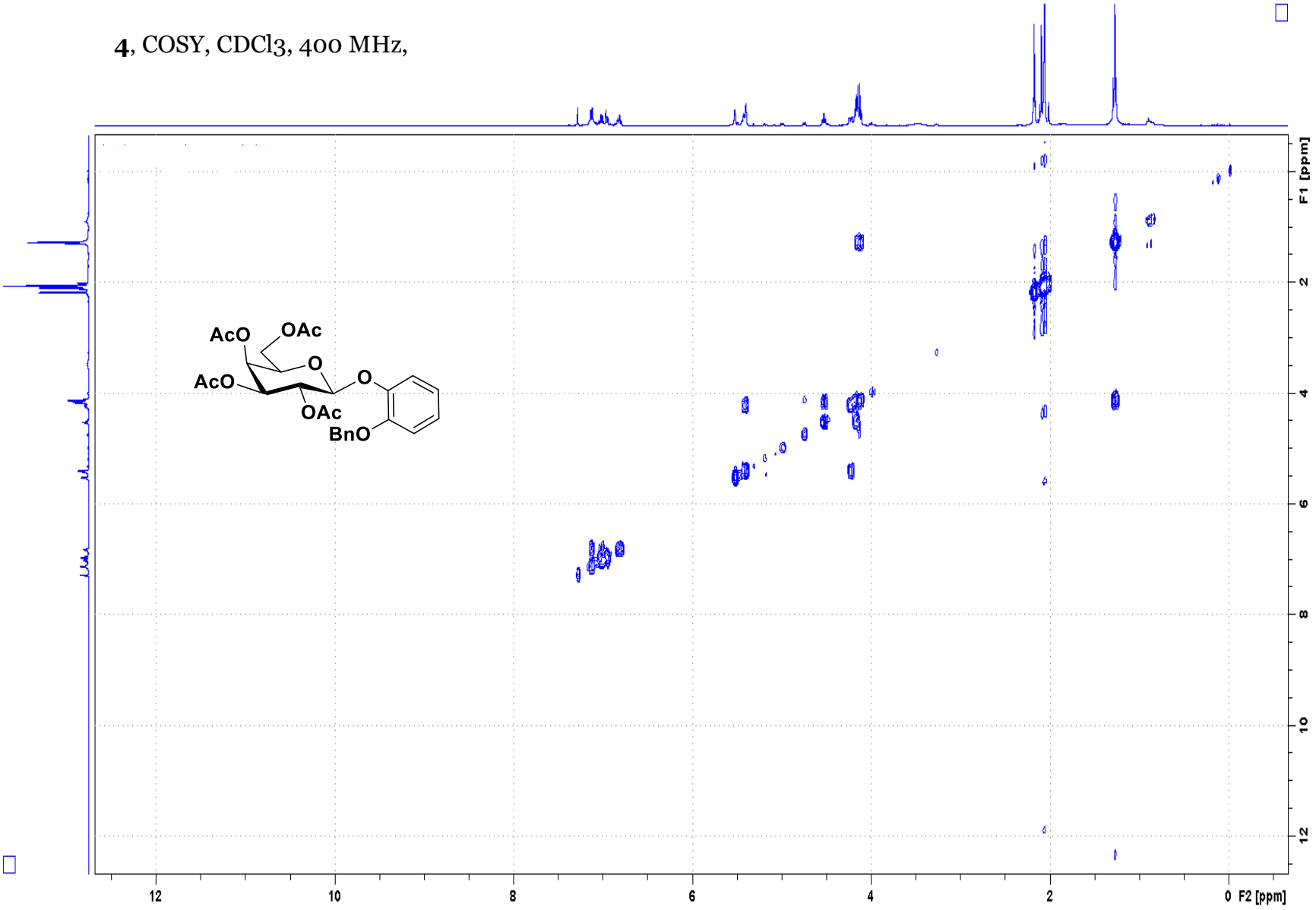

4, HSQC, CDCl3, 400 MHz,

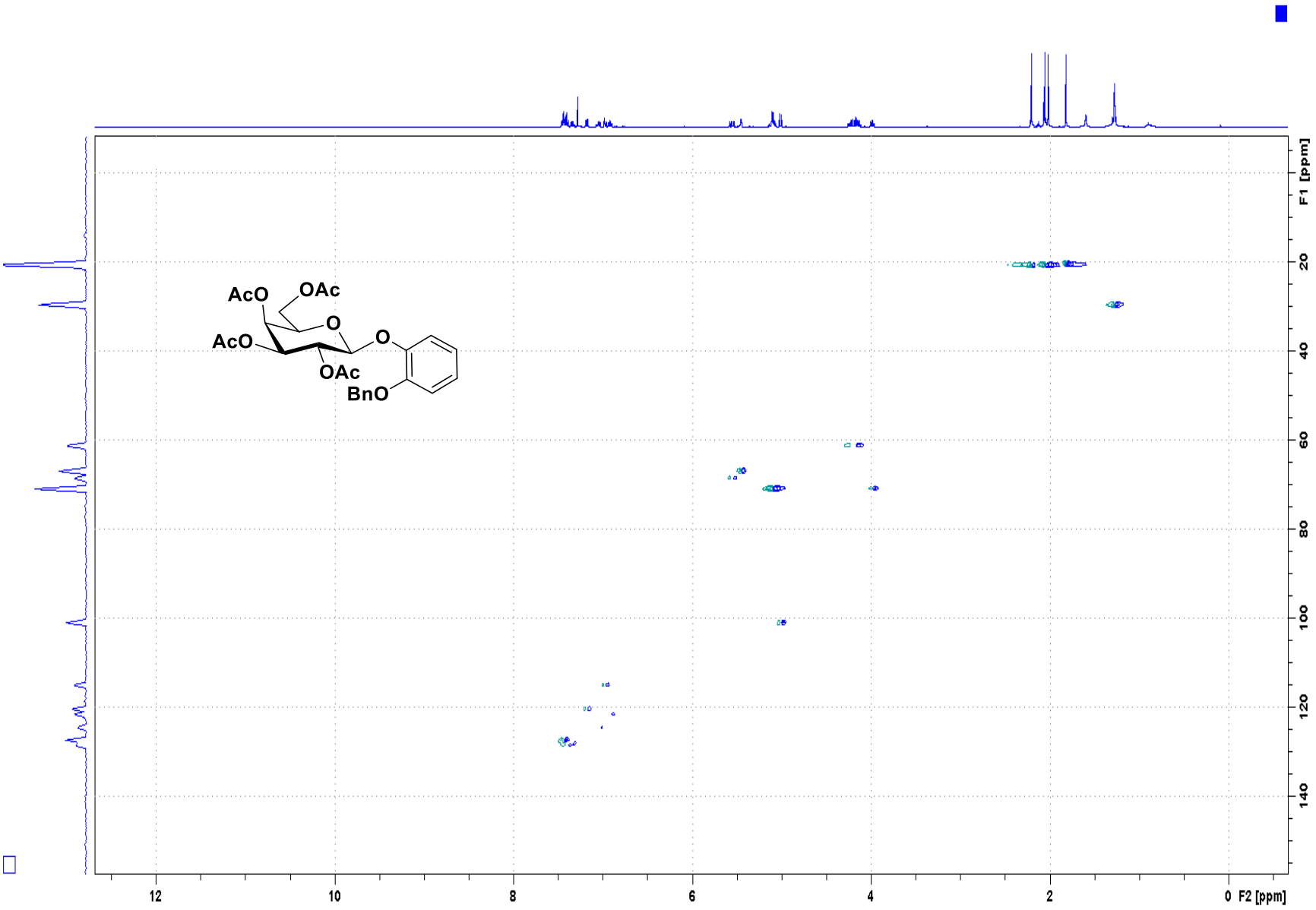

GC, ^{1}H NMR, D_2O,400 MHz,

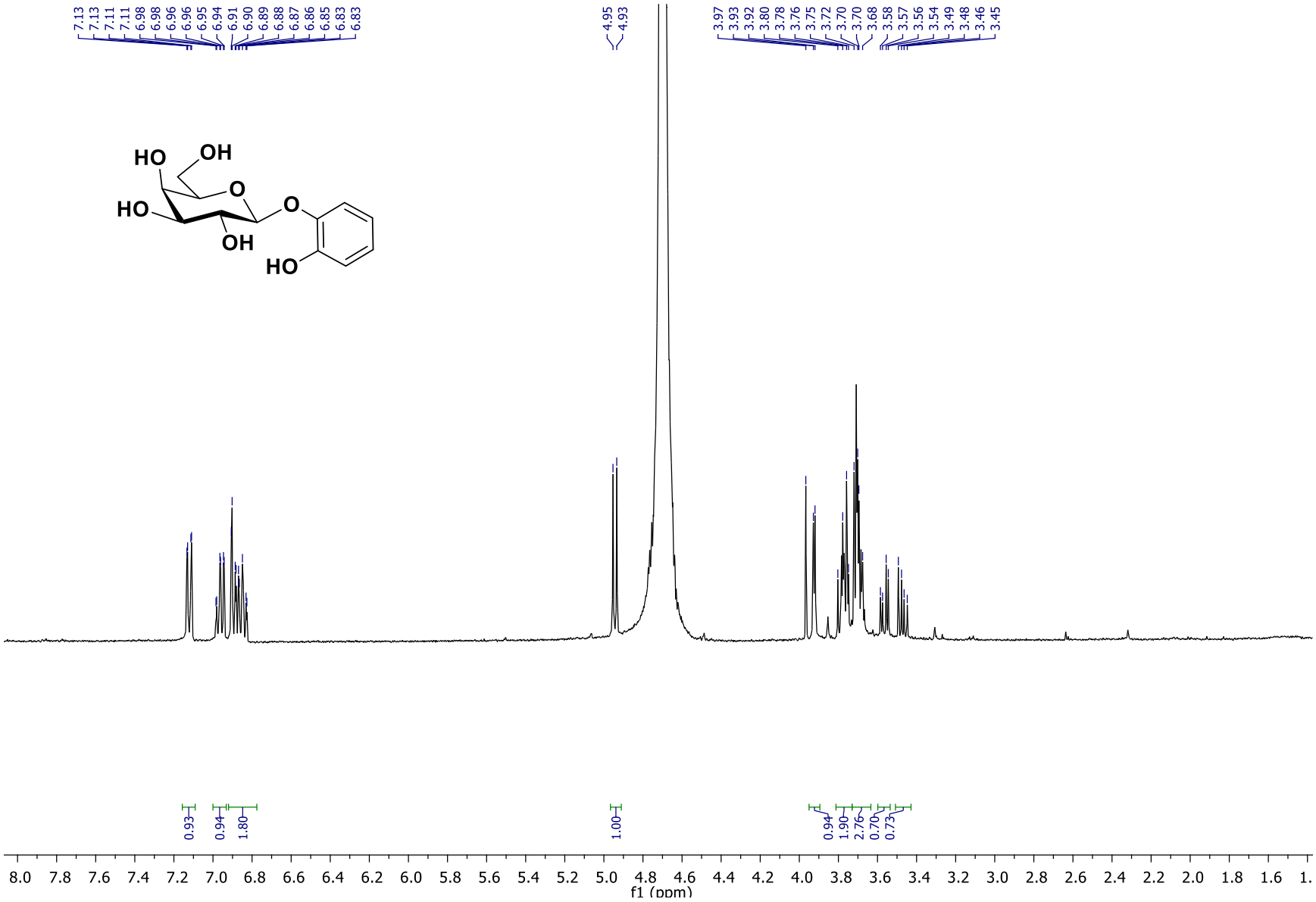

GC, ^{13}C NMR, D_2O, 400 MHz,

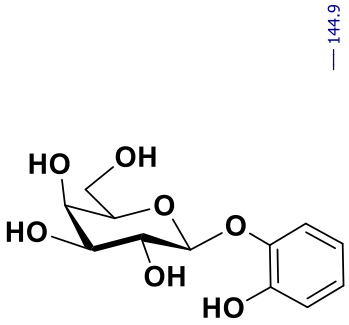

GC, COSY, D_2O , 400 MHz,

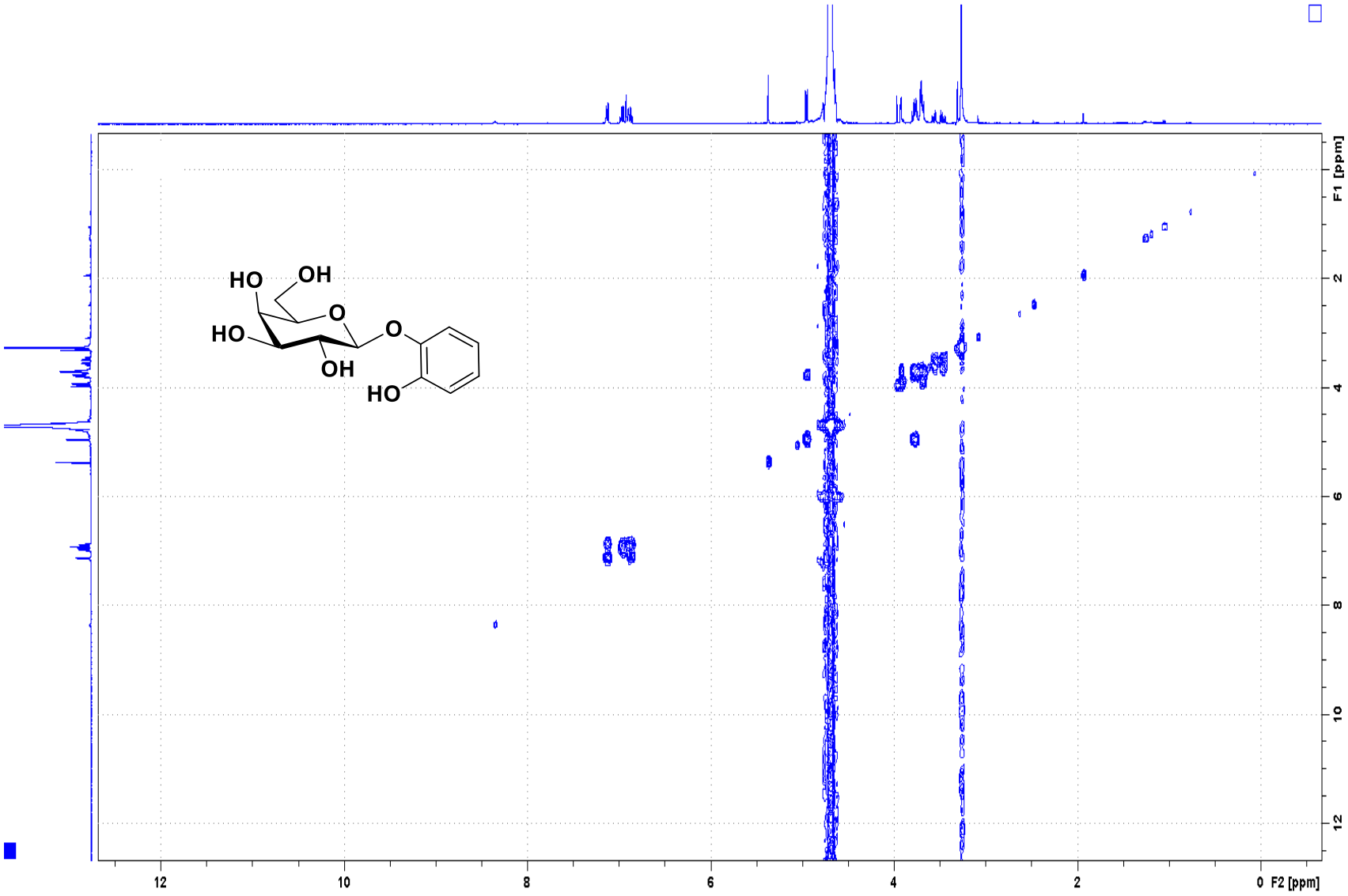

GC, HSQC, D_2O,400 MHz,

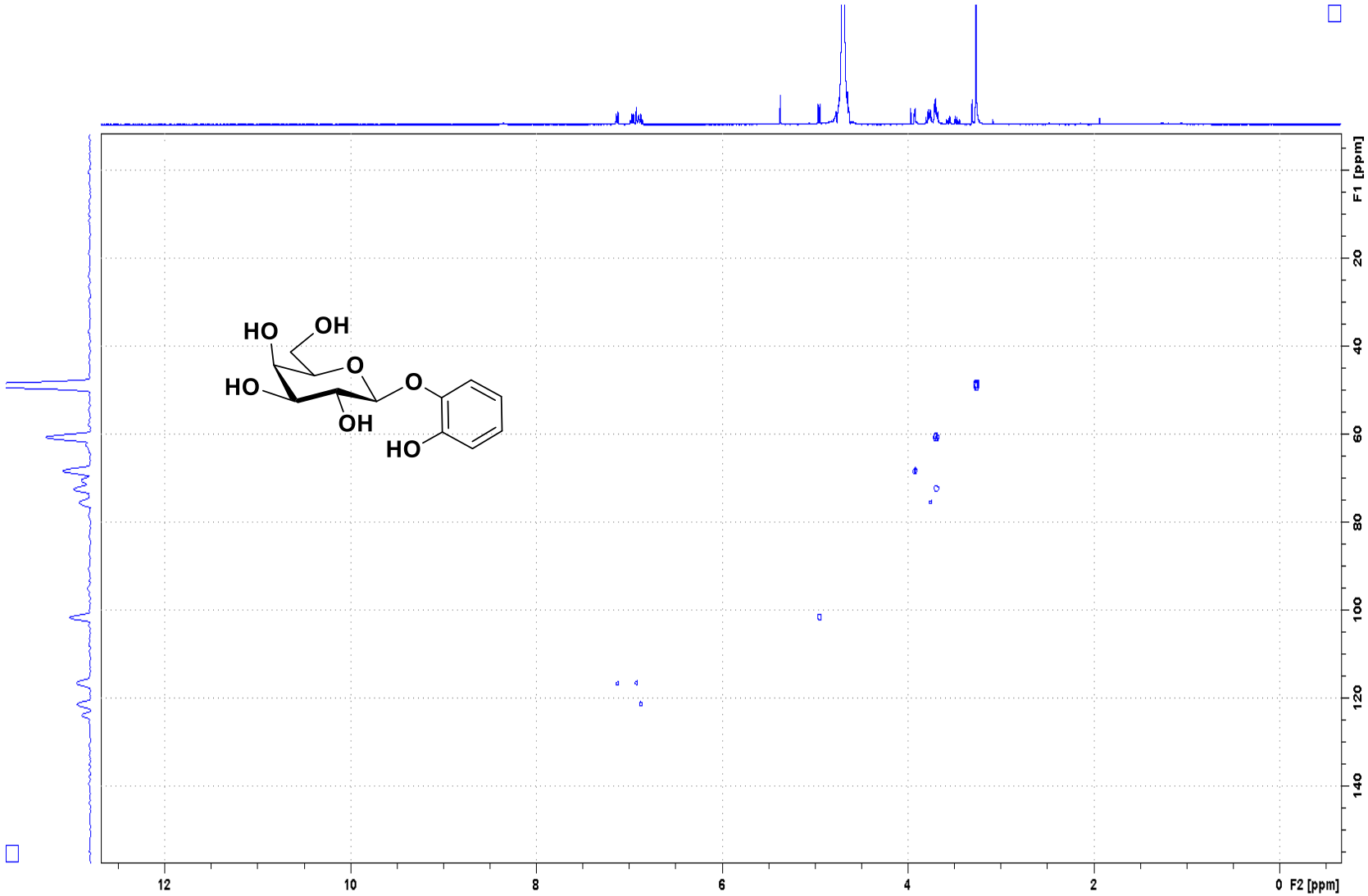

4, ^{1}H NMR, $CDCl_3$, 400 MHz

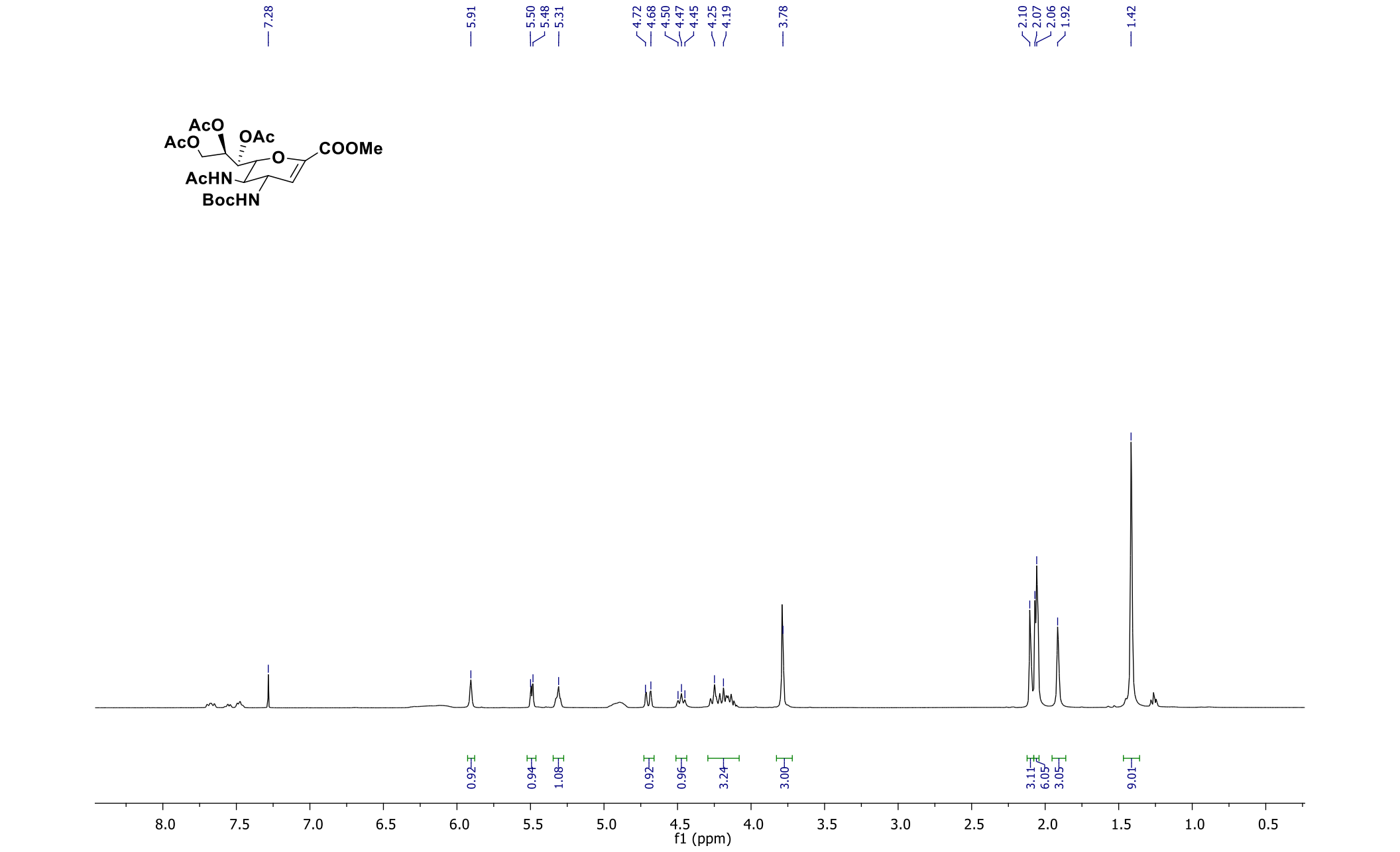

6, ^{1}H, $CDCl_3$, 400 MHz

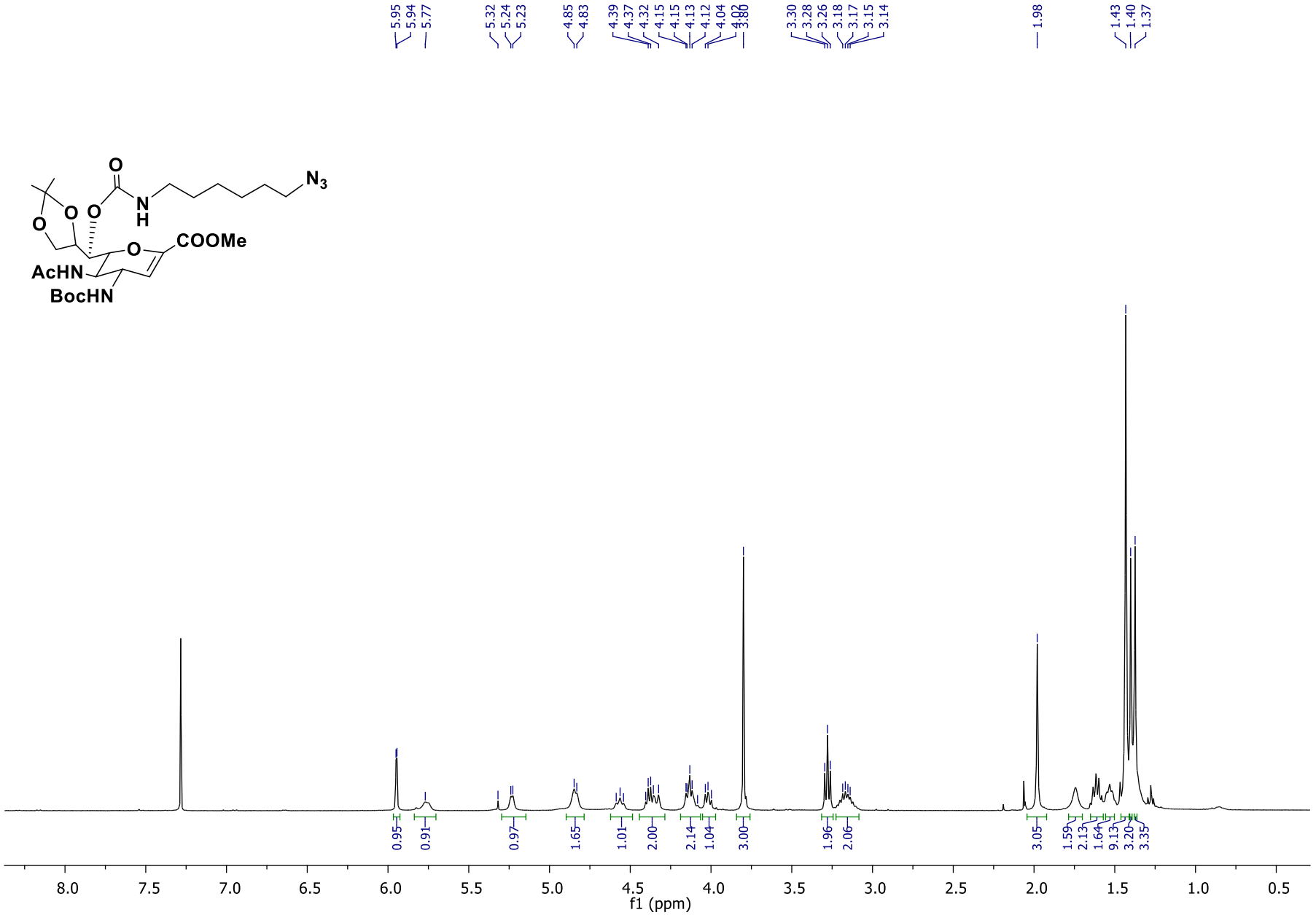

7, ^{1}H, $CDCl_3$, 400 MHz

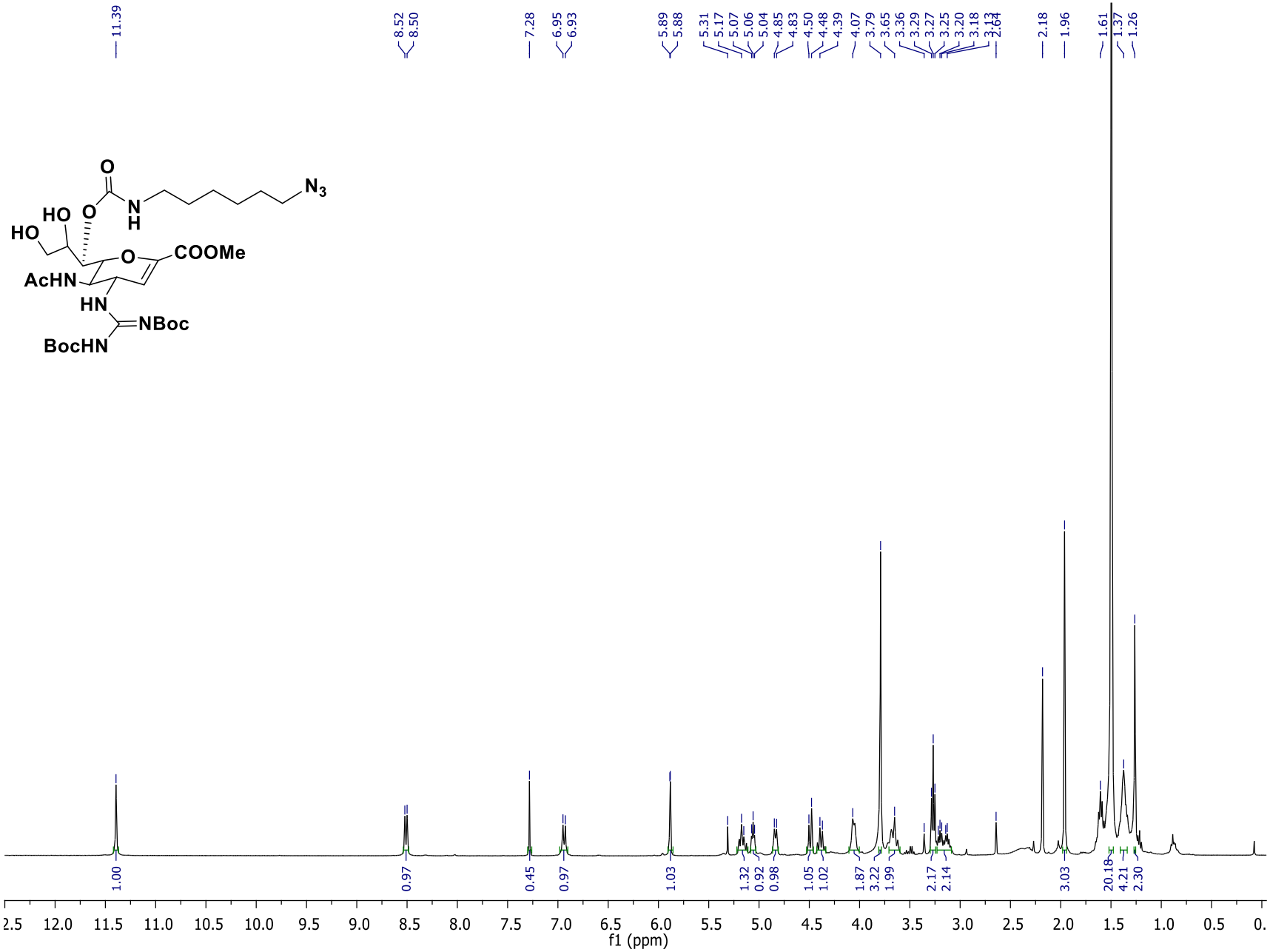

9, ^{1}H NMR, $CDCl_3$, 400 MHz

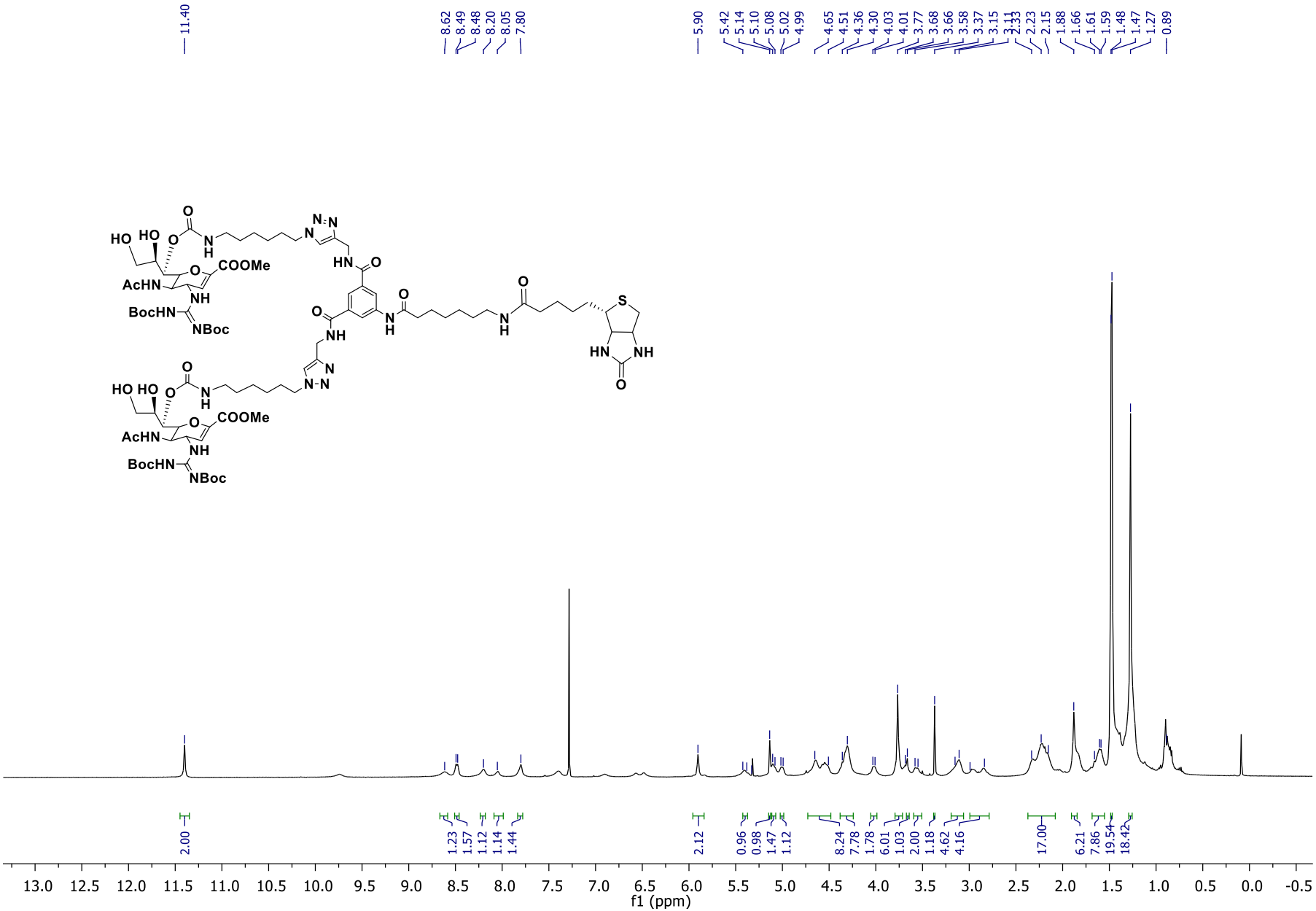

9, ^{13}C, $CDCl_3$, 400 MHz

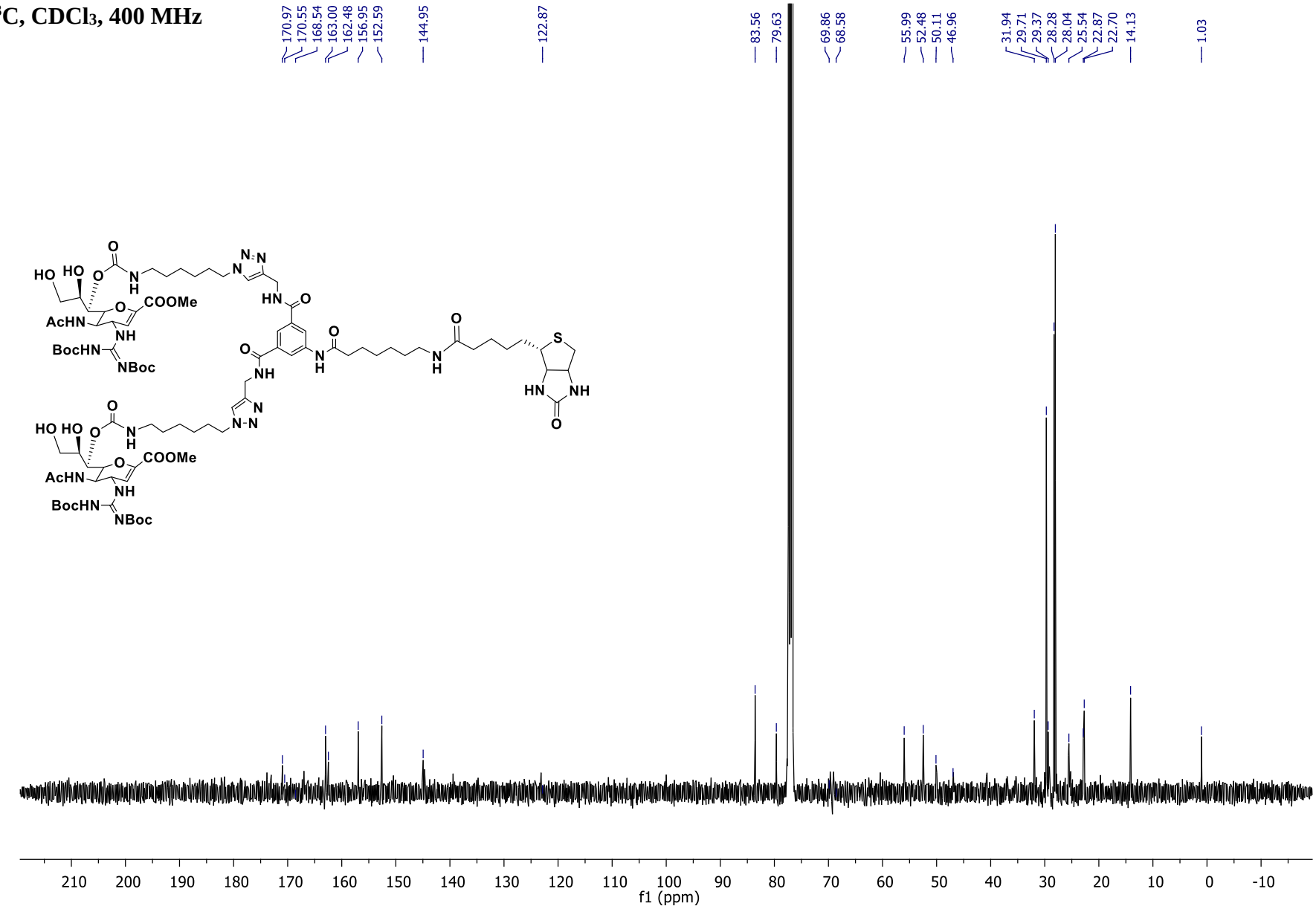

9, COSY, $CDCl_3$, 400 MHz

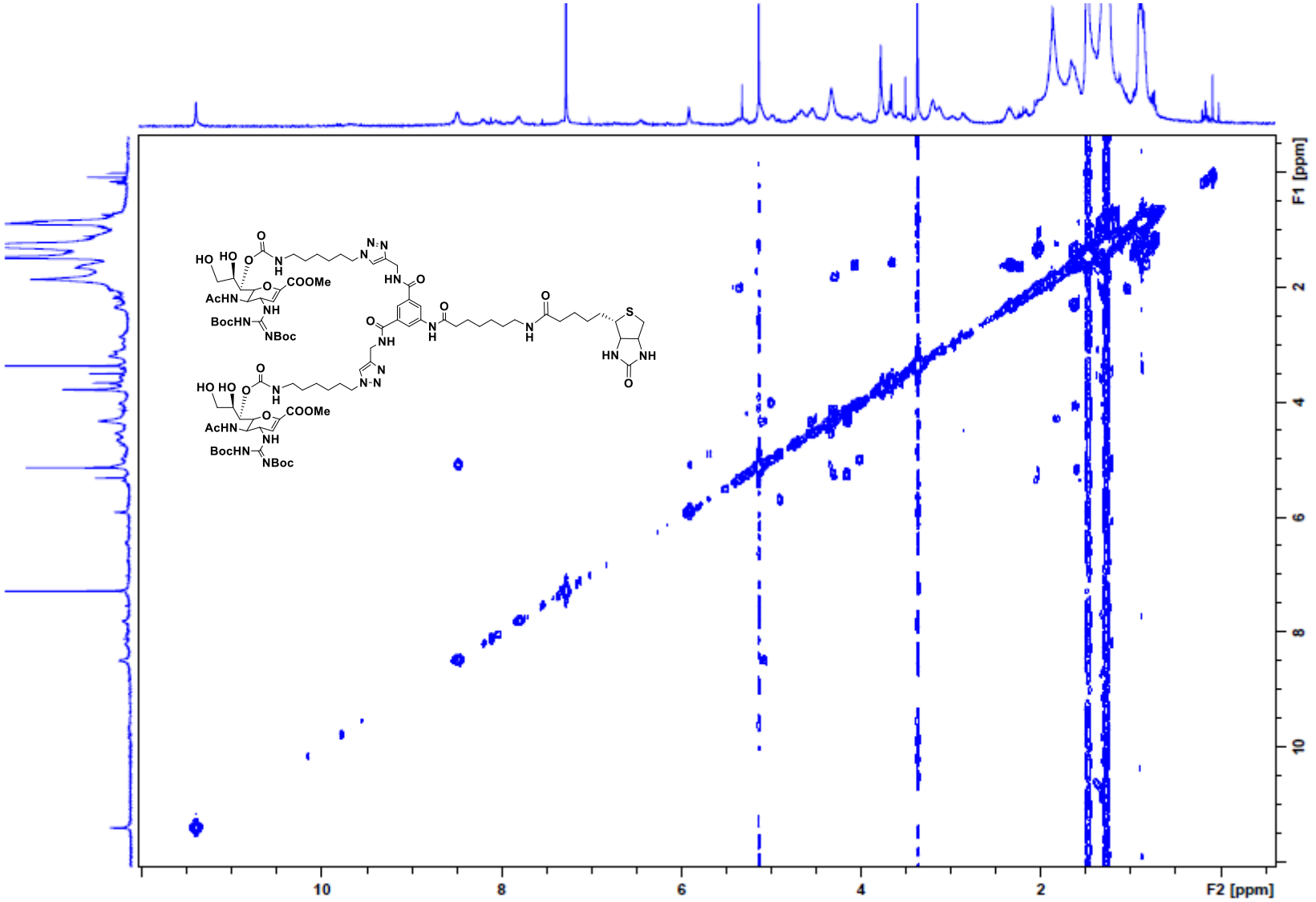

9, HSQC, $CDCl_3$, 400 MHz

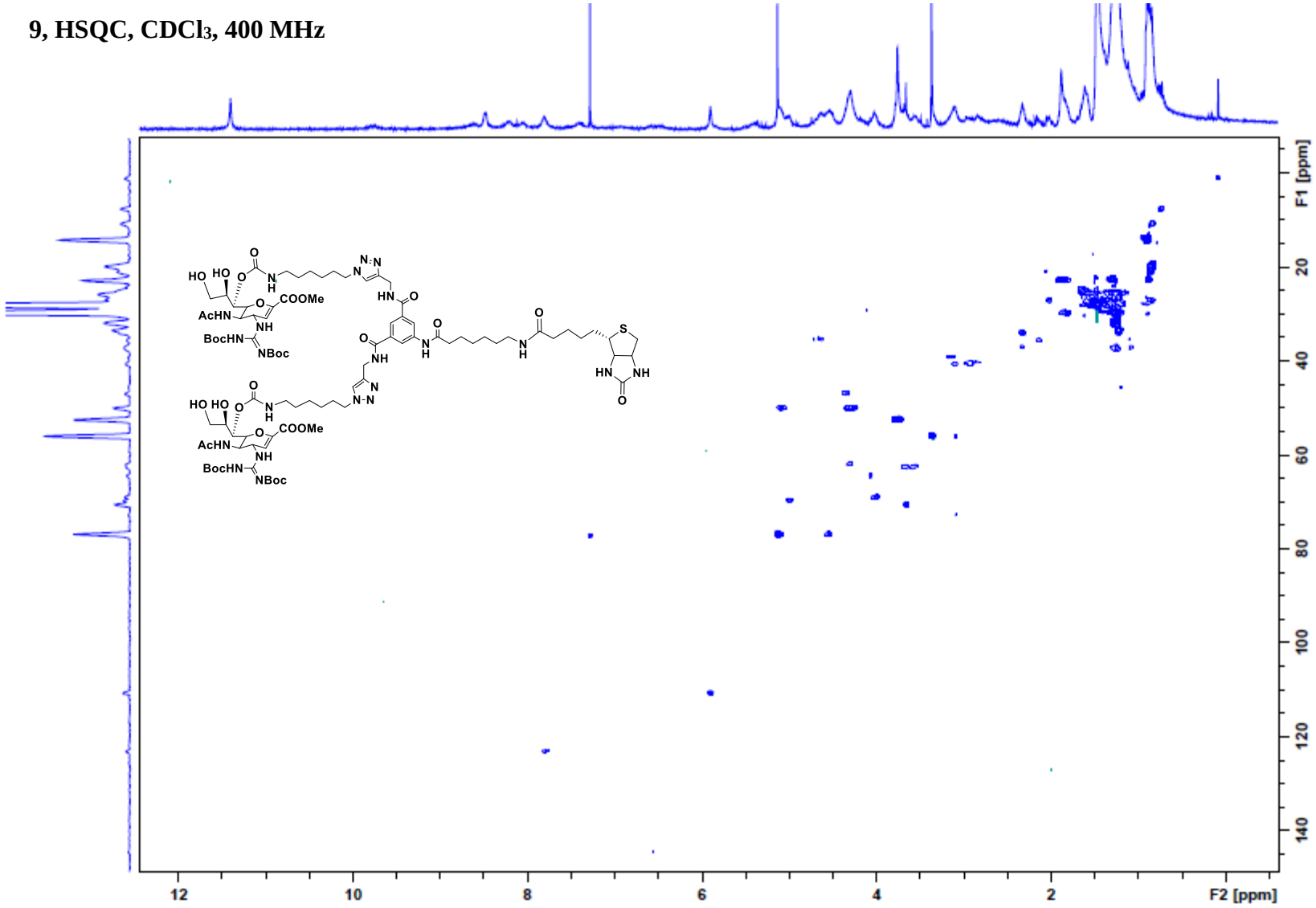

AD-R 1H NMR, 400 MHz

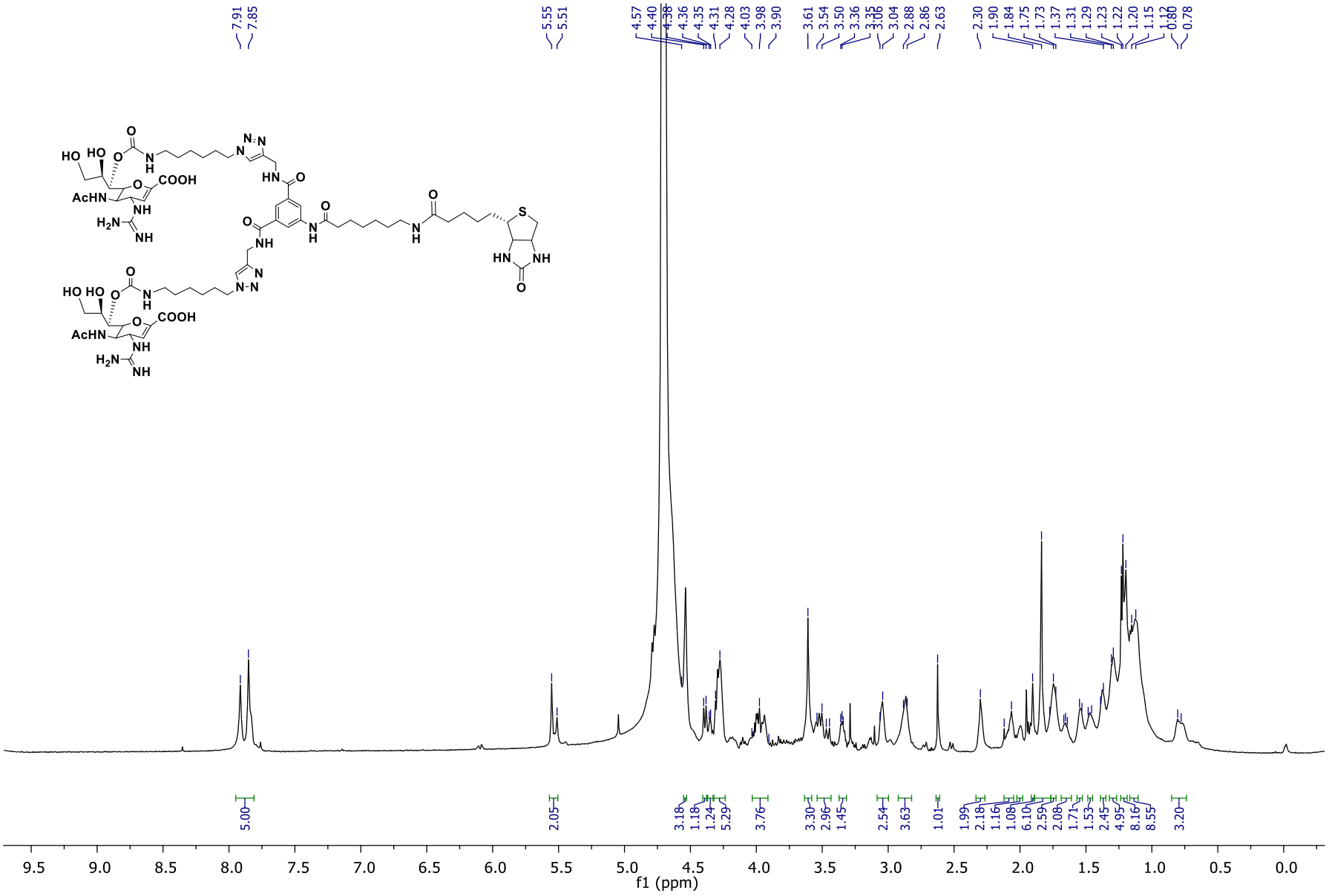

AD-R ^{13}C NMR, D_2O, 100 MHz

175.81
171.12
168.40
163.56
163.26
162.92
156.22
135.81
134.94
129.36
123.92
122.55
115.34
110.03
104.85
100.00
78.67
75.23
71.90
71.50
69.64
68.54
62.53
51.87
50.32
47.39
40.35
35.00
28.44
28.00
27.79
27.51
26.01
25.67
25.11
21.85
20.00

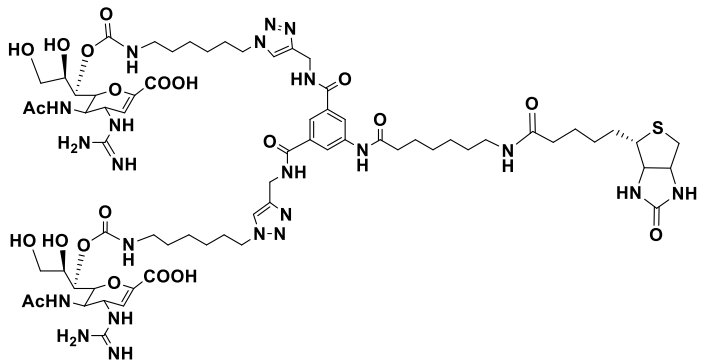

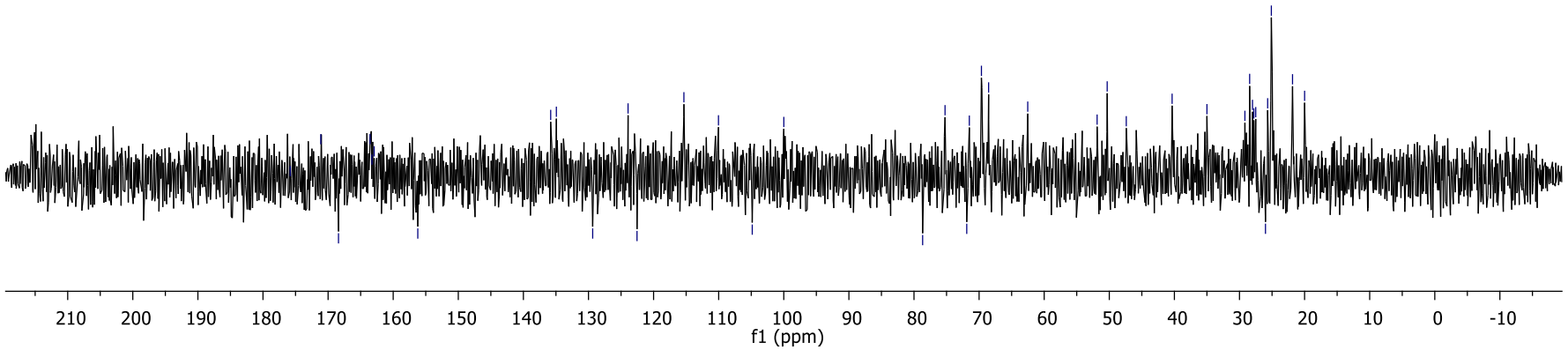

AD-R, COSY, D_2O, 400 MHz

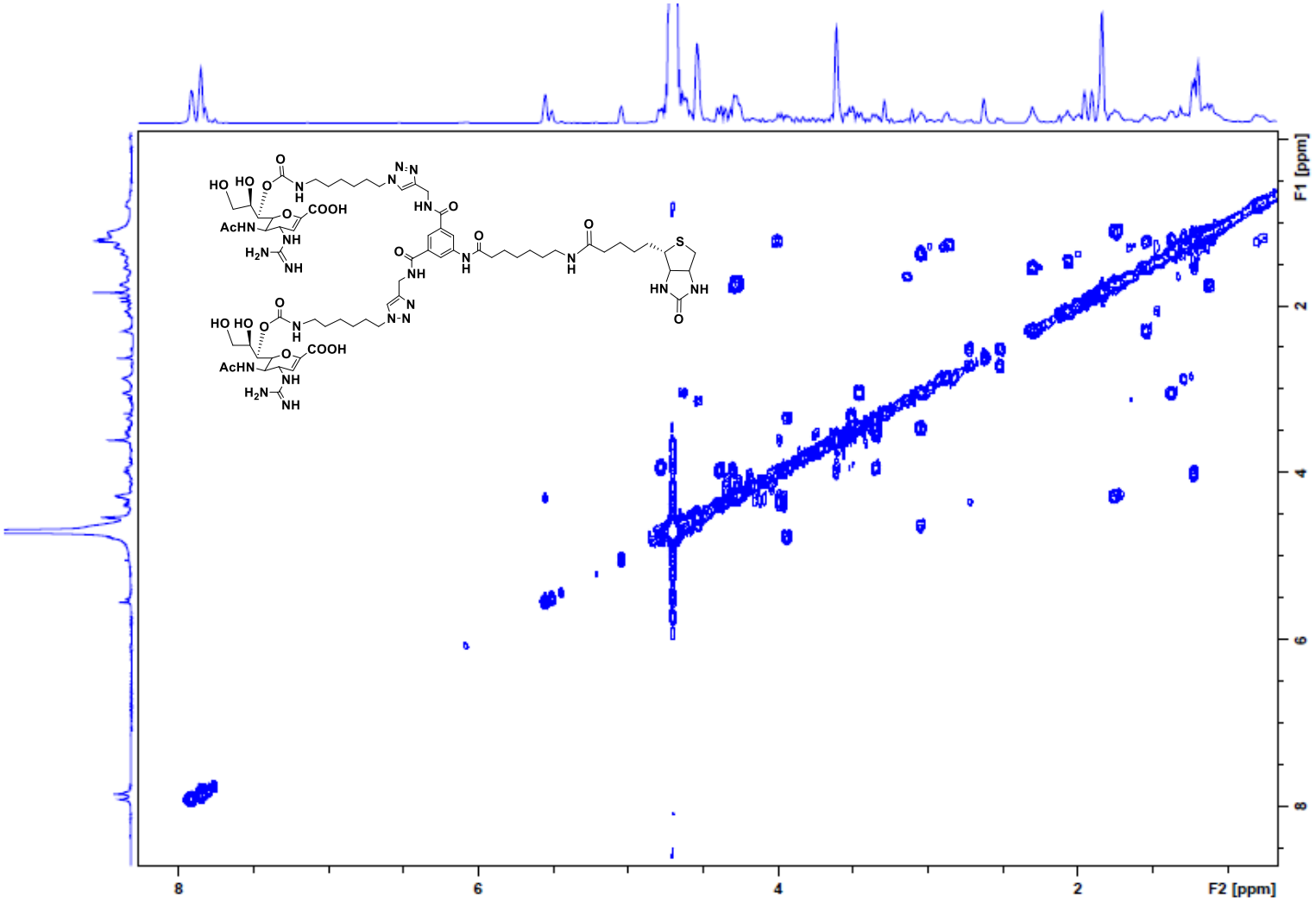

AD-R, HSQC , 400MHz

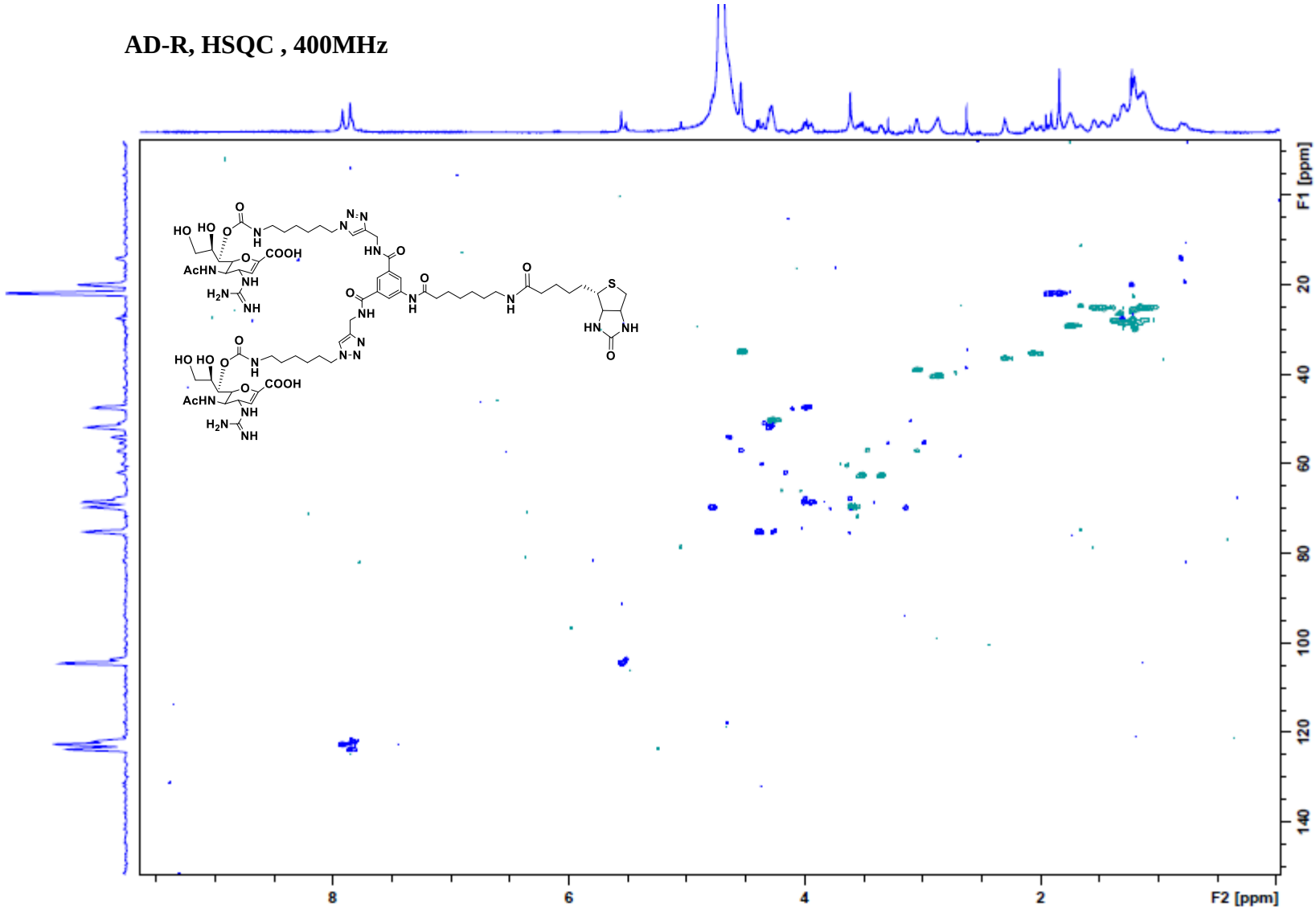

Appendix B. Raw data from biological assays

Plaque Assays:

Dilution of viruses (pfu/ml): 10^{-4} 10^{-5} 10^{-6}

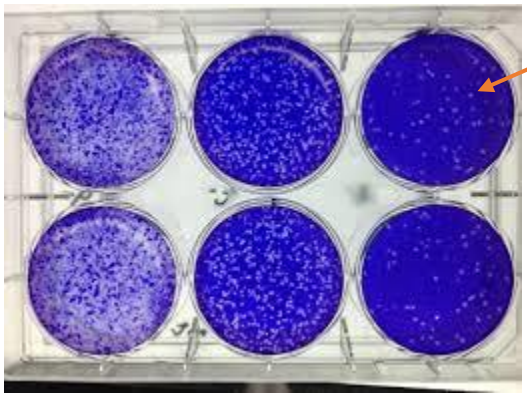

Figure 47*. Plaque Assay for Influenza virus A/Brisbane/57/2009.*

The assay was done in duplicate. Each well consisted of 4.5X 106 cells and the cells were seeded 24 h prior to performing the assay to obtain around 80% cell confluency. Each cell was then treated with 450 µL of viral culture with different dilutions (10^{-4}, 10^{-5}, 10^{-6} pfu/ml of virus) for an hour with shaking every 15 mins. After an hour of incubation with the virus, each well was washed twice and then media supplemented with 0.2ug/ml of TPCK treated Trypsin was added and the cells were allowed to grow for 3 days before checking for plaques.

The number of plaques was calculated using the following formulae

Pfu/ml= (no of plaques/ d x V)

Where, d= dilution of virus

V=volume of diluted virus added to each well.

After the plaque assay for Influenza virus A/Brisbane/57/2009 strain, the pfu/ml was calculated using the above formula as pfu/ml=1.207 X 10^7

The titer values of the different Influenza viral strain obtained from Plaque assays.

Catalogue	Influenza Virus	Strain	(pfu/ml)
NR-15268	A/New York/18/2009	H1N1	1.5 X 10^8
NR-3177	A/Aichi/2/1968	H3N2	1.8 X 10^8
NR-21667	A/New Jersey/8/76	H1N1	2.5 X 10^7
NR-12283	A/Brisbane/10/2007	H3N2	6.75 X 10^7
NR-13658	A/California/04/2009	H1N1	1.2 X 10^7
NR-41800	A/Wisconsin/67/2005	H3N2	1.5 X 10^7
NR-31657	A/Brisbane/59/2007	H1N1	7.0 X 10^7
NR-3223	A/Texas/36/91	H1N1	2.5 X 10^7
NR-12281	A/Solomon Islands/03/2006	H1N1	6.5X 10^6

Growth curves for *E. coli*:

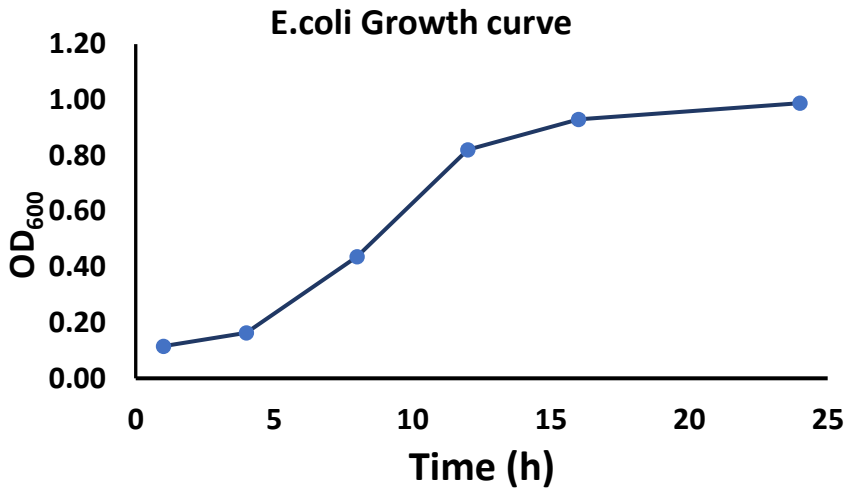

E.coli growth curve:				
Time (h)	OD600		AVG	STDEV
1	0.11	0.121	0.1155	0.007778
4	0.1623	0.164	0.16315	0.001202
8	0.43	0.443	0.4365	0.009192
12	0.812	0.83	0.821	0.012728
16	0.92	0.939	0.9295	0.013435
24	0.987	0.989	0.988	0.001414

The *E. coli* B (ATCC 11303) samples were grown in Luria-Bertani (LB) broth for 24 h at 37^0C, supplemented with a final concentration of 1 mM isopropyl β -D-thiogalactopyranoside (IPTG) for the induction of β-galactosidase enzyme. The OD values were taken every 4 hours to get the growth curve for E.*coli*. The cells were harvested by centrifuging them at 2500 rpm for 5 min

and re-suspended in sterile PBS buffer. 1% Triton was added to the *E. coli* cells to lyse and release the β - galactosidase enzyme.

Limit of detection of *E. coli*. with GP; All assays were done in triplicates.

E.coli						
time-15 min						
pfu/ml	**Glucose M**	**Average**	**Glucose M**	**p valuer**	**STD**	**control**
10^5	97,98,89	94.66667	37.66667		4.932883	57
10^4	76,79,73	76	19	0.008668	3	
10^3	65,68,67	66.66667	9.666667	0.017565	1.527525	
10^2	62,61,63	62	5	0.015902	1	
10^1	57,60,61	59.33333	2.333333	0.143248	2.081666	
10^0	57,59,58	58	1	0.393854	1	

E.coli						
time-30 min						
pfu/ml	**Glucose Me**	**Average**	**Glucose M**	**p valuer**	**STD**	**control**
10^5	101,105,103	103	46		2	57
10^4	83,86,89	86	29	0.002163	3	
10^3	67,72,73	70.66667	13.66667	0.003847	3.21455	
10^2	66,62,63	63.66667	6.666667	0.042153	2.081666	
10^1	64,60,61	61.66667	4.666667	0.304559	2.081666	
10^0	59,61,60	60	3	0.303342	1	

Detection of A/Aichi/2/1968 and *S. pneumoniae with SP(OMe)$_2$ and SP respectively.*

Detection of 10^4 pfu/ ml Aichi (A/2/1968/H3N2)				
	Glucose Meter Reading			
Time(min	Average (	Δ Glucose	Standard Dev	
0	59.66667	2.666667	1.154701	
15	66.66667	9.666667	1.527525	
30	69.66667	12.66667	2.081666	
60	77.33333	20.33333	0.57735	
Detection of S. pneumonia 10^6 CFU/ml				
	Glucose Meter Reading			
Time(min	Average (	Δ Glucose	Standard Dev	
0	137.6667	0	2.081666	
15	139	1.333333	3	
30	138	0.333333	2	
60	140	2.333333	2	

\

Limit of detection of A/Aichi/2/1968 strain with SP(OMe)$_2$; All the assays were done in triplicates.

Aichi/2/1968						
15 mins						
pfu/ml	Glucose M	p value	Glucose M	Average Δ	STD	control
10^4	66,67,68		67	10	1.5	57
10^3	64,63,64	0.0137	63	6	1.0	
10^2	62,61,62	0.0132	62	5	0.6	
10^1	62,61,61	0.5185	62	5	0.6	
10^0	61,61,64	0.5813	62	5	1.7	
	time-30 min					
pfu/ml	Glucose M	p value	Glucose M	Average Δ	STD	control
10^4	77,78,77		77	20	0.6	57
10^3	68,71,68	0.008536	69	12	2.1	
10^2	63,62,63	0.01625	63	6	0.6	
10^1	61,60,63	0.2667	61	4	1.5	
10^0	61,60,59	0.2846	60	3	1.0	

Limit of detection of A/Solomon Islands/3/2006 strain with $SP(OMe)_2$; All the assays were done in triplicates

Solomon Islands						
	time-15 min					
pfu/ml	**Glucose M**	**p value**	**Glucose M**	**Average Δ**	**STD**	**control**
10^6	95, 90, 94		93	36	2.645751	57
10^5	84,88,88	0.036288	86.66667	29.66667	2.309401	
10^4	80,84,83	0.073918	81	24	1.732051	
10^3	77,69,73	0.036967	79.66667	22.66667	0.57735	
10^2	63,64,62	0.042455	69.66667	12.66667	2.081666	
10^1	60,61,63	0.200173	68.33333	11.33333	1.527525	
10^0	57,60,65	0.809315	67	10	1	
concentration of Virus						
	time-30 min					
pfu/ml	**Glucose M**	**p-value**	**Glucose M**	**Average Δ**	**STD**	**control**
10^6	100, 102,98		100	43	2	57
10^5	86,89,88	0.001412	87.66667	30.66667	1.527525	
10^4	83,84,83	0.027122	83.33333	26.33333	0.57735	
10^3	75,73,77	0.013255	81.33333	24.33333	2.309401	
10^2	70,66,72	0.064171	75	18	2	
10^1	61,63,65	0.048108	71.66667	14.66667	1.154701	
10^0	64,61,60	0.468594	70	13	1	